Ebola Virus RNA Editing: Characterization of the Mechanism and Gene Products.

by

Masfique Mehedi B.Sc., M.Sc.

A Thesis submitted to the Faculty of Graduate Studies of

The University of Manitoba

in partial fulfillment of the requirements of the degree of

DOCTOR OF PHILOSOPHY

Department of Medical Microbiology

University of Manitoba

Winnipeg

COPYRIGHT PERMISSION

A thesis/practicum submitted to the Faculty of Graduate Studies of the University of Manitoba in partial fulfilment of the requirement of the degree of

DOCTOR OF PHILOSOPHY

THIS THESIS HAS BEEN EXAMINED AND APPROVED.

Thesis supervisor, Dr. Heinz Feldmann, M.D., Ph.D.

Associate Professor of Medical Microbiology, University of Manitoba &

Chief, Laboratory of Virology, Rocky Mountain Laboratories, DIR, NIAID, NIH, Hamilton, MT

Dr. Kevin Coombs, Ph.D.

Professor of Medical Microbiology &

Associate Dean (Research), Faculty of Medicine, University of Manitoba

Dr. Steven Pind, Ph.D.

Assistant Professor, Biochemistry and Medical Genetics, University of Manitoba

External Examiner, Dr. Paul A Rota, Ph.D.

Adjunct Professor, Emory University & University of Georgia, &

Measles Team Lead, MMR and Herpes virus Laboratory Branch, Centers for Disease Control and Prevention (CDC), Atlanta, GA

ABSTRACT

EBOLA VIRUS RNA EDITING: CHARACTERIZATION OF THE MECHANISM AND GENE PRODUCTS.

Masfique Mehedi, B.Sc., M.Sc.

University of Manitoba, 2012

Ebola virus (EBOV) is an enveloped, negative-sense single-stranded RNA virus that causes severe hemorrhagic fever in humans and nonhuman primates. The EBOV glycoprotein (GP) gene encodes multiple transcripts due to RNA editing at a conserved editing site (ES) (a hepta-uridine stretche). The majority of GP gene transcript is unedited and encodes for a soluble glycoprotein (sGP); a defined function has not been assigned for sGP. In contrast, the transmembrane glycoprotein ($GP_{1,2}$) dictates viral tropism and is expressed through RNA editing by insertion of a nontemplate adenosine (A) residue. Hypothetically, the insertion/deletion of a different number of A residues through RNA editing would result in another yet unidentified GP gene product, the small soluble glycoprotein (ssGP). I have shown that ssGP specific transcripts were indeed produced during EBOV infection. Detection of ssGP during infection was challenging due to the abundance of sGP over ssGP and the absence of distinguishing antibodies for ssGP. Optimized two- dimensional (2-D) gel electrophoresis verified the expression of ssGP during infection. Biophysical characterization revealed ssGP is a disulfide-linked homodimer that is exclusively N-glycosylated. Although ssGP appears to share similar structural properties with sGP, it does not have the same anti-inflammatory function.

Using a new rapid transcript quantification assay (RTQA), I was able to demonstrate that RNA editing is an inherent feature of the genus *Ebolavirus* and all species of EBOV produce multiple GP gene products. A newly developed dual-reporter minigenome system was utilized to characterize EBOV RNA editing and determined the conserved ES sequence and cis-acting sequences as primary and secondary requirements for RNA editing, respectively. Viral protein (VP) 30, a transcription activator, was identified as a contributing factor of RNA editing— a proposed novel function for this largely uncharacterized viral protein. Finally, I could show that EBOV RNA editing is GP gene-specific because a similar sequence located in L gene did not serve as an ES, most likely due to the lack of the necessary cis-acting sequences. In conclusion, I identified a novel soluble protein of EBOV whose function needs further characterization. I also shed light into the mechanism of EBOV RNA editing, a potential novel target for intervention.

ACKNOWLEDGEMENTS

This has been a wonderful learning endeavor with the Department of Medical Microbiology, University of Manitoba. I would like to thank my dear committee members Kevin Coombs and Steven Pind for their comments and guidance over the years. I would like to extend my sincere gratitude toward my external reviewer, Paul A Rota (CDC, Atlanta, GA) for reviewing my thesis.

I have been extremely fortunate to have Heinz Feldmann as my supervisor. It is difficult to express in words, but definitely I owe a huge debt of gratitude to him for his patient guidance, precious encouragement, valuable advice, and tremendous support in my graduate study and helping me bloom my research potential.

I would like to thank members of the Special Pathogens Program, National Microbiology Lab, Winnipeg for providing generous support; especially, Darryl Falzarano for his unconditional support in my research training, Thomas Hoenen, Allison Groseth, and Marko Zivcec for their cloning lessons that helped me in my research, and Hideki Ebihara for providing minigenome plasmids and his valuable suggestion in my research.

I am also thankful to Jochen Seebach & Hans-Joachim Schnittler, University of Munster, Germany for their help with the experimental procedures of the transendothelial

resistance (TER) measurement and to Garett Westmacott & Keding Cheng for their help with the mass spectrometry.

I am grateful to the National Institutes of Health for the Pre-Doctoral Fellowship to do research at the Rocky Mountain Laboratories (RML), Hamilton, MT. My heartiest thanks go toward the members of the Laboratory of Virology for their numerous supports in my research, especially Ricki Feldmann for the biosafety level 4 training and Shelly Robertson for helping with the flow cytometer. I am thankful to Stacy Ricklefs, Research Technology Branch, RML for help in the development of the rapid transcript quantification assay.

I am obliged to the University of Manitoba for providing me the graduate student entrance scholarships (2006-07), graduate student scholarships (2008), and Dean's award (2008) in the Manitoba Health Research Poster Competition; to the Canadian Institutes of Health Research (CIHR) for the Silver award (2008) in the CIHR poster competition; to the American Society of Virology (ASV) for the travel award (2011) to attend the ASV conference.

Last, but not least, I am grateful to my wife (Farhana Yesmen) for being patient and providing constant encouragements.

DEDICATION

This thesis is dedicated to my beloved parent.

TABLE OF CONTENTS

LIST OF TABLES

LIST OF FIGURES

LIST OF APPENDICES

LIST OF COPYRIGHTED MATERIALS

Figure 11- 13, 16, 18 – 23 reproduced with permission

Mehedi M., D. Falzarano, J. Seebach, X.Hu, M. S. Carpenter, H. J. Schnittler, & H. Feldmann. A new Ebola virus nonstructural glycoprotein expressed through RNA editing. Journal of Virology, 2011. Vol 85(11), pp 5406-5414.

LIST OF ABBREVIATION

2-D	two dimensional
A	adenine/adenosine
aa	amino acid
Abs	antibodies
ADAR	adenosine deaminase acting on RNAs
AGM	African green monkey
AFLP	amplified fragment length polymorphism
apoB	apolipoprotein B
APOBEC	apolipoprotein B mRNA editing enzyme
BEBOV	*Bundibugyo ebolavirus*
BSL	biosafety level
$CD4^+$	cluster of differentiation 4
$CD8^+$	cluster of differentiation 8
CDC	Centers for Disease Control and Prevention
CIEBOV	*Cote d'Ivoire ebolavirus*
CPE	cytopathic effect
cps	count per second
Da	daltons
DAPI	4',6-diamidino-2-phenylindole
DC	dendritic cell
DIGE	differential gel electrophoresis
DMEM	Dulbecco's modified Eagle's medium
DMSO	dimethyl sulfoxide
DRC	Democratic Republic of Congo
dsRNA	double-stranded ribonucleic acid
DTT	dithiothreitol
EBOV	Ebola viruses
eGFP	enhanced green fluorescence protein
ELISA	enzyme linked immunosorbent assay
EHF	Ebola hemorrhagic fever
Env	envelope
ER	endoplasmic reticulum
ES	editing site
ESI	electrospray ionization
FACS	fluorescence activated cell sorting
FAM	6 carboxyfluorescein
FBS	fetal bovine serum
G	guanine
GP	glycoprotein
$GP_{1,2}$	transmembrane glycoprotein
HA	hemagglutinin
HDV	Hepatitis Delta virus
HDVrib	HDV ribozyme

HEK293	human endothelial kidney cell line
HEPES	hydroxyethyl piperazineethanesulfonic acid
HPLC	high pressure liquid chromatography
HUVEC	human umbilical vein endothelial cells
Huh7	Hepatocarcinoma cell line
Hz	Hertz (cycles per second)
IAA	iodoacetamide
IFN	interferon
IL	interleukin
IPG	immobilized pH gradient
IR	intergenic region
IRF	interferon regulatory factor
ITO	indium tin oxide
kDa	kilodalton
kVh	kilo volt hour
L	RNA dependent RNA polymerase
LB	Luria broth
LC	liquid chromatography
Ldr	leader sequence
MA-ZEBOV	mouse-adapted *Zaire ebolavirus*
MAb	monoclonal antibody
Mac	macrophages
MARV	Marburg virus
mCherry	red fluorescence protein
MHF	Marburg hemorrhagic fever
MOI	multiplicity of infection
MS	mass spectrometry
MS/MS	tandem mass spectrometry
MWCO	molecular weight cut-off
m/z	mass divided by charge
NHP	nonhuman primate
NIAID	National Institute of Allergy and Infectious Diseases
NIH	National Institutes of Health
NLS	nuclear localization signal
NNS	Negative-strand non-segmented single-stranded
NP	nucleoprotein
NS	non-structural
NTR	nontranslated region
ORF	open reading frame
P	phosphoprotein
PAGE	polyacrylamide gel electrophoresis
PBS	phosphate-buffered saline
pen/strep	penicillin/streptomycin
PFA	paraformaldehyde
PFU	plaque forming unit
p*I*	isoelectric point

PreGP	precursor glycoprotein
PVDF	polyvinylidene difluoride
RBS	receptor binding site
RBD	receptor binding domain
RdRP	RNA-dependent RNA polymerase
REBOV	*Reston ebolavirus*
RML	Rocky Mountain Laboratories
RNP	ribonucleoprotein complex
RPMI	Roswell Park Memorial Institute medium
RT-PCR	reverse transcriptase polymerase chain reaction
RTQA	rapid transcript quantification assay
SDS	sodium dodecyl sulphate
SEBOV	*Sudan ebolavirus*
sGP	secreted glycoprotein
SP	signal peptide
ssGP	small soluble glycoprotein
KO	knock-out
TER	transendothelial resistance
Tlr	trailer sequence
TNF-α	tumor necrosis factor-α
U	uridine
VHF	viral hemorrhagic fever
VLP	virus-like particle
VP	virion protein
VP24	viral protein 24
VP30	viral protein 30
VP35	viral protein 35
VP40	viral protein 40
vRNA	viral RNA (genomic)
WT	wild-type
ZEBOV	*Zaire ebolavirus*

1. INTRODUCTION

1.1. History of Filoviral Hemorrhagic Fever

Filoviruses are the most virulent of the hemorrhagic fever-causing viruses (arenaviruses, bunyaviruses, filoviruses, and flaviviruses) and have the highest case fatality rates of any of these viruses (Jahrling et al., 2007). Two genera of filoviruses (*Ebolavirus* and *Marburgvirus*) cause lethal hemorrhagic fever in both humans and nonhuman primates (NHPs), which have occurred in sporadic outbreaks occurring mostly in Africa. The pathogenicity of each filovirus varies from asymptomatic to a highly lethal infection with a case fatality rate of up to 90% (Bray, 2009; Fisher-Hoch and McCormick, 1999; Swanepoel et al., 1996). Marburg hemorrhagic fever (MHF) was first recognized during simultaneous outbreaks of Marburg virus (MARV) in Marburg and Frankfurt, Germany in August, 1967. The MARV outbreak started in a pharmaceutical factory where laboratory workers had been processing organs from African green monkeys (AGMs) (*Cercopithecus aelhiops*) imported from Uganda (Kissling et al., 1968; Martini et al., 1968a). Several weeks later two MARV cases were also reported in Belgrade, Yugoslavia (now Serbia), in which a veterinarian was infected while performing a necropsy on a dead monkey that was also imported from Uganda; he subsequently infected his wife (Anthony Sanchez, 2007; Kuhn, 2008). Despite the initial identification of MHF in Germany, filoviruses are considered to be largely endemic to Africa. Except for the initial 1967 MARV cases, most MHF outbreaks have occurred sporadically in East Africa, within 500 miles of Lake Victoria (Mehedi et al., 2011), the exceptions are a small cluster of MARV cases in Zimbabwe in 1975 (Conrad et al., 1978) and the recent largest MHF outbreak in Uige, Angola in 2004-05 (Towner et al., 2006).

Introduction

Ebola hemorrhagic fever (EHF) was first reported in two simultaneous outbreaks in Sudan and Zaire, now Democratic Republic of Congo (DRC), in 1976. The first Ebola virus (EBOV) cases were reported from an outbreak that started in a cotton factory at Nazara in Sudan. There were 67 cases in June and July and the epidemic increased over time with the identification of an additional 213 cases in the neighboring areas of Maridi, Tembura, and Juba. These outbreaks lasted until November and extensive person-to-person transmission was reported. The epidemics were controlled by following strict barrier nursing techniques and basic public health principles. There was no proven link between these two epidemics. EBOV was isolated from the infected patients of both outbreaks. The virus was named after a small river in northwestern Zaire, because that was thought to be the place where one of the first EHF cases occurred (Feldmann and Klenk, 1996; King et al., 2011; Kuhn, 2008).

Numerous EBOV outbreaks have occurred across Africa (Figure 1 and Table 1), but it is likely that many small localized outbreaks may have not been reported due to lack of infrastructure in affected areas (Kuhn, 2008). In 1979 EBOV re-emerged in Nzara and Yambio, which are located in southern Sudan, near the border with Zaire. The initial patient was a 45-year-old man who worked in the same cotton factory where the EBOV outbreak occurred in 1976. This man was admitted to the Nzara Hospital and was suspected of playing a role in virus dissemination by nosocomial infections (Baron et al., 1983; Feldmann and Klenk, 1996). Then after 15 years, in 1994, another EBOV outbreak was reported near the Tai Forest in Cote d'Ivoire when a

Genus	**Species**	**Year isolated**	**location**	**# Cases (fatality rate in %)**	**Reference**
Marburgvirus	*Lake Victoria marburgvirus*	1967	Marburg and Frankfurt, Germany; Belgrade; Yugoslavia (now Serbia)	32 (23)	(Feldmann et al., 1996b; Kuhn, 2008; Martini et al., 1968b; Siegert et al., 1968)
		1975	Johannesburg, South Africa (originated in present Zimbabwe)	3 (33)	(Feldmann and Klenk, 1996; Gear et al., 1975)
		1980	Kisumu and Nairobi, Kenya	2 (50)	(Smith et al., 1982)
		1987	Mombasa, Kenya	1 (100)	(Feldmann and Klenk, 1996; Johnson et al., 1996)
		1998-00	Democratic republic of Congo (DRC)	154 (83)	(Bausch et al., 2006)
		2004-05	Uige, Angola	252 (90)	(Bausch et al., 2008; Kuhn, 2008)
		2007	Uganda	4 (25)	(Towner et al., 2009)
		2008	USA	1 (0)	(MMWR, 2009)
		2008	Netherland	1(100)	(Timen et al., 2009)
Ebola virus	*Zaire ebolavirus*	1976	Zaire (Yambuku)	318 (88)	(Kuhn, 2008)
		1977	DRC	1 (100)	(Anthony Sanchez, 2007; Feldmann and Klenk, 1996)
		1994-97	Booue, Gabon & Johannesburg, South Africa	37 (57)	(Anthony Sanchez, 2007)
		1995	DRC	315 (77)	(Anthony Sanchez, 2007)
		2001-02	Mekembo district, Gabon	65 (82)	(Casillas et al., 2003)
		2001-02	Mbomo district and Kelle district, DRC	58 (75)	(Casillas et al., 2003)

		2002-03	DRC	143 (89)	(Formenty et al., 2003)
		2007	DRC	264 (71)	(Groseth et al.; Rec, 2007)
		2009	Germany	1 (0)	(Günther et al., 2011)
	Sudan ebolavirus	1976	Maridi, Sudan	284 (53)	(Kuhn, 2008)
		1979	Southern Sudan	34 (65)	(Feldmann and Klenk, 1996)
		2000-01	Gulu, Masindi, and Mbarara district, Uganda	425 (53)	(Casillas et al., 2003; Kuhn, 2008)
		2004	Sudan	17 (41)	(Rec, 2005)
		2011	Uganda	1 (100)	(Groseth et al.)
	Reston ebolavirus	1989	Philadelphia, USA	4 (0)	(Feldmann and Klenk, 1996; Kuhn, 2008)
		1992	Italy	epizootic	(Anthony Sanchez, 2007; Feldmann and Klenk, 1996)
		1996	Luzon, Philippines	epizootic	(Kuhn, 2008)
		1996	USA	epizootic	(Anthony Sanchez, 2007)
	Tai forest ebolavirus	1994	Tai national forest, Cote d'Ivoire	1 (0)	(Hartman et al., 2010; Le Guenno et al., 1995)
	Bundibugyo ebolavirus	2007	Bundibugyo district, Uganda	149 (25)	(Hartman et al., 2010; Towner et al., 2008)
Cuevavirus	*LIoviu ebolavirus*	2002	Cueva del Lloviu, Spain	No outbreak	(Negredo et al., 2011)

Table 1. **Filovirus outbreaks since discovery in 1967**.

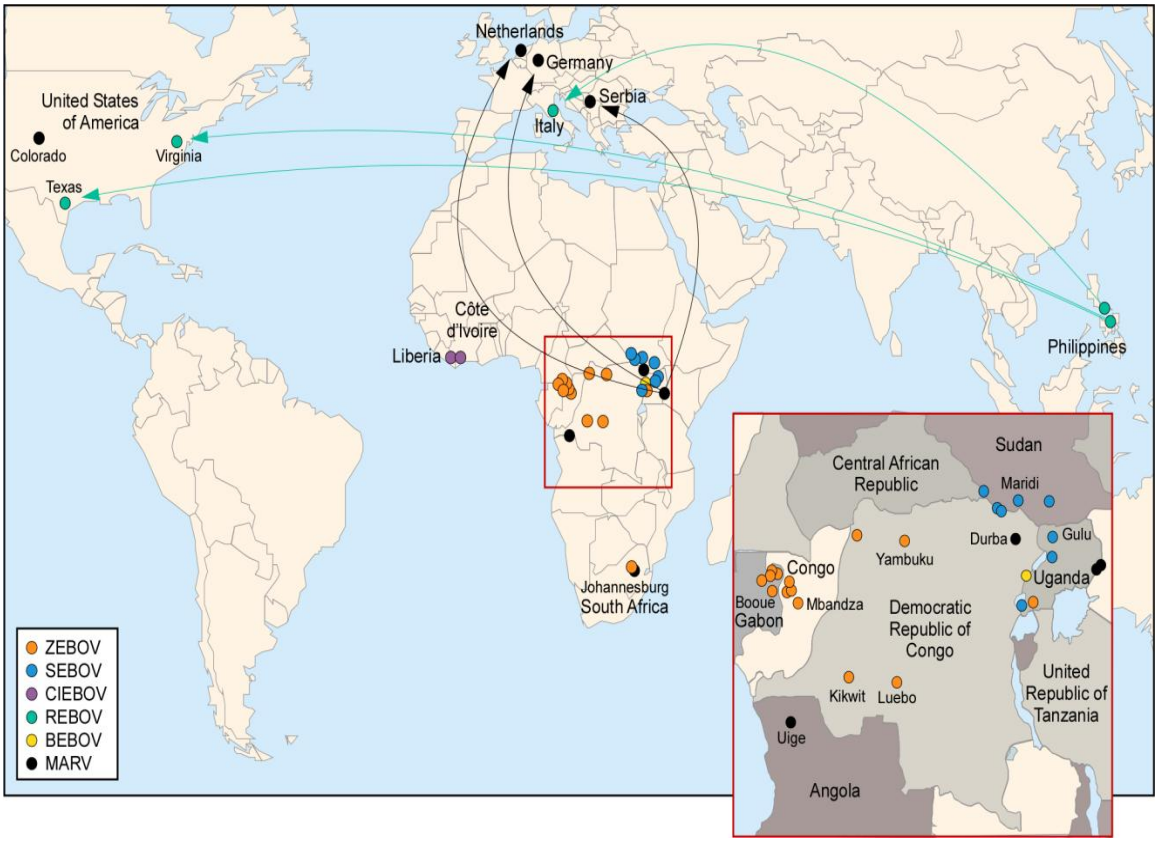

Figure 1. **Locations of filovirus outbreaks/episodes.** Ebola virus: *Zaire ebolavirus* (ZEBOV), *Sudan ebolavirus* (SEBOV), *Reston ebolavirus* (REBOV), *Cote de'Ivoire ebolavirus* (CIEBOV), and *Bundibugyo ebolavirus* (BEBOV) are shown in orange, blue, green, magenta, and yellow, respectively. Marburg Virus: *Lake Victoria marburgvirus* (MARV) is shown in black. REBOV epizootics occurred in nonhuman primate (NHP) facilities located at several places in the USA and in Italy, which were linked to importation of NHPs from the Philippines. MARV was discovered in 1967 in Germany and Serbia during an outbreak associated with NHPs imported from Uganda.

veterinarian was infected by a new EBOV species after performing a necropsy on a chimpanzee (Le Guenno et al., 1999). This new EBOV species, *Cote d'Ivoire ebolavirus* (CIEBOV), recently renamed *Tai Forest ebolavirus*, was isolated from both the chimpanzee and the veterinarian who had performed the necropsy (King et al., 2011; Kuhn, 2008). There were several EBOV outbreaks reported in Gabon and in Kikwit in the 1990s (Georges-Courbot et al., 1997; Kuhn, 2008); the frequency of outbreaks was higher in 2002 and 2003 in those areas (WHO, 2002, 2003a, b) than in subsequent years. In 2002-03, numerous dead chimpanzees, gorillas, and duikers were discovered and EBOV was isolated from a gorilla carcass, suggesting a potential cause for the decreasing gorilla and chimpanzee populations in DRC (Kuhn, 2008; Palacios et al., 2007). After the initial *Sudan ebolavirus* (SEBOV) outbreak in 1976, SEBOV remerged in 1979 and 2004 in southern Sudan, and in 2001 in Uganda (Kuhn, 2008).

Reston ebolavirus (REBOV), suspected to be the only EBOV that is nonpathogenic to humans but pathogenic to NHPs, was first isolated from a colony of cynomolgus macaques in Reston, Virginia, USA, that had been imported from the Philippines. Macaques from the Philippines were also identified as the source for two consecutive REBOV outbreaks that occurred in 1992 in Sienna, Italy and in 1996 in Alice, Texas, USA (Kuhn, 2008).

In 2007 a new EBOV species, *Bundibugyo ebolavirus* (BEBOV), was isolated during an EHF outbreak in Uganda (King et al., 2011; MacNeil et al., 2010; Towner et al., 2008). More recently, a tentative new filovirus genus, *Cuevavirus*, has been proposed after discovery of a distinct EBOV sequence, designated *Lloviu ebolavirus*, in dead insectivorous bats in Spain; however, this virus has yet to be isolated (Negredo et al.,

2011). A summary of confirmed filovirus outbreaks is presented in Table 1; Figure 1 shows the location of filovirus outbreaks.

1.2 Filovirus Classification

1.2.1 Virus Taxonomy

The family *Filoviridae* belongs to the order *Mononegavirales*, which includes all single-stranded negative-sense RNA viruses including the family *Bornaviridae*, *Rhabdoviridae*, and *Paramyxoviridae*. This *Filoviridae* family consists of two established genera, *Marburgvirus* and *Ebolavirus;* in addition, a new genus, tentatively named *Cuevavirus*, has been postulated (Kuhn et al., 2010) (Table 2). The *Marburgvirus* genus consists of only one virus species, *Lake Victoria marburgvirus*. In contrast, there are five virus species in the *Ebolavirus* genus: *Zaire ebolavirus*, *Sudan ebolavirus*, *Reston ebolavirus*, *Cote d'Ivoire ebolavirus* (current name *Tai Forest ebolavirus*), and *Bundibugyo ebolavirus* (King et al., 2011). The *Cuevavirus* genus has one species provisionally named *Lloviu ebolavirus;* however, this virus has yet to be isolated (Negredo et al., 2011).

1.2.2 Biohazard Classification

EBOV and MARV are considered highly lethal pathogens that have the potential to be misused in biowarfare programs or bioterrorist attacks (Becker, 2007). The Centers for Disease Control and Prevention (CDC) has designated EBOV and MARV as Category A agents that pose a serious threat to public health because of their ease of transmission and high mortality (Workgroup, 2000). These viruses are biosafety level

Family	Genus	Species
Filoviridae	*Marburgvirus*	*Lake Victoria marburgvirus*
	Ebolavirus	*Bundibugyo ebolavirus*
		Cote d'Ivoire ebolavirus (*Tai Forest ebolavirus*)
		Reston ebolavirus
		Sudan ebolavirus
		Zaire ebolavirus
	Cuevavirus (tentative)	*Lloviu cuevavirus* (tentative)

Table 2. **Taxonomy of *Filoviridae***.

(BSL) 4 pathogens; therefore, a high containment laboratory is mandatory in order to work with these viruses.

1.3. Filovirus Ecology, Natural Reservoir, and Transmission

Although EBOV and MARV are distributed throughout central Africa, ecological niche modeling shows differences in geographic distribution. MARV tends to be present in drier areas in eastern, south-central, and western Africa, while EBOV tends to be found in the humid rain forests of central and western Africa (Peterson et al., 2004; Peterson et al., 2006; Pinzon et al., 2005). Interestingly, similar climate conditions are present in the Philippines, where REBOV is endemic. Meteorological data have indicated that an increase in filovirus activity correlated with an unusual precipitation pattern (lower than average rainfall) from 1994-96 (Pinzon et al., 2004; Tucker et al., 2002). It has been suggested that ecological disruption due to various human activities such as agriculture, deforestation, hunting, military conflicts, and other changes in the ecosystem may play a role in filovirus outbreaks as all of these may bring humans in closer contact with the natural reservoir of filoviruses (Kuhn, 2008).

Initially, bats [*Tadarida (mops) trevori*] were thought to be a potential reservoir for filoviruses, because they were associated with the 1976 EBOV outbreak (Breman et al., 1999). NHPs were also suspected as a filovirus reservoir because many outbreaks directly involved contact with NHPs (Le Guenno et al., 1995), but experimentally infected animals show rapid lethal disease progression, a fact that against NHPs being an effective reservoir. Due to repeated association of filovirus outbreaks with gold mines, it was suspected that the reservoir host might be an animal found in or in close proximity to

natural or artificial caves (Bausch et al., 2006; Swanepoel et al., 1996). Recently, African fruit bats (*Rousettus aegypticus*) have been identified as a natural reservoir for MARV (Towner et al., 2007). Furthermore, thousands of small vertebrates have been collected during EBOV outbreaks in Gabon and DRC, but only fruit bats have been found positive for EBOV and MARV-specific antibodies (Abs). Epidemiological studies have demonstrated a direct link between migrating fruit bats and recent EBOV outbreaks in DRC in 2007 (Leroy et al., 2009). It has been shown that ZEBOV can replicate in infected fruits bats; however, virus antigen was detected only in endothelial cells of the lung tissue of a bat sacrificed on day 8 post-infection, but virus isolation was unsuccessful (Swanepoel et al., 1996). More recently the genome of a new, genetically distinct filovirus, Lioviu virus, has been sequenced from dead insectivorous bats in Cueva del Lloviu, Spain (Negredo et al., 2011).

Human-to-human transmission of EBOV does occur through direct contact with virus-contaminated body fluids such as blood, vomitus, urine, feces, breast milk, saliva, and respiratory secretions. Caregivers of infected patients are at high risk of infection and epidemiological studies have found that family members who are actively involved in patient care and burial procedures are at high risk of infection (Bray, 2003; Dowell et al., 1999; Sarwar et al., 2011). Despite the highest standards of protection, researchers working in high containment laboratories can and have been infected as a result of accidental needle sticks (Anthony Sanchez, 2007; Günther et al., 2011; Kortepeter et al., 2008).

1.4 Ebola Hemorrhagic Fever (EHF)

EBOV is one of the most severe hemorrhagic fever-causing viruses for humans, with case fatality rates as high as 90% (Leroy et al., 2011). Typically EHF starts with "flu-like" symptoms that rapidly develop into multi-organ failure, which is characterized by hepatic dysfunction, hemorrhages, capillary leakage, hypotension, and shock. Similar hemorrhagic symptoms were also reported in NHPs experimentally infected with ZEBOV, SEBOV, REBOV, BEBOV, and CIEBOV. However, REBOV appears to be asymptomatic in humans and only one symptomatic case of CIEBOV has been reported (Anthony Sanchez, 2007; Feldmann et al., 2003; Kuhn, 2008).

1.4.1 Disease Symptoms, Pathology, and Diagnosis

The incubation period of EHF is 4-16 (mean 7) days. Initial disease symptoms are frontal headache, weakness, arthralgia, and radiating myalgia in the cervical and lumbar muscles with increase of muscle rigidity. Spasms of the masseter and tremors in the head and arm have also been reported in severe cases. Other frequent symptoms are malaise, sore throat, fever, abdominal pain, upper respiratory tract symptoms (oral dryness, pharyngitis, glossitis, dry cough, and spastic sounds in the lung), and diarrhea. These symptoms in the initial phase (5-8 days) of the disease are nonspecific and are not consistent between individuals. Severe dysphagia and dyspnea develop in a minority of patients. After the initial phase, patients either recover slowly or progress into the second phase (organ phase) of the disease (Kuhn, 2008). This phase is characterized by a rash (not all cases) and severe cases present with hemorrhagic manifestations. Hemorrhagic symptoms may last 3-5 days and usually result in a fatal outcome (Kuhn, 2008).

Survivors during the 1995 ZEBOV outbreak experienced neither tachypnea nor massive blood loss (Kuhn, 2008). For survivors, the convalescent phase is usually long. Complete loss of appetite, profound prostration, and weight loss are common. Importantly, psychiatric sequelae, including confusion, anxiety, restlessness and aggressive behavior, have been reported. Asymptomatic EHF patients were reported in two outbreaks, in 1994 and 1996. Asymptomatic infections seem to be associated with early inflammatory responses and not genotypic changes in the causative virus (Leroy et al., 2000; Leroy et al., 2002).

EBOV pathology was studied in tissue samples from infected people who died in the 1976 and 1995 ZEBOV outbreaks in DRC. In these cases, cells of the reticuloendothelial systems, epithelial cells, and fibroblasts were found to be infected. The liver, kidneys, and lymph nodes were the major target organs. One unique observation, fatty degeneration of the liver, was described in particular in the 1976 ZEBOV outbreak. Focal necrosis of the hepatocytes and Kupffer cells throughout the lobes were observed in the liver. Pathology was also observed in kidneys, with moderate necrosis and calcification of the tubules (Kuhn, 2008; Murphy, 1978). Hematological changes, in particular thrombocytopenia, leukopenia, and later leukocytosis, were reported in ZEBOV infected patients (Kuhn, 2008). There was an increase in liver enzymes such as serum glutamic pyruvic transaminase (SGPT) and serum glutamic oxaloacetic transaminase (SGOT) in EHF patients (Formenty et al., 1999). Virus was also detected in skin and mucous membranes, adnexal structures, and cutaneous blood vessels (Peters, 1997). ZEBOV infection in NHPs showed a similar disease course to that seen in humans (Baskerville et al., 1978; Davis et al., 1997; Jaax et al., 1996; Johnson et al.,

1995). Because of the difficulties involved in obtaining human specimens, experimental NHP (rhesus and cynomolgus macaques, and AGMs) EBOV infections have provided most of the information available today on disease pathology (Ryabchikova et al., 1999). Most of the livers of infected NHPs were friable with an obvious reticulated pattern, periorbital dermis was seen with bilateral petechiae, and glandular stomach was seen with petechiae in mucosa/submucosa during necropsy (Davis et al., 1997). Histological findings indicated depletion, apoptosis, and necrosis of lymphoid cells in the lymphoid tissue. A significant congestion of the marginal zone sinuses was observed in the spleen. In addition, infection was obvious in the red pulp of the spleen due to the formation of huge aggregates of free virions, extensive fibrin deposition, and abundant necrotic cells (Davis et al., 1997). EBOV inclusions and virions were observed in circulating monocytes and macrophages in lymph nodes, spleen, liver, lung, skin, and lamina propria of the tongue and ileum (Davis et al., 1997).

Identification of EHF in tropical areas during the early phase of outbreaks is difficult because the clinical symptoms of EHF are similar to numerous tropical diseases such as shigellosis, meningococcal septicemia, relapsing fever, yellow fever, anthrax, malaria, typhoid fever, and rickettsial infections. However, the presence of a cluster of cases with a prodromal fever that turns into hemorrhagic diatheses with evidence of person-to-person transmission indicates the potential of a viral hemorrhagic fever (VHF). Importantly, EHF shows a characteristic rash (although not in every case) and disease progression seems more severe than with any other VHF (Anthony Sanchez, 2007; Grolla et al., 2005). Even though diagnosis of an individual suspect case for VHF outside the epidemic area is difficult, extensive testing and the patient's travel history are helpful for

diagnostics. Clinical diagnosis of EHF is typically confirmed at reference laboratories. Standard laboratory diagnostic samples are whole blood or serum; alternatively, urine, saliva, or oral swabs can be used. Viral genome detection using reverse transcriptase-polymerase chain reaction (RT-PCR) and viral antigen detection using enzyme linked immunosorbent assay (ELISA) are the most common diagnostic tests for acute infections. Antibody detection can be performed using ELISA, immunofluorescence assay (IFA), and immunoblotting. Antigen-capture ELISA, immunohistochemistry (IHC), and fluorescence assay can be used for virus detection in tissue samples. Virus isolation or visualization of viruses using electron microscopy are used as confirmatory diagnostic tests (Anthony Sanchez, 2007; Bray, 2009).

1.4.2 Treatment and Prevention

To date there are no effective treatments for EHF. During the 1995 ZEBOV outbreak, eight patients were treated with blood that had been donated by five survivors of the disease; seven of the treated patients survived. Although this indicates that blood transfusion has a beneficial effect, this claim was contested because these eight patients received better nursing than average patients and they had already survived 11 days before starting the treatment (Mupapa et al., 1999; Sadek et al., 1996; Sadek et al., 1999). Ribavirin, an antiviral drug shown to be useful in treating several other hemorrhagic fevers has not been effective against EBOV infections both *in vitro* and *in vivo* (e.g. NHP) (Huggins, 1989; Ignatyev et al., 2000). Equine IgG with high titer neutralizing Abs (EBOV specific) showed success in treatment of infected guinea pigs but not in NHPs; similarly, human interferon (IFN) treatment was effective in infected rodents but unsuccessful in the NHP model. It is assumed, due to the lack of success in NHP models

(Emond et al., 1977; Geisbert et al., 2010; Huggins et al., 1999; Jahrling et al., 1996), that these therapies have little likelihood of being effective in human patients. Transcription and replication inhibitors (e.g. RNA interference, antisense oligonucleotides) have shown success in both rodent and NHP models, but costs, the requirement for intravenous application, and sequence specificity might limit their therapeutic use (Feldmann and Geisbert, 2011; Geisbert et al., 2006; Geisbert et al., 2010; Warfield et al., 2006).

Treatment with recombinant nematode anticoagulant protein c2, a potent inhibitor of tissue-factor initiated blood coagulation, significantly increased the survival of EBOV infected NHPs. Survival was associated with decreased activation of coagulation and fibrinolysis, and dampened the expression of pro-inflammatory cytokines and chemokines, particularly interleukin-6 (IL-6) and monocyte chemoattractant protein-1 (MCP-1) (Geisbert et al., 2003a). U18666A, cholesterol inhibitor and a novel benzylpiperazine admantane diamide-derived compound that was identified through a screening library of small molecules, blocked EBOV transmembrane glycoprotein ($GP_{1,2}$)-mediated entry in an *in vitro* pseudotyped virus infection system (Carette et al., 2011; Côté et al., 2011). These studies identified a potential target, virus entry, for EBOV therapy. A recent study using antibody therapy demonstrated that an EBOV-specific polyclonal antiserum can protect NHPs from lethal ZEBOV challenge (Dye et al., 2012). A monoclonal antibody (MAb) with enhanced potency to bind the mucin-like domain of the EBOV glycoprotein has been generated as an immunoprotectant against EBOV for human use (Zeitlin et al., 2011). Phosphorodiamidate morphilino oligomers (PMOs), synthetic antisense oligonucleotide analogs, interfere in the translational process by duplex formation with RNA. The potency of neutrally charged PMO was enhanced by

the chemical modified version PMOPlus, which contain positively-charged piperzine groups along with the molecular backbone. PMOPlus targeting EBOV viral protein (VP)35 mRNA has protected mice (Swenson et al., 2009) and NHPs against EBOV challenge (Warren et al., 2010).

Developed countries have their own contingency plans to tackle not only imported cases but also laboratory exposures by proper isolation and intensive care units (Risi et al., 2010; Smith et al., 2006). In contrast, developing countries in Africa (EBOV endemic area) have minimum health-care support and a lack of personal protective equipment and sterile equipment for injection to prevent infection (Feldmann and Geisbert, 2011). It has been known that humans are accidental victims of EBOV infection due to an unknown exposure to the reservoir; therefore, there is no obvious strategy for preventing primary EBOV infection. However, early recognition of a cluster of cases and rapid intervention are currently the best practices for disease control because virus transmission occurs through close contact with infected individuals. This includes rapid identification of cases, isolation of patients using strict barrier nursing techniques, use of proper personal protective equipment, practicing proper medical procedures (according to professional health care protocols for contagious diseases) and proper burial management (Anthony Sanchez, 2007; Ascenzi et al., 2008; Kuhn, 2008).

1.4.3 Vaccine Development

Several animal models, including NHPs (rhesus and cynomolgus macaques, and AGMs) and rodents (mice, hamsters, and guinea pigs) have been used to study EBOV pathogenesis and some of them were used to test different vaccine platforms (Lupton et

al., 1980; Reed and Mohamadzadeh, 2007; Tsuda et al., 2011; Wang et al., 2006). Venezuelan equine encephalitis (VEE) virus replicon particles (VRP) based on an attenuated strain of VEE expressing EBOV $GP_{1,2}$, nucleoprotein (NP), VP24, VP30, VP35 or VP40 were shown to be protective in mice against lethal EBOV challenge (Olinger et al., 2005; Wilson et al., 2001; Wilson and Hart, 2001). Cynomolgus macaques were protected against EBOV challenge by a vaccination regime of DNA prime and adenovirus (AdV)-boost expressing ZEBOV GP— the first successful vaccine study in NHPs (Sullivan et al., 2000). Moreover, this DNA/ AdV platform for ZEBOV and SEBOV vaccination showed cross-protection in an NHP model against BEBOV challenge (Hensley et al., 2010). Vesicular stomatitis virus (VSV) has been used to make a live attenuated vaccine for EHF by expressing EBOV $GP_{1,2}$ instead of VSV glycoprotein (VSV/EBO-$GP_{1,2}$). This vaccine platform has demonstrated protection in both mice and NHP models against lethal EBOV challenge (Garbutt et al., 2004; Jones et al., 2005). Post-exposure use of this vaccine platform showed considerable protection in mice, guinea pigs, and NHPs (Feldmann et al., 2007). Despite success in both prophylactic and post-exposure treatment in the NHP model, the VSV-based platform has not yet been approved for humans because of safety concerns (Feldmann et al., 2007; Geisbert et al., 2008; Jones et al., 2005). A respiratory virus vaccine platform based on human parainfluenza virus 3 (HPIV3) expressing EBOV $GP_{1,2}$ or NP completely protected guinea pigs and partially protected NHPs against lethal EBOV challenge (Bukreyev et al., 2007; Bukreyev et al., 2006). However, pre-existing immunity in target populations might be an issue for HPIV3 and AdV-based vaccine platforms (Kobinger et al., 2006; Yang et al., 2008). EBOV virus-like particles (VLPs) (similar morphology to

authentic virus particle but replication incompetent), containing VP40 and $GP_{1,2}$ protect mice and NHPs following either intramuscular or intraperitoneal vaccination against lethal EBOV challenge (Feldmann and Geisbert, 2011; Warfield et al., 2003). Despite being safe, the VLP vaccine required booster immunizations for protection of NHP against lethal challenge, which might limit its use for emergency applications (Feldmann and Geisbert, 2011). Human trials have been initiated with DNA- and AdV-based vaccines. DNA vaccines expressing EBOV $GP_{1,2}$, NP or SEBOV $GP_{1,2}$ generated antibodies to at least one of the proteins when used in a recent human trial (Martin et al., 2006). Non-replicative recombinant AdV vectors expressing ZEBOV $GP_{1,2}$ and SEBOV $GP_{1,2}$ resulted in $CD4^+$ or $CD8^+$ responses in less than half of the vaccinated individuals. However, patients with pre-existing AdV Abs showed lower response rates and antibody titers (Ledgerwood et al., 2010; Martin et al., 2006).

1.5 EBOV Morphology and Structure

EBOV particles are predominantly filamentous in nature but U or 6-shaped or spherical particles can be found (Anthony Sanchez, 2007) (Figure 2A&B). Virus particles are composed of an internal helical nucleocapsid, an outer-unit membrane envelope, and a surface projection layer consisting of $GP_{1,2}$ spikes (Anthony Sanchez, 2007; Beniac et al., 2012) (Figure 2C). EBOV particles are approximately 80-90 nm in diameter and on average 900-1000 nm in length (Beniac et al., 2012; Bharat et al., 2012). Like other non-segmented negative-sense single-stranded (NNS) viruses the EBOV genome is also encapsidated by the NP. The NP-RNA complex assembles into the helical nucleocapsid with other viral proteins (Ruigrok et al., 2011)and serves as the template for genome replication (Bharat et al., 2012). Three proteins – NP, the minor matrix protein VP24, and

the polymerase cofactor VP35 – form the 50 nm diameter helical nucleocapsid (Huang et al., 2002). The VP24-VP35 heterodimer bridge holds the adjacent NP molecule horizontally (Beniac et al., 2012). VP30 is a component of the nucleocapsid by its interaction with NP, but it is dispensable for nucleocapsid formation. It has been suggested that it resides in the interior side of the nucleocapsids, not on the peripheral bridge (Beniac et al., 2012; Groseth et al., 2009; Huang et al., 2002). Interestingly, EBOV particles have shown extensive polyploidy, and in one instance 22 genome copies were observed in a viral particle. The filamentous shape may provide EBOV an advantage in disseminating in infected tissues by diapedesis of virus budding through epithelial layers (Beniac et al., 2012).

1.6 EBOV Genome

EBOV has a 18.9 kilobase (kb) long, NNS RNA genome with seven linearly arranged genes 3’ (leader)-NP-VP35-VP40-GP-VP30-VP24-L-(trailer) 5’ (Breman et al., 1999) (Figure 3). EBOV genes have conserved transcriptional start (3’CUC/ACUUCUAAUU) and stop signals [UAAUUCAAAAA(A)]. It has been reported that transcription starts exactly with the first nucleotide of the start signal and terminates at the consensus stop signal with a poly A-tail (Mühlberger, 2007; Muhlberger et al., 1996).

A. B. C.

Figure 2. **Morphology and structure of EBOV**. (A) Electron micrograph image of EBOV-infected Vero E6 cells showing virus budding out from the infected cell membrane; (B) Electron micrograph image of a single EBOV particle. Both images are kindly provided by Dr. Victoria Wahl-Jensen. (C) Schematic of an EBOV virion. The transmembrane glycoprotein ($GP_{1,2}$) forms spikes on the virion surface. The nucleoprotein (NP), viral protein (VP) 35, VP 30, and RNA-dependent RNA polymerase (L) form the ribonucleoprotein (RNP) complex together with the genomic RNA. VP40 and VP24 are the major and minor matrix proteins, respectively.

Gene overlaps have been observed between VP35-VP40, GP-VP30, and VP24-L. Short intergenic regions (IR) (varying in length and nucleotide composition) separate non-overlapping genes (NP-VP35, VP40-GP, and VP30-VP24) (Mühlberger, 2007; Sanchez, 2007) (Figure 3). The 3' termini of the EBOV genome (leader) is short (on average 50-70 bases), but the 5' termini of the genome (trailer) is variable in length. Interestingly, the extreme termini of the leader and trailer sequences are conserved, show greater complementarity, and are thought to form a secondary structure (stem-loop) (Sanchez, 2007; Sanchez et al., 1993). Each EBOV gene, except for the GP gene, codes for a single structural protein that is translated from a monocistronic mRNA. This mRNA sequence is the complementary copy of the negative-strand of the respective gene (Volchkov et al., 1999). Interestingly, the GP gene organization and expression is different because it contains an editing site (ES) (a hepta uridine stretch), which is conserved in all EBOV species. The ZEBOV RNA-dependent RNA polymerase (RdRP), L, edits the GP gene transcript at the ES, thus producing multiple proteins from the same gene (Sanchez, 2007).

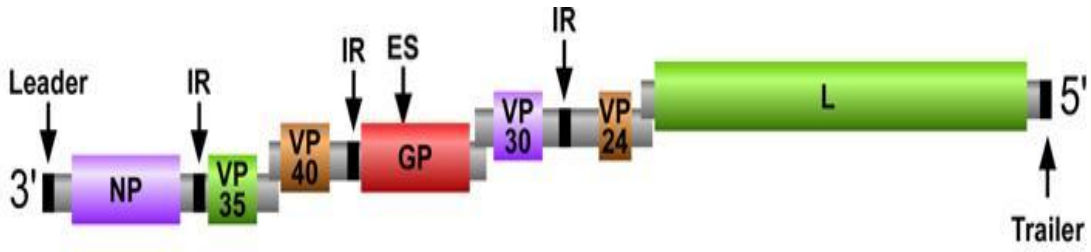

Figure 3. **Schematic illustration of the *Zaire ebolavirus* genome**. Seven genes are linearly arranged on the non-segmented negative-sense single-stranded RNA genome. All structural proteins are chronologically expressed from the 3' termini of the genome in the order nucleoprotein, NP; polymerase cofactor, VP35; matrix protein, VP40; transmembrane glycoprotein, $GP_{1,2}$; transcription activator protein,VP30; minor matrix protein,VP24; and RNA dependent RNA polymerase, L. The genome possesses non coding sequences at the 3' and 5' termini designated leader and trailer sequences, respectively. Genes are flanked by conserved start and stop signals, which overlap between genes VP35 and VP40, GP and VP30, VP24 and L. The non-overlapping genes are separated by intergenic region (IR) of variable length. The GP gene has an editing site (ES), which allows site-specific RNA editing to produce multiple proteins.

1.7 EBOV Life Cycle

1.7.1 Attachment and Entry

The EBOV $GP_{1,2}$ is a type 1 transmembrane glycoprotein that forms spikes on the virion surface, and mediates binding and entry into target cells (Elliott et al., 1985; Feldmann and Klenk, 1996). A definitive receptor for EBOV entry has not been identified; however, several cell surface proteins have been proposed as being involved in EBOV entry. $GP_{1,2}$ is highly glycosylated; therefore, it is proposed that $GP_{1,2}$ interacts with C-type lectins during the early stage of infection (Figure 4). A pseudotyped lentivirus expressing EBOV $GP_{1,2}$ showed enhanced entry via dendritic cell (DC)-specific intracellular adhesion molecule (ICAM)-3-grabbing non-integrin (DC-SIGN) or L-SIGN expressing non-permissive Jurkat cells (Alvarez et al., 2002; Simmons et al., 2003). DC-SIGN is a type II membrane protein with a C-type lectin extracellular domain, and it plays an important role in host cellular migration and immune response. L-SIGN is a homolog of DC-SIGN and it is expressed on the surface of endothelial cells in the liver, lymph node sinuses and placental villi (Alvarez et al., 2002; Bashirova et al., 2001). Although there has been experimental evidence of an interaction between the glycan cap or mucin-like domain of EBOV $GP_{1,2}$ with C-type lectins, deleting either of these domains did not reduce virus transduction efficiency. Therefore, it appears that C-type lectins act as an entry enhancement factor rather than as a specific cellular receptor that mediates virus entry (Hunt et al., 2012). Human macrophage galactose- and acetylgalactose-amine-specific C-type lectin (hMGL), which is expressed on the surface of immature DC and macrophages, was also identified as a potential factor for EBOV entry (Takada et al., 2004). Another endothelial cell surface protein, the lymph node

sinusoidal endothelial cell C-type lectin (LSECtin/CLEC4G), has been shown to interact with EBOV (Figure 4). Although LSECtin is similar to DC-SIGN, it recognizes only N-acetylglucosamine and not mannose or N-acetyl-galactosamine moieties (Dominguez-Soto et al., 2007; Gramberg et al., 2005). The β-integrin adhesion receptor on cells, a surface adhesion molecule involved in cell-cell adhesion, migration, proliferation, differentiation and apoptosis, has been identified as playing a role in EBOV entry (Arnaout et al., 2005; Takada et al., 2000). However, no direct interaction is evident between any part of $GP_{1,2}$ and a member of the β-integrin family of proteins (Hunt et al., 2012). Folate receptor-α (FR-α), a glycosyl-phosphatidylinositol-linked (GP_1-linked) protein that is highly conserved in many mammalian species, was identified as a co-factor in EBOV entry (Casillas et al., 2003; Lee et al., 1996). Similarly, three members of the Tyro3 family tyrosine kinase receptors (TAM) (i.e. Ax1, Dtk, and Mer), which are found on the plasma membrane of various cell types involved in cell migration and are highly conserved in different mammalian species, were reported to play a role in EBOV entry (Shimojima et al., 2006). Increased Axl expression on the cell surface increased EBOV entry via macropinocytosis but it is not considered an EBOV entry receptor due to insufficient evidence of direct interaction with $GP_{1,2}$ (Hunt et al., 2012). T-cell immunoglobulin and mucin domain-1 (TIM-1) expressed on mucosal epithelia from the trachea, cornea, and conjunctiva was proposed as an EBOV entry receptor. TIM-1 interacts with the mucin-like domain of $GP_{1,2}$ and this interaction is enhanced with removal of the glycan cap (Kondratowicz et al., 2011).

It has been suggested that EBOV may use multiple receptors (non-lectin) for attachment and internalization (Freeman et al., 2010; Miller and Chandran, 2012).

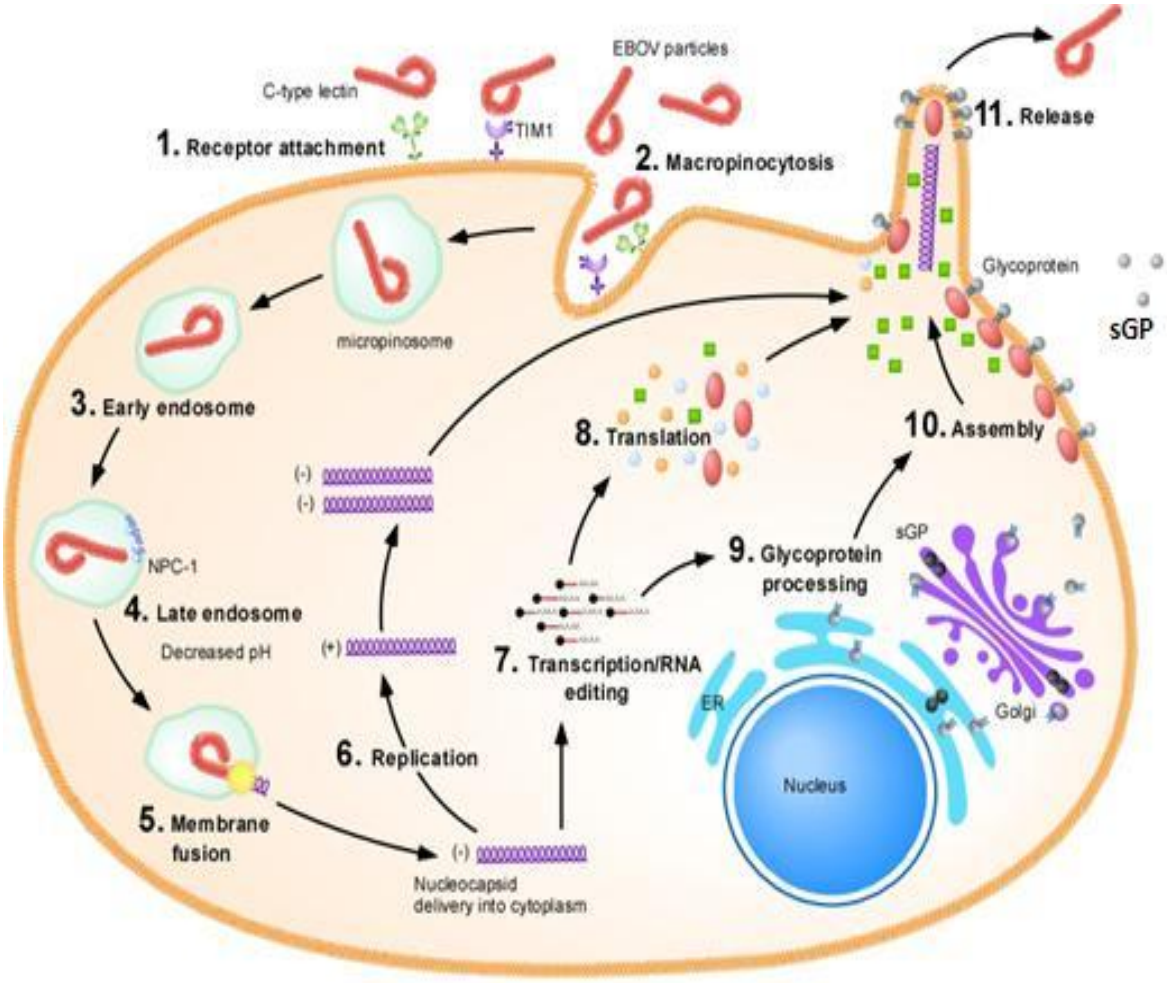

Figure 4. **EBOV life cycle.** 1. Interaction between $GP_{1,2}$ and the potential host cell receptor(s) or attachment factor(s) (such as C-type lectins and/or T-cell immunoglobulin and mucin domain 1) on the cell surface. 2. Entry via macropinocytosis. 3. Early endosome formation. 4. Trafficking to the late endosome and GP processing ($GP_{1,2}$ cleavage by endosomal cysteine proteases); potential interaction with Neuman-Pick type C1 (NPC1). 5. Late endosome/ lysosome fusion. Fusion releases encapsidated genome into the cytoplasm. 6. Replication generating complementary (+) strand RNA which serves as a template for the synthesis of (-) strand RNA. 7. Transcription of viral genes and co-transcriptional RNA editing at the GP gene editing site. 8. Translation. 9. Glycoprotein processed through endoplasmic reticulum (ER) and Golgi complex; non-structural soluble glycoprotein (sGP) secreted from the infected cells. 10. Assembly. 11. Progeny virion release.

Pseudotyped virus systems have been used for most of the studies characterizing entry; therefore, the roles of candidate molecules in entry have yet to be verified during EBOV infection.

It has been suggested that like most of the enveloped viruses EBOV enters cells by receptor-mediated endocytic pathways such as macropinocytosis, clatherin-mediated endocytosis, caveolin-mediated endocytosis, and clatherin- and caveolin- independent endocytosis (Conner and Schmid, 2003; Dolnik et al., 2008). Endocytic pathways depend on a large number of lipid rafts; and, different studies have confirmed the involvement of lipid rafts in entry using pseudotyped systems (Bavari et al., 2002; Empig and Goldsmith, 2002; Yonezawa et al., 2005). EBOV may enter different cell types using different entry mechanisms (Dolnik et al., 2008). A recent study showed that ZEBOV enters cells independently of clathrin, caveolae, and dynamin (Saeed et al., 2010). EBOV entry requires cholesterol in the cell membrane, and the uptake mechanism is related to macropinocytosis and this process seems $GP_{1,2}$ dependent (Nanbo et al., 2010; Saeed et al., 2010). In addition, several studies on EBOV entry also emphasized macropinocytosis as a virus internalization process because virions are too big to fit into smaller endocytic vesicles (Figure 4). However, virus uptake seems to be depend on $GP_{1,2}$ rather than virion size or morphology. Receptor-mediated binding potentially initiates macropinocytosis because macropinocytosis needs external stimulation to activate the signal cascade that induces alterations in the actin filament dynamics and triggers plasma membrane ruffling and blebs. This process results in the entrapment of large volumes of extracellular fluid. Interestingly, single membrane fission is adequate to close a macropinosome, which is regulated by a number of host factors (such as kinases) (Aleksandrowicz et al., 2011;

Mercer and Helenius, 2009; Miller and Chandran, 2012; Nanbo et al., 2010; Saeed et al., 2010).

A series of events during EBOV internalization in endosomes leads to viral membrane fusion, allowing the virus genome to be delivered into the cytoplasm. The fusogenic cleavage product GP_2 plays an important role in this process (Weissenhorn et al., 1998a). In the early stage of fusion, endosomal proteases, especially cysteine proteases (cathepsin L and cathepsin B), proteolytically cleave GP_1, generating a key 19 kilodalton (kDa) GP_1 intermediate. A third endo/lysosomal factor, thiol reductase, has an inhibitory effect on the cysteine proteases in a low pH environment, thus allowing fusion to occur in endo/lysosomal compartments (Chandran et al., 2005; Schornberg et al., 2006). Although several *in vitro* studies have shown that cysteine proteases contribute to EBOV $GP_{1,2}$ processing, their role for EBOV infection *in vivo* has yet to be confirmed (Miller and Chandran, 2012). In addition, cathepsin involvement in EBOV entry is cell-type dependent (Martinez et al., 2010). A more recent study confirmed that 19 kDa GP_1 binds to the lysosomal membrane and triggers fusion at low pH (Brecher et al., 2012). In addition, the cholesterol transporter, Neiman-Pick C1 (NPC1) has been identified as an EBOV entry factor. This has been confirmed independently by another group by using small molecule inhibitors (Carette et al., 2011; Côté et al., 2011). NPC1 is a multipass membrane protein localized to late endosomes and lysosomes that plays a part in lysosomal efflux of low-density lipoprotein-derived cholesterol. NPC1 contributes to EBOV genome release into the cytoplasm by initiating GP dependent fusion between viral and cellular membranes (Carstea et al., 1997; Côté et al., 2011; Miller and Chandran, 2012).

1.7.2 Transcription & Replication

After fusion of the viral and cellular endosomal membranes, the viral nucleocapsid is released into the cytoplasm. EBOV transcription and replication take place in the cytoplasm of the infected cell (Figure 4). Like other NNS RNA viruses, EBOV encodes its own RdRP. The RdRP recognizes the encapsidated RNA genome rather than naked RNA as a template for transcription and replication. Similar to other NNS RNA viruses, EBOV transcription is controlled by an inherent feature of polymerase entry at a single 3'-proximal site followed by compulsory sequential transcription of linearly arranged genes. The level of gene expression is controlled not only by gene position, but also by cis-acting sequences that are located at the beginning and the terminal region of each gene as well as the intergenic junction (Mühlberger, 2007; Whelan et al., 2004). EBOV transcription start signals are thought to form stable RNA secondary structures, which are involved in the VP30-driven regulation of early transcription (Mühlberger, 2007). EBOV replication requires a replicative intermediate, the RNA antigenome – a full length positive-sense genome that is encapsidated with NP produced during transcription. The viral polymerase then uses the antigenome as a template for progeny genome synthesis. The ribonucleoprotein (RNP) complex plays an important role in replication and transcription, including capping and polyadenylation (Mühlberger, 2007). EBOV NP and VP40 were shown to accumulate and form inclusion bodies during viral infection. These inclusion bodies are found in a highly organized region in the cytoplasm where viral morphogenesis occurs by assembling nucleocapsids for progeny virions (Kolesnikova et al., 2002; Ryabchikova and Price, 2004).

1.7.3 Budding

The order of sequential steps in EBOV budding are still unknown. However, two contrasting mechanisms have been proposed: a "submarine-like" budding and a "rocket-like" protrusion. Electron tomography of filovirus budding steps confirms that in the initial stage released infectious virus particles are filamentous, but that over time they change into spherical particles (Welsch et al., 2010). The matrix proteins of *Mononegavirales* have been shown to be the driving force for particle assembly and budding. Matrix proteins can interact with and polymerize at the cellular membrane and link other viral proteins to form the final shape and structure of virions (Figure 4). This ability to interact with multiple partners is dependent on conformational changes of the matrix protein. EBOV matrix protein, VP40, has an N-terminal oligomerization and C-terminal membrane binding domain that have a unique fold and are connected by a flexible linker (Dessen et al., 2000; Garoff et al., 1998; LENARD, 1996). N-terminal sequences of VP40 regulate the oligomerization in the lipid raft of the plasma membrane during the virus budding process (Panchal et al., 2003). VP40 is able to easily transition into a ring like structure (either an octamer or hexamer) due to its metastable conformation (Dolnik et al., 2008). Another EBOV protein, NP, has been shown to serve as the backbone of the nucleocapsids and plays a role in virus budding (Bray, 2009).

1.8 EBOV Pathogenesis and Evasion of Host Immune Response

EBOV targets antigen-presenting cells (APC) such as monocytes, macrophages and DCs for replication. Virus can spread into tissue macrophages in the liver, spleen, and other organs (Schnittler and Feldmann, 1998; Zaki and Goldsmith, 1999). It has been

speculated that uncontrolled elevation of host immune responses might contribute to the fatal outcome in EHF patients. Sequential blood samples from EBOV-infected patients during an outbreak in DRC in 1995 allowed scientists to study the serum cytokine profile. Fatal cases showed increased levels of IL-2, IL-10, IFN-γ, tumor necrosis factor (TNF)-α, and IFN-α compared to patients that survived (Villinger et al., 1999). A closer look at the immune response against EBOV infection was revealed by comparing the immune responses of survivors and of those who died from EHF during outbreaks between 1994 and 1996 in Gabon. During these outbreaks humoral and T-cell responses from the symptomatic patients showed that early and vigorous humoral responses against NP, VP35, and VP40 were associated with survival. In addition, cytotoxic cell activation was observed in patients at the recovery stage of disease. In fatal cases, responses were characterized by defective humoral responses and by early T-cell activation followed by T-cell apoptosis (Baize et al., 2002; Baize et al., 1999). Importantly, in fatal cases the immunological responses were disrupted by EBOV infection of APCs, which are key components of the innate and adaptive immune responses (Bosio et al., 2003; Geisbert et al., 2003c; Mahanty et al., 2003). EBOV infection of NHPs revealed that infected macrophages not only release cytokines and chemokines but also elevate the production of cell surface adhesion and procoagulant molecules, which increased endothelial permeability and destroyed endothelial cells. These events during infection probably contribute to hemorrhagic diathesis and shock (Geisbert et al., 2003c; Hensley et al., 2002; Stroher et al., 2001).

EBOV has several strategies to block cellular responses to type I IFN and multifunctional cytokines that regulate innate and adaptive immune responses (Cárdenas,

2010). In particular, EBOV VP35 blocks the initial steps in IFN production, thus inhibiting phosphorylation and activation of IRF regulatory factors- 3 and 7 (IRF-3 & 7), transcription factors responsible for orchestrating cellular antiviral programs (Barnes et al., 2002; Basler et al., 2003; Levy et al., 2002). EBOV VP24 also plays a role in immune evasion by inhibiting IFN signaling through the common Janus Kinase and signal transducer and activator of transcription (JAK-STAT) pathway. In particular, it blocks the interaction between phosphorylated STAT1 (PY-STAT1) and nuclear transport protein, karyopherin α-1, thus inhibiting nuclear translocation. Thus, VP24 has been shown to play an important role in the impairment of both type I and type II IFN signaling (Leung et al., 2006; Mateo et al., 2010). EBOV $GP_{1,2}$ has an immunosuppressive-like domain, which may be involved in host cell immune evasion (Volchkov et al., 1992). *In vitro* studies with EBOV VLPs showed that interaction between the $GP_{1,2}$ on VLPs and the toll-like receptor 4 (TLR4) resulted in the release of proinflammatory cytokines and suppression of cytokine signaling 1 (SOCS1) in a human monocytic cell line and a human endothelial kidney cell line (HEK293) stably expressing the TLR4/MD2 complex. It has been reported that SOCS1 regulates IFN-dependent pathways by not only reducing IFN-β production but also reducing STAT1 phosphorylation (Prêle et al., 2008).

1.9 EBOV Proteins

1.9.1 Nucleoprotein (NP)

NP is encoded by the first gene of the EBOV genome and encapsidates the viral genome via a hydrophobic domain present in the N-terminal region. It also serves as the

backbone of the nucleocapsids and plays a role in virus budding (Bray, 2009). A mutational study determined that the NP is important for virion capsid assembly and plays a major role in replication and transcription, along with VP24 and VP35 (Huang et al., 2002; Muhlberger et al., 1999). Structural studies have confirmed that NP, VP35, and VP24 are the main components required for the formation of a double layered nucleocapsid. VP35 and VP24 form the bridge (VP35-VP24 heterodimer) located on the periphery of the nucleocapsid that holds the NP molecules together horizontally. This not only proves that NP interacts independently with VP35 and VP24 but also implies that VP35 and VP24 can interact with each other and also interact with different sites on the NP (Beniac et al., 2012). Interestingly, both asymptomatic and symptomatic EHF patients showed a higher level of NP-specific antisera than that of sera against other EBOV proteins, such as VP40, VP35, and $GP_{1,2}$ (Baize et al., 1999; Leroy et al., 2000). As NP is the most abundant protein and antibodies are present in both survivors and fatal cases, antigen-capture ELISA based on NP is a commonly accepted method to rapidly detect EBOV antigen (Ikegami et al., 2003).

1.9.2 Viral Protein (VP)35

Similar to other NNS viruses, the EBOV second gene encodes a phosphoprotein (VP35) known as a polymerase cofactor (Cozelmann, 2004). VP35 shows similarities with other NNS phosphoproteins (Mühlberger et al., 1998). It is a 35 kDa protein, and constitutes nearly 25% of the virion protein content (Elliott et al., 1985). *In vitro* studies of EBOV nucleocapsid assembly confirm that VP35 is necessary, in combination with NP and VP24, for nucleocapsid formation (Beniac et al., 2012; Huang et al., 2002). VP35 has also been identified as an IFN antagonist that affects type I IFN gene activation by

inhibiting IRF-3 function (Basler et al., 2000). The IFN antagonistic function is dependent on its C-terminal IFN inhibitory domain (IID) that binds to dsRNA and interferes with dsRNA-dependent protein kinase R (PKR) activity; however, dsRNA binding-independent inhibition of IFN signaling has also been observed (Cárdenas et al., 2006; Feng et al., 2007; Schumann et al., 2009). VP35 is also identified as a potent inhibitor of RNA interference (RNAi), an innate antiviral response in mammalian cells (Haasnoot et al., 2007). VP35 also has an inhibitory effect on the IFN pathway that is regulated by PKR. By interfering with multiple IFN-mediated pathways, VP35 strongly facilitates virus spread and dissemination (Feng et al., 2007).

1.9.3 Viral Protein (VP)40

VP40 is the matrix protein based on its position in the genome, its hydrophobicity, and its abundance in the virion; however, it shares neither sequence nor structural homology with matrix proteins from other NNS RNA viruses (Bukreyev et al., 1993; Timmins et al., 2004). This abundant protein is the major part of the virion and underlies the virion envelope membrane where it plays an important role in maintaining the structural integrity of the virus particle. It is a multifunctional protein that associates with the cellular membrane and plays a major role in both virus particle morphogenesis and viral egress from infected cells (Feldmann and Klenk, 1996; Neumann et al., 2004; Ruigrok et al., 2000; Timmins et al., 2004; Timmins et al., 2001). VP40 has proline-rich motifs (both PPxY and PTAP) in the C-terminal domain that mediate the association with cellular proteins such as human neural precursor cell expressed developmentally down-regulated protein 4 (Nedd4) and tumor susceptibility gene 101 (Tsg101) (Harty et al., 2000; Licata et al., 2003; Yasuda et al., 2003). The VP40 N-terminal domain is

responsible for VP40 oligomerization. Analysis of the crystal structure of VP40 revealed the mechanism of its conversion from a monomeric conformation to a hexameric or octameric form. Four antiparallel homodimers (N-terminal domain) of VP40 form a disk-shaped octameric form, which supports RNA binding (Dessen et al., 2000; Gomis-Rüth et al., 2003; Ruigrok et al., 2000; Timmins et al., 2001). It has been shown that the VP40 octameric form is not crucial for VLP formation *in vitro*, but that RNA binding via the VP40 octameric form is important in virus morphogenesis (Hoenen et al., 2005). The coat protein complex II (COPII) transport system is used by VP40 for intracellular transport to the plasma membrane— this is evident by the interaction between a component of the COPII system, Sec24C, and VP40 (residues 303-307) (Yamayoshi et al., 2008). Co-expression of VP40 and $GP_{1,2}$ in mammalian cells results in the production of filamentous virus-like particles that resemble infectious EBOV particles. This may indicate that $GP_{1,2}$ and VP40 interact during virus infection (Bray, 2009; Noda et al., 2002). Interestingly, VP40 alone can mediate the production of filamentous VLPs (Bray, 2009; Jasenosky et al., 2001).

1.9.4 Viral Protein (VP)24

VP24 is a membrane-associated secondary matrix protein that may be involved in linking VP40 and $GP_{1,2}$ to the RNP. It is a 24 kDa hydrophobic protein and a minor component of the EBOV virion. VP24 has an association with the lipid membrane, and it localizes to the plasma membrane and perinuclear region in infected cells, suggesting that it may play a role in virus assembly and budding (Anthony Sanchez, 2007; Bray, 2009; Han et al., 2003). VP24 facilitates the assembly of functional nucleocapsid (Hoenen et al., 2006b). VP24 also plays an important role in host cell immune evasion as an IFN

antagonist by inhibiting IFN-α/β and IFN-γ signaling, thereby blocking nuclear accumulation of STAT1. VP24 specifically recruits the nuclear transport protein, karyopherin-α-1, blocking its interaction with tyrosine PY-STAT1, which impairs type I and type II IFN signaling (Leung et al., 2006; Reid et al., 2006). Interestingly, it has been shown that VP24 plays an important role in virus adaptation in mice (Bray et al., 1998; Ebihara et al., 2006) and guinea pigs (Volchkov et al., 2000).

1.9.5 Viral Protein (VP)30

The EBOV genome encodes several proteins necessary for transcription and replication. In addition to NP, VP35, and L, VP30 is a transcription factor, which is encoded by the fifth gene of the genome. Similar to pneumovirus M2-1, EBOV VP30 is a zinc-binding protein. Among the negative-sense RNA viruses these two viruses are unique in terms of requiring an additional factor for transcription and replication (Modrof et al., 2003; Mühlberger et al., 1998; Whelan et al., 2004). There have been several studies to characterize VP30-based transcriptional activation; however, the precise mechanism is not fully understood. Using a monocistronic minigenome assay, which is an artificial system for viral transcription and replication, it has been shown that VP30 regulates a very early stage of transcription, most likely early anti-termination. Importantly, VP30 dependent transcription is influenced by the RNA secondary structure formed by the promoter-proximal transcription start signal of the NP gene and a downstream-located sequence (Mühlberger, 2007). Similar to NP, VP30 binds to RNA (Bray, 2009). It contains an arginine-rich region (residues, 26-40) at the N-terminus that supports pH-dependent RNA binding (John et al., 2007). However, VP30 is not required for transcription reinitiation between genes at the internally positioned gene start sites

(Mühlberger, 2007; Weik et al., 2002). The oligomerization of VP30, mediated by hydrophobic amino acids at positions 94-112, is important for virus transcription, but phosphorylation negatively regulates transcription (Hartlieb et al., 2003; Modrof et al., 2002). Phosphorylation of VP30 is assumed to be a vital factor determining whether the protein regulates transcription activation or assembly. VP30 has two regions (a basic cluster around Lys180 and Glu197) that NP presumably interacts with, and these interactions might provide two different functions. The VP30 N-terminal domain mediates the interaction with the NP-RNA helical-coil structure; in contrast, the C-terminal domain mediates the interaction with NP-RNA nucleocapsid complexes, allowing transport to the assembly site and incorporation into virions (Hartlieb et al., 2007). It has been proposed that VP30 might regulate virus transcription activity, and may govern the balance between transcription and replication. However, increased VP30 concentration suppressed transcription (Ascenzi et al., 2008). In addition to its role as a transcription activator, VP30 is involved in nucleocapsid assembly and interacts with NP-derived inclusion bodies (Muhlberger, 2002).

1.9.6 RNA Dependent RNA Polymerase (L)

EBOV L is a large protein, that drives both transcription and replication with the help of other EBOV proteins (Volchkov et al., 1999). The EBOV L gene shows sequence similarity with other NNS L proteins, particularly MARV and certain paramyxoviruses. Importantly, they all have a 2'-O-ribose methyltransferase domain activity that mediates capping of viral mRNAs (Ferron et al., 2002). It has been reported that the RNA-GDP polyribonucleotidyltransferase domain is involved in L-mediated capping (Ogino and

Banerjee, 2007). The L protein also contains linear conserved domains that are common for L proteins of NNS RNA viruses (Volchkov et al., 1999).

1.9.7 Glycoproteins (GP)

The EBOV surface contains glycoprotein spikes, which are composed of the only transmembrane glycoprotein, expressed from the fourth gene in the genome. $GP_{1,2}$ is a major pathogenicity factor, as it mediates virus entry through receptor binding and membrane fusion (Takada et al., 1997). The EBOV GP gene contains a unique ES leading to the modulation of multiple transcripts through RNA editing. The most abundant transcript of the GP gene is unedited and encodes for a soluble glycoprotein (sGP) that is subsequently proteolytically cleaved into Δ-peptide and mature sGP (Figure 5). The less abundant transcript is edited by the insertion of an extra non-template adenosine (A) residue at the ES, resulting in a frame-shift allowing expression of $GP_{1,2}$ (Figure 5). The ratio of sGP to $GP_{1,2}$ specific transcripts is 4:1 (Sanchez et al., 1996; Volchkov et al., 1995).

1.9.7.1 Soluble Glycoprotein (sGP)

sGP is encoded from the unedited GP gene transcript, and is the most abundant GP gene product. Its signal peptide (SP) (first 1-32 aa) is cleaved by the cellular signalase. Furin cleavage results in the mature sGP and the carboxy-terminal cleavage fragment, Δ-peptide, a secreted peptide (Volchkova et al., 1999). sGP has been detected in the serum of infected humans (Sanchez et al., 1996; Volchkova et al., 1998). sGP is a homodimeric soluble protein that is arranged in a parallel orientation through intermolecular disulfide bonds between paired Cys53-Cys53’ and Cys306-Cys306’

residues. In addition, there are intramolecular-disulfide bonds between Cys108-Cys135 and Cys121-Cys147 within each monomer. A recent study has shown that ZEBOV sGP forms a structural complex with GP_1 (Iwasa et al., 2011). sGP is consistently post-translationally N-linked glycosylated at residues N40, N204, N228, N257, and N268 and infrequently at N238 (Falzarano et al., 2006; Sanchez et al., 1998; Volchkov et al., 1995). sGP is also C-mannosylated at residue W288 (Falzarano et al., 2007). It has been postulated that sGP potentially blocks EBOV-neutralizing antibodies (Kindzelskii et al., 2000; Yang et al., 1998). It has also been suggested that sGP potentially interferes with the innate immune response by binding to CD16b and inhibiting neutrophil activation (Kindzelskii et al., 2000; Yang et al., 1998); however, several studies could not confirm the finding (Maruyama et al., 1998; Sui and Marasco, 2002). In contrast to $GP_{1,2,}$ sGP did not induce macrophage activation nor did it increase the permeability of endothelial cells (Wahl-Jensen et al., 2005a; Wahl-Jensen et al., 2005b). A recent study showed that sGP counteracts the permeability-increasing effect of the pro-inflammatory mediator TNF-α, and thereby may interfere with leukocyte extravasation (Falzarano et al., 2006; Wahl-Jensen et al., 2005a).

1.9.7.2 Δ-Peptide

Δ-peptide is a secreted glycopeptide generated through proteolytic cleavage from the precursor sGP (cleaved by furin at the 324 aa position). The length of this protein (40-48 aa) varies depending on the EBOV species. It has a molecular weight of 10-14 kDa, which is higher than predicted due to post-translational processing, e.g. O-glycosylation and sialylation (Volchkova et al., 1999).

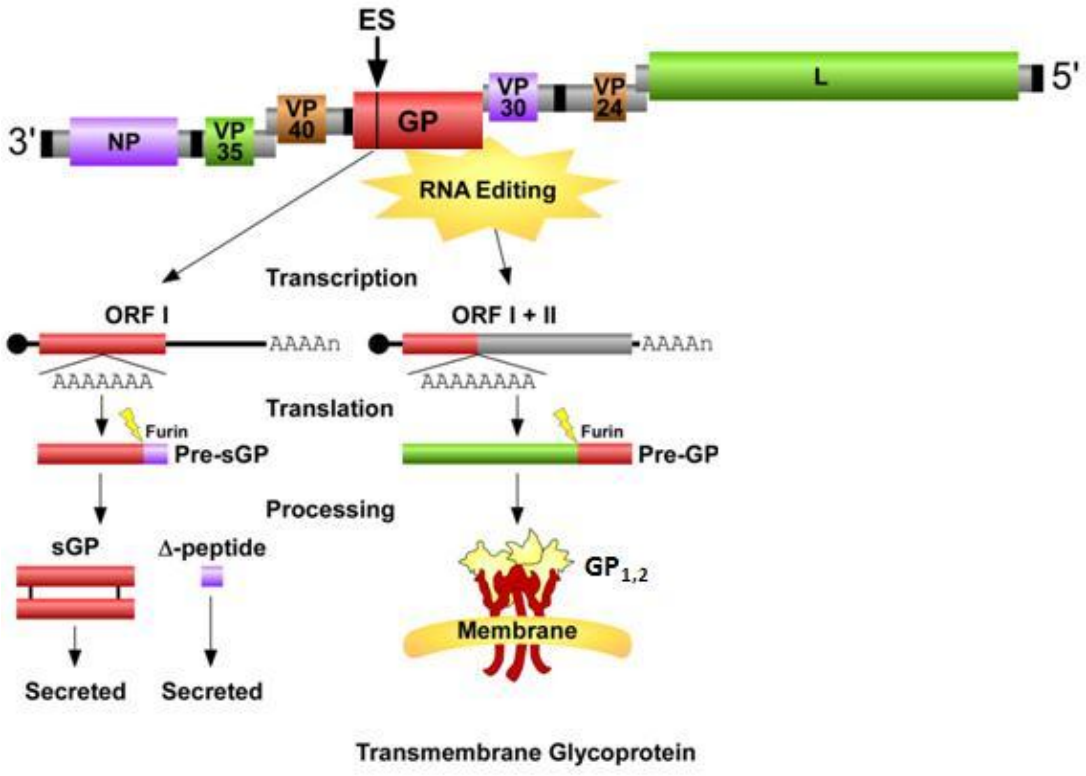

Figure 5. **Glycoprotein (GP) gene products**. GP gene has a conserved editing site (ES). During transcription the viral polymerase L edits GP gene-derived transcripts at the ES leading to multiple protein products. The majority of GP gene transcripts is unedited, and encode Pre-sGP that is proteolytic processed (signal peptide cleavage and furin cleavage) into the mature soluble glycoprotein (sGP) and the secretory Δ-peptide. Two monomeric sGP form a homodimer with parallel orientation. The transmembrane glycoprotein ($GP_{1,2}$) is expressed from the edited transcript as a precursor (Pre-GP) and cleaved by furin into GP_1 and GP_2 to form the trimeric surface glycoprotein (GP_1 and GP_2 disulfide-linked). This figure is adapted from (Falzarano, 2010) with permission.

There is no function identified for the Δ-peptide; however, it has been shown that Δ-peptide potentially inhibits virus entry as demonstrated by the use of pseudotyped retroviruses expressing either EBOV or MARV $GP_{1,2}$ (Radoshitzky et al., 2011).

1.9.7.3 Transmembrane Glycoprotein ($GP_{1,2}$)

The EBOV $GP_{1,2}$ is a class 1 viral membrane fusion glycoprotein, similar to the human immunodeficiency virus (HIV-1) envelope (Env) and the influenza virus hemagglutinin (HA) protein (Harrison, 2008; Lee and Saphire, 2009; Malashkevich et al., 1999; Weissenhorn et al., 1998b). $GP_{1,2}$ is processed from a precursor glycoprotein (PreGP) by furin cleavage, resulting in the 130-140 kDa N-terminal fragment GP_1 and a 24-26 kDa C-terminal fragment, GP_2. GP_1 and GP_2 are joined to one another by a disulfide bond to form a ~150 kDa heterodimer. This disulfide bond between Cys53 of GP_1 and Cys609 of GP_2 is formed before furin cleavage. PreGP also undergoes co- and post-translational modifications such as SP cleavage, N-glycosylation, and O-glycosylation and these glycosylations account for one third of PreGP's apparent molecular weight. $GP_{1,2}$ is transported to the cell surface using the classical endoplasmic reticulum (ER) pathway, where it remains anchored in the cell membrane by a hydrophobic domain in the C-terminus of GP_2 (Dolnik et al., 2004; Feldmann et al., 2001; Sanchez et al., 1998; Volchkov et al., 1995; Volchkov et al., 1998). $GP_{1,2}$ forms spike (a metastable non-covalently attached trimer of heterodimers) on the virion surface. The crystal structure of this protein has been resolved in an immune complex with the neutralizing MAb F_{ab} KZ52 (Lee et al., 2008; Sanchez et al., 1996; Sanchez et al., 1998). A putative receptor binding domain (RBD) is present in GP_1 (54-201 aa) (Kuhn et al., 2006). In this domain at least 19 residues have been found to be important for attachment

and entry (Brindley et al., 2007; Manicassamy et al., 2005; Mpanju et al., 2006). Recently, an HIV-based pseudotype system revealed that Arg64 and Lys95 are involved in receptor binding; it was also shown that Ile170 is important for viral entry but is not directly involved in receptor binding (Wang et al., 2011). While GP_1 attaches to the target cells, GP_2 is responsible for the fusion of viral and cellular membranes. GP_2 contains the internal fusion loop and heptad repeats (HR1 and HR2). The GP_2 ectodomain possesses coiled-coil and disulfide-bonded loops (Malashkevich et al., 1999; Weissenhorn et al., 1998a; Weissenhorn et al., 1998b). After entry, $GP_{1,2}$ is further cleaved by endosomal cathepsin L and B, resulting in the trimming of GP_1 at loop residues 190-213. Eventually the 450 kDa trimeric $GP_{1,2}$ forms a truncated product, a 39 kDa protein, consisting of trimmed GP_1 and the entire GP_2. These cathepsin cleavages expose the RBD on the remaining GP_1, which facilitates fusion of the viral and cellular membranes (Bale et al., 2011; Chandran et al., 2005; Dube et al., 2009; Schornberg et al., 2006). $GP_{1,2}$ is the major antigenic determinant of EBOV and it was found to initiate innate immune responses by inducing a pro-inflammatory response similar to that of lipopolysaccharides (LPS) and by suppressing SOCS1. SOCS1 is known for regulating IFN-dependent pathways by decreasing IFN-β production and STAT1 phosphorylation. Therefore, $GP_{1,2}$ is also involved in host cellular immune evasion (Martinez et al., 2007; Okumura et al., 2010; Prêle et al., 2008).

1.10 RNA Editing

Transcriptional editing or RNA editing is the process of alteration of a genome transcript during or after transcription. It results in alteration of the open reading frame (ORF). RNA editing was first discovered in the kinetoplastid protozoa, where insertion

and deletion of uridylates (Us) occurs in the mitochondrial pre-mRNA by a post-transcriptional process (Brennicke et al., 1999; Stuart et al., 1997). RNA editing mechanisms are diverse, ranging from nucleotide modification, such as cytidylates (C) to uridylates (U) and adenosines (A) to inosines (I) deaminations, to insertion of non-templated nucleotide(s). Although RNA editing may occur post-transcriptionally in prokaryotes (Brennicke et al., 1999), in viruses, especially paramyxoviruses' P genes, and in mitochondrial RNA editing of eukaryotes (e.g. *Physarum polycephalum*), it occurs co-transcriptionally (Brennicke et al., 1999; Hausmann et al., 1999a). The mechanism of *Physarum polycephalum* editing is rather complex and its specificity is unclear. Approximately 1000 different sites in its 60 kb genome have been found where single or dinucleotides of either C or U were inserted by RNA editing (Visomirski-Robic and Gott, 1997a, b). In contrast, paramyxovirus RNA editing is simpler and occurs in the P/V gene where only guanylate (G) residues are added at a defined 3'-U_nC_n-5' site. All the members of *Paramyxovirinae*, except human parainfluenza virus type-1 (HPIV-1), perform editing, also known as pseudo-template transcription, which was first described for Simian virus 5 (SV5) in the *Rubulavirus* genus. A genetically programmed insertion of G residues during transcription generates three distinct mRNA species with common ORFs located upstream and altered ORFs downstream of the ES. Paramyxoviruses use a stuttering process for RNA editing, which has been described by a competitive kinetic model (Cozelmann, 2004; Hausmann et al., 1999a; Kolakofsky et al., 1993; Kolakofsky and Hausmann, 1998; Thomas et al., 1988). Briefly, the RdRP stalls, probably due to changes in stability between the template–nascent strand hybrid at the vicinity of the editing sequence. As a result, the RdRP can go through one or more cycle of polymerase

and nascent strand realignment followed by template transcription. The number of cycles and the number of nucleotide insertions during this process are controlled by the ES sequence and cis-acting sequences (Whelan et al., 2004). Members of the *Morbilivirus* and *Respirovirus* genera and Newcastle disease virus (NDV) produce a genome-encoded P ORF from the P gene, but insertion of one G residue at the ES produces the V ORF (or D ORF for human parainfluenza virus type-3, HPIV-3). In contrast, members of the *Rubulavirus* genus encode a V ORF that is a faithful copy of the P gene, but insertion of two G residues at the ES encodes the P protein. Similarly, in members of the *Henipavirus* genus, V and W ORFs are produced from the P gene during transcription by inserting one or two G residues at the ES, respectively (Cozelmann, 2004; Hausmann et al., 1999a; Kulkarni et al., 2009). In contrast to paramyxovirus site-specific RNA editing (insertion of nontemplate G residue), RNA editing (base substitution) by the cellular editing enzyme adenosine deaminase acting on RNA (ADAR) has been observed in both the genomic and antigenomic RNA of Hepatitis Delta virus (HDV) (Casey and Gerin, 1995; Zheng et al., 1992).

1.10.1 EBOV RNA Editing

RdRPs of NNS RNA viruses share the ability to polyadenylate their mRNAs in response to specific template signals residing within the terminal sequences of genes (Whelan et al., 2004). RdRP-driven editing or pseudo-templated transcription has been observed in the paramyxoviruses, which is similar to polyadenylation in its mechanism. A similar editing phenomenon has been identified for EBOV. EBOV produces more than one transcript from the GP gene during transcription— one example of an efficient use of a small genome (Hausmann et al., 1999a; Robert A. Lamb, 2007; Whelan et al., 2004).

The unedited transcript encodes the sGP (Sanchez et al., 1996; Volchkov et al., 1995). $GP_{1,2}$ is only expressed following RNA editing, which occurs at a site of seven consecutive U residues (genomic sense), resulting in the insertion of an additional A residue in the transcript and a subsequent +1 shift in the extended ORF (Sanchez et al., 1996; Volchkov et al., 1995). In contrast, MARV, a distinct member of the same family, lacks the ES and produces only $GP_{1,2,}$ from unedited GP gene transcripts (Sanchez et al., 1996). Interestingly, a knockout of the ES in ZEBOV resulted in a significant increase in cytopathogenicity compared to wild-type virus, indicating the importance of RNA editing for EBOV replication (Alazard-Dany et al., 2006; Volchkov et al., 2001).

Cotranscriptional RNA editing has been well studied in the prototypic *Respirovirus,* Sendai virus (SeV), by determining cis-acting sequences that are involved in editing. Sequences in the conserved editing motif 3'-U_nC_n-5'as well as the upstream six nucleotides modulate the number of G residue insertions. Remarkably, specific alterations within the conserved motif sequence changed editing from a precisely controlled G residue insertion to an uncontrolled A residue insertion (similar to polyadenylation) (Cozelmann, 2004; Hausmann et al., 1999a; Hausmann et al., 1999b). Interestingly, all paramyxoviruses that show P gene editing, follows the "rule of six". This rule reflects the requirement for NP to bind six nucleotides in the encapsidated genome (Egelman et al., 1989). There is no evidence for the "rule of six" with EBOV; however, recent structural studies using cryo-electron tomography revealed that EBOV likely packages six RNA bases per copy of NP. Although it has been suggested that EBOV editing occurs co-transcriptionally as in paramyxoviruses, the EBOV RNA editing mechanism has not been characterized (Bharat et al., 2012; Calain et al., 1999;

Kolakofsky et al., 1998; Muhlberger et al., 1999; Whelan et al., 2004). The importance of cis-acting sequences upstream of the ES in the paramyxoviruses was demonstrated through mutational analysis (Kolakofsky et al., 1998), which also suggests that the viral RdRP can distinguish between editing and polyadenylation (Iseni et al., 2002). Similarly, it can be speculated that structural features (cis-acting sequences) and/or other viral factors contribute to EBOV RNA editing.

1.11 Objective and Hypothesis

1.11.1 Significance

EBOV is an enveloped, NNS RNA virus that causes severe hemorrhagic fever in humans and NHPs. EBOV is one of the most pathogenic communicable agents, with no approved treatment or prophylaxis; therefore, it is on the list of potential biological weapons. As such, EBOV is considered a high-priority (category A) pathogen (Becker, 2007). A better understanding of the virus biology is needed to discover novel intervention strategies. EBOV $GP_{1,2}$ is encoded by the GP gene and plays a major role in EBOV parthogenesis by dictating virus cell tropism, mediating virus entry, and being the major target of the host humoral immune response. On the other hand, EBOV sGP has been identified in abundance during infection, but a clearly defined function remains unidentified. EBOV utilizes a rare mechanism, single-site-specific RNA editing, to produce the structural $GP_{1,2}$ from the GP gene. Hypothetically, the insertion of different numbers of A residues would result in another yet unidentified gene product (Anthony Sanchez, 2007; Feldmann et al., 2001; Volchkov et al., 1995). Among NNS RNA viruses, RNA editing has previously only been described for the paramyxovirus phosphoprotein

(P) gene, where it regulates expression of important viral proteins with IFN-antagonistic functions. Therefore, a better understanding of the mechanism of EBOV RNA editing and the identification and characterization of all editing-driven viral proteins are of paramount importance and may lead to the identification of new viral targets for intervention therapy.

1.11.2 Hypotheses

This thesis is based on three related hypotheses:

1. EBOV produces an additional nonstructural protein as a result of RNA editing.
2. RNA editing is an inherent feature of all EBOV species.
3. RNA editing is regulated by cis-acting sequences and other viral factors.

1.11.3 Objectives

To test the hypotheses, the studies presented in this thesis are built on the following objectives:

1. To identify and characterize if an addiotnal glycoprotein produce through EBOV GP gene RNA editing.
2. To identify RNA editing as a shared mechanism of all members of the genus, *Ebolavirus*.
3. To determine the minimal structural requirements (cis-acting sequences) for EBOV RNA editing and identify potential viral factors involved in RNA editing.

1.11. 4. Justification.

RNA editing is one of the mechanisms for protein diversification, and consequently contributes to evolution (Gerber & Keller, 2001; Hajduk & Ochsenreiter, 2010). Viral structural proteins produced through RNA editing (i.e. EBOV $GP_{1,2}$ and the HDV large antigen, LDAg) play essential roles in virus life cycles (A. Sanchez, T. W. Geisbert, H. Feldmann, 2007; Shih, Chuang, Liu, & Lo, 2004). Similarly, viral nonstructural proteins produced through RNA editing have been shown to contribute to viral pathogenesis. For example, Nipah virus V and W play a role in host immune response evasion (Shaw, Cardenas, Zamarin, Palese, & Basler, 2005; Shaw, García-Sastre, Palese, & Basler, 2004). Detection and characterization of a new EBOV protein expressed through RNA editing would be a novel contribution to a better understanding of the EBOV life cycle. RNA editing is a rare mechanism that allows EBOV to increase its genome coding capacity— one example of how the virus efficiently utilizes its small genome. Interestingly, all EBOV species possess the conserved ES in the GP gene; however, RNA editing has only been described for ZEBOV, the type species of the Ebolavirus genus. Therefore, it remains unknown whether RNA editing is an inherent feature of all EBOV. Determining this might lead to a better understanding of EBOV pathogenesis. In contrast to the paramyxoviruses, the EBOV RNA editing mechanism has not been studied; therefore, we do not yet know what the structural requirements are and whether additional viral factor(s) are involved. Hence, another goal of this study is to characterize the EBOV RNA editing by determining the minimum structural requirements (e.g. cis-acting sequences) and additional viral factor(s) in this process. These studies might lead to the identification of new targets for therapeutic intervention.

2. MATERIALS AND METHODS

2.1 Cells and Media

2.1.1 Maintenance of Mammalian Cell Lines

Vero E6 (ATCC CRL-1586) (AGM kidney cell line), Huh7 (human liver cell line) and 293T (human embryonic kidney cell line) cells were cultured in Dulbecco's modified Eagle's Medium (DMEM) (Sigma-Aldrich) with high glucose, 10% (v/v) fetal bovine serum (FBS) (heat inactivated) (Invitrogen), 1% L-glutamine (2 mM) (Invitrogen), and 100 U/ml penicillin/ streptomycin (pen/strep) (100 ug/ml) (Gibco) under 5% CO_2 in a humidified incubator at 37^0C.

2.1.2 Isolation and Culture of Primary Human Cells

Whole venous blood was collected from healthy donors in accordance with a protocol approved by the Institutional Review Board for Human Subjects, National Institute of Allergy and Infectious Diseases (NIAID), National Institutes of Health (NIH). The blood was used to isolate human polymorphonuclear leukocytes (PMNs) and monocytes/macrophages. Human umbilical cord endothelial cells (HUVECs) were isolated from human umbilical cords, donated from local hospitals in Dresden, Germany, according to a previously established procedure under an approved local ethics protocol (Schnittler et al., 1990).

2.1.2.1 Primary Human Monocytes/Macrophages

A conical tube (50 ml) filled with 15 ml Ficoll-Paque plus (GE Healthcare) was slowly overlaid with EDTA blood without disturbing the interface. The tube was

centrifuged at 450 xg for 30 min at room temperature, followed by aspiration of the upper plasma layer without disturbing the buffy coat. The remaining cells were washed with phosphate buffered saline (PBS) twice (total 50 ml, centrifuged at 300 xg for 10 min), diluted in cold (4^0C) MACS buffer (Miltenyi Biotec) to $1x10^7$cells per 80 ul, and incubated with anti-CD14 magnetic beads (Miltenyi Biotec) (one-fifth of the cell volume) for 15 min at 4^0C. After incubation, cells were washed with 10 volumes of MACS buffer (centrifuged at 300 xg for 10 min). Cells were resuspended in MACS buffer to $1x10^8$ cells per 500 ul and applied to a prewashed MACS LS column (Miltenyi Biotec). The column was washed 3 times with 3 ml cold (4^0C) MACS buffer before elution. Elution of primary human monocytes was done into a 15 ml tube by removing the column from the magnetic field after addition of 5 ml cold (4^0C) MACS buffer using a plunger. Eluted cells were then centrifuged at 300 xg for 10 min and resuspended in warm (37^0C) Roswell Park Memorial Institute (RPMI) 1640 medium (Sigma) without human serum. $3x10^5$cells/well were seeded in a 24-well plate for incubation for 15-30 min at 37^0C. Medium was replaced with RPMI containing 10% AB human serum (heat inactivated) (Invitrogen). Human primary monocytes were maintained in RPMI with 10% AB human serum (heat inactivated), 1% glutamine, 1% pen/strep, and 1% non-essential amino acids (Invitrogen) under 5% CO_2 in a humidified incubator at 37^0C and differentiated into macrophages over several days.

2.1.2.2 Primary Human Neutrophils

Blood was collected using heparin tubes (BD Bioscience) (1 ml of 1000 U/ml heparin per 50 ml blood) and mixed 1:1 (v/v) with a sterile solution of 3% dextran and 0.9% NaCl for sedimentation. For sedimentation neutrophil isolation medium (35 ml

0.9% NaCl, 20 ml 1.7% NaCl, 12 ml Hypaque-Ficoll, and 20 ml distilled water) were prepared and disbursed into several 50 ml conical tubes. The top layer from the dextran-blood mixture was transferred into a fresh tube after 20 min sedimentation, and centrifuged immediately at 500-700 xg for 10 min at room temperature. The cell pellet was resuspended in 10 ml 0.9% NaCl, and 10 ml Ficoll was underlayed followed by centrifugation at 500 xg, with a low brake setting, for 17 min at room temperature. The cell pellet was resuspended in 20 ml distilled water, mixed by pipetting for 20-30 sec, centrifuged at 500 xg for 10 min at room temperature, resuspended in 20 ml 1.7% NaCl, and centrifuged again at 500 xg for 10 min at room temperature. Purified neutrophils were resuspended in RPMI medium with 10 mM 4-(2-hydroxyethyl)-1-piperazineethanesulfonic acid (HEPES).

2.1.2.3 Primary Human Umbilical Vein Endothelial Cells

Endothelial cells were isolated from the human umbilical cord using a previously established procedure (Schnittler et al., 1990). Briefly, the cord was rinsed in 70% ethanol, both ends were cut and a blunt end needle was inserted into the umbilical vein. The cord was stabilized with a sterile hemostat at one end and washed several times with pre-warmed (37^0C) PBS. After three washes the other end of the cord was clamped with a second sterile hemostat. Collagenase solution, containing 0.5 mg/ml collagenase II (Sigma) in PBS, was added to the vein and incubated for 12 min at 37^0C in PBS. The cord was washed with 70% ethanol followed by drying to remove residual ethanol. One end of the cord was cut just inside one of the hemostats to collect the collagenase solution in M199 complete medium (M119 with 10% FBS, 1% pen/strep, and 1% bovine lens growth factor) (Invitrogen). The cell suspension was centrifuged at 230 xg for 5 min at

23^0C, resuspended in 10 ml M199 complete medium, and transferred into a T25 tissue culture flask that was pre-treated with 0.5% porcine gelatin in PBS for 1 hr at 37^0C. Cells were maintained overnight in 5% CO_2 at 37^0C in a humidified incubator, washed in PBS to remove any erythrocytes, and incubated further in fresh M199 complete medium.

2.1.3 Bacterial Cells

Escherichia coli (E. coli) of the XL-1 Blue strain (genotype: *recA1 endA1 gyr96, thi-1 hsdR17 supE44 relA1 lac* [*F'proAB* lac^q *ZΔM15 tn10* (tet^r)]) were used for all cloning procedures unless otherwise stated. To prepare competent cells, 0.5 ml of an overnight culture was added to 50 ml of LB-Lauria/Lenox (0.5% NaCl) broth (LB) and propagated under shaking at 37^0C until an optical density of 0.5-0.8 at 600 nm was reached. Cells were incubated for 20 min on ice, centrifuged at 2500 xg for 10 min at 4^0C, and resuspended in transformation storage solution (TSS) buffer [85% LB, 10% polyethylene glycol, 5% dimethyl sulfoxide (DMSO) and 50 mM $MgCl_2$]. Cells were stored as 50 ul aliquots at -80^0C.

2.2 Virus Infection

2.2.1 Virus Strains

ZEBOV prototype strain Mayinga, ZEBOV strain Kikwit, mouse-adapted ZEBOV (MA-ZEBOV) strain Mayinga (Bray et al., 1998), SEBOV strain Boniface, REBOV strain Pennsylvania, CIEBOV, and BEBOV were used in this study.

2.2.2 *In Vitro* Infection

Vero E6 or Huh7 cells (approximately 90% confluent) were infected with ZEBOV strain Mayinga (this prototype strain was used for all infectious work unless otherwise stated) using an multiplicity of infection (MOI) of 1 and incubated for 1 hr at 37^0C. Subsequently, medium was replaced and cells were maintained in Opti-MEM (Invitrogen) at 37^0C for the appropriate time period.

Vero E6 cells ($3x10^5$) were also infected separately with ZEBOV strain Mayinga, SEBOV, REBOV, CIEBOV, and BEBOV using an MOI of 0.1. Infected cells were maintained in DMEM with 1% FBS at 37^0C.

Monocyte-derived macrophages ($3x10^5$) were infected separately with ZEBOV strain Mayinga, SEBOV, REBOV, CIEBOV, and BEBOV using an MOI of 0.1. Infected cells were maintained in RPMI with 10% AB human serum at 37^0C.

2.3 Cloning and Site-directed Mutagenesis

2.3.1 Recombinant ssGP (r.ssGP) and Recombinant sGP (r.sGP) Expression Plasmids

Recombinant expression of both ssGP and sGP were done with or without an N terminal tag using mammalian expression plasmids. For tagged proteins, the ORF for ZEBOV ssGP without its SP was amplified by two-step RT-PCR from purified ZEBOV vRNA. Briefly, in the first step (cDNA synthesis) 3 ul RNA (50 ng/ul), 1 ul 10 mM deoxyribonucleotide triphosphate (dNTP) mix, 1ul 50 uM forward primer (Appendix 1A), and 12 ul RNAse free water were mixed and incubated at 65^0C for 5 min followed by the addition of 5 ul 5x First-strand buffer (Invitrogen), 1 ul 0.1 M dithiothreitol (DTT), 1 ul 25 mM Mg_2Cl_2, 0.5 ul RNAseOUT (40 U/ul) (Invitrogen), and 0.5 ul SuperScript III

(200 U/ul) (Invitrogen) and incubated at 55^0C for 60 min. 2 ul of this first-strand reaction was used for PCR amplification in the second step using sequence-specific primers (Appendix 1A). A PCR reaction mix was prepared with 10 ul 5x HF iProof reaction buffer (Bio-Rad), 1 ul 10 mM dNTP mix, 1 ul 10 mM forward primer, 1 ul 10 mM reverse primer, 1 ul 25 mM Mg_2Cl_2 , 1 ul DMSO, 0.5 ul HF iProof DNA polymerase (2 U/ul) (Bio-Rad), and 32.5 ul of sterile distilled water. The thermal cycling conditions were programmed for an initial denaturation at 98^0C for 30 sec, followed by 30 cycles of a 10 sec denaturation at 98^0C, a 15 sec annealing at 65^0C, and an extension step with 1 kb/minute at 70^0C, followed by a final extension at 72^0C for 7 min. In this way, PCR fragments for both putative forms of ssGP (ssGP6A and ssGP9A containing 6A and 9A residues at the ES, respectively) were generated this was followed by cloning into the eukaryotic expression plasmid, pDISPLAY (Invitrogen) (pDISPLAY-ssGP6A and pDISPLAY-ssGP9A) using BglII and PstI restriction sites. This plasmid is known to direct the expression of foreign glycoproteins through a vector-specific SP and adds an N-terminal HA-tag. r.sGP expression was achieved using the expression plasmid, pDISPLAY-sGP (Wahl-Jensen et al., 2005a), which was kindly provided by Dr. Victoria Wahl-Jensen. For untagged proteins, the ssGP (ssGP9A, this form was used in further experiments unless otherwise stated) and sGP ORFs with their authentic SPs were generated by PCR amplification using the method described above. These PCR amplified products were then cloned into a different eukaryotic expression plasmid, pCAGGS (Appendix 3A) (Niwa et al., 1991) (pCAGGS-sGP and pCAGGS-ssGP) using EcoRI and XhoI restriction sites.

2.3.2 Cys53 Mutated r.ssGP

The amino acid, cysteine (Cys) at position 53 in the ssGP was mutated into glycine (Gly) using a protocol similar to that provided by the site-directed mutagenesis kit (Strategene). Briefly, the mutagenesis PCR reaction mix consisted of 1 ul DNA template (pDISPLAY-ssGP) (50 ng/ul), 10 ul 5x HF iProof reaction buffer, 1 ul 10 mM dNTP mix, 1.25 ul 125 ng/ul forward primer, 1.25 ul 125 ng/ul reverse primer, 1 ul 25 mM Mg_2Cl_2, 1 ul DMSO, 0.5 ul HF iProof DNA polymerase (2 U/ul), and 32.5 ul of sterile distilled water. The thermal cycle conditions were programmed for an initial denaturation at 98^0C for 30 sec, followed by 16 cycles of a 10 sec denaturation at 98^0C, a 15 sec annealing at 70^0C, and an extension step with 1 kb/min at 72^0C.

2.3.3 Minigenome

The GP gene ORF was inserted into the published ZEBOV minigenome plasmid by replacing the chloramphenicol acetyltransferase (CAT) reporter gene (Muhlberger et al., 1999). The minigenome contains the ZEBOV genome leader [the entire 3'nontranslated region (NTR) of the NP gene] (472 nt) and trailer [the entire 5'NTR of the L gene] (731 nt) sequences, and was kindly provided by Dr. Hideki Ebihara. For this, the minigenome plasmid was altered at two nucleotide positions in order to remove BsmB1 sites using site-directed mutagenesis allowing the insertion of the GP gene using the BsmB1 sites. The GP minigenome was rescued as described later (Figure 6).

A truncated GP gene minigenome was created by introducing 110 nt of the ZEBOV GP gene [covering the conserved ES with 45 nucleotide (nt) up- and 58 nt downstream] instead of the GP ORF into the minigenome plasmid. Similarly, a truncated

L gene minigenome was created by introducing 110 nt of the ZEBOV L gene (covering the ES-like sequence with 45 nt up- and 58 nt downstream) into the minigenome plasmid.

The recombinant plasmids, pCAGGS-NP, pCAGGS-VP30, pCAGGS-VP35, and pCAGGS-L containing the ORFs for ZEBOV NP, VP30, VP35, and L, respectively, and pCAGGS-T7 expressing the T7 bacteriophage polymerase were used in minigenome rescues. The plasmids were kindly provided by Dr. Hideki Ebihara.

2.3.4 Dual-reporter Minigenome

The sub-cloning plasmid, pATX-MCS (Appendix 3B) was used for generating a dual-reporter cassette. First, 110 nt of the GP gene (described earlier) was cloned into the pATX-MCS. The ORF for the enhanced green fluorescent protein (eGFP; without stop signal) was introduced upstream of the 110 nt using sequence-specific primers with BsmB1 sites (Appendix 1B). Similarly, the ORF for a second fluorescent reporter (red fluorescent protein, mCherry, without start and stop signals), was introduced downstream of the 110 nt. At the C-terminus of the mCherry ORF, two nuclear localization signals (NLS) were introduced. To test the expression of the two reporter genes from the dual-reporter cassette prior to cloning it into the minigenome plasmid, the whole cassette (eGFP-110 nt-mCherry-NLS) was introduced into an expression plasmid pCAGGS using SacI and NheI restriction sites. For a control, an edited version of the GP gene ES containing dual-reporter cassette (eGFP-111 nt-mCherry-NLS) was generated by introducing an additional A residue into the ES, followed by cloning into the same expression plasmid. Finally, the dual-reporter cassette with the wild-type ES (eGFP-110 nt-mCherry-NLS) was cloned into the ZEBOV minigenome plasmid (Figure 7).

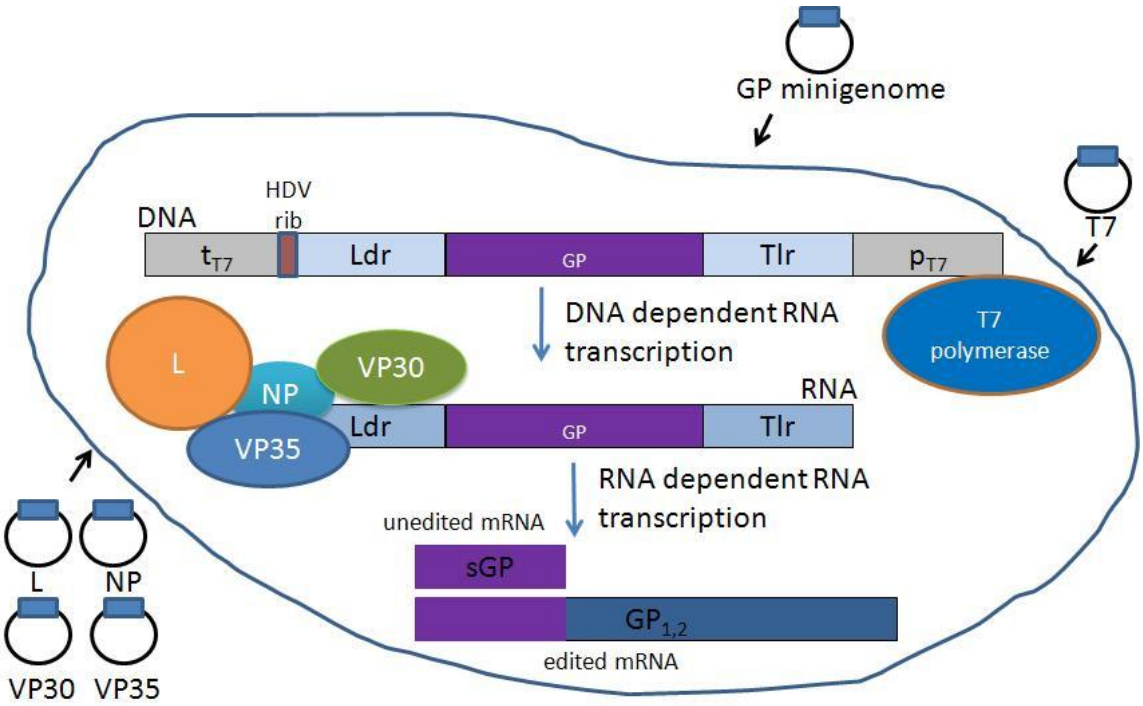

Figure 6. **GP minigenome rescue.** The GP gene ORF was cloned between the ZEBOV leader (Ldr), the entire 3' nontranslated region (NTR) of the NP gene and the trailer (Tlr), the entire 5' NTR of L gene. This (Ldr-GP gene ORF-Tlr) is then flanked by the T7 polymerase terminator (t_{T7}) and promoter (p_{T7}) in the ZEBOV minigenome plasmid. Rescue was done by transfecting cells with multiple plasmids [the minigenome plasmid, the helper plasmids expressing ZEBOV NP, L, VP30, or VP35 for a functional ribonucleoprotein (RNP) complex, and the T7 polymerase for DNA-dependent RNA transcription from the minigenome plasmid]. T7 driven transcription provides genomic sense of the GP minigenome cassette (Ldr-GP gene ORF-Tlr). The hepatitis delta virus ribozyme (HDV rib) sequence driven cleavage provides the authentic leader sequences allowing binding of the reconstituted ZEBOV RNP complex for RNA-dependent transcription of the GP gene generating multiple transcripts [here sGP (unedited) and $GP_{1,2}$ (edited)].

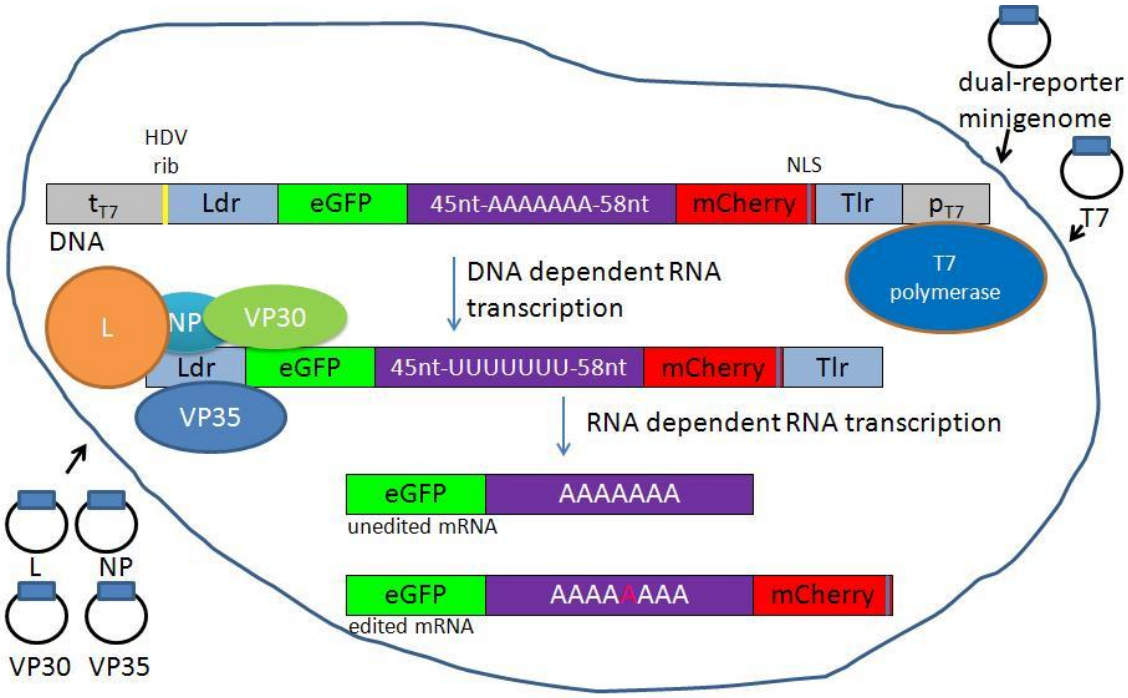

Figure 7. **Dual-reporter minigenome rescue.** The dual-reporter cassette (eGFP-110 nt-mCherry-NLS) was introduced between ZEBOV leader (Ldr), the entire 3' nontranslated region (NTR) of the NP gene and the trailer (Tlr), the entire 5' NTR of L gene. This (Ldr-eGFP-110 nt-mCherry-NLS-Tlr) is then flanked by the T7 polymerase terminator (t_{T7}) and promoter (p_{T7}) in the ZEBOV minigenome plasmid. Cells were transfected with multiple plasmids (minigenome plasmid; helper plasmids expressing ZEBOV NP, L, VP30, and VP35 for a functional RNP complex, and T7 polymerase for DNA-dependent RNA transcription of the minigenome). T7 driven transcription provides genomic sense of the dual-reporter cassette (Ldr-eGFP-110 nt-mCherry-NLS-Tlr). The hepatitis delta virus ribozyme (HDV rib) sequence driven cleavage provides the authentic Ldr allowing RNA-dependent RNA transcription of the reporter genes through the functional ZEBOV RNP complex. During transcription multiple transcripts are produced (unedited and edited) due to RNA editing.

2.3.5 Mutations and Deletions in the Dual-reporter Minigenome

The third or sixth A residue of the GP gene ES in the dual-reporter minigenome plasmid was independently mutated to a G residue using site-directed mutagenesis (Figure 8A). Multiple deletions were introduced into the up- and downstream sequences of the ES in the dual-reporter minigenome as outlined in Figure 8A using PCR-driven technology.

Furthermore, point-mutations were introduced at the leader sequence (the entire 3' NTR of the NP gene; Ldr) of the dual-reporter minigenome plasmid using site-directed mutagenesis (Appendix 1C) to destabilize the predicted secondary structure (stem-loop) formed by nucleotides 56-78 (genomic sense) (Weik et al., 2002) (Figure 8B).

Two potential stem-loops were observed in the upstream sequence (45 nt) of the ES using the RNA secondary structure prediction available at the mfold webserver (http://mfold.rna.albany.edu/?q=mfold) (Zuker, 2003). The first potential stem-loop is formed by the first 24 nt (1-24 nt, plus sense), whereas the second potential stem-loop is formed by the end of the sequence (38- 45 nt, plus sense). Using the XRNAmute webserver (http://www.cs.bgu.ac.il/~xrnamute/XRNAmute) (Churkin et al., 2011) three point mutations (C3T, A18G, and G24T) were introduced using site-directed mutagenesis that were predicted to destabilize the putative stem-loop formed by first 24 nucleotides (Figure 8A). Subsequently, two different combinations of mutations (5'38GA and 39GA or 5'G39A and C44T) were introduced into the predicted second stem-loop for destabilization (Figure 8A).

A.


Truncated GP gene (110 nt)
CCCGAAATTGATACAACAATCGGGGAGTGGGCCTTCTGGGAAACTAAAAAAACCTCACTAGAAAAATTCGCAGTGAAGAGTTGTCTTTCACAGTTGTATCAAACGGAGCC
Mutated ES (3rd A to G)
CCCGAAATTGATACAACAATCGGGGAGTGGGCCTTCTGGGAAACTAAGAAAACCTCACTAGAAAAATTCGCAGTGAAGAGTTGTCTTTCACAGTTGTATCAAACGGAGCC
Mutated ES (6th A to G)
CCCGAAATTGATACAACAATCGGGGAGTGGGCCTTCTGGGAAACTAAAAAGACCTCACTAGAAAAATTCGCAGTGAAGAGTTGTCTTTCACAGTTGTATCAAACGGAGCC
9 nt upstream deletion
GATACAACAATCGGGGAGTGGGCCTTCTGGGAAACTAAAAAAACCTCACTAGAAAAATTCGCAGTGAAGAGTTGTCTTTCACAGTTGTATCAAACGGAGCC
18 nt upstream deletion
-ATCGGGGAGTGGGCCTTCTGGGAAACTAAAAAAACCTCACTAGAAAAATTCGCAGTGAAGAGTTGTCTTTCACAGTTGTATCAAACGGAGCC
27 nt upstream deletion
TGGGCCTTCTGGGAAACTAAAAAAACCTCACTAGAAAAATTCGCAGTGAAGAGTTGTCTTTCACAGTTGTATCAAACGGAGCC
45 nt upstream deletion
-AAAAAAACCTCACTAGAAAAATTCGCAGTGAAGAGTTGTCTTTCACAGTTGTATCAAACGGAGCC
13 nt downstream deletion
CCCGAAATTGATACAACAATCGGGGAGTGGGCCTTCTGGGAAACTAAAAAAACCTCACTAGAAAAATTCGCAGTGAAGAGTTGTCTTTCACAGTTGT
22 nt downstream deletion
CCCGAAATTGATACAACAATCGGGGAGTGGGCCTTCTGGGAAACTAAAAAAACCTCACTAGAAAAATTCGCAGTGAAGAGTTGTCTTT
31 nt downstream deletion
CCCGAAATTGATACAACAATCGGGGAGTGGGCCTTCTGGGAAACTAAAAAAACCTCACTAGAAAAATTCGCAGTGAAGA
49 nt downstream deletion
CCCGAAATTGATACAACAATCGGGGAGTGGGCCTTCTGGGAAACTAAAAAAACCTCACTAG
58 nt downstream deletion
CCCGAAATTGATACAACAATCGGGGAGTGGGCCTTCTGGGAAACTAAAAAAAC-
45 nt up- and 58 nt downstream deletion
-AAAAAAA--
3 mutations to destabilize stem-loop at 1-24 nt
CCTGAAATTGATACAACAGTCGGTGAGTGGGCCTTCGGGAAACTAAAAAAACCTCACTAGAAAAATTCGCAGTGAAGAGTTGTCTTTCACAGTTGTATCAAACGGAGCC
2 mutations to destabilize stem-loop at 38-45 nt
CCCGAAATTGATACAACAATCGGGGAGTGGGCCTTCTAAGAAACTAAAAAAACCTCACTAGAAAAATTCGCAGTGAAGAGTTGTCTTTCACAGTTGTATCAAACGGAGCC
2 mutations to destabilize stem-loop at 38-45 nt
CCCGAAATTGATACAACAATCGGGGAGTGGGCCTTCTGAGAAATTAAAAAAACCTCACTAGAAAAATTCGCAGTGAAGAGTTGTCTTTCACAGTTGTATCAAACGGAGCC

B.

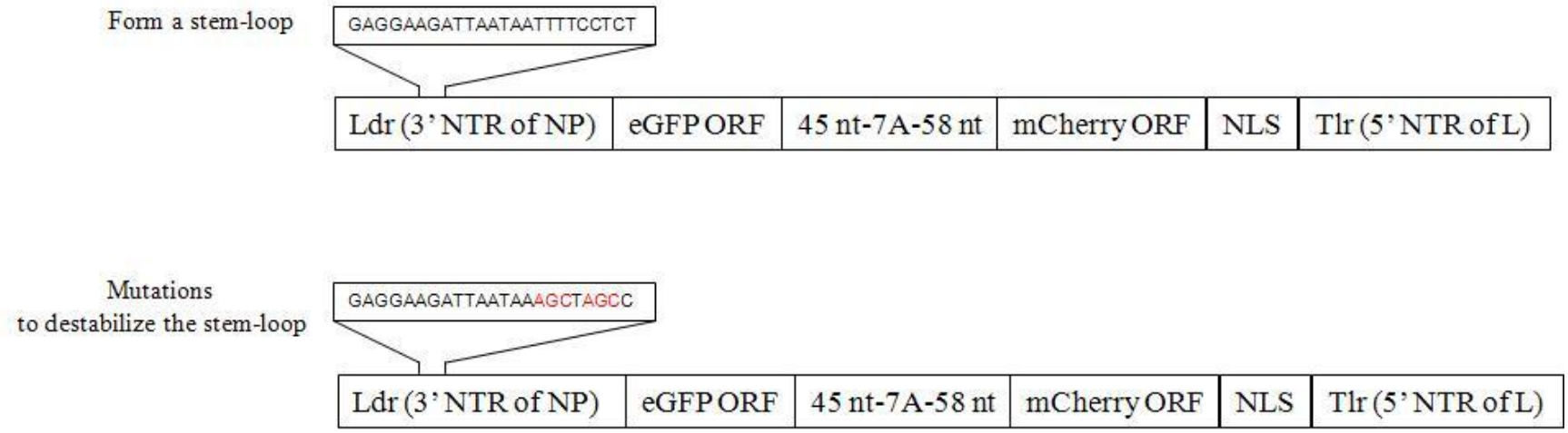

Figure 8. Mutations and deletions in the dual-reporter minigenome. A. Scheme of the deletions and point mutations (in red) in the truncated GP gene dual-reporter minigenome plasmid. Green is showing the nucleotide sequences form secondary structure (stem-loop) (predicted) **B.** Scheme of the mutations (in red) introduced into the leader (Ldr) sequence [the entire 3' nontranslated region (NTR) of the NP gene] (bottom image) to destabilize the predicted stem-loop at this region (56-78 nt; nt numbers are refer to the genome sequence of ZEBOV and sequence are shown in DNA sense) (top image) in the dual-reporter minigenome plasmid.

For control purposes, a T7 polymerase driven plasmid was generated for expression of the two reporters by introducing the dual-reporter cassette (eGFP-110 nt-mCherry-NLS) into the pTM1 vector (kindly provided by Dr. Thomas Hoenen) using EcoRI and XhoI restriction sites.

All constructs were verified by sequencing either at the Research Technology Branch, Rocky Mountain Laboratories (RML), Hamilton, MT, USA or the DNA Core Facility, National Microbiology Laboratory, Winnipeg, Canada.

2.4 r.ssGP and r.sGP Production

293T and Vero E6 cells were seeded in T150 tissue culture flasks so that they were 80% confluent the next day. Cells were transfected with plasmids pDISPLAY-HAtag-sGP/ssGP and pCAGGS-sGP/ssGP using FuGENE6 (Roche). Briefly, 3.8 ml Opti-MEM, 114 ul FuGENE6, and 38 ul DNA (1 ug/ul) were mixed and incubated for 30 min at room temperature. Cell culture medium was replaced with 16 ml Opti-MEM prior to adding the transfection mix at room temperature, followed by incubation at 37^0C. Supernatants from the transfected cells were collected 72 hr post-transfection (this time-point was used for all experiments unless otherwise stated) and centrifuged at 5000 xg for 15 min to remove residual cell debris. The anti-HA affinity matrix (Roche) was equilibrated with buffer supplied by the manufacturer (Appendix 2A). Subsequently, the supernatant was mixed with the HA affinity matrix and incubated overnight at 4^0C under shaking in a 50 ml tube. The solution was added onto the column (Roche) and washed a minimum of three times with the provided wash buffer (Appendix 2A). For elution of the bound HA-tagged protein, 1 ml of HA peptide (American Peptide Company; thawed

prior to use) was added to the matrix and incubated for 30 min at 37^0C without shaking. The matrix was added onto the column and the HA-tagged protein was collected in the flow-through (this step was repeated twice). The HA-matrix was reused for purification of the same protein according to manufacturer's instructions using regeneration buffer (Appendix 2A).

Purified proteins were concentrated with an Amicon Ultra 4 (Milipore) using a molecular weight cut-off (MWCO) of 30 kDa. The concentrations of purified proteins were determined by the DC-protein assay (Bio-Rad). Proteins (r.ssGP and r.sGP) were aliquoted and stored at -20°C.

2.5 ssGP Transcript Detection

Vero E6 or Huh7 cells were infected with ZEBOV strain Mayinga at an MOI of 1. Total cellular RNA was extracted 4 days post-infection using Trizol LS reagent (Invitrogen). ZEBOV GP cDNA was synthesized from extracted total RNA using a GP-specific oligo-dT primer (ACCGGTTTTTTTTTTTTTT) with SuperScript III (described in 2.3.1). Subsequently, a fragment covering the GP gene ES was amplified using GP sequence-specific primers (Appendix 1D) and high-fidelity Taq DNA polymerase (Roche). The amplified 330 bp PCR fragment was purified using the QIAquick PCR purification kit (QIAGEN) and cloned into TOPO TA 2.1 PCR cloning vector (Invitrogen) using One Shot Top10 chemically competent *E. coli* cells (Invitrogen) and SOC medium (Invitrogen). These transformed cells were plated on LB agar containing X-gal (Invitrogen) and incubated overnight for blue-white colony screening. The white bacterial clones were sequenced to determine the ratios of GP gene-specific transcripts encoding for sGP, $GP_{1,2,}$ and ssGP.

For *in vivo* confirmation, mice were infected intraperitoneally with 200 ul of MA-ZEBOV [100 plaque forming unit (PFU)]. Animals were euthanized 4 days post-infection, and liver samples were collected. RNA was extracted from liver tissue using the RNeasy kit (QIAGEN). Extracted RNA was utilized to determine the ratio of the GP gene transcripts using the same strategy as described above for the *in vitro* procedure.

To determine heterogeneity at the ES in genomic RNA, Vero E6 cells were infected with ZEBOV at an MOI of 1. Virus was harvested 4 days post-infection and RNA was extracted for RT-PCR analysis. Instead of an oligo-dT primer, a genome RNA specific primer (AGAGTAGGGGTCGTCAGGTCC) that binds upstream of the GP gene was used for cDNA synthesis; the subsequent amplified GP gene editing region (330 bp) (described above) was sequenced to determine the ratio of distinct vRNA templates in virus particles.

To control for Taq DNA polymerase errors during amplification as the source for the introduction of non-template A residue(s) at the ES, a synthetic positive sense RNA (AUAGAAUUCUCGGGGAGUGGGCCUUCUGGGAAACUAAAAAAACCUCACUAGAAAAAUUCGCAGUGAAGAGUUGUCGAAUUCCGU) (Thermo Fisher Scientific) was synthesized and used as the template for RNA amplification. The product was cloned and sequenced as described earlier.

2.6 Protein Analysis

EBOV sGP and ssGP are predicted to be processed similarly and nearly identical in size. Therefore, several methods were applied to first verify expression either from

transfected or infected cells and second to distinguish both proteins in the absence of specific (discriminating) antibodies.

Tissue culture supernatants from transfected and/or infected cells were centrifuged at 2,000 xg for 10 min at room temperature to remove cell debris. In the case of viral infection, supernatants were further centrifuged at 21,000 xg for 30 min at room temperature to remove viral particles. The clarified supernatants were concentrated with an Amicon Ultra-4 (30 kDa MWCO), and if derived from EBOV infections were inactivated with sodium dodecyl sulfate (SDS) (final concentration 1%) and boiling (10 min). Similarly, for detection of sGP and $GP_{1,2,}$ supernatants from Vero E6 cells infected with representative strains of all EBOV species using an MOI of 0.1 were harvested 4 days post-infection. Supernatants were first centrifuged at 1000 rpm for 10 min to remove cells. Supernatants were concentrated using an Amicon Ultra-4 (10 kDa MWCO) at 10,000 rpm for 15 min. Cell pellets were also collected and inactivated by the above mentioned SDS (final concentration 2%) & heat treatment. To simplify separation of glycoproteins (sGP and ssGP), proteins were treated overnight with N-glycosidase F (PNGaseF) (New England Biolabs, NEB) to remove all N-linked carbohydrates from glycoproteins (see below).

2.6.1 Removal of Carbohydrates

PNGaseF removes all N-linked glycans from glycoproteins, whereas endoglycosidase H (Endo H; NEB) specifically removes high-mannose type N-linked carbohydrates. To efficiently remove O-linked glycans, proteins were treated with O-glycanase (endo-α-N-acetylgalactosaminidase) (Iwase and Hotta, 1993) in combination

with different exoglycosidases [sialidase A, β(1-4)-galactosidase, β-N-acetylglucosaminidase, and N-glycanase] (Prozyme). All digestions were performed for 3 hr (except PNGaseF) according to the manufacturer's instructions. Briefly, 9 ul of protein solution was denatured in 10x denaturing buffer (NEB) for 10 min at 99^0C followed by overnight incubation at 37^0C in a reaction mix containing 2 ul 10x G7 buffer, 2 ul 10x NP40, 2 ul of enzyme (PNGaseF) (NEB), and 4 ul distilled water. Deglycosylated proteins were analyzed by SDS-polyacrylamide gel electrophoresis (SDS-PAGE).

2.6.2 SDS-PAGE

SDS-PAGE under either reducing (addition of β-mercaptoethanol) or non-reducing conditions were used to separate proteins (i.e. r.sGP, r.ssGP, with or without HA-tag and sGP, ssGP, and $GP_{1,2}$). For this, proteins were mixed with 4x SDS loading buffer and boiled for 10 min. SDS-PAGE gels were prepared at the appropriate concentration (10–15% separating gels; 4% stacking gel) (Appendix 2F) and proteins were loaded. Gels were run for 2 hr at 120 volt (V). For detection, proteins were transferred to polyvinylidene difloride (PVDF) membranes.

2.6.3 Two Dimensional (2-D) Gel Electrophoresis

To better discriminate proteins of similar biochemical characteristics and size, 2-D gel electrophoresis was applied. For this, supernatants from transfected (for r.ssGP and r.sGP) and ZEBOV infected (MOI of 1.0) (for ssGP and sGP) Vero E6 cells were desalted using a 2-D Clean-Up Kit (GE Healthcare) and resuspended in 2-D rehydration buffer (7 M Urea, 2 M thiourea, 2% CHAPS). Protein samples (15 ug) were loaded onto a 7 cm pH 4-7 NL immobilized pH gradient (IPG) strip (GE Healthcare) using the

following treatment profile: 15 hr 30 V passive rehydration, 0.2 kilo volt hour (kVh) stepped to 300 V, 0.3 kVh gradient to 1000 V, 4.5 kVh gradient to 5000 V, 3 kVh stepped to 5000 V. The IPG strip was equilibrated for 15 min in equilibration buffer (75 mM Tris-HCl pH 8.8, 6 M urea, 30% glycerol, 2% SDS, and 0.002% bromophenol blue) containing 1% w/v DTT followed by 15 min in equilibration buffer containing 2.5% iodoacetamide (IAA). The IPG strip was applied on a 12% Bis-Tris gel (Invitrogen). The gel was transferred to a PVDF membrane using the iBlot dry blotting system (Invitrogen).

2.6.4 Protein Detection

PVDF membranes were blocked overnight with 5% skim milk in PBS followed by antibody incubation. For HA-tagged proteins (r.ssGP and r.sGP), membranes were incubated for 1 hr at room temperature with a 1/10,000 dilution of anti-HA-peroxidase (Roche). For untagged proteins (r.ssGP, r.sGP, ssGP, sGP, and $GP_{1,2}$) membranes were incubated with a 1/10,000 dilution of mouse MAb 42/3.7 (anti-$GP_{1,2}$/sGP/ssGP) (kindly provided by Dr. Ayato Takada) followed by a 1/10,000 dilution of goat anti-mouse IgG conjugated with peroxidase (H+L) (KPL). Protein visualization was done with the ECL Plus Western blotting detection kit (GE Healthcare).

2.6.5 2-D Difference Gel Electrophoresis (2-D DIGE)

2-D DIGE was used to better separate proteins of similar biochemistry and size. Secreted proteins derived from transient expression in 293T cells (r.ssGP, r.sGP) as well as from infected Vero E6 cell (MOI of 1) supernatants (ssGP & sGP) were labelled with fluorescent CyDyes (Cy3 = r.ssGP, Cy2 = r.sGP, and Cy5 = supernatant from ZEBOV

infected Vero E6 cells) (Appendix 10A) following the procedures described in the Ettan DIGE system user manual (GE Healthcare). Briefly, 50 ug of protein sample was incubated with 400 picomole (pmol) of dye for 30 min, followed by a 10 min lysine quench (1 ul of 10 mM lysine). The labelled samples were mixed and incubated in an equal volume of 2x 2-D sample buffer (7 M Urea, 2 M thiourea, 4% CHAPS, 130 mM DTT, 1% IPG buffer) for 10 min at room temperature. After reduction, samples were brought to a volume of 450 ul with 1x 2-D sample buffer (7 M Urea, 2 M thiourea, 4% CHAPS, 65 mM DTT, 0.5% IPG buffer). Isoelectric focusing (IEF) (first dimension) was performed using 24 cm pre-cast IPG strips (GE Healthcare) with a linear pH range of 3-10 as described above for 2-D electrophoresis. The strip was then directly applied to a 10% isocratic SDS-PAGE gel for electrophoresis at 15°C overnight at 2 W/gel with a maximum current setting of 400 mA using the Ettan DIGE unit (GE Healthcare). The gels were scanned while still in the glass plates on a Typhoon 9400 scanner (GE Healthcare) at absorption wavelengths of 489 nm, 550 nm, and 649 nm and emission wavelengths of 506 nm, 570 nm, and 670 nm for Cy2-, Cy3-, and Cy5-labeled proteins, respectively. Resolution was set to 100 microns, sensitivity = 450-600 V.

2.6.6 Mass Spectrometry

Mass spectrometry was used to distinguish between sGP (r.sGP) and ssGP (r.ssGP) based on the prediction that formic acid digestion of ssGP (r.ssGP) would generate a unique shorter terminal peptide than that of sGP (r.sGP) (Appendix 5). Freshly made 2% formic acid (200 ul) was used for protein digestion at 108^0C for 2 hr and peptide detection was done by nanoflow liquid chromatography-electrospray ionization-tandem mass spectrometry (nanoLC-ESI-MS/MS) (QSTAR, AB-Sciex). Before digestion

and mass spectrometry analysis a reduction/alkylation step was performed. Briefly, protein (i.e. 20 ug r.ssGP) in a NH_4HCO_3 solution (Appendix 2B) was added onto a 3 kDa MWCO filter tube (pre-washed with 100 ul 100 mM NH_4HCO_3 solution) and centrifuged at 11,200 xg for 30 min followed by two in-column incubation steps; first, 100 ul 100 mM DTT solution at 37^0C for 1 hr, followed by 100 ul 65 mM iodoacetamide (IAA) solution at room temperature for 30 min in the dark. After this treatment the column was centrifuged at 11,200 xg for 30 min followed by a wash-step using 100 ul 100 mM NH_4HCO_3 solution (centrifuged at 11,200 xg for 1 hr). Similarly, formic acid in-gel digestion of purified protein (r.ssGP) was done. Briefly, proteins were separated on 10% reducing SDS-PAGE gel and visualized by Coomassie staining. The gel was washed several times with distilled water; the corresponding piece was cut and mixed with 600 ul 100 mM NH_4HCO_3 and 400 ul acetonitrile, followed by short spin to settle the gel piece at the bottom of the tube. The gel piece was washed two times with 200 ul acetonitrile, followed by treatment with 600 ul 100 mM NH_4HCO_3 for 5 min at room temperature, 400 ul acetonitrile for 10 min at room temperature and a wash with 200 ul acetonitrile to remove the Coomassie stain. Following the reduction/alkylation step, formic acid digestion was done as described above. The samples were vacuum-dried for storage. The samples were diluted and applied to the nanoLC-ESI-MS/MS according to the standard protocol (QSTAR, AB-Sciex) at the Proteomics Core Facility, National Microbiology Lab, Winnipeg, Canada. Spectra analysis and peak assignment was performed with in house software. A targeted MS/MS was utilized for focusing the peptide of interest [the data acquisition software was restricted to look for intense peptide (2^+ and 3^+ ions) in a narrower mass window]. Subsequently, the fragmentation spectrum was searched against

the database Mascot (Matrix Science). Both manual and automated searches for the ssGP terminal peptide were performed during the analysis.

2.7 ssGP Function

2.7.1 Neutrophil Binding

Isolated PMNs (99%) (10^6 cells) were incubated with 20 μg/ml of either purified HA-tagged r.sGP or r.ssGP for 30 min on ice. PMNs were centrifuged for 7 min at 456 xg at 4˚C and washed with ice-cold buffer (PBS with 2% goat serum). Washed PMNs were incubated with 100 μl of anti-HA-PE (Miltenyi Biotec) (1/10 dilution in wash buffer) for 30 min on ice. For control purposes, an isotype mouse IgG1-PE (Miltenyi Biotec) was used. Subsequently, cells were washed twice in ice-cold 250 μl wash buffer and analyzed by fluorescence-activated cell sorting (FACS).

2.7.2 Barrier Function Analysis of Endothelial Cells

Impedance microscopy has been used widely to measure the transendothelial electrical resistance (TER) of a cultured cell monolayer. The TER is a measurement for changes in paracellular permeability (Claude, 1978; DePaola et al., 2001; Falzarano et al., 2006; Powell, 1981; Seebach et al., 2000; Seebach et al., 2005; Wahl-Jensen et al., 2005b).

2.7.2.1 Chamber Slides Preparation

Chamber slides were prepared for the impedance spectroscopy as described elsewhere (Wahl-Jensen et al., 2005b). Briefly, indium tin oxide (ITO)-coated chamber slides (multi-well) (Delta Technologies Ltd.) were sonicated at 40^0C for 15 min and

washed extensively in reverse osmosis water. Next, the chamber slides were treated with sterile gelatin (0.5% PBS) for 1 hr at 37^0C, fixed with 2% glutaraldehyde in water for 5 min at room temperature, treated with 70% ethanol, and washed five times with sterile water. Moreover, the chambers were treated with a glycine solution (22.2 mM glycine in PBS) overnight at room temperature and washed five times with sterile PBS. HUVECs were seeded on the chamber slides that were pre-incubated with endothelial cell growth media (ECGM) containing growth factors (PromoCell) for 5 min at room temperature. The cells were kept in ECGM in a humidified incubator at 37^0C until confluent.

2.7.2.2 Impedance Spectroscopy

To measure TER, an alternating voltage was applied to the multi-channel rheological *in vitro* system (Figure 9) (MOS Technologies) and is described in detail elsewhere (Dieterich et al., 2000; Schnittler et al., 1993). The impedance magnitude was measured at frequencies between 10 Hz and 1 MHz between the three small, independent ITO electrodes in the chamber and one large counter electrode, which is applied by the rotation of the cone and plate of this system (Figure 9). Without a cell monolayer the impedance of the system is basically a series connection of an ohmic resistor (characterized by the resistance of the medium) and a constant phase element (represented by the electrode) (Figure 9A). A cell monolayer covering the electrode increases the impedance; it has been shown that this increment can be from 10^3 Hz to $3x10^5$ Hz (Seebach et al., 2000). Based on the applied frequency, alternating current passes through the intercellular junction and/or may traverse the monolayer transcellularly. The transcellular path can be

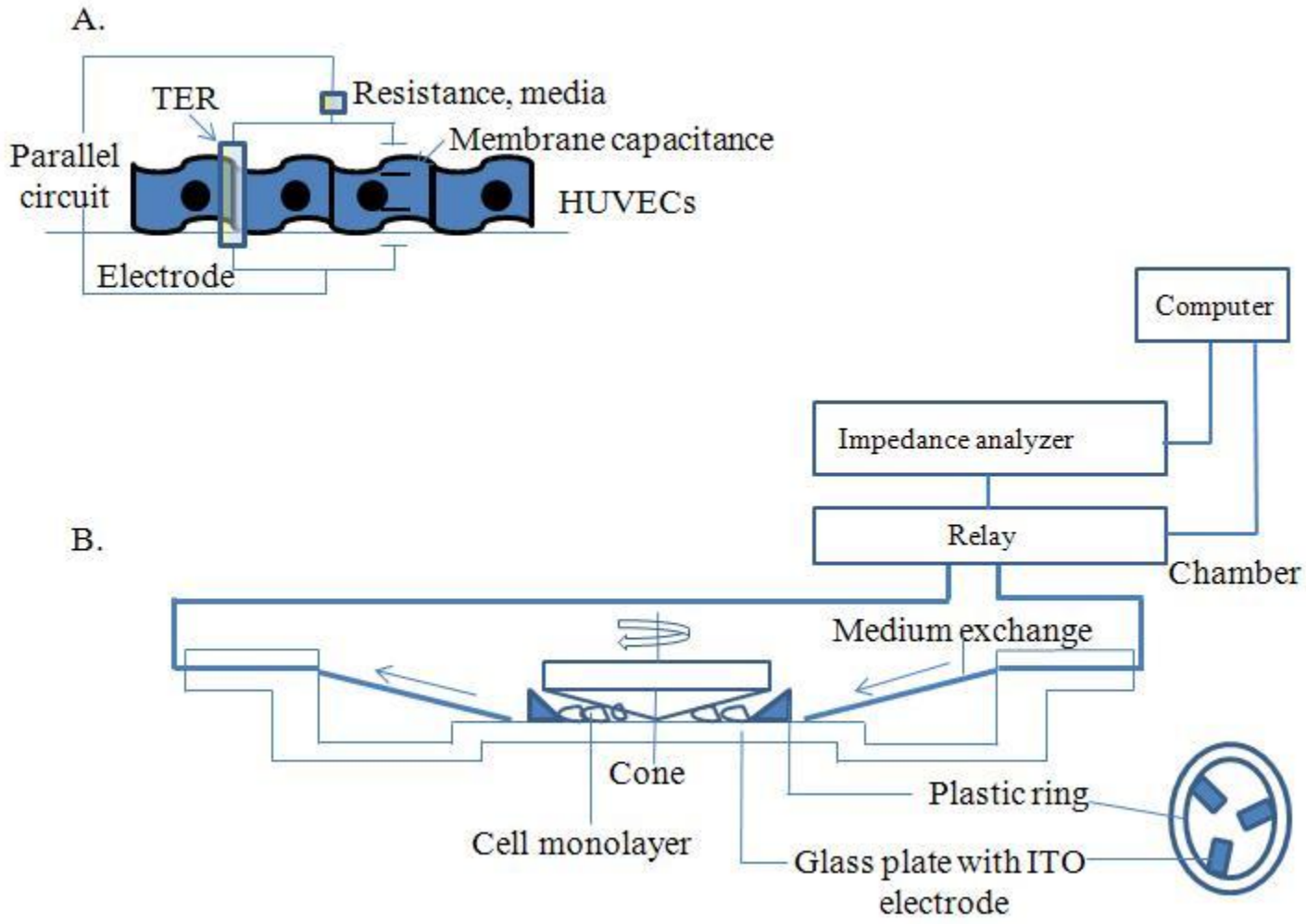
A.
TER
Resistance, media
Membrane capacitance
Parallel circuit
HUVECs
Electrode
B.
Computer
Impedance analyzer
Relay
Chamber
Medium exchange
Cone
Cell monolayer
Plastic ring
Glass plate with ITO electrode

Figure 9. **A. Scheme for the measurement of transendothelial resistance (TER).** The TER was calculated by measuring the impedance magnitude (the ratio between the amplitude of an alternating voltage applied to the system and the amplitude of the associated alternating current) at frequencies range from 10 Hz to 1 MHz between the electrode area of the ITO slide and a counter electrode. Without a human umbilical cord endothelial cell (HUVEC) monolayer, the system impedance is basically a series connection of an ohmic resistor (resistance of medium) and a constant phase component (electrode). HUVEC monolayers covering the electrode increase the impedance. Based on the applied frequency alternating current passes through the intercellular junction and may traverse the monolayer transcellularly. The cell membrane behaves as a capacitor with an approximate constant value while the paracellular path performs as an ohmic resistor (i.e. TER) at certain frequencies. Here, this ohmic resistor can be utilized to determine the tightness of cell-to-cell contacts. **B. The cone and plate rheological chamber is utilized to measure TER.** The cone rotates at a set speed supplying a calibrated shear force evenly across the cells in a chamber that contains three ITO electrodes that measure TER. This figure is adapted from (Falzarano, 2010) and MOS Technologies (http://www.glpnet.de/mos-technologies/technologie/index.php) with permission.

characterized by an approximate constant membrane capacitance (a theoretical value for a confluent monolayer equivalent to 0.5 mF/cm^2) while the paracellular path performs as an ohmic resistor (i.e. TER) at certain frequencies. This ohmic resistor can be utilized to determine the tightness of cell-to-cell contacts (Seebach et al., 2000; Wegener et al., 1999). Once HUVECs were confluent (Janshoff et al., 1996), they were equilibrated for 1-2 hr to establish a baseline TER prior to addition of proteins such as TNF-α (1 ng/ml) (R&D Systems), r.ssGP or r.sGP (30 ug/ml) to the cell monolayer.

The TER was calculated from the resulting spectra as described elsewhere (Seebach et al., 2000). Custom software based on the visual programming language LabVIEW (National Instruments, Germany) was utilized for data acquisition and analysis. All electrical resistance data are presented as normalized to baseline resistance values (TER/TER0). TER data are shown as mean +/- standard error. Data were compared an unpaired t-test. Values were considered to be statistically significant when *P* was <0.05.

2.8 Detection of RNA Editing

2.8.1 Development of a Rapid Transcript Quantification Assay (RTQA)

A new rapid transcript quantification assay (RTQA) was designed based on amplified fragment length polymorphism (AFLP) to quantify site-specific single nucleotide polymorphism (due to non-template nucleotide insertion) in RNA transcripts using the Genetic Analyzer 3730xl (Applied Biosystems). To validate the assay two fragments of the ZEBOV GP gene [45nt-ES(7A)-58nt=110 nt and 45nt-ES(8A)-58nt=111 nt] were generated from DNA containing plasmids encoding sGP and $GP_{1,2}$,

respectively (Appendix 1D). These two PCR fragments were utilized in various combinations (100:00, 90:10, 80:20, 70:30, 60:40, 50:50, 40:60, 30:70, 20:80, 10:90, and 0:100) to cover a broad range of transcript ratios between edited and unedited transcripts for quantification using the Genetic Analyzer 3730xl.

For quantification of GP gene transcripts, RNA was extracted from cells 48 hr post-transfection using the AllPrep DNA/RNA mini kit (QIAGEN). Briefly, cells were treated with 600 ul freshly made RLT buffer (QIAGEN) (with β marcaptoethanol) and passed through the QIAshredder (QIAGEN) at 19800 xg for 3 min. The solution from the QIAshredder was poured into an AllPrep spin column (QIAGEN) and centrifuged for 30 sec at 8000 xg. 600 ul of 70% ethanol was added to the collected solution and poured into the RNeasy column (QIAGEN) and centrifuged for 30 sec at 8000 xg. 350 ul of RW1 buffer (QIAGEN) was added into the column and centrifuged for 30 sec at 8000 xg. 70 ul RDD buffer (QIAGEN) and 10 ul RNase-free DNAse set (QIAGEN) were mixed and poured into the column and incubated at room temperature for 15 min. 350 ul of RW1 buffer was added and centrifuged for 30 sec at 8000 xg. The previous two steps were repeated once. 500 ul RPE buffer (QIAGEN) was added and centrifuged for 30 sec at 8000 xg. RNA was eluted in a new tube with RNase-free water.

To quantify GP gene transcripts *in vitro*, Vero E6 cells were infected with different EBOV strains representing the five species using an MOI of 0.1. Total RNA was extracted from infected cells using the RNeasy kit. Similarly, to quantify GP gene transcripts *in vivo* blood and liver samples from ZEBOV (strain Kikwit) infected macaques (kindly provided by Dr. Andrea Marzi) were used for RNA extraction using the QIAamp Viral RNA (QIAGEN) and RNeasy kit, respectively.

Materials and Methods

First-strand synthesis was done using an oligo-dT primer and SuperScript III (described in 2.3.1). First-strand synthesis was also done using a vRNA template using a genome specific primer instead of an oligo-dT primer. The first-strand synthesis product (cDNA-RNA hybrid) was purified using the QIAquick PCR purification kit. Purified first-strand reactions were utilized for PCR amplification using HF iProof DNA Polymerase in 20 ul reactions consisting of 1 ul template, 4 ul 5x HF reaction buffer, 0.4 ul 10 mM dNTP mix, 0.5 ul 20 uM 6 carboxyfluorecein (FAM)-labeled forward primer, 20 uM 0.5 ul reverse primer, 13.4 ul water, and 0.2 ul HF iProof DNA polymerase (2 U/ul). Thermal cycling conditions were programmed for an initial denaturation at 98^0C for 30 sec, followed by 30 cycles of a 10 sec denaturation at 98^0C, a 15 sec annealing at 55^0C, and a 15 sec extension at 72^0C, followed by a final extension at 72^0C for 7 min. The labeled final product was diluted 1:400 with water and 1 ul was added to a mix of 10.5 ul HiDi Formamide (Applied Biosystems) and 0.5 ul GeneScan LIZ-120 Size Standard (Applied Biosystems), heat denatured for 3 min at 95^0C, snap-cooled on ice, and separated with the Genetic Analyzer 3730xL. A FAM-labeled forward primer (Appendix 1E) allows labeled PCR product analysis in the genetic analyzer. An internal size standard GeneScan-120 LIZ (Applied Biosytems) was used for this fluorescence-based DNA electrophoresis system for sequencing and fragment analysis that provides an automated and rapid quantification. The electropherogram provides multiple peaks (labeled by LIZ) for the product being analyzed (here unedited and edited fragments) (Figure 10).

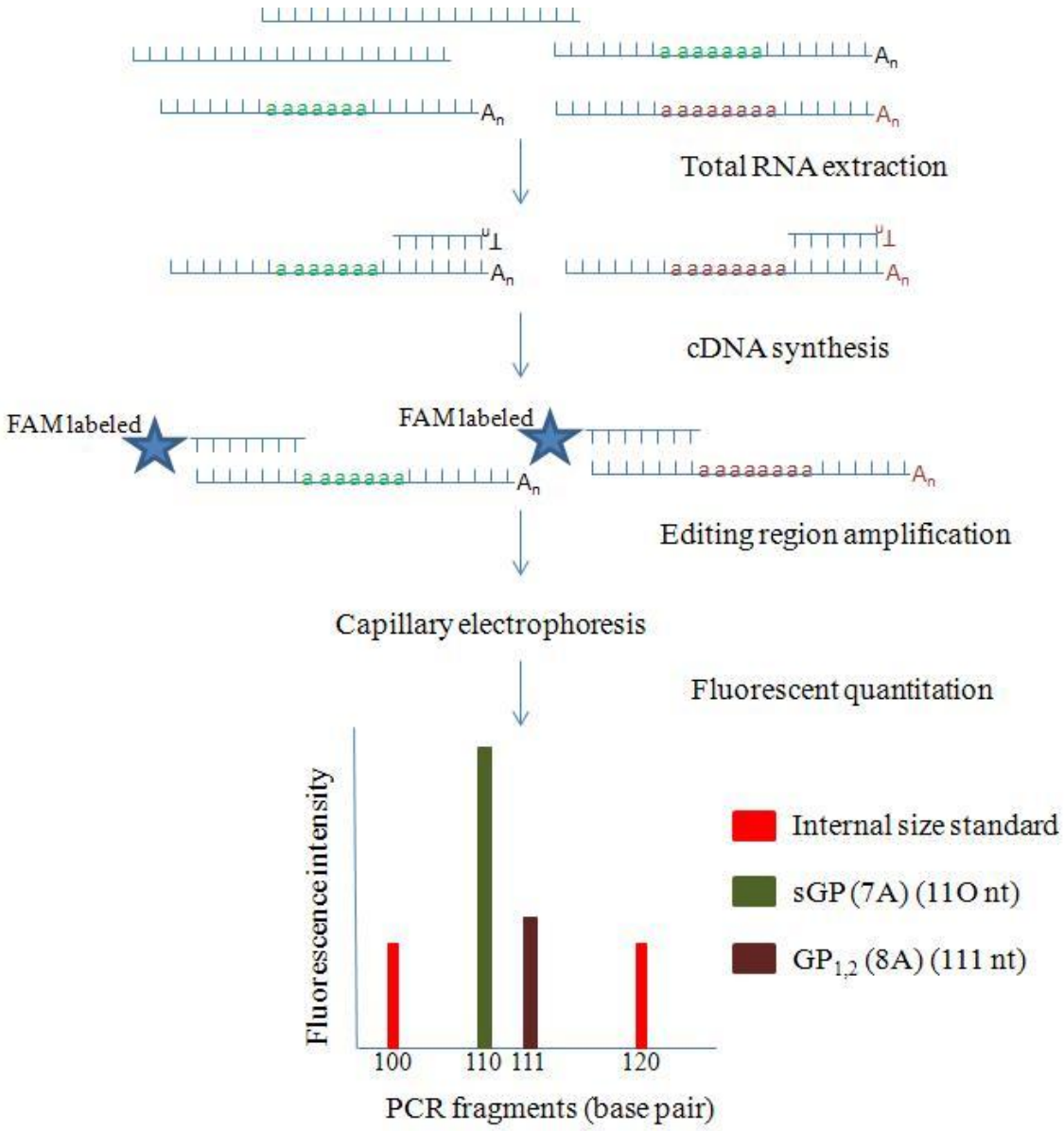

Figure 10. **The rapid transcript quantification assay (RTQA).** cDNA was synthesized from total RNA using an oligo-dT primer followed by primer specific PCR amplification of the editing region. PCR fragments differing by a single nucleotide were differentiated using the capillary electrophoresis based Genetic Analyzer 3730xl (Applied Biosystems). Internal size standard allows separation and detection of PCR fragments. GeneMapper software v4.0 (Applied Biosystems) analyzes and quantifies allele specific signals based on the abundance of FAM-labeled PCR products.

Quantification of GP gene transcripts obtained from RNA editing (unedited, 7A and edited, 8A) was done by analyzing the PCR fragment profiles for 7A and 8A genotyping using the GeneMapper v4.0 (Applied Biosystems). Peak designations were inferred according to the bin set established by 7A and 8A fragments (Appendix 13). The relationship of 7A to 8A genotypes for each sample was calculated using a curve fit equation (6^{th} order polynomial) from the standard curve generated from 7A- and 8A-transcripts (Appendix 13).

2.9 Characterization of RNA Editing

2.9.1 Minigenome Rescue

Six-well plates were coated with a Poly D-lysine (Invitrogen) in PBS by incubating the bottom surface for 30 min 37^0C in the CO_2 incubator. 293T cells were seeded the day before to get 50-60% confluent cells for transfection. A typical transfection mix with TransIT-LT1 transfection reagent (Mirus) for one well of a six-well plate contained the following: 1 ul VP30 (75 ng/ul), 1 ul VP35 (125 ng/ul), 1 ul NP (125 ng/ul), T7 polymerase (250 ng/ul), 1 ul L (1000 ng/ul), 1 ul minigenome plasmid (250 ng/ul), 250 ul Opti-MEM, and 7.5 ul Trans-LT1. The solution was added, mixed, and incubated for15-30 min at room temperature. The transfection mix was added to the well slowly and incubated for 48 hr at 37^0C in a CO_2 incubator. 24 hr post-transfection the medium was replaced with DMEM with 2% FBS.

2.9.2 *In Vitro*-transcription of Minigenome DNA

Minigenome plasmids were *in vitro*-transcribed using the MAXIscript T7 Kit (Ambion). First, plasmid DNA was linearized by restriction enzyme digestion (e.g.

Sma1). For this, 4 ul of plasmid (500 ng/ul), 3 ul Sma1, 5 ul NEB buffer 4, and 38 ul distilled water were mixed and incubated at room temperature (25^0C) for 2 hr followed by incubation at 65^0C for 20 min. 2.5 ul 0.5M EDTA, 5 ul 5 M ammonium acetate, and 100 ul 100% ethanol were added and incubated for 20 min at -20^0C to precipitate DNA. The supernatant was removed after centrifugation at 15000 xg for 20 min, and the pellet was diluted with nuclease free water. Linearized plasmid DNA was used for *in vitro*-transcription. Briefly, 2 ul DNA (500 ng/ul), 2 ul 10x transcription buffer, 1 ul 10 mM ATP, 1 ul 10 mM CTP, 1 ul 10 mM GTP, 1 ul 10 mM UTP, 2 ul T7 enzyme MAXiscript and 10 ul distilled water were mixed and incubated for 30 min at 37^0C. 2 ul of Turbo DNase1 mix (Ambion) was added and incubated for 15 min at 37^0C. To stop the reaction, 1ul of 0.5 M EDTA was added. Transcripts were precipitated by adding 30 ul of distilled water, 5 ul 5 M ammonium acetate, and 3 volumes of 100% ethanol and incubated at -20^0C overnight. After centrifugation at 13000 rpm for 15 min at 4^0C, the pellet was washed with 100 ul ice cold 70% ethanol and resuspended in RNAse free water.

293T cell monolayers (50% confluent) were transfected with the TransIT-LT1 transfection reagent. Briefly, 1 ul VP30 (75 ng/ul), 1 ul VP35 (125 ng/ul), 1 ul NP (125 ng/ul), 1 ul L (1000 ng/ul), 250 ul Opti-MEM, and 7.5 ul Trans-LT1 were mixed and incubated for 15-30 min at room temperature. The transfection mix was added to a six-well plate slowly, and incubated for 24 hr at 37^0C in the CO_2 incubator. mRNA transfection was done using the TransIT-mRNA transfection kit (Mirus). Briefly, 1 ug of RNA transcript, 250 ul of Opti-MEM, 2.5 ul mRNA boost reagent, 2.5 ul mRNA TransIT-mRNA reagent were mixed and incubated at room temperature for 5 min. The

mix was added slowly to a six-well plate and incubated for 48 hr at 37^0C in the CO_2 incubator. After 24 hr post-transfection medium was replaced with DMEM with 2% FBS.

2.9.3 Detection and Quantification of Reporter Proteins

2. 9.3.1 Confocal Microscopy

For confocal microscopy, cover slips in a six-well plate were submerged with Poly D-lysine (Invitrogen) in PBS for 30 min and washed twice with PBS. 293T cells were seeded on the coverslip, and transfection was done as described in 2.9.1. At 48 hr post-transfection, coverslips were washed with PBS, fixed with 4% paraformaldehyde (PFA), and stained with ProLong Gold Antifade reagent with 4',6-diamidino-2-phenylindole (DAPI) (Invitrogen). The coverslips were mounted on glass bases. Confocal images were obtained by a Zeiss LSM710 confocal microscope with a 63x objective. Following sequential excitation for DAPI, eGFP, and mCherry, fluorescence images (blue, green, and red) of the same cell were saved and processed using ZEN software (Zeiss).

2.9.3.2 Epi-Fluorescence Microscopy

Slides prepared for confocal microscopy were analyzed under an AXIO Imager M1 epi-fluorescence microscope (Zeiss) for fluorescence signal quantification. Mean fluorescent intensity (MFI) was measured for the same area for both fluorescent reporters (eGFP and mCherry) using the ImageJ software 1.44p (Abràmoff et al., 2004). MFI was calculated with standard deviation and standard error.

2.9.3.3 Fluorescence Activated Cell Sorting (FACS)

Supernatant from the transfected cells was discarded, and cells were harvested with trypsin treatment [250 ul 0.5% trypsin (Invitrogen) into a single well of a six-well plate for 1 min]. The cells were washed twice (centrifuged at 300 xg for 5 min) with sterile PBS on ice, fixed with 2% PFA, and washed with PBS containing 2% FBS. Cells were analyzed on a LSR II Flow Cytometer (BD Biosciences). Live cells were gated first for eGFP signals, followed by mCherry signal quantification. For each sample at least 100,000 events were analyzed. Data analysis was performed using FlowJo software package (TreeStar Inc.).

2.10 Statistical Analysis

Analysis was done using GraphPad Prism version 5.00 for Windows, GraphPad Software, San Diego California USA, www.graphpad.com.

2.11 Ethics and Biosafety Statements

All infectious EBOV *in vitro* and *in vivo* work was performed in the BSL4 laboratories at the National Microbiology Laboratory, Winnipeg, Canada or the Rocky Mountain Laboratories, Hamilton, USA. Animal experiments were performed under approved institutional animal-use documents and according to the guidelines of the Canadian Council on Animal Care (CCAC) or the American Association of Laboratory Animal Care (AALAC).

3. RESULTS

3.1 Identification of a New EBOV Small Soluble Glycoprotein (ssGP)

3.1.1 Detection of ssGP Transcript

3.1.1. 1 Quantification of ssGP Transcript by sequencing

During transcription the ZEBOV polymerase edits the GP gene at the conserved ES, resulting in multiple transcripts that encode for multiple proteins. The primary GP gene product is sGP that is produced from the unedited transcript, whereas the edited transcript produces $GP_{1,2}$. It has been shown that the ratio between transcripts that encode for sGP and $GP_{1,2}$ is approximately 80:20 (Volchkov et al., 1995). In this thesis, I hypothesized that RNA editing produces a distinct additional transcript that encodes for a second nonstructural protein, the ssGP, as this had been postulated before (Figure 11) (Anthony Sanchez, 2007; Feldmann et al., 2001; Volchkov et al., 1995). I first tried to identify ssGP-specific transcripts by determining GP gene-specific transcripts during EBOV infection. For *in vitro* analyses, Vero E6 cells (the most widely used cell line for EBOV propagation) were infected with ZEBOV using an MOI of 1. At 4 days post-infection total RNA was harvested from infected cells, followed by first-strand synthesis using a GP gene-specific oligo-dT primer. A fragment of 330 bp covering the GP gene ES region (Appendix 4) was amplified by PCR using a GP gene-specific primer-pair, cloned into the TOPO TA vector, and subsequently sequenced using the method established by Sanger (Sanger and Coulson, 1975).

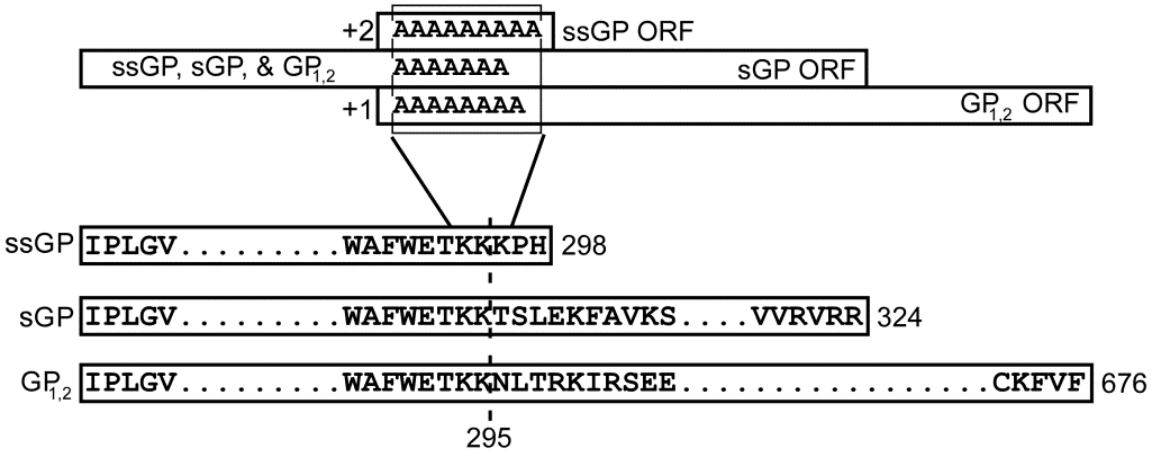

Figure 11. **ZEBOV GP gene putative open reading frames (ORFs).** The most abundant GP gene product, soluble glycoprotein (sGP) is encoded from an unedited transcript; the structural protein, transmembrane glycoprotein ($GP_{1,2}$) is encoded from an edited transcript; a hypothetical protein, small soluble glycoprotein (ssGP) is potentially encoded from a distinct edited transcript. Putative ORFs for ssGP, sGP and $GP_{1,2}$ are depicted (top). An alignment of the primary amino acid (aa) sequences shows that ssGP, sGP, and $GP_{1,2}$ are identical for the first 295 aa from the N-terminus including the signal peptide (SP; 1-32 aa), but differ in their C-terminal portion (bottom).

Positive clones differed from each other only by the number of A residues present at the ES within the 330 bp fragment. Based on the number of A residues at the ES, transcripts were identified as specific for either sGP (7A), $GP_{1,2}$ (8A), or ssGP (6A or 9A). A total of 224 clones were sequenced and the ratio of transcripts encoding for sGP, $GP_{1,2,}$ and ssGP was determined as 71:24:5, respectively (Figure 12). A human liver cell line (Huh7) was also used to determine GP gene-specific transcripts because liver is one of the primary target organs for EBOV infection in humans and NHPs. A similar transcript ratio was observed in ZEBOV infected Huh7 cells (MOI of 1) with 4% of the transcript being ssGP specific (Figure 12).

Next, I attempted to identify the presence of ssGP-specific transcripts during *in vivo* ZEBOV infection. BALB/c mice were infected with MA-ZEBOV (100 PFU), and at 4 days post-infection animals were euthanized. Total RNA was extracted from liver. A total of 260 clones were analyzed using the methods described above and the ratio of RNA transcripts was determined to be 67: 31: 2 for sGP, $GP_{1,2,}$ and ssGP, respectively (Figure 12).

3.1.1.2 Specificity of RNA Editing

Although editing was largely a specific event, a small proportion of transcripts (3% of all analyzed clones) showed the insertion of multiple A residues at the ES during both *in vitro* and *in vivo* infection. The number of A residues inserted ranged from 1 to 24. In addition, a few clones with a single A residue deletion were observed that encode for a variant of ssGP. No transcripts were detected with less than six A residues (Figure 13).

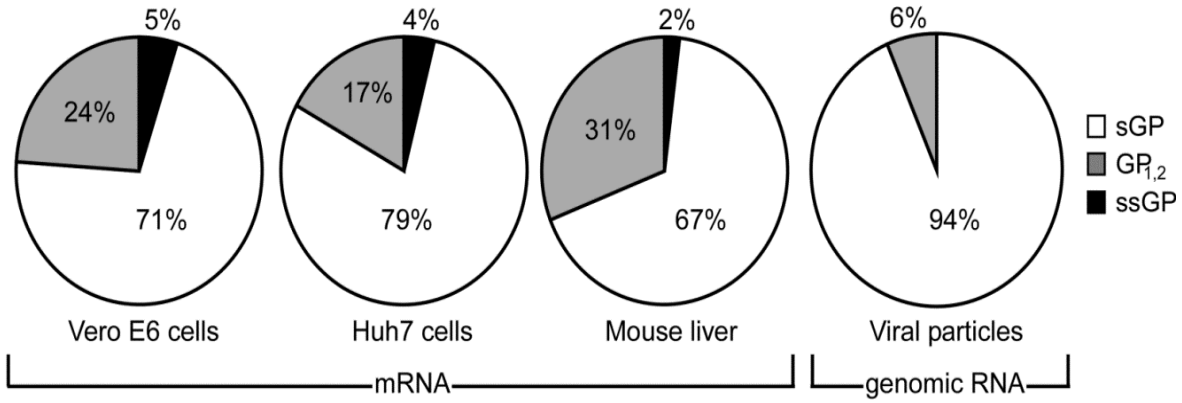

Figure 12. **ssGP specific transcripts are produced *in vitro* and *in vivo*.** Vero E6 and Huh7 cells were infected with ZEBOV (MOI of 1) and mice were infected with MA-ZEBOV (100 PFU). RNA was extracted from infected cell cultures, virus particles, and mouse liver. The ES region from transcripts (mRNA) and the vRNA (genomic RNA) was amplified (330 bp fragment), cloned and sequenced. A total of 224 (Vero E6), 132 (Huh7), 260 (mouse liver), and 109 (viral genome) clones were analyzed. ssGP transcripts were detected to a smaller degree from both *in vitro* and *in vivo* infection as compared to the major transcripts (sGP and $GP_{1,2}$).

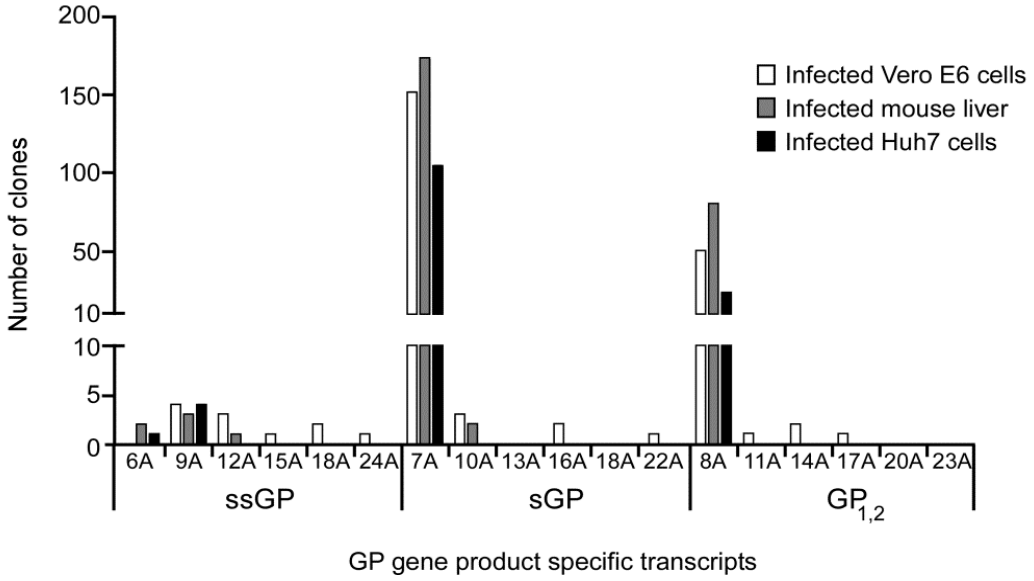

Figure 13. **Specificity of RNA editing.** The vast majority of clones from transcripts (97%) showed either 7 (sGP), or 8 ($GP_{1,2}$) adenosine (A) residues at the ES. In addition, 9 (ssGP) A residues were observed at the ES for ssGP. The remaining 3% of clones analyzed contained multiple A residues, which would lead to the incorporation of additional lysine(s) in the primary amino acid sequence. With the rare exception of a single A residue deletion (encodes ssGP) no other deletions were found at the ES.

To exclude the possibility that editing occurred during reverse transcription and PCR amplification, a synthetic positive sense RNA including the ES and surrounding sequences was subjected to the same procedures. Neither insertion nor deletion of nucleotide was observed by sequencing from more than 50 clones, thus confirming that A residues are introduced as a result of editing by the viral polymerase rather than the Taq DNA polymerase (data not shown).

To exclude the possibility that insertions or deletions are already existing in viral genomic RNA, total RNA was extracted from virus particles and subjected to the same procedures. The vast majority (94%) of 109 clones showed wild-type sequence at the ES (7A residues), 6% of the clones were identified to carry 8A residues at the ES (Figure 12). This finding was not unexpected as an 8A virus was previously plaque purified and isolated (Sanchez et al., 1993; Volchkov et al., 2001). However, vRNA genomes with 9A or 6A residues at the ES (encoding directly for ssGP) were not detected, indicating that such viruses might not be viable (Figure 12).

3.1.2 Detection of ssGP during ZEBOV Infection

3.1.2.1 Transient Expression of r.ssGP and r.sGP

The GP gene products $GP_{1,2}$ (676 aa) and sGP (324 aa) are identical over the first 295 N-terminal amino acids; however, they differ in their C-terminal portions and their structures (Figure 11) (Anthony Sanchez, 2007; Barrientos et al., 2004; Barrientos et al., 2007; Falzarano et al., 2006; Feldmann et al., 2001). This is also expected for the hypothesized nonstructural ssGP, which theoretically should represent a truncated version of sGP. All GP gene-specific products carry the same SP (1-32 aa); therefore, it is

expected that like other GP gene-specific products putative nonstructural ssGP has the same processing pathway undergoing similar co- and post-translational modifications.

For characterization and control purposes, recombinant proteins (r.ssGP and r.sGP) were expressed with or without an N-terminal HA tag using the mammalian expression vectors pDISPLAY (Figure 14 A&B) and pCAGGS (Figure 15A), respectively. The expression of HA-tagged r.ssGP6A (265 aa) and r. ssGP9A (266 aa) in 293T cells was confirmed by immunoblotting using Anti-HA peroxidase (Figure 14C). Similarly, expression of untagged r.ssGP and r.sGP in Vero E6 cells was confirmed by immunoblotting using MAb 42/3.7. This MAb recognizes an epitope in the N-terminal portion of the proteins common to all GP gene products (Takada et al., 2007a; Takada et al., 2007b), therefore it was expected to also detect ssGP (Figure 15B).

3.1.2.2 ssGP is Secreted During Infection

Vero E6 cells were infected with ZEBOV strain Mayinga using an MOI of 1. In parallel, Vero E6 cells were transfected with r.ssGP and r.sGP expression plasmids. The supernatants from infected and transfected cells were subjected to an overnight digestion with PNGaseF, and the proteins were analyzed in 15% SDS-PAGE, followed by immunoblotting using MAb 42/3.7 (Figure 16). Two bands were identified in the supernatant of ZEBOV infected cells with the more prominent displaying a MW of approximately 33 kDa, which correlates in size with deglycosylated r.sGP (Figure16, lanes 2 & 3).

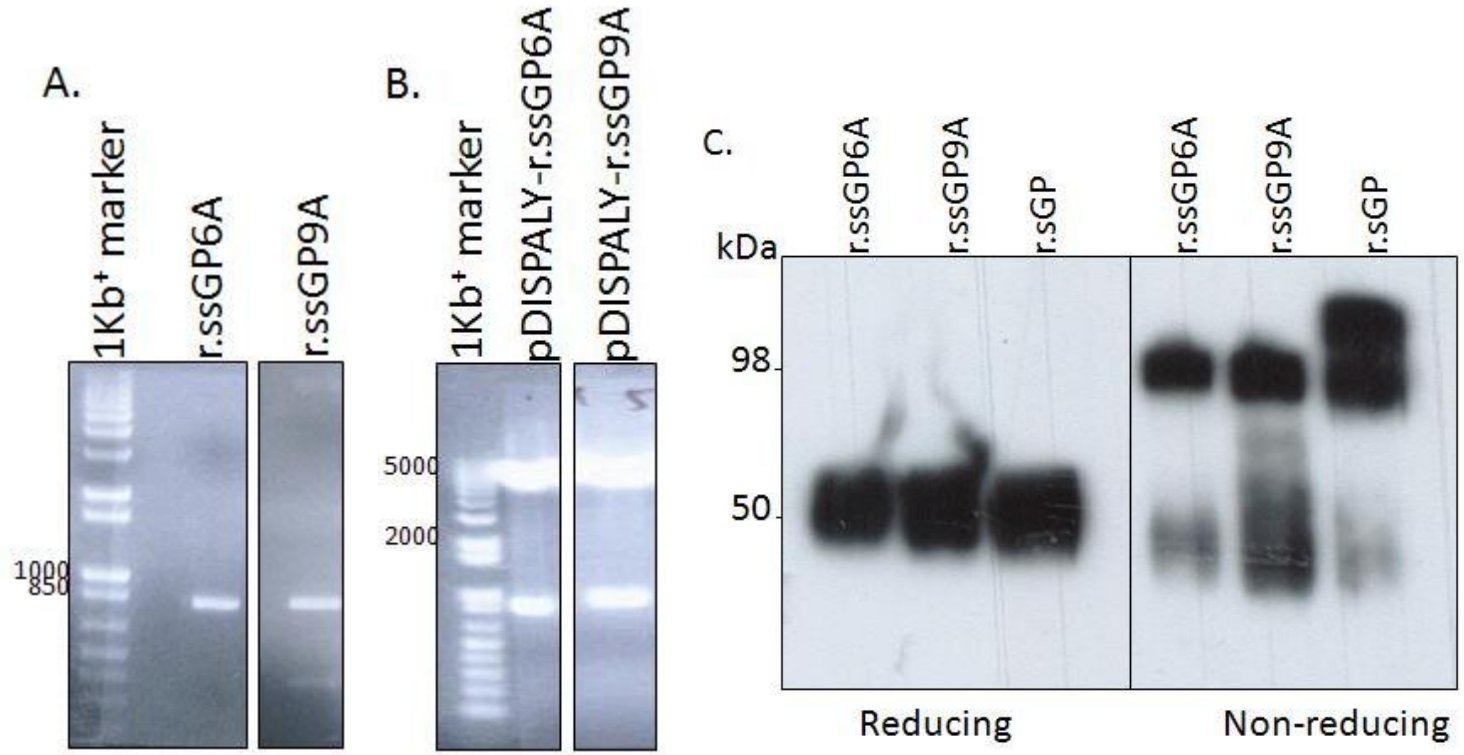

Figure 14. **recombinant ssGP (HA-tagged) expression.** Two different transcripts are potentially produced due to RNA editing that encode for ssGP either by deleting a single A residue at the editing site (ES) (ssGP6A) or by inserting two A residues at the ES (ssGP9A). **A.** PCR fragments of both forms of ssGP. **B.** Restriction enzyme digested expression plasmid, pDISPLAY containing either ssGP6A or ssGP9A. **C.** Expression of r.ssGP and r.sGP was verified by transfecting appropriate plasmids in 293T cells. Proteins were detected by immunoblotting using Anti-HA peroxidase (1:10,000 dilution). r.ssGP6A and r.ssGP9A were secreted from the transfected 293T cells and migrated similarly with r.sGP following reducing (50 kDa) (left panel) and non-reducing (100 kDa) (right panel) SDS-PAGE.

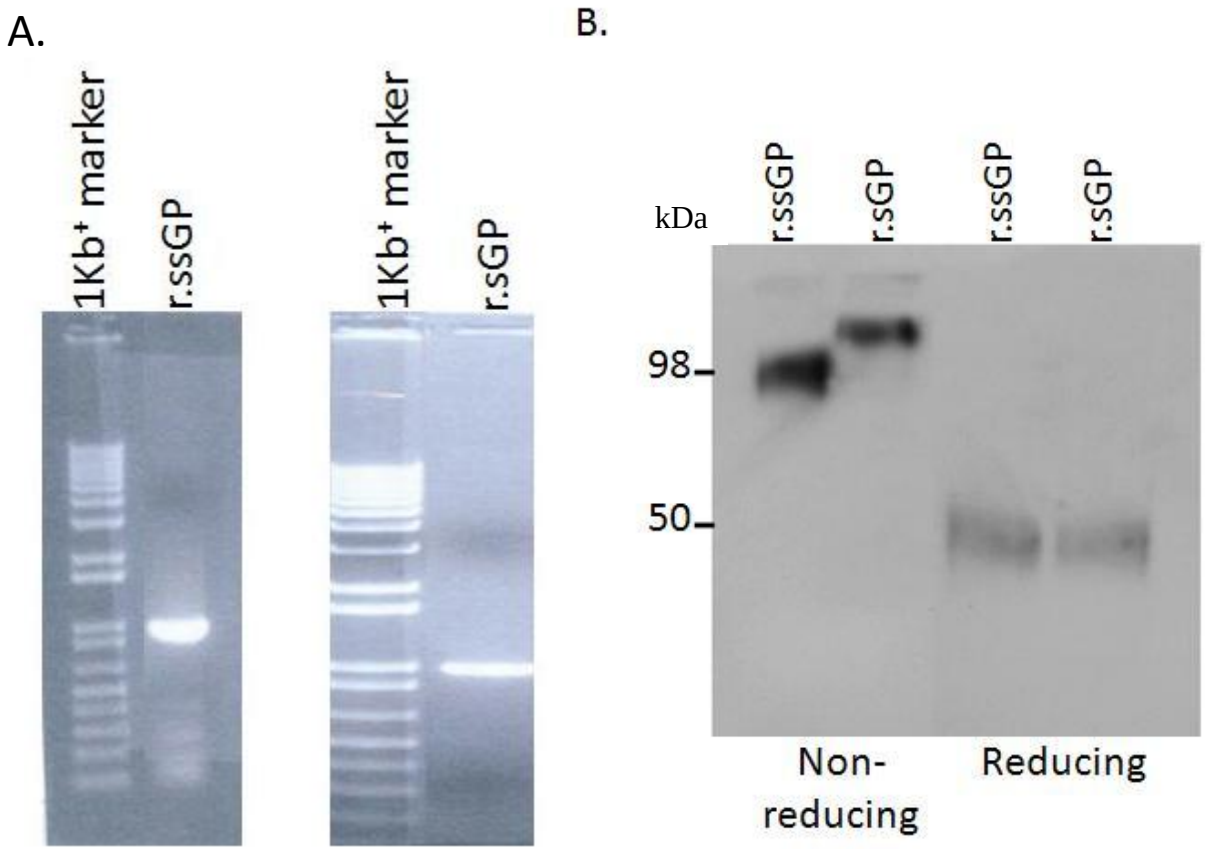

Figure 15. **Recombinant ssGP and sGP (without any tag) expression. A.** The agarose gel shows PCR fragments encoding r.ssGP (ssGP9A) and r.sGP for insertion into the expression plasmid pCAGGS. **B.** Expression of un-tagged r.ssGP and r.sGP was verified in Vero E6 cells at 72 hr post-transfection. Proteins were detected by immunoblotting using MAb 42/3.7 (1:10,000 dilution). r.ssGP migrated similarly to r.sGP on reducing SDS-PAGE, but slightly faster under non-reducing conditions.

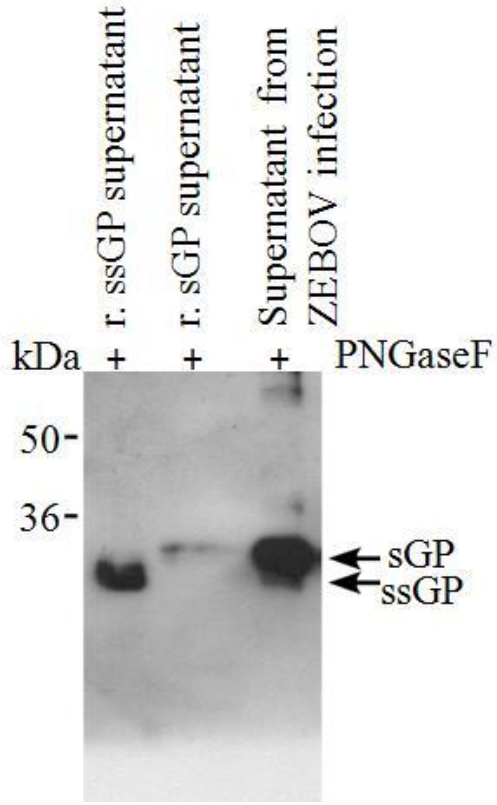

Figure 16. **ssGP is secreted during ZEBOV infection.** PNGaseF treated supernatants from infected Vero E6 cells (MOI of 1) and transfected Vero E6 cells (r.ssGP and r.sGP) were run longer time on a 15% reducing SDS-PAGE gel. Proteins were detected by immunoblotting using MAb 42/3.7 (1:10,000 dilution) and secondary anti-mouse IgG (H+L) (KPL).

The weaker, lower MW band (approximately 30 kDa) co-migrated with deglycosylated r.ssGP and likely represents ssGP that is produced and secreted during ZEBOV infection (Figure 16, lanes 1 & 3). This provided the first indication of ssGP expression and secretion during ZEBOV infection.

3.1.2.3 Confirmation of ssGP Secretion during EBOV Infection

To verify ssGP expression during infection, I used nanoLC-ESI-MS/MS for the identification of the ssGP specific C-terminal peptide. Comparison of amino acid sequences between ssGP and sGP revealed that only the C-terminal two amino acids are unique to ssGP (Appendix 5). Trypsin digestion was unable to produce peptides that allowed for discrimination between ssGP and sGP. Therefore, I used formic acid digestion to generate a C-terminal ssGP-specific peptide (282-TIGEWAFWETKKPH-297; 1830.9173 Da MW) differing from the one generated for sGP digestion (282-TTIGEWAFWETKKTSLEKFAVKSCLSQLYQTEPKTSVVRVRR-324; 4775.5228 Da MW) (Appendix 6). In the control experiment, purified r.ssGP was treated with formic acid and subjected to nanoLC-ESI-MS/MS analysis, and the double (916 m/z) and triple charged ion (611 m/z) for the C-terminal ssGP-specific peptides were detectable (Figure 17A). The fragmentation spectrum was searched against the database Mascot (Matrix Science) (James et al., 1994) resulting in correctly annotated peaks of the y and b series ion for peptide 282-TIGEWAFWETKKPH-297 (Figure 17B). Subsequently, supernatants from ZEBOV infected Vero E6 cells (MOI of 1) were subjected to in-gel formic acid digestion followed by nanoLC-ESI-MS/MS. However, neither the double nor triple charged ion of the ssGP-specific unique peptide was detectable, despite multiple attempts (data not shown).

A.

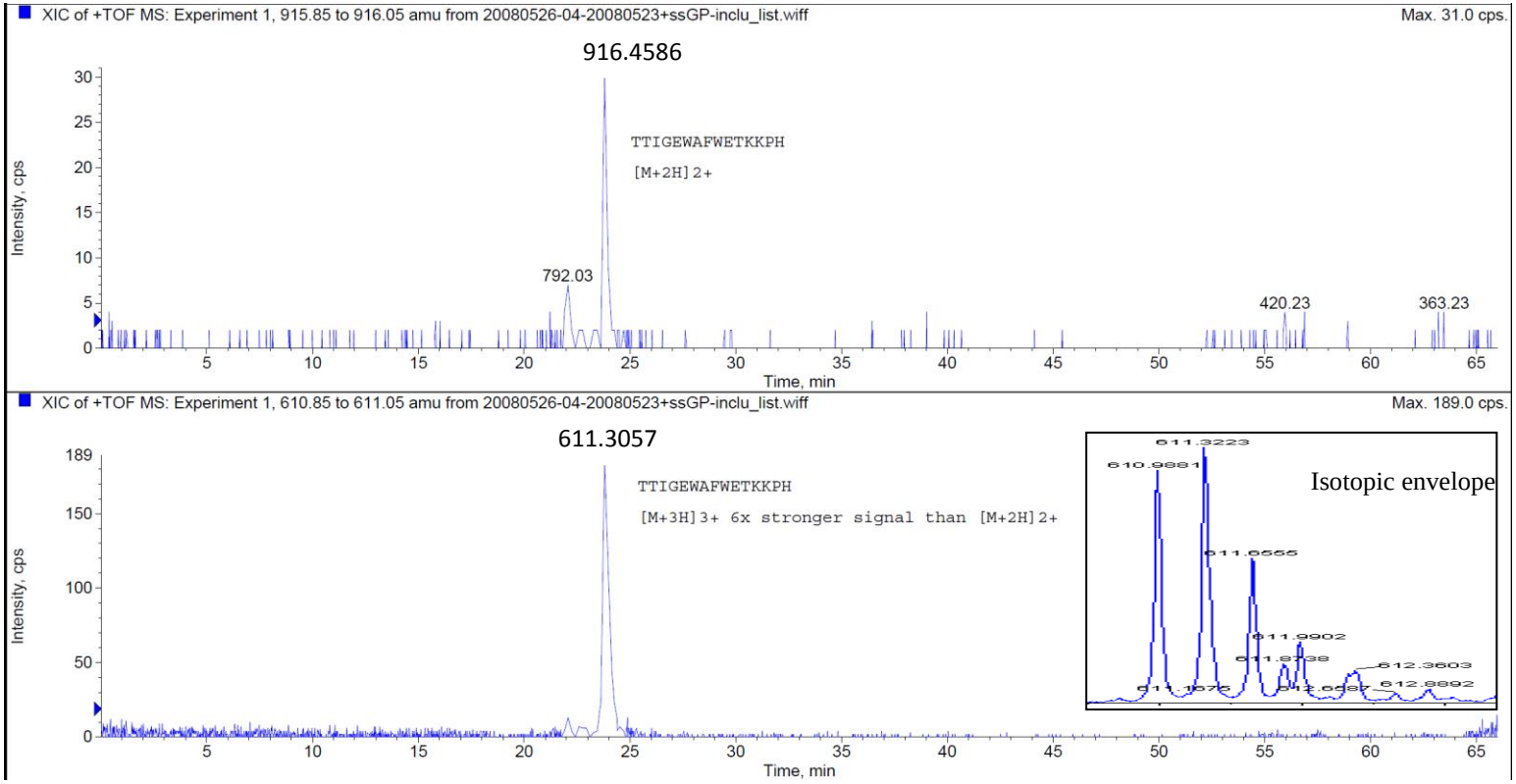
XIC of +TOF MS: Experiment 1, 915.85 to 916.05 amu from 20080526-04-20080523+ssGP-inclu_list.wiff
Max. 31.0 cps.
916.4586
TTIGEWAFWETKKPH
[M+2H]2+
792.03
420.23
363.23
Intensity, cps
Time, min
XIC of +TOF MS: Experiment 1, 610.85 to 611.05 amu from 20080526-04-20080523+ssGP-inclu_list.wiff
Max. 189.0 cps.
611.3057
TTIGEWAFWETKKPH
[M+3H]3+ 6x stronger signal than [M+2H]2+
Isotopic envelope
611.3223
610.9881
611.6555
611.9902
612.3603
612.8892
Intensity, cps
Time, min

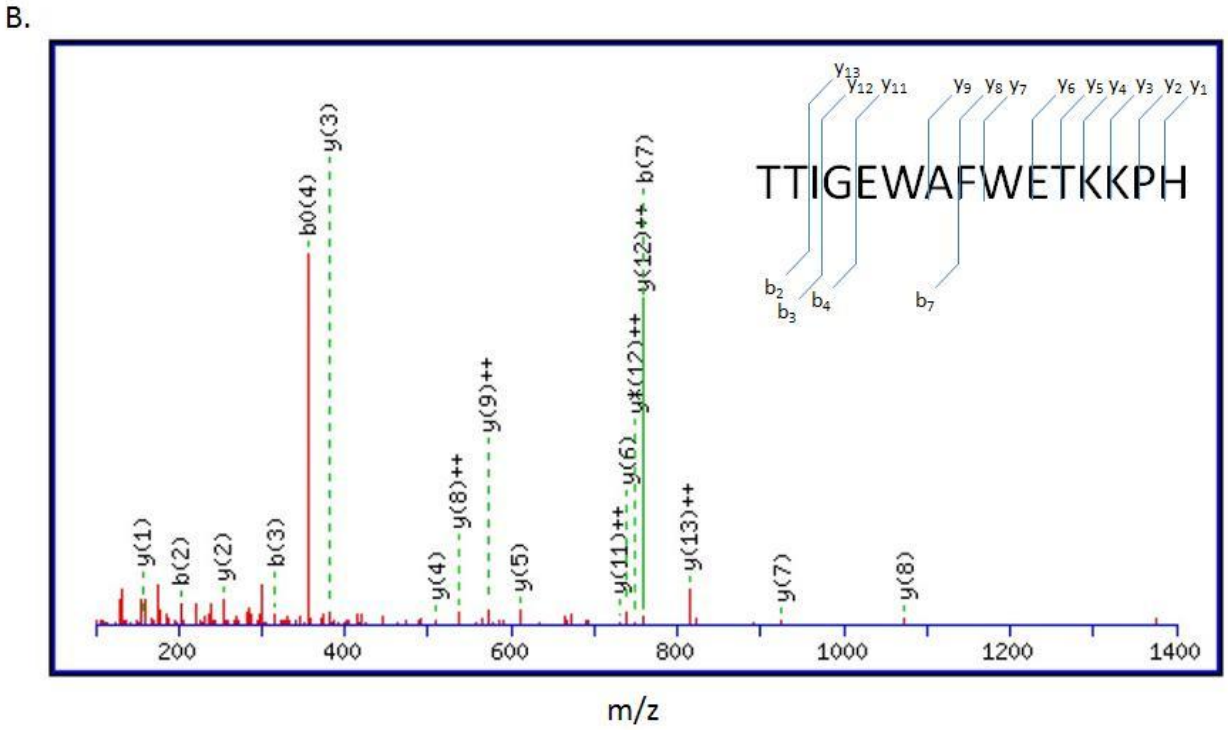

Figure 17. **ssGP-specific peptide can be detected by mass spectrometry. A.** Formic acid digested purified r.ssGP was analyzed on a nanoflow liquid chromatography-electrospray ionization-tandem mass spectrometryc (nanoLC-ESI-MS/MS). The extracted ion chromatogram of the ssGP C-terminal unique peptide (282-TIGEWAFWETKKPH-297) showed the monoisotopic peak for ions [double (2^+) (top) and triple (3^+) (bottom)]. Triple charged ion signals were detected stronger than double charged ion signals. The multi-charge envelope (isotopic envelope) for the peptide from triple charged ion signals is shown (inset of the bottom image). **B.** Fragmentation spectrum was searched against the database Mascot (Matrix Science) resulting in correctly annotated peaks of the y and b series ions for 282-TIGEWAFWETKKPH-297.

Results

To overcome the limitations in one-dimensional SDS-PAGE in separating ssGP from sGP, 2-D gel electrophoresis was utilized next. For control purposes, Vero E6 cells were transfected with the recombinant plasmids pCAGGS-ssGP or pCAGGS-sGP and supernatants were harvested at 72 hr post-transfection. In parallel, Vero E6 cells were infected with ZEBOV using an MOI of 1. Supernatants were harvested at 4 days post-infection. Harvested supernatants from transfected and infected cells were subjected to PNGaseF treatment overnight. Proteins were applied to 2-D gel electrophoresis using a narrow pH range (pH 4-7) in the first dimension and 12% SDS-PAGE in the second dimension. Following the second dimension, immunoblotting was performed using MAb 42/3.7, which detects ZEBOV GP gene products. r.sGP and r.ssGP were clearly separated based on their p*I* and MW (ssGP is predicted to be smaller than sGP), demonstrating the suitability of the approach to discriminate between the two similar secreted proteins (Figure 18 left panel, Appendix 7 & 8). Both proteins appeared in different isoforms, possibly reflecting certain co- and/or post-translational modifications besides N-glycosylation (Figure 20). A similar pattern was observed when supernatant derived from ZEBOV-infected cells was analyzed, confirming the expression of both proteins during infection (Figure 18, right panel). The apparent weaker expression of ssGP correlates with the lower transcript numbers as determined earlier (Figure 12). ssGP secretion during EBOV infection was also confirmed by 2-D DIGE analysis. Basically, purified r.ssGP and r.sGP were labeled with Cy5 and Cy3 dyes, respectively. Both labeled proteins displayed similar differences in MW and p*I* on 2-D DIGE (Appendix 9) as had been observed with regular 2-D gel electrophoresis (Figure 18). When r.sGP (Cy2-labeled) and r.ssGP (Cy3-labeled) were mixed with Cy5-labeled

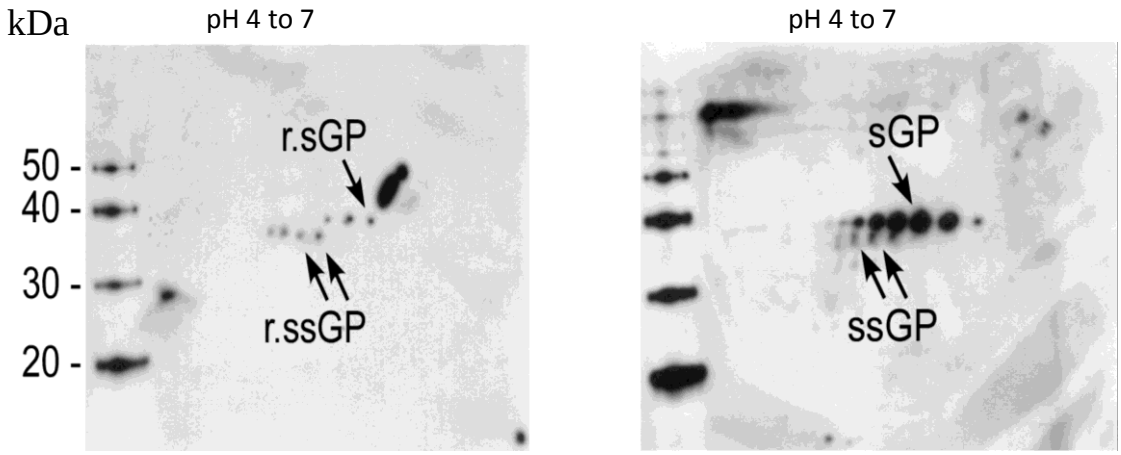

Figure 18. **ssGP detection by 2-D gel electrophoresis.** PNGaseF treated supernatants fromVero E6 cells transfected with pCAGGS-sGP and pCAGGS-ssGP (left panel) and ZEBOV infected Vero E6 cells (MOI of 1) (right panel) were separated by 2-D gel electrophoresis: pH (4-7) in the first dimension and 12% SDS-PAGE in the second dimension. sGP and ssGP were detected using 42/3.7 MAb (1:10,000 dilution).

proteins derived from ZEBOV-infected cell supernatant and run on 2-D DIGE, detection of both proteins was confirmed at their predicted MW and p*I* (Appendix 10).

3.1.3 Biophysical Properties of ssGP

3.1.3.1 ssGP is a Dimer

$GP_{1,2}$ and sGP have been shown to form disulfide-linked homotrimers and homodimers, respectively (Barrientos et al., 2004; Barrientos et al., 2007; Falzarano et al., 2006; Sanchez et al., 1998). There was a clear differentiation in ssGP migration on SDS-PAGE under reducing and non-reducing conditions (Figure 15B, lanes 1 & 3). Under non-reducing condition r.ssGP migrated as a 100 kDa protein, similar but slightly faster than r.sGP, suggesting that ssGP also has a dimeric structure (Figure 15B, lanes 1 & 2), whereas under reducing conditions sGP and ssGP show a nearly identical migration (Figure 15B, lanes 3 & 4). Cysteine residues at positions 53 (Cys53) and 306 (Cys306) are responsible for intermolecular disulfide bond formation in sGP (Barrientos et al., 2004; Falzarano et al., 2006). Since Cys306 is not present in the ssGP, Cys53 was replaced by a glycine (gly) residue using site-directed mutagenesis and expression was analyzed under reducing and non-reducing SDS-PAGE. Only the monomeric form was detected for the mutated ssGP, suggesting that oligomerization of ssGP is also dependent on an intermolecular disulfide bond between two adjacent Cys53 molecules (Figure 19).

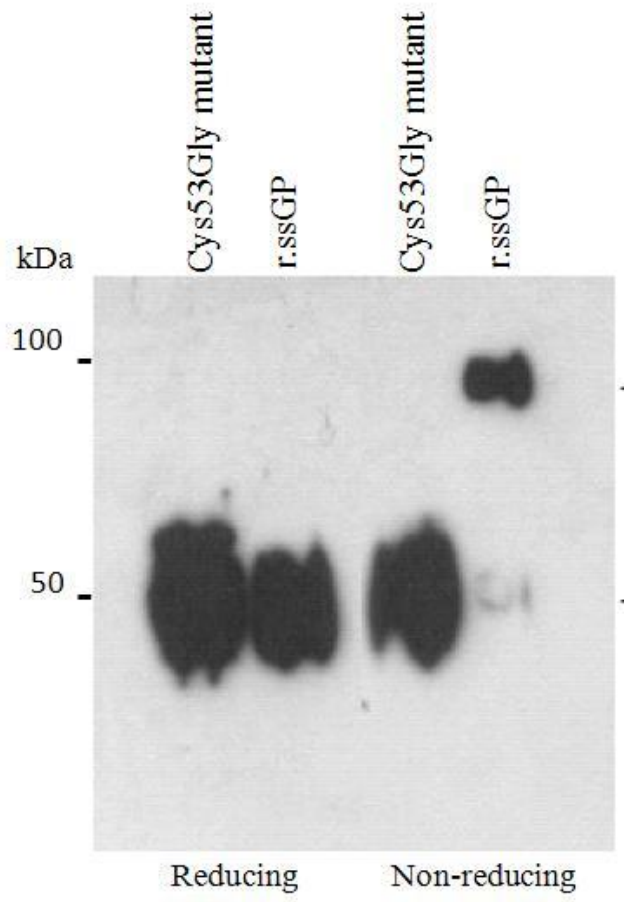

Figure 19. **Cysteine at position 53 is responsible for dimerization.** Site-directed mutagenesis was performed at amino acid position 53 (cysteine to glycine) and plasmid DNA was transfected into 293T cells. Proteins were detected by immunoblotting using Anti-HA peroxidase (1:10,000 dilution). Mutated ssGP was unable to oligomerize and appeared in the monomeric form only.

3.1.3.2 ssGP is N-glycosylated

The predicted MW for ssGP is approximately 29.5 kDa, but it migrates on reducing SDS-PAGE gel as a 50 kDa protein, similar to sGP (Figure 15B). It is known that $GP_{1,2}$ is heavily N- and O-glycosylated, whereas sGP seems to only carry N-glycans (Anthony Sanchez, 2007; Feldmann et al., 1994; Feldmann et al., 2001; Sanchez et al., 1998; Volchkova et al., 1998; Volchkova et al., 1999). Therefore, glycosylation as one form of post-translational processing was predicted for ssGP as well. For glycosylation analysis untagged r.ssGP and r.sGP were treated overnight with PNGaseF to remove all the N-linked carbohydrates before separation on reducing SDS-PAGE and immunoblotting analysis. Deglycosylated r.ssGP migrated with a lower MW (approximately 30 kDa) than deglycosylated r.sGP (approximately 33 kDa) indicating that ssGP contains N-glycans similar to sGP (Figure 20A) (Appendix 11). Endo H treatment of r.ssGP, which removes all mannose-type N-linked carbohydrates, did not result in a MW shift, indicating that ssGP N-glycosylation is mainly of the complex hybrid type (Figure 20B).

3.1.3.3 ssGP is not O-glycosylated

ssGP was further analyzed for O-glycosylation. O-glycanase removes core O-linked carbohydrates by breaking the bond between Gal β (1-3) GalNAc (N-acetyl galactosamine) and serine/threonine. In order for O-glycanase to work properly, additional monosaccharides need to be removed first from the core structure by exoglycosidases (Figure 21A). Treatment of r.ssGP with different exoglycosidases in

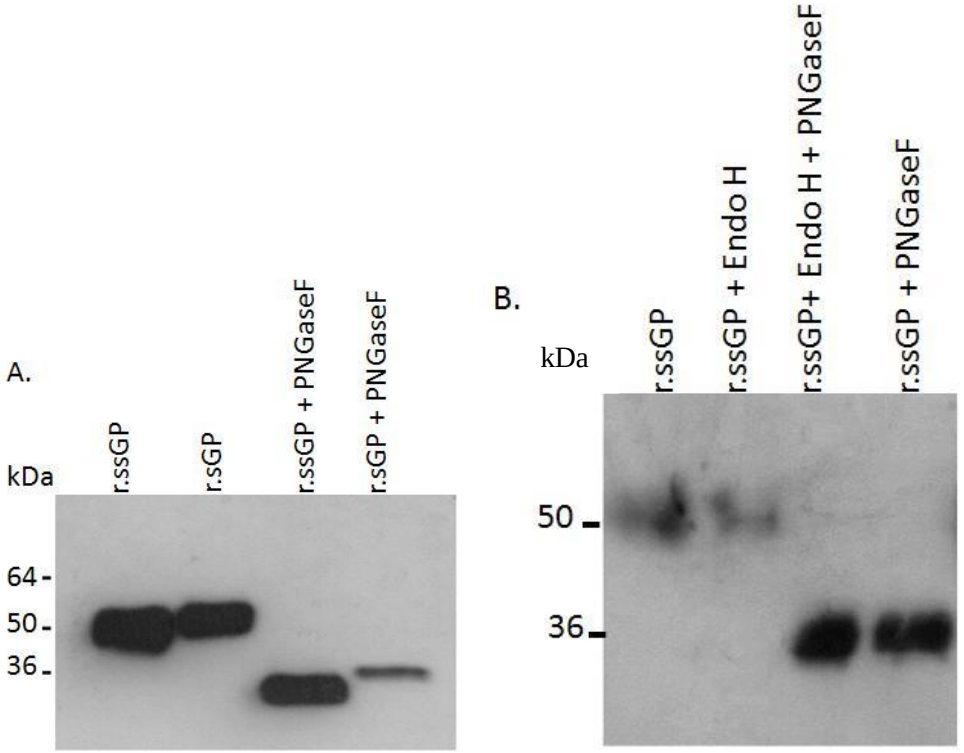

Figure 20. ssGP is glycosylated. A. ssGP contains N-linked carbohydrates. Proteins were treated with PNGaseF, separated under reducing 10% SDS-PAGE, and detected by immunoblotting using MAb 42/3.7 (1:10,000 dilution). The observed MW shift between treated and untreated proteins revealed N-linked glycosylation for ssGP similar to sGP. B. **ssGP does not contain high-mannose type N-linked carbohydrates.** HA-tagged r.ssGP was treated with Endo H (cleaves asparagine-linked high-mannose oligosaccharides, but not highly processed oligosaccharides from glycoprotein) and /or PNGaseF [cleaves all asparagine-linked (N-linked) oligosaccharides] and analyzed under reducing 10% SDS-PAGE followed by immunoblotting using Anti-HA peroxidase (1:10,000 dilution). No MW shift was observed between ssGP treated with/without Endo H indicating N-glycosylation with the complex hybrid type rather than the high-mannose type.

A.

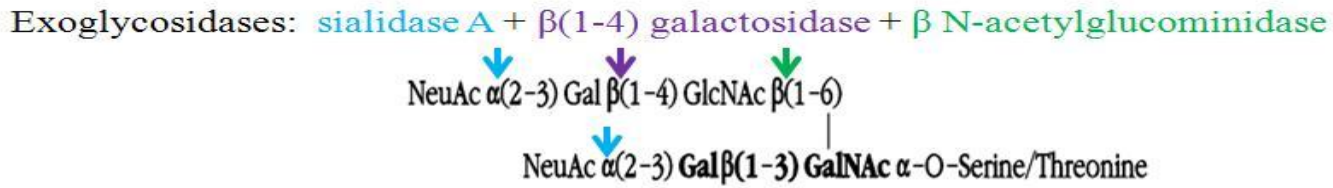
Exoglycosidases: sialidase A + β(1-4) galactosidase + β N-acetylglucominidase
NeuAc α(2-3) Gal β(1-4) GlcNAc β(1-6)
NeuAc α(2-3) Galβ(1-3) GalNAc α-O-Serine/Threonine

B.

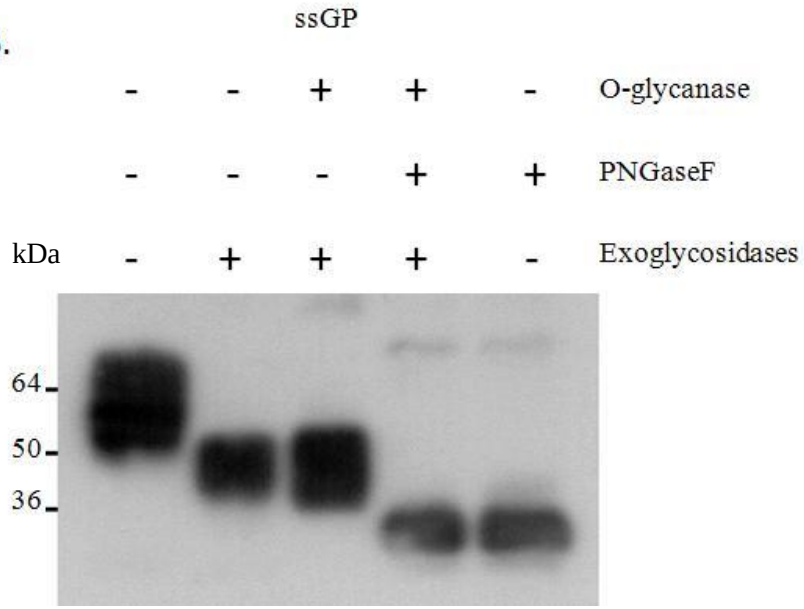
ssGP
- - + + - O-glycanase
- - - + + PNGaseF
kDa - + + + - Exoglycosidases
64
50
36

Figure 21: ssGP does not contain O-linked carbohydrates. A. Scheme for the specificity of certain exoglycosidases on one of the core type structures of O-linked glycans (Glyco-O-Glycanase technical information, Prozyme). **B.** HA-tagged r.ssGP was treated with different exoglycosidases, O-glycanase, N-glycanase (PNGaseF) or combinations of these glycosidases and subsequently analyzed on reducing 10% SDS-PAGE followed by immunoblotting. Lane 1, r.ssGP untreated; lane 2, r.ssGP treated with the exoglycosidases [sialidase A, β (1-4) galactosidase, and β-N-acetylglucosaminidase]; lane 3, r.ssGP treated with exoglycosidases [sialidase A, β (1-4) galactosidase, and β-N-acetylglucosaminidase] and O-glycanase; lane 4, r.ssGP treated with exoglycosidases [sialidase A, β (1-4) galactosidase, and β-N-acetylglucosaminidase], O-glycanase, and N-glycanase; lane 5, r.ssGP treated with N-glycanase. Protein detection was done using Anti-HA peroxidase (1:10,000 dilution). No obvious MW shift was observed between lanes 2 & 3 and lanes 4 & 5, indicating the absence of O-linked glycosylation on ssGP. However, MW shifts were observed between lane 1 and lane 2 due to exoglycosidase cleavage of N-linked carbohydrates.

combination with O-glycanase did not result in a MW shift following separation on reducing 10% SDS-PAGE, indicating that ssGP does not carry O-linked carbohydrates (Figure 21B), similar to what has been previously reported for sGP (Anthony Sanchez, 2007; Feldmann et al., 2001; Volchkova et al., 1998).

3.1.4 Studies to Determine ssGP Function

3.1.4.1 ssGP does not Bind to Neutrophils

Previously, it has been speculated that the nonstructural protein sGP plays a role in the pathogenesis of EHF (Sanchez et al., 1999). Previously it has been reported that sGP binds to human neutrophils via the IgG Fc receptor IIIb (FcγRIIIb, CD16b) and inhibits early neutrophil activation (Kindzelskii et al., 2000; Yang et al., 1998). Therefore, I performed ssGP binding experiments with neutrophils; however, neither ssGP nor sGP were found to bind to neutrophils in this study (Figure 22), supporting previous data that could not confirm a specific interaction between sGP and human neutrophils (Maruyama et al., 1998; Sui and Marasco, 2002).

3.1.4.2 ssGP does not have an Anti-inflammatory Function

The structural and biochemical similarities between ssGP and sGP would suggest that ssGP may function similarly to sGP. One of the established functions of sGP is its ability to have an anti-inflammatory function by stabilizing the endothelial barrier (Wahl-Jensen et al., 2005b). To determine whether ssGP could also function as an anti-inflammatory protein, endothelial cells were treated with TNF-α and ssGP. In contrast to results with sGP, no rescue effect was noted with added ssGP (Figure 23). In addition, as

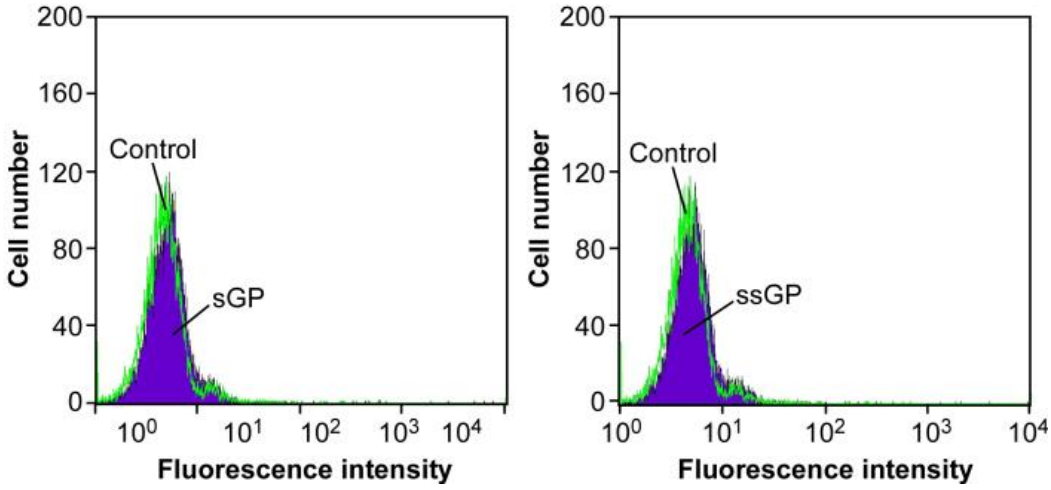

Figure 22. **ssGP does not Bind to Neutrophils.** Primary human neutrophils (10^6) were incubated with purified HA-tagged r.ssGP or HA-tagged r.sGP (20 ug/ml) for 30 min at 4^0C and subsequently stained with Anti-HA-PE (mouse mAb anti-HA conjugated to R-phycoerythrin) (1: 10 dilution) (Miltenyi Biotech) and analyzed by using a Flow Cytometry. Here control (Neutrophils + Anti-HA-PE) and ssGP (Neutrophils + ssGP+Anti-HA-PE), sGP (Neutrophils + sGP+Anti-HA-PE). For control purposes, an isotype mouse IgG1-PE (Miltenyi Biotech) was used. The lack of a shift in fluorescence intensity (green) between untreated and treated neutrophils indicates that neither sGP nor ssGP binds to the surface of human neutrophils (violet).

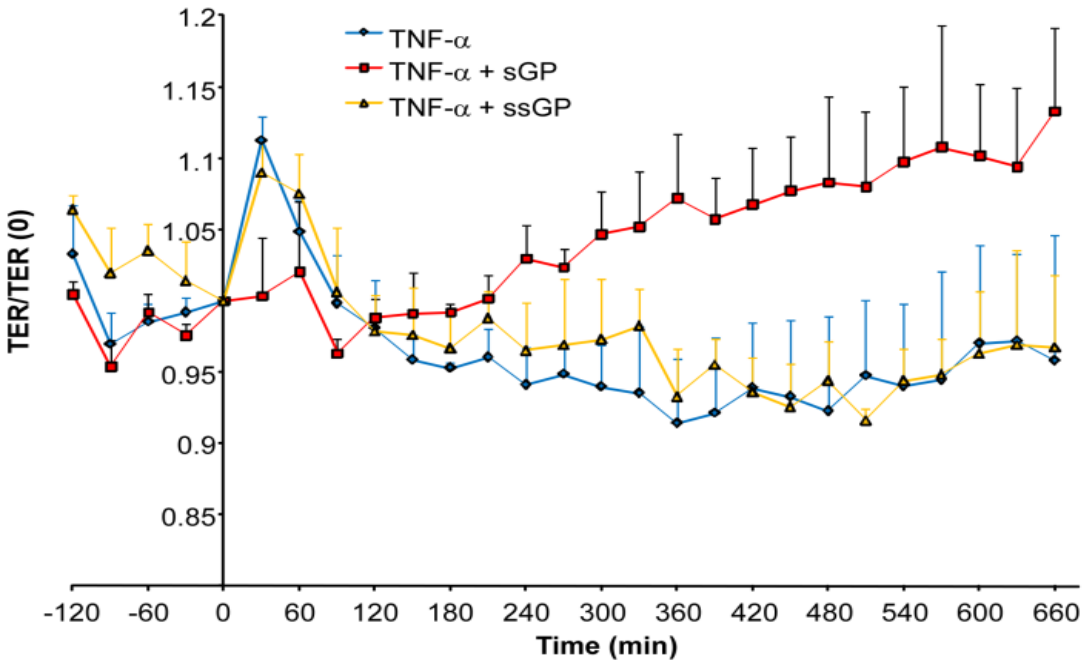

Figure 23. **ssGP does not affect endothelial barrier function.** Human umbilical vein endothelial cells (HUVECs) were equilibrated for 2 hr to generate a baseline transendothelial resistance (TER). TNF-α (1 ng/ml) with and without ssGP or sGP (30 ug/ml) were added to the medium as indicated and the chambers were monitored by impedance spectroscopy. There was a significant difference ($p<0.05$) at 360 min between the TER of cells treated with TNF-α alone and cells treated with TNF-α and sGP, while there was no significant difference between cells treated with TNF-α alone and TNF-α and ssGP. Each point represents mean +/- standard deviation of 3 replicates.

previously shown for sGP, ssGP alone did not affect the endothelial barrier function (data not shown).

3.2 RNA Editing is an Inherent Feature of the Genus *Ebolavirus*

Like ZEBOV, all other species of EBOV including the new species (*Bundibugyo ebolavirus*) contain the conserved GP gene ES (a hepta uridine stretch) (Figure 24). In contrast, *Marburgvirus*, the only other genus within the family *Filoviridae*, has no ES and thus expresses only the transmembrane glycoprotein from an unedited GP gene transcript. Therefore, all species of EBOV may produce multiple glycoproteins; however, this has so far only been studied for ZEBOV. A panel of polyclonal Abs were developed based on conserved peptide sequences, which detect transiently expressed sGP and $GP_{1,2}$ (Ou et al., 2011).Therefore, the second objective of my study was to test that RNA editing is an inherent feature of the genus *Ebolavirus* and that all EBOV express multiple glycoproteins encoded by the GP gene.

3.2.1 Development of a Rapid Assay for the Quantification of Transcripts Generated Through Viral RNA Editing

For the detection of multiple transcripts that differ by only a single nucleotide, a rapid transcript quantification assay (RTQA) was developed. This rapid assay does not utilize restriction enzyme digestion and ligation like the most commonly used method, AFLP, to determine single nucleotide polymorphism (Mueller and Wolfenbarger, 1999; Vos et al., 1995). To evaluate the assay for the detection and quantification of transcripts that differ by a single nucleotide, such as those encoding sGP and $GP_{1,2}$, two PCR

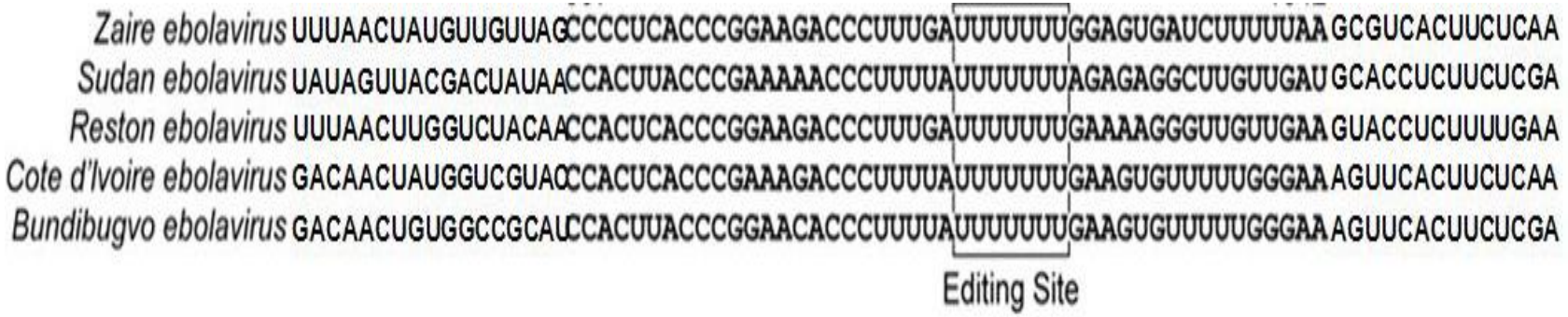

Figure 24. **The GP gene editing site (ES) is conserved among all Ebola viruses.** An alignment of the GP gene sequences (sequences are shown in negative sense) (Clone Manager version 9, Scientific and Educational Software) demonstrates the conservation of the ES for all EBOV species (shown in the box). GeneBank accession numbers: *Zaire ebolavirus* (AF086833), *Sudan ebolavirus* (AY729654), *Reston ebolavirus* (AF522874), *Cote d'Ivoire ebolavirus* (FJ217162), and *Bundibugyo ebolavirus* (FJ217161).

fragments representing unedited and edited transcripts of the EBOV GP gene were generated. The DNA was mixed in different known ratios and quantified using RTQA (Appendix 12 & 13). After establishing the assay, the methodology was applied to quantify transcripts from both *in vitro* and *in vivo* ZEBOV infections (Figure 25). Transcript ratios between sGP and $GP_{1,2}$ in infected Vero E6 cells was 5:1 as previously shown for ZEBOV (Volchkov et al., 1995). This method further quantified GP gene transcripts in two main target organs derived from ZEBOV infected NHP (in liver 5:1 and in blood 9:1)(Figure 25). When RTQA quantification was applied to genomic RNA derived from *in vitro* and *in vivo* infections, mostly unedited ES sequences (7U) were found, indicating that transcript polymorphism primarily occurs through RNA editing and not transcription of distinct genome pools (Figure 25).

3.2.2 All EBOV Species Produce Multiple GP gene Transcripts during infection

Vero E6 cells and primary human macrophages were infected with representative members of all the EBOV species (MOI of 0.1) and GP gene transcripts were quantified at 24, 96, and 144 hr post-infection. In ZEBOV infected cells, GP gene transcript ratios between unedited and edited were (5:1) and thus comparable with results, obtained by the cloning sequence approach for GP gene transcript quantification, reported in this thesis (Figure 12) and published earlier by others (Volchkov et al., 1995) (Figure 26A). Similar and slightly higher transcript ratios (ranging from 15-40%) were found with all human pathogenic EBOV species in both cell types studied (Figure 26C-E). The human apathogenic REBOV showed a considerably lower editing frequency of about 10% (Figure 26B). For all EBOV species the transcript ratios did not change significantly over time (Figure 26).

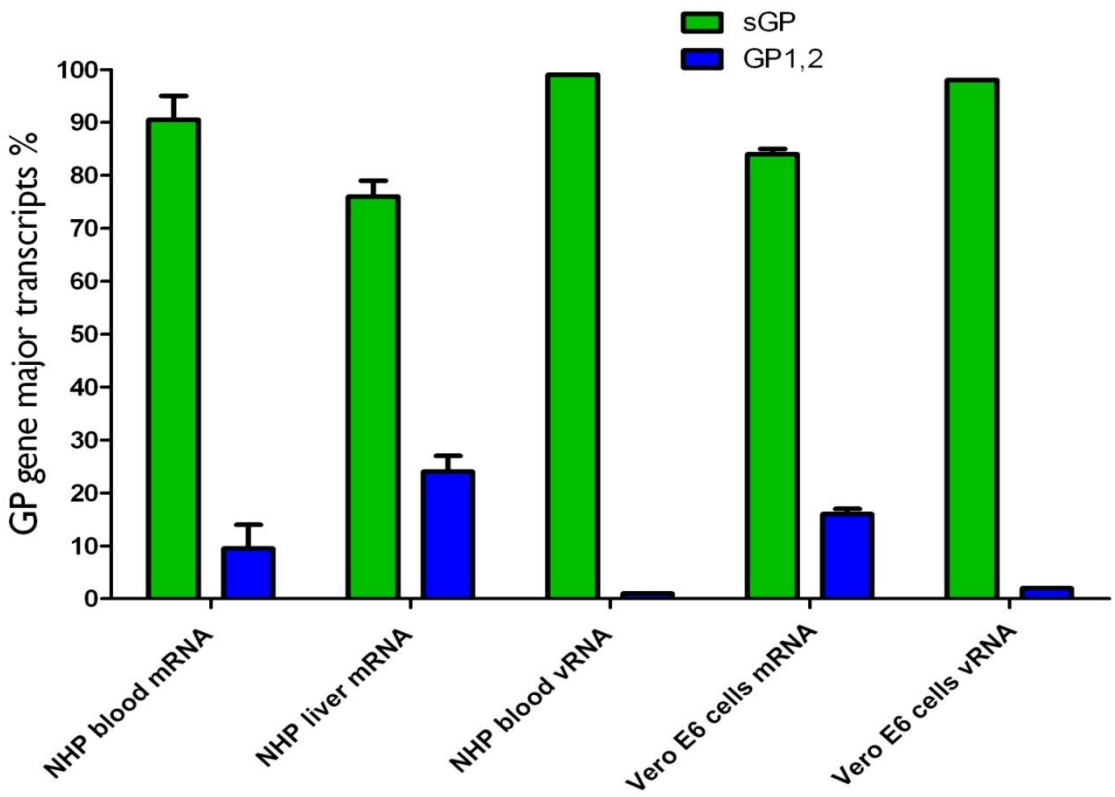

Figure 25. Q**uantification of *Zaire ebolavirus* (ZEBOV) RNA editing.** Transcripts (mRNA) and genomic RNA (vRNA) polymorphism were quantified using the rapid transcript quantification assay (RTQA) from RNA derived from ZEBOV infected nonhuman primates (NHPs) (100 PFU) and Vero E6 cells (MOI of 0.1). Mean and standard deviation of three independent transcript quantification (mRNA) from two infected animal samples are shown with exception for vRNA quantification (three independent transcription quantification from one animal sample).

A.

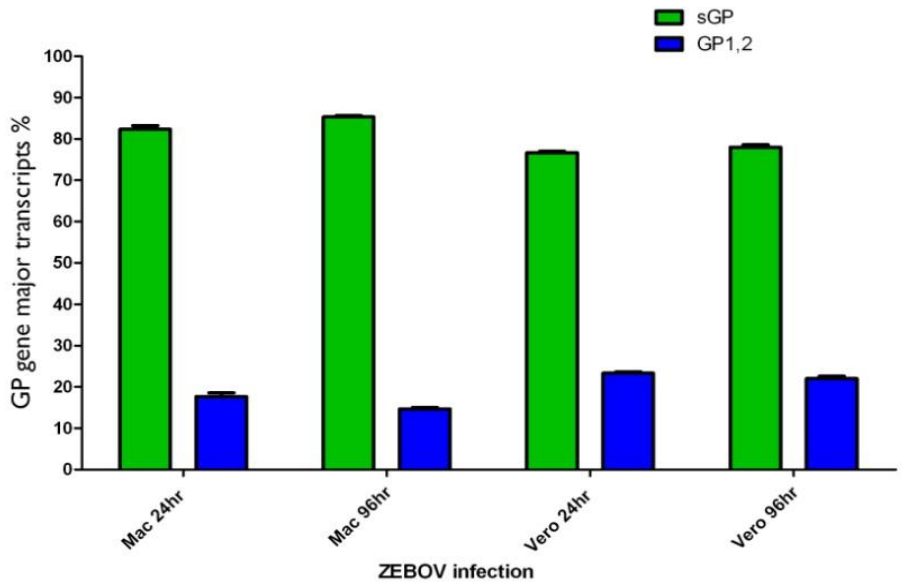
sGP
GP1,2
GP gene major transcripts %
100
90
80
70
60
50
40
30
20
10
0
Mac 24hr
Mac 96hr
Vero 24hr
Vero 96hr
ZEBOV infection

B.

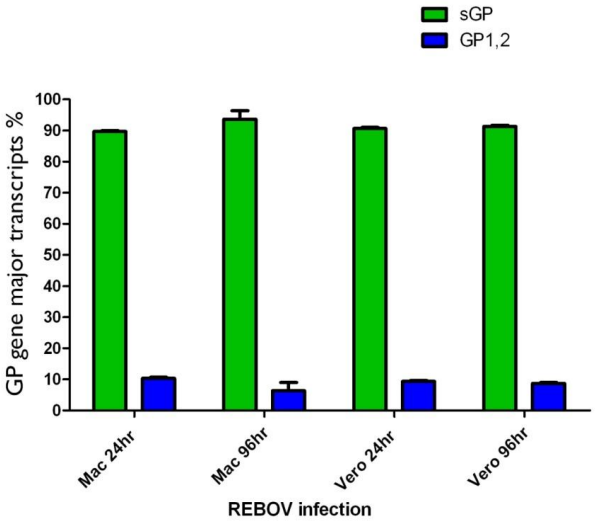
sGP
GP1,2
GP gene major transcripts %
100
90
80
70
60
50
40
30
20
10
0
Mac 24hr
Mac 96hr
Vero 24hr
Vero 96hr
REBOV infection

C.

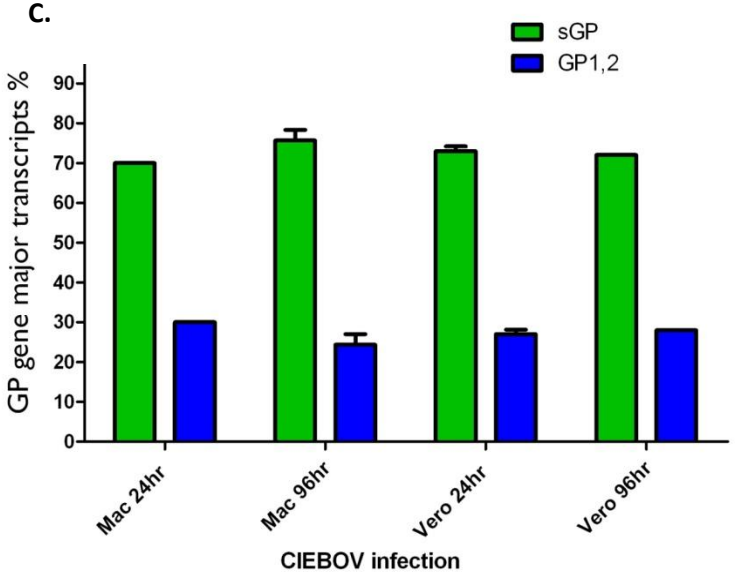
sGP
GP1,2
GP gene major transcripts %
90
80
70
60
50
40
30
20
10
0
Mac 24hr
Mac 96hr
Vero 24hr
Vero 96hr
CIEBOV infection

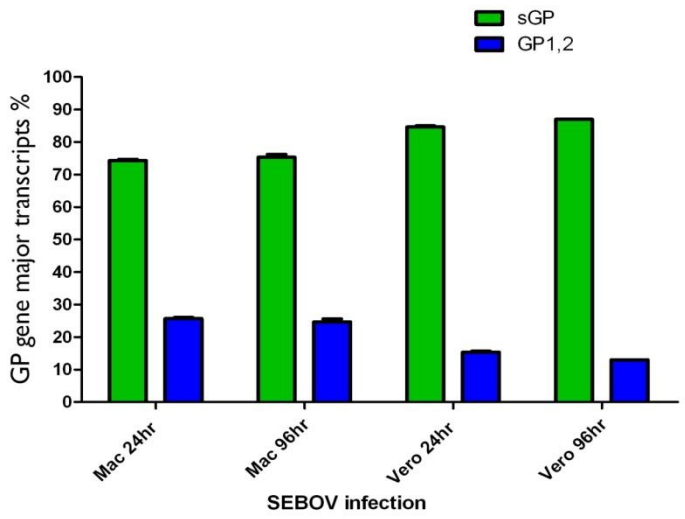
sGP
GP1,2
GP gene major transcripts %
100
90
80
70
60
50
40
30
20
10
0
Mac 24hr
Mac 96hr
Vero 24hr
Vero 96hr
SEBOV infection

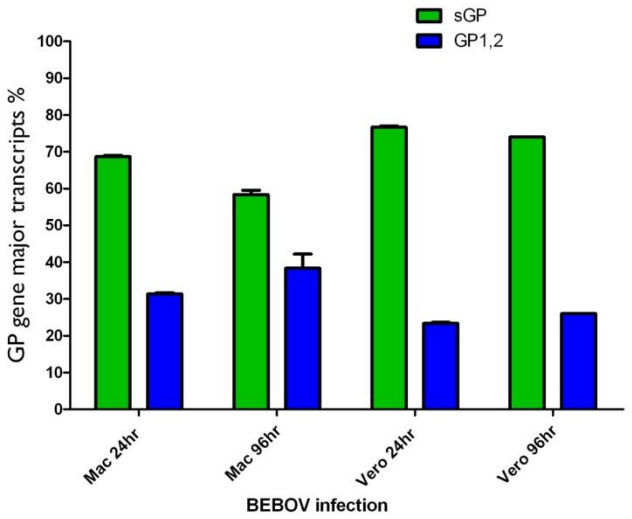
sGP
GP1,2
GP gene major transcripts %
100
90
80
70
60
50
40
30
20
10
0
Mac 24hr
Mac 96hr
Vero 24hr
Vero 96hr
BEBOV infection

Figure 26. **All EBOV species perform RNA editing of their GP gene.** Vero E6 cells (Vero) and primary human macrophages (Mac) were infected with representative members of all known EBOV species: (A) *Zaire ebolavirus* (ZEBOV) (strain Mayinga), (B**)** *Reston ebolavirus* (REBOV) (strain Pennsylvania), (C**)** *Cote d'Ivoire ebolavirus* (CIEBOV) (strain Boniface), (D**)** *Sudan ebolavirus* (SEBOV), and **(E)** *Bundibugyo ebolavirus* (BEBOV) using an MOI of 0.1. Quantification was done using the rapid transcript quantification assay (RTQA) in triplicate from three independent infections at 24 and 96 hr post-infection. All EBOV species produce multiple GP gene transcripts through RNA editing. Error bars: mean +/- standard deviation of 3 replicates.

To confirm expression of distinct GP gene products, SDS-PAGE analysis followed by immunoblotting using a cross-reactive GP-specific MAb was performed. For infection with all EBOV species, expression of sGP (~50 kDa) and $GP_{1,2}$ (GP_1 fragment ~150 kDa) could be confirmed at 4 days post-infection in the supernatant of infected Vero E6 cells (Figure 27). As demonstrated before for ZEBOV (Figure 20A), sGP expressed by all EBOV was N-glycosylated (Figure 28).

3.3 Characterization of EBOV RNA Editing

3.3.1 Development of a Minigenome system to study RNA editing

The minigenome system allows studying virus transcription and replication without the use of infectious virus. This is important for highly virulent viruses such as EBOV, because it lowers the containment level from BSL4 to BSL2. Here, I have utilized the ZEBOV minigenome system to study RNA editing. For this, the reporter cassette in the ZEBOV minigenome clone was replaced by the full-length GP gene coding region to study transcription and expression of sGP and $GP_{1,2}$. This modified EBOV minigenome (GP minigenome) was successfully rescued in 293T cells and demonstrated proper gene transcription, RNA editing, and protein translation (Figure 29, lane 1). RTQA was used to quantify transcripts and confirmed the previously found ratio of 80:20 for transcripts encoding sGP (unedited) and $GP_{1,2}$ (edited) (Figure 30) (Volchkov et al., 1995).

A truncated GP minigenome covering the GP gene ES (45 nt -7A- 58 nt =110 nt) showed a similar (slightly increased) ratio of edited versus unedited transcripts indicating

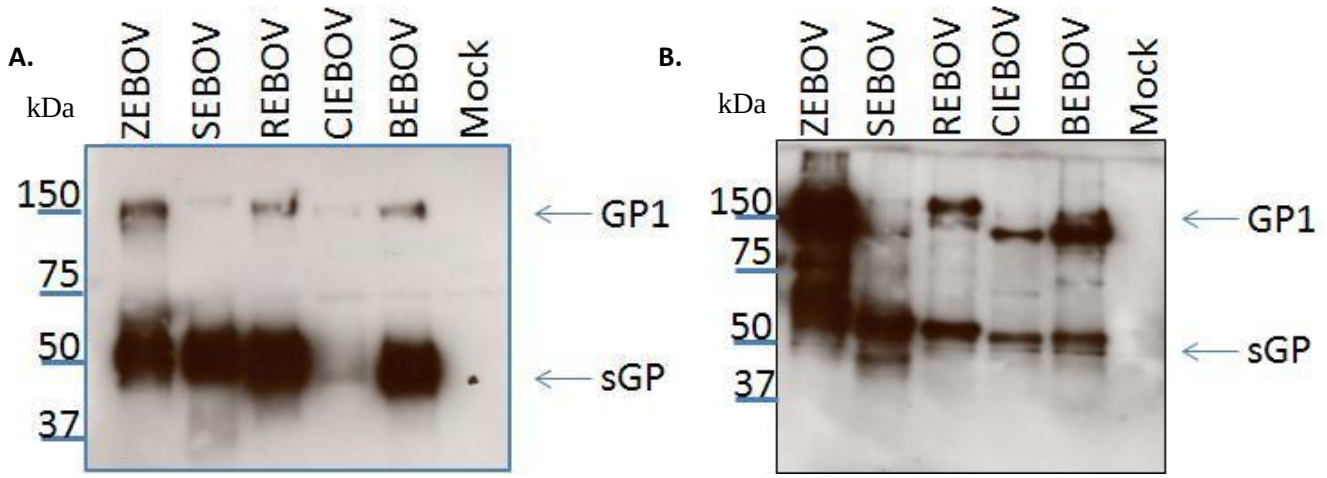

Figure 27. **All EBOV express sGP and $GP_{1,2}$.** Supernatants (A) and cell pellets (B) from Vero E6 cells infected with *Zaire ebolavirus* (ZEBOV) (strain Mayinga), *Reston ebolavirus* (REBOV) (strain Pennsylvania), *Cote d'Ivoire ebolavirus* (CIEBOV) (strain Boniface), *Sudan ebolavirus* (SEBOV), and *Bundibugyo ebolavirus* (BEBOV) (MOI of 0.1) (4 days post-infection) were run on 10% SDS-PAGE. sGP and GP_1 (the larger fragment of $GP_{1,2}$) were detected by immunoblotting using the 42/3.7 MAb (1:10,000 dilution). All proteins appeared similar in size on reducing SDS-PAGE.

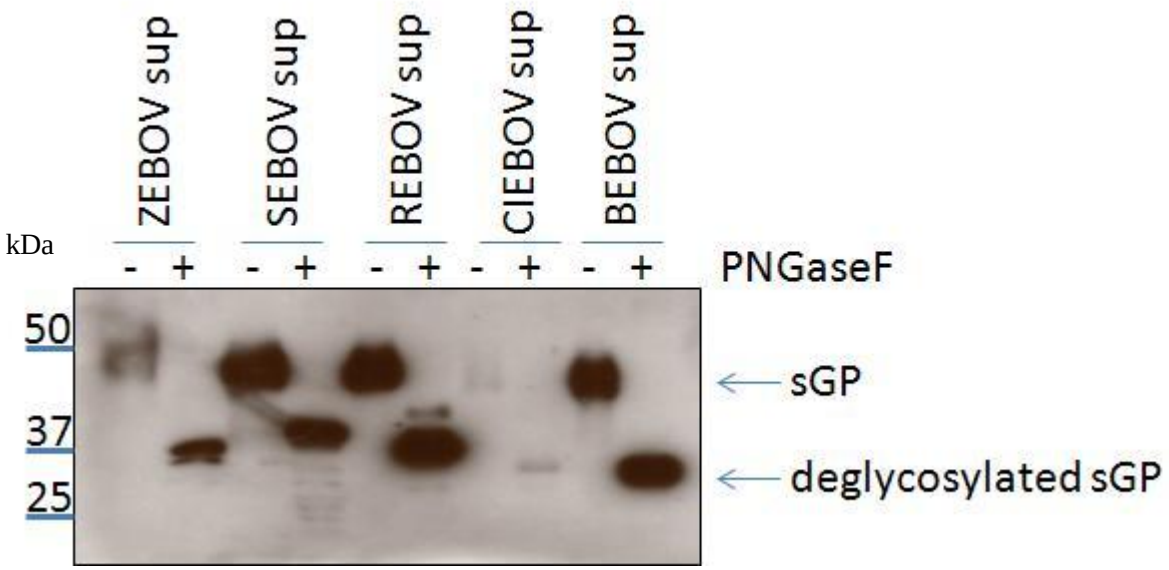

Figure 28. **sGP expressed by all EBOV is N-glycosylated.** Supernatants from the EBOV infected Vero E6 cells with *Zaire ebolavirus* (ZEBOV) (strain Mayinga), *Reston ebolavirus* (REBOV) (strain Pennsylvania), *Cote d'Ivoire ebolavirus* (CIEBOV) (strain Boniface), *Sudan ebolavirus* (SEBOV), and *Bundibugyo ebolavirus* (BEBOV) (MOI of 0.1) were treated overnight with PNGaseF and run on 10% SDS-PAGE. Proteins were detected by immunoblotting using the 42/3.7 MAb (1:10,000 dilution). PNGaseF sensitivity of all sGPs confirms their N-glycosylation.

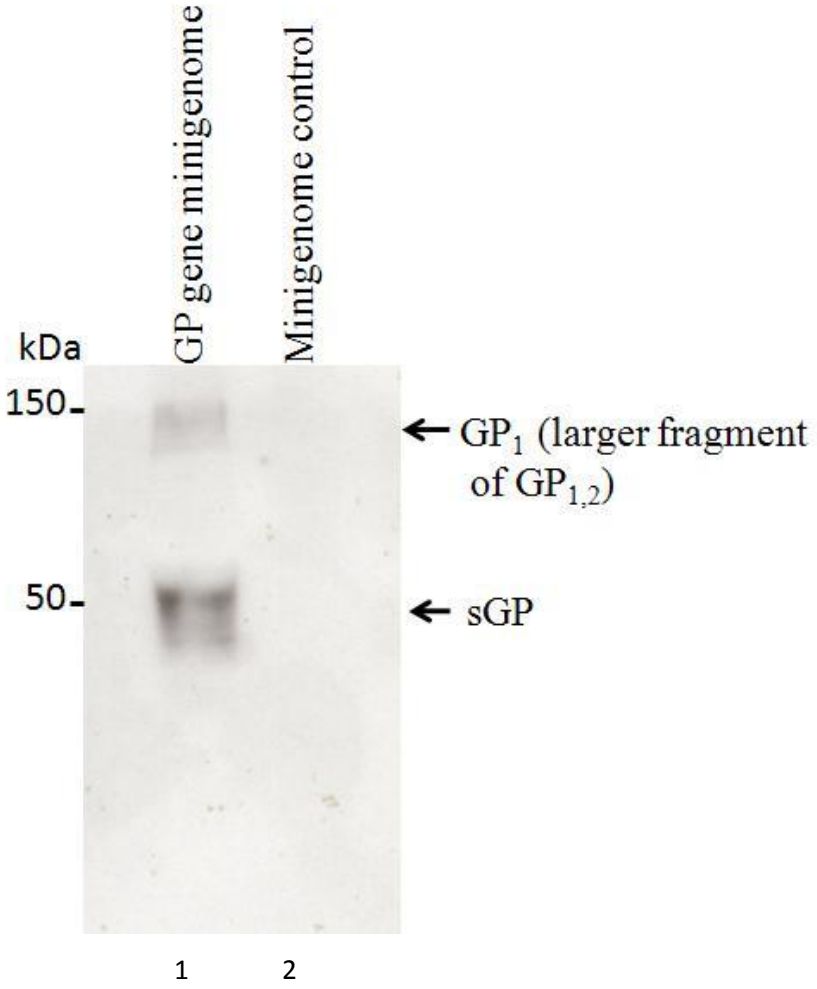

Figure 29. **A *Zaire ebolavirus* (ZEBOV) minigenome expresses distinct glycoproteins through RNA editing.** 293T cells were transfected with the GP minigenome DNA (schematic is shown in Figure 6). Cells were harvested at 72 hr post-transfection, and proteins were subjected to 10% reducing SDS-PAGE. Lane 1, cell pellet from GP minigenome. Lane 2, cell pellet from GP minigenome without using viral polymerase plasmid (minigenome negative control). Proteins were detected by immunoblotting using the 42/3.7 MAb (1:10,000 dilution). sGP and GP_1 detection confirmed proper transcription and editing with this minigenome system.

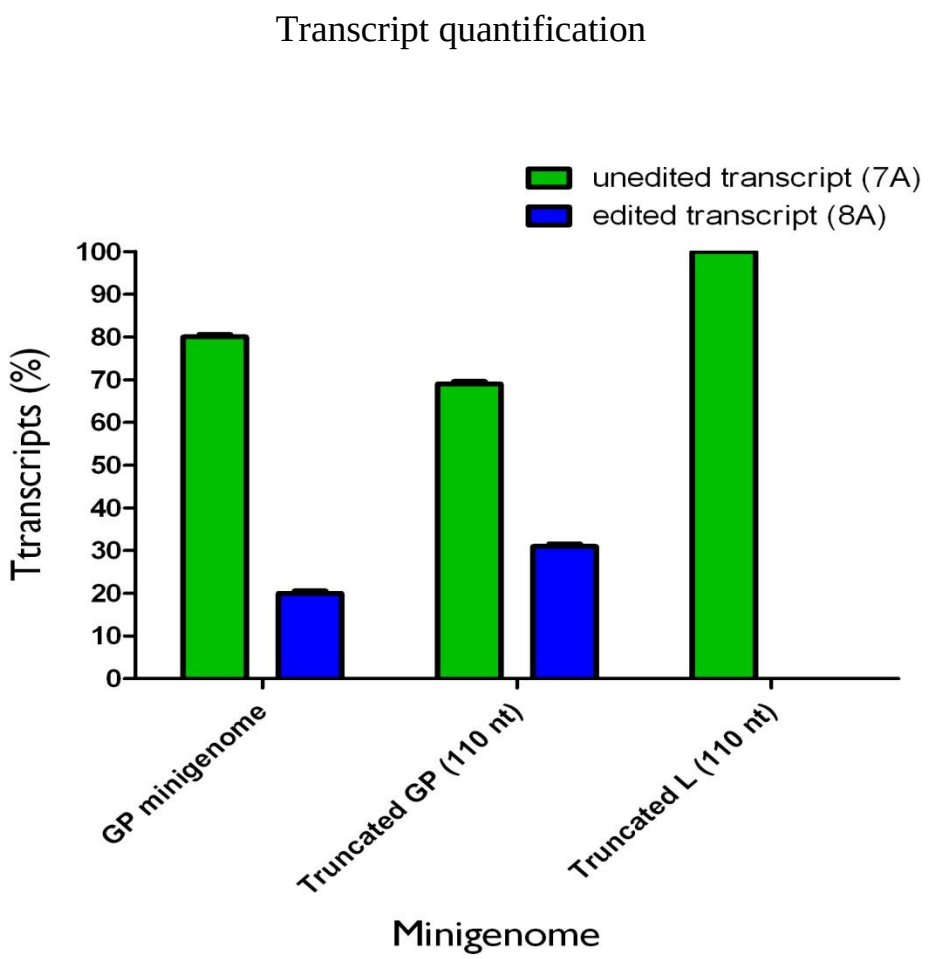

Figure 30. **RNA editing is GP gene specific.** 293T cells were transfected with the GP minigenome RNA, truncated GP minigenome RNA or truncated L minigenome RNA. Cells were harvested 48 hr after transfection and transcripts (unedited and edited) were quantified by the rapid transcript quantification assay (RTQA) using respective primers for GP and L gene sequences. Edited transcripts were detected with the minigenomes encoding for the GP gene full-length and truncated ORFs but not with the minigenome encoding the truncated L ORF indicating that RNA editing is GP gene-specific. Quantification was done in triplicates from three independent minigenome rescues. Error bars: mean +/- standard deviation of 3 replicates.

that this truncated minigenome can be used as a model system to further study structural requirements for RNA editing (Figure 30). A minigenome containing a truncated L ORF including a putative L gene ES did not support RNA editing, indicating that this site is not used for RNA editing, despite fulfilling the primary sequence requirements. This strongly suggests the importance of cis-acting sequences for RNA editing (Figure 30).

In the following experiments the minigenome system was used in two different ways. In a few experiments, simultaneous transfection of only plasmid DNA including the minigenome plasmid, the EBOV-specific helper plasmids encoding NP, VP35, VP30 and L, and the plasmid encoding T7 bacteriophage polymerase was performed (schematically shown in Figure 6). In most cases, however, the minigenome plasmid DNA was first *in vitro*-transcribed to generate RNA (minigenome RNA) using the T7 promoter. This was done to avoid potential issues with remaining plasmid DNA for subsequent analysis. For minigenome RNA transfections, 293T cells were first transfected with the EBOV helper plasmids encoding NP, VP35, VP30, and L, followed by transfection of the minigenome RNA 48 hr later. In both cases, transcripts and reporter protein expression were analyzed using the established RTQA and FACS (unless otherwise stated), respectively. In the following experimental description, I will refer to minigenome DNA or minigenome RNA transfection when addressing the above described procedures.

3.3.2 Dual-reporter Minigenome for studying EBOV RNA Editing

To use the successfully established truncated GP minigenome system to confirm RNA editing at the protein level, I developed a dual-reporter cassette with an upstream

eGFP ORF and a downstream mCherry ORF. The two ORFs are connected by the truncated GP gene ES (110 nt sequence) in such a way that only in case of RNA editing would mCherry expressed (dual-reporter minigenome) (Figure 31). These fluorescence reporters are far apart in terms of their respective excitation and emission spectra, therefore background signal is negligible in their respective channels and allows better separation between the signals (Appendix 14). The C-terminal end of mCherry contains an NLS (Figure 31D) for easy discrimination of the cytoplasmic eGFP (no RNA editing) and nuclear localization of the expressed eGFP-mCherry fusion protein (RNA editing). As a pilot experiment, the cassette (eGFP-110nt-mCherry-NLS) was cloned into the plasmid pCAGGS for transient expression in 293T cells (Figure 32). To mimic RNA editing a 7 and an 8A ES version of the cassette were transiently expressed. As predicted, the 7A construct resulted in cytoplasmic expression of eGFP and no expression of mCherry (Figure 32, top panel). The 8A version (eGFP-ES111nt-mCherry-NLS) resulted in expression of the eGFP-mCherry fusion protein which, due to the C-terminal NLS, localized to the nucleus (Figure 32, bottom panel). The quantification of the fluorescence signals from the expressed proteins was done using FACS (Appendix 15). This proved the feasibility of the dual-reporter casette to study RNA editing at the protein level. Furthermore, RTQA was able to quantify respective transcripts from the transient expression of the dual-reporter cassette (data not shown). In a next step, the dual-reporter cassette was introduced into the ZEBOV minigenome plasmid (dual-reporter minigenome) to study EBOV polymerase-driven RNA editing (schematically shown in Figure 7). 293T cells were transfected with the dual-reporter minigenome DNA as described in 2.9.1. At 48 hr post-transfection, eGFP signals were observed both in the

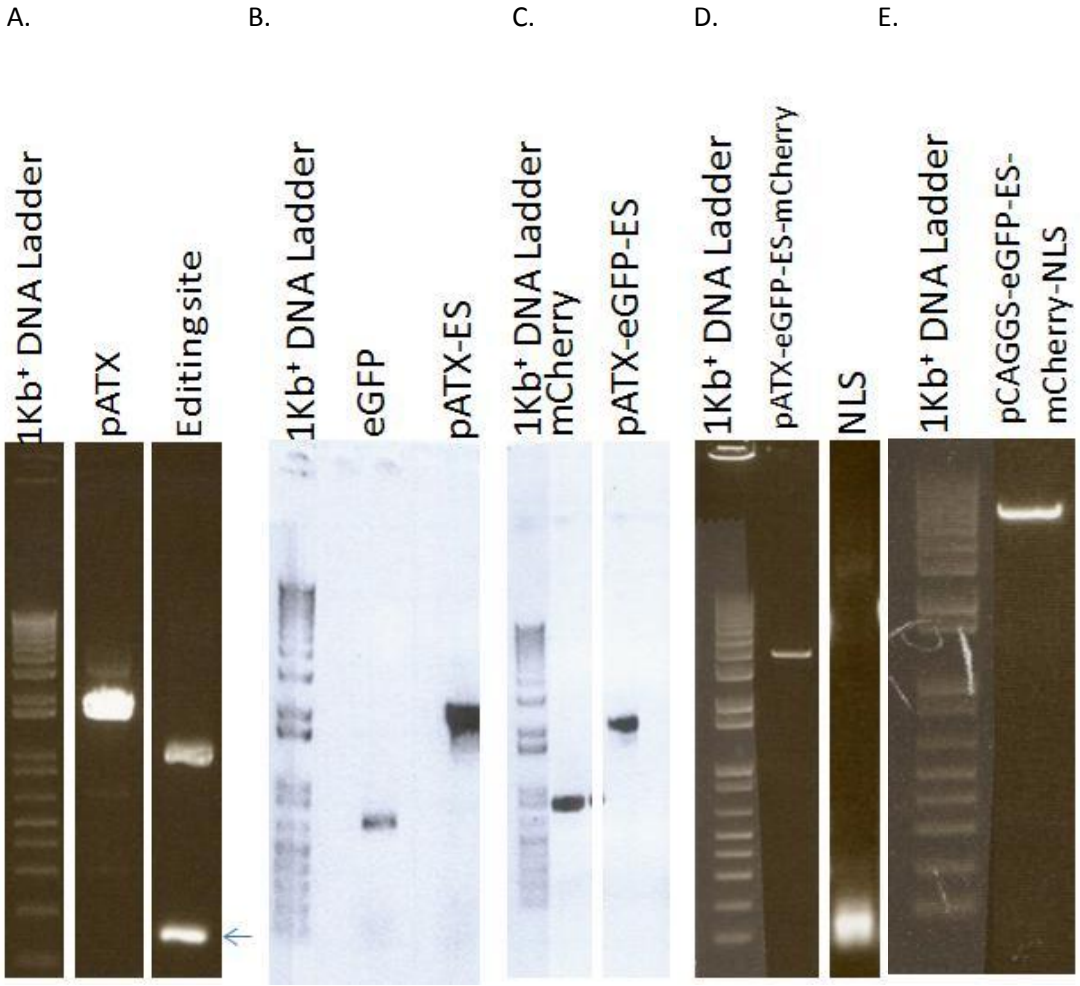

Figure 31. **Generation of a dual-reporter cassette. A.** PCR fragment (110 nt) covering the GP gene ES (lane 2) for insertion into the sub-cloning plasmid pATX. **B.** PCR amplified eGFP ORF for insertion into pATX-ES(110 nt). **C.** PCR amplified mCherry ORF for insertion into pATX-eGFP-ES(110 nt). **D.** PCR amplified NLS for insertion into pATX-eGFP-ES(110 nt)-mCherry. **E.** PCR amplified entire minigenome cassette [eGFP-ES(11ont)-mCherry-NLS] inserted into the expression plasmid pCAGGS.

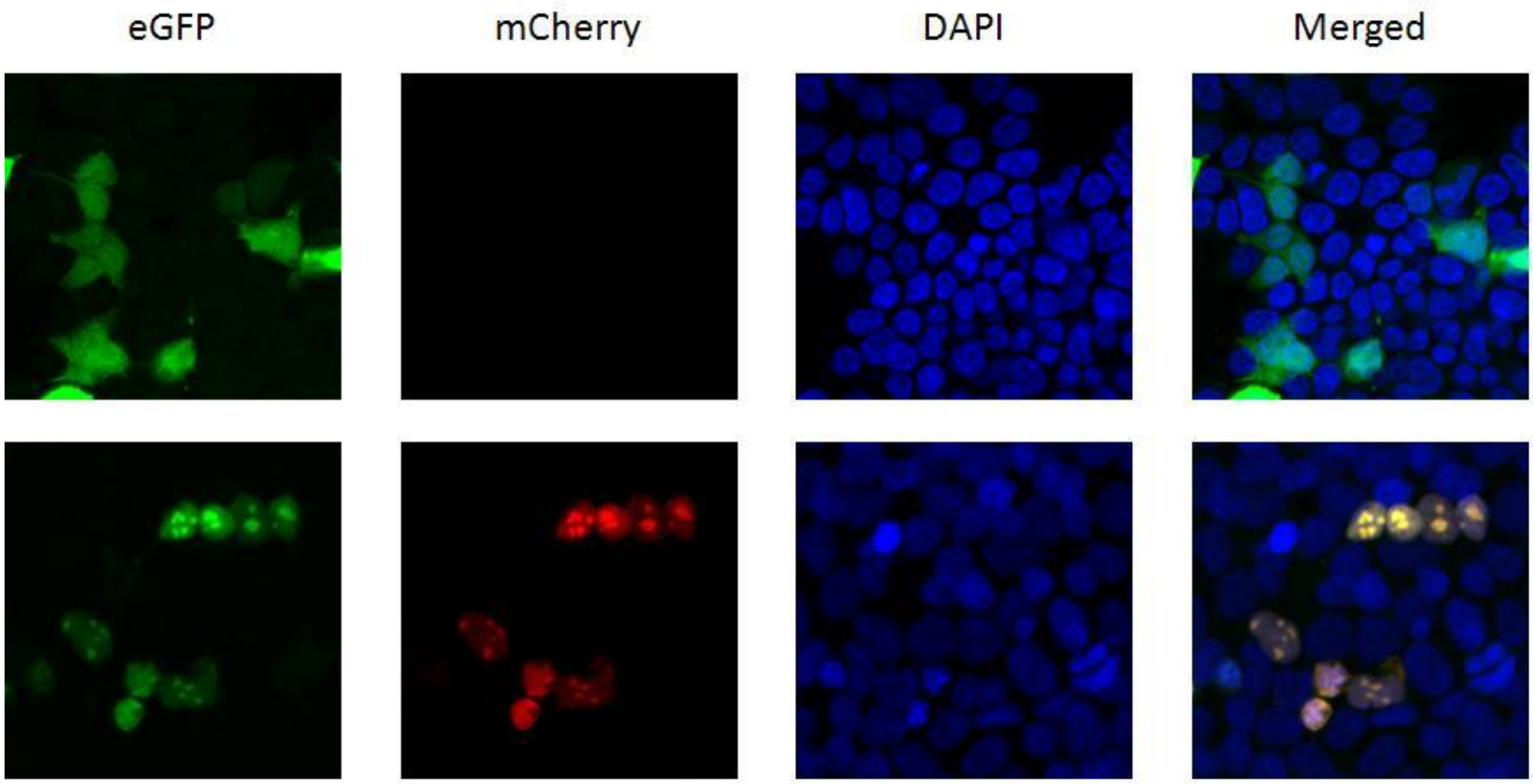

Figure 32. **Reporter proteins are expressed from the dual-reporter cassette (pilot experiment).** In the top panel the dual-reporter cassette with 7 adenosine residues at the GP gene ES (eGFP-110 nt-mCherry-NLS) is expressed following transfection in 293T cells. This allows for cytoplasmic eGFP expression but no mCherry expression (not in frame). The bottom panel shows transient expression in 293T cells after transfection of the dual-reporter cassette with 8 adenosine residues in the GP gene ES (eGFP-111 nt-mCherry-NLS). This allows for expression of the eGFP-mCherry fusion protein which localized to the nucleus due to the C-terminal NLS.

cytoplasm (encoded by the unedited transcript) and nucleus as a fusion protein with mCherry (encoded by the edited transcript) (Figure 33, top panel).The nuclear localization of the fusion protein is mediated through the incorporated NLS. This confirms that RNA editing occurs in the minigenome system. No expression of either protein was observed when the L expression plasmid was omitted from the transfection (negative control) (Figure 33, middle panel).

To exclude plasmid DNA contamination (dual-reporter minigenome DNA) as a template for PCR amplification during transcript quantification by RTQA, *in vitro*-transcribed dual reporter minigenome RNA was transfected into 293T cells along with the necessary helper plasmids as described in 2.9.2. RNA editing was identified following minigenome RNA transfection (Figure 33 bottom).

Like other NNS RNA viruses, ZEBOV transcription occurs in the cell cytoplasm, which reduces the possibility of cellular polymerase driven transcription/RNA editing that might occur in the cell nucleus. However, it has been shown that other viral polymerases can edit EBOV mRNA (Volchkov et al., 1995). To rule out the possibility of T7-driven editing during DNA dependent RNA transcription from the minigenome DNA, the dual-reporter cassette was introduced into the pTM1 vector under the control of the T7 promoter. T7-driven expression of the dual-reporter cassette failed to produce edited transcript as evidenced by undetectable mCherry signal (Appendix 16).

3.3.3. Requirements for EBOV RNA Editing

3.3.3.1The ES is a primary requirement for RNA Editing.

Results

To investigate the structural requirements for RNA editing, mutations were introduced into the primary ES sequence by replacing the A residue at position 3 or 6 by a G residue. *In vitro*-transcribed minigenome RNA was transfected into 293T cells and reporter gene expression was analyzed 48 hr post RNA transfection. RNA editing was abolished after introduction of the single mutations as demonstrated by only eGFP expression and no evidence for mCherry expression (Figure 34). This indicates the importance of the primary ES sequence for RNA editing. However, rare nuclear eGFP signals were observed in some cells due to the known inherent ability of eGFP to occasionally translocate to the nucleus (Seibel et al., 2007). In addition to fluorescence reporter visualization, fluorescence signals (eGFP and mCherry) were quantified from eGFP expressing cells by FACS. For this, total signals from the dual-reporter minigenome were set to 100% (standard). Despite the importance of the primary ES sequence for RNA editing (described above), a dual-reporter minigenome containing only the ES without surrounding up- and downstream cis-acting sequences showed dramatically reduced RNA editing, as evidenced by reduced mCherry expression (encoded only by the edited transcript) (Figure 34 & 35). Deletion of one, either the up- or downstream cis-acting sequences, resulted in reduced RNA editing activity, which, however, was higher than that of the minigenome with just the ES sequence and no surrounding cis-acting sequences (Figure 35). This indicates that both up- and downstream cis-acting sequences are important for RNA editing. The FACS based quantification result was supported by reporter expression visualization, shown for only ES dual-reporter minigenome rescues (Figure 34) and by transcript quantification shown

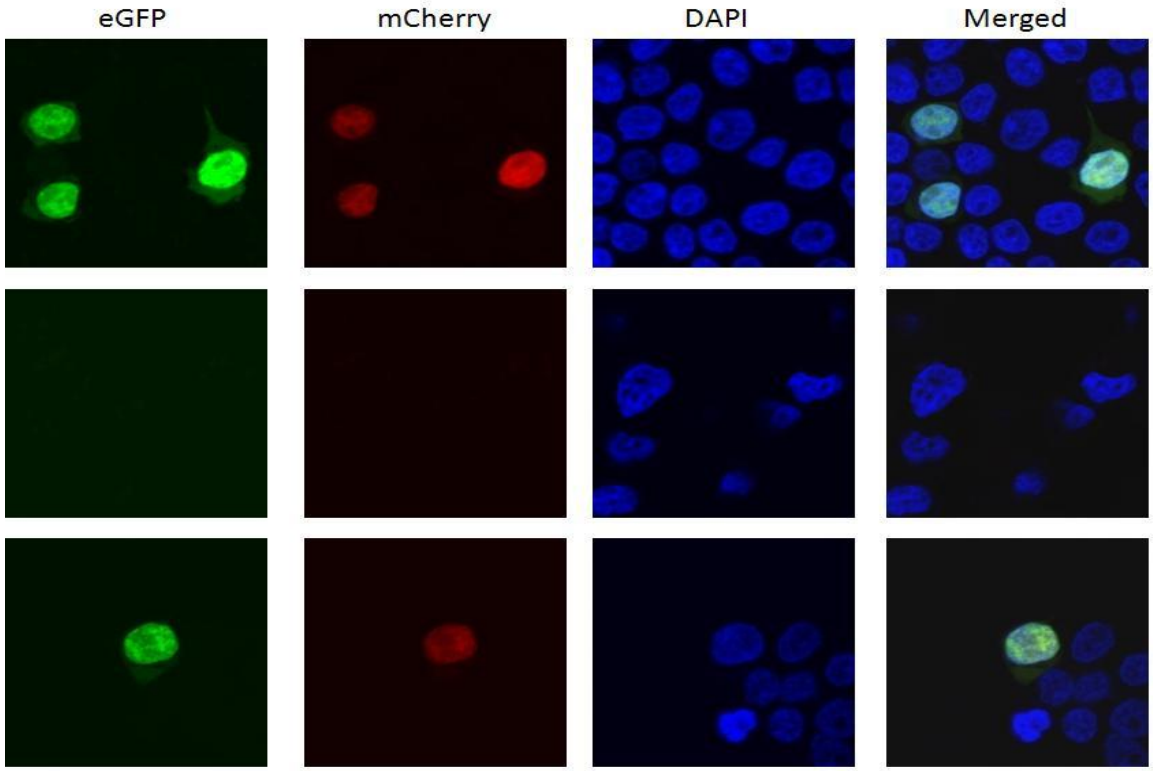

Figure 33. **RNA editing using the dual-reporter minigenome system.** The dual-reporter minigenome DNA was transfected into 293T cells. Expression was analyzed by fluorescence microscopy 48 hr post-transfection. The top panel shows cytoplasmic and nuclear eGFP expression as well as nuclear mCherry expression, indicating that editing occurs. The middle panel is a control experiment omitting the expression plasmid for the *Zaire ebolavirus* (ZEBOV) polymerase (no transcription). The bottom panel shows expression following transfection of 293T cells with *in vitro*-transcribed dual-reporter minigenome RNA along with the necessary helper plasmids.

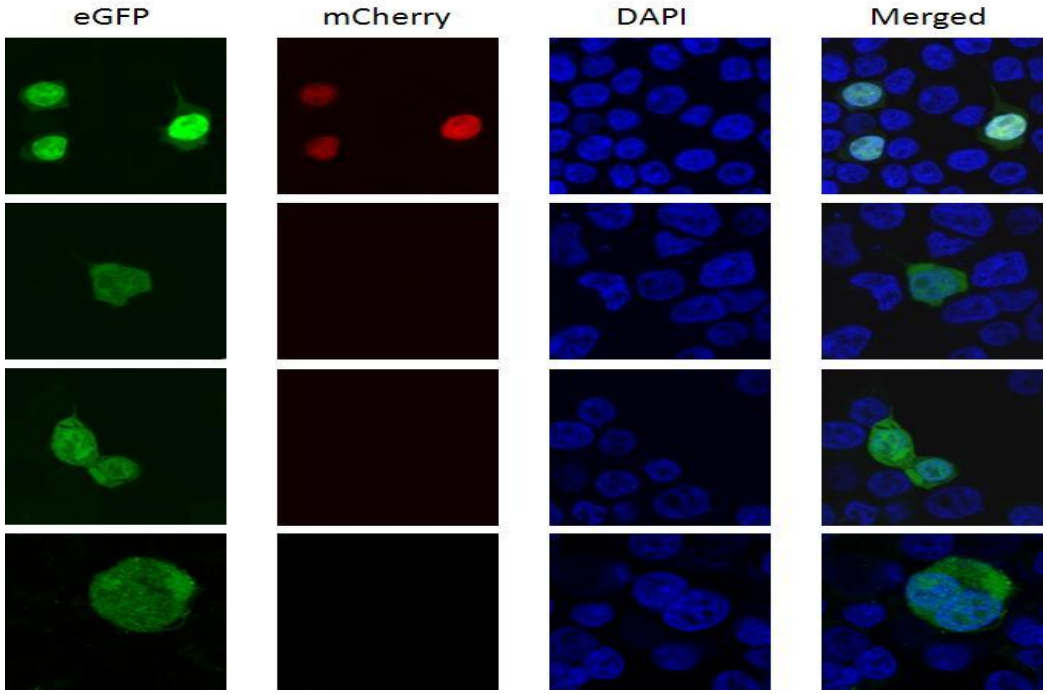

Figure 34. **The editing site (ES) sequence is important for RNA editing.** *In vitro*-transcribed minigenome RNA was transfected into 293T cells and reporter genes expression was analyzed at 48 hr post-transfection. Mutations in the primary ES sequence [A to G replacement at position 3 in the conserved ES (AAGAAAA) or 6 (AAAAAGA)] abolished editing as indicated by eGFP only and no mCherry expression (edited transcripts only) (upper and lower middle panels). The conserved ES (no surrounding up- and downstream cis-acting sequences) alone cannot support editing as indicated by eGFP only and no evidence for mCherry expression (edited transcripts only) (bottom panel). Transfection of unaltered dual-reporter minigenome DNA (positive control) resulted in RNA editing (upper panel).

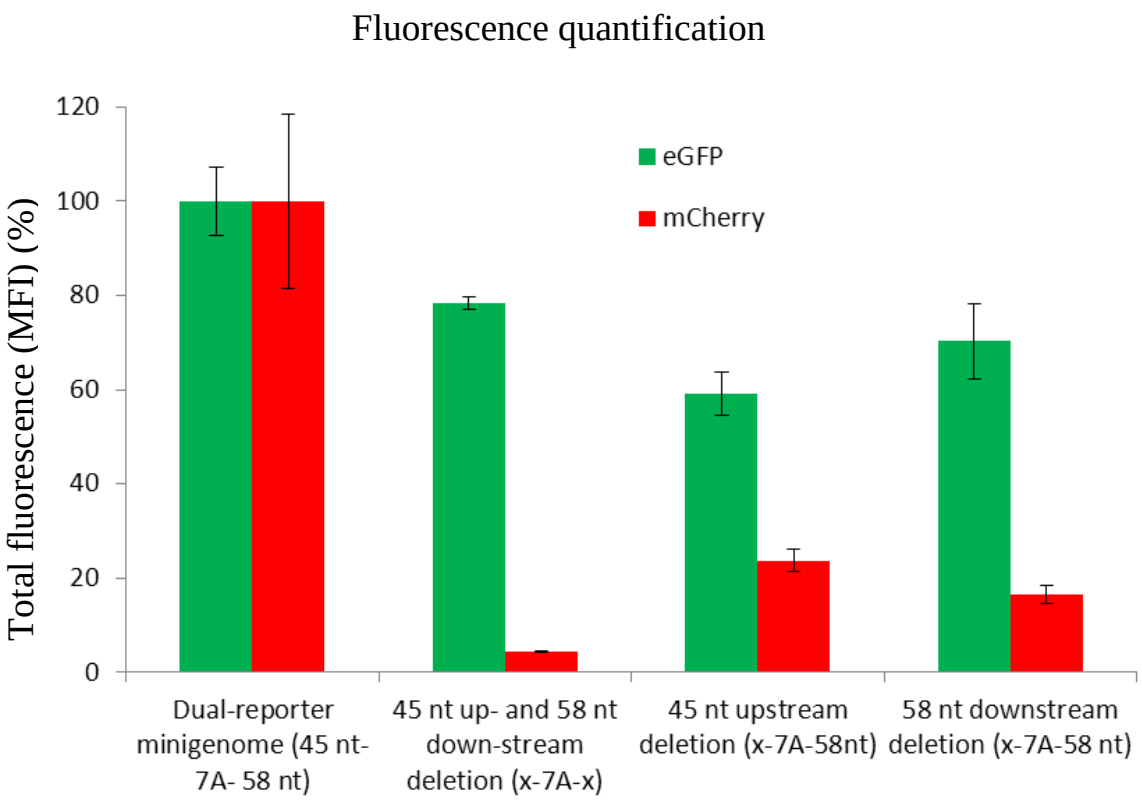

Figure 35: **Up- and downstream cis-acting ES sequences are important for RNA editing**. *In vitro*-transcribed dual-reporter minigenome RNA was transfected into 293T cells and reporter expression was analyzed 48 hr post-transfection by fluorescence activated cell sorting (FACS). For quantification, total eGFP and mCherry signals [mean fluorescence intensity (MFI)] from the unaltered dual reporter minigenome were set to 100% (standard). Deletion of the 45 nt up- and 58 nt downstream cis-acting ES sequences resulted in drastically reduced RNA editing (mCherry signal reduction). Furthermore, deletion of either the 45 nt up- or 58 nt downstream cis-acting ES sequences resulted in less reduced RNA editing. Error bars: mean+/- standard deviation of 3 replicates.

here for the mutant with the upstream cis-acting sequences deleted (a 10-fold reduction of edited RNA transcripts) (Figure 36).

3.3.3.2 The region of 18 nt up- and 9 nt downstream of the ES are important for RNA editing

The up- and downstream cis-acting sequences surrounding the ES were subjected to deletion analysis as shown in Figure 8A. Transfection of dual-reporter minigenome DNA into 293T cells and analysis of protein expression 48 hr post-transfection determined that the region of 18 nt up- and 9 nt downstream of the ES is sufficient to support RNA editing (Figure 37). Further deletions have not been undertaken.

3.3.3.3 VP30 is a Putative Factor for RNA Editing

Transcription of the ZEBOV minigenome is totally dependent on the expression of ZEBOV L, NP, and VP35 (data not shown), but not VP30 (Figure 38). However, overall reporter expression (eGFP) was reduced in the absence of VP30 (Figure 38A). Interestingly, minigenome assays lacking VP30 showed a dramatic reduction in mCherry expression, indicating a putative role of this protein for RNA editing (Figure 38A & B). This observation was confirmed when fluorescence signals were quantified using ImageJ software (Appendix 18 and 19).

It has been shown that VP30 functions as a transcription activator by overcoming a secondary structure (stem-loop) within the 3' leader sequences just upstream of the NP gene transcriptional start-site (Weik et al., 2002). To determine if VP30 putative role in RNA editing is independent of its function in transcript activation, I compared RNA

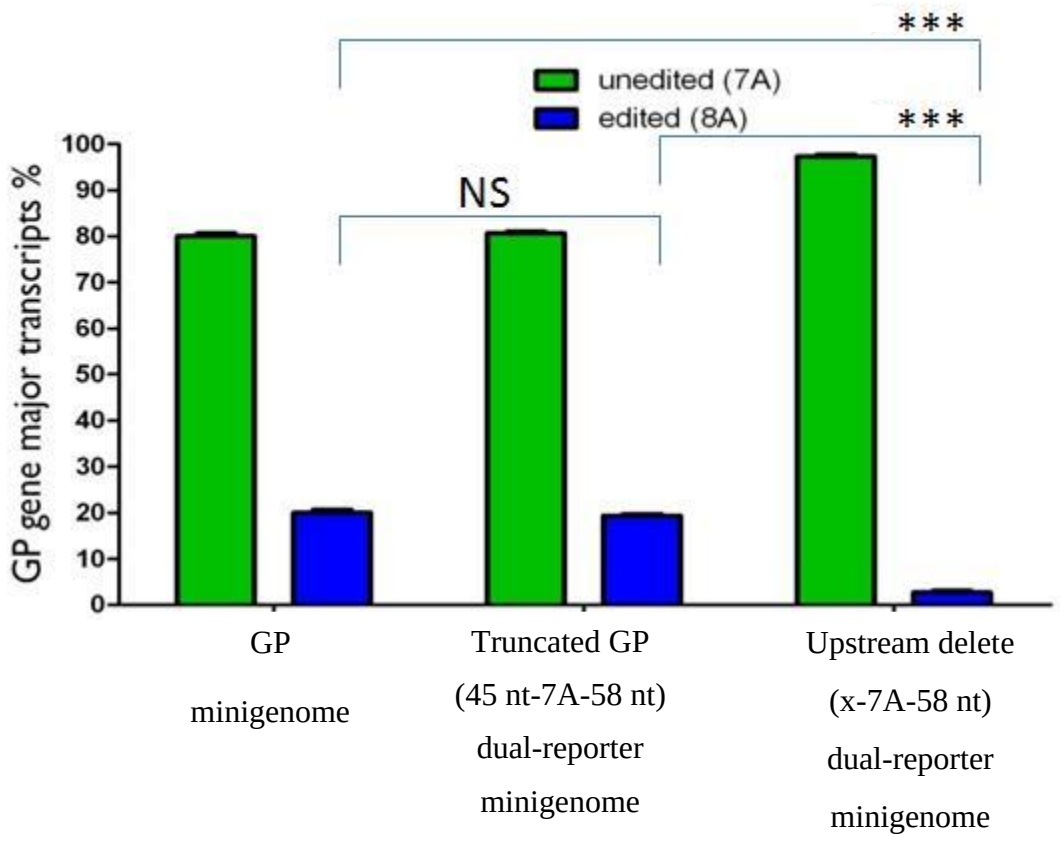

Figure 36: **Deletion of upstream cis-acting editing site (ES) sequence reduced RNA editing.** *In vitro*-transcribed dual-reporter minigenome RNA was transfected into 293T cells and transcripts were analyzed 48 hr post-transfection. Transcripts were quantified by the rapid transcript quantification assay (RTQA) in triplicate from three independent minigenome rescues. A significant reduction (n= 3, two tailed unpaired t-test P< 0.001) in RNA editing (10-fold reduction in edited transcripts) was observed when the upstream cis-acting sequences were deleted. Error bars: mean+/- standard deviation of 3 replicates.

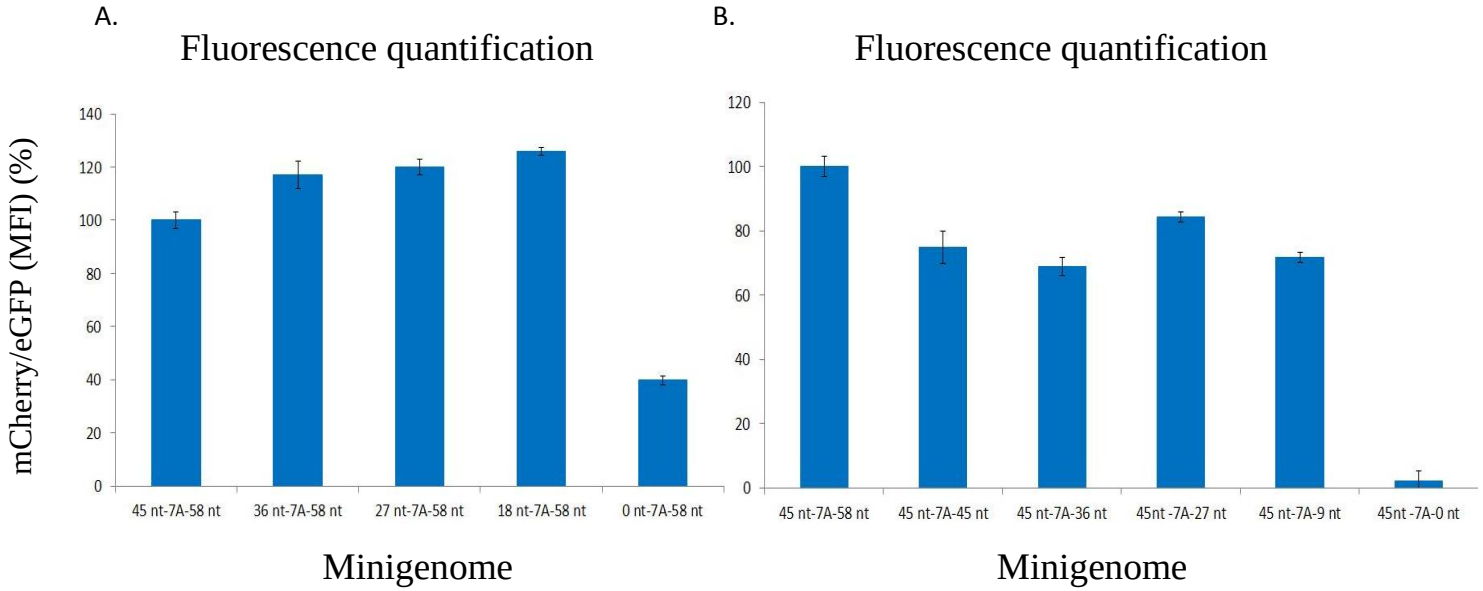

Figure 37. **The region of 18 nt up- and 9 nt downstream of the editing site (ES) is sufficient to support RNA editing.** A series of up- and downstream deleted dual-reporter minigenomes were generated (Figure 8A). The minigenome DNA was transfected into 293T cells and reporter protein expression was analyzed by fluorescence activated cell sorting (FACS) at 48 hr post-transfection. Flourescence signals (eGFP and mCherry) were quantified and mCherry signals were normalized with eGFP signals and presented here. This normalized signal from the unaltered dual-reporter minigenome (45 nt-7A- 58 nt) was set to 100% (standard). While comparing fluorescence signals from the deleted minigenomes with the standard there was no significant reduction in the mCherry signal (normalized with eGFP signal) for as small as 18 nt upstream (A) and 9 nt downstream (B) of the ES, whereas these was for longer deletions, suggesting that cis-acting sequence between 18 nt up- and 9 nt downstream of the ES are sufficient to support RNA editing. Error bars: mean+/- standard deviation of 3 replicates.

editing between a wild-type minigenome and a minigenome with a 3' leader stem-loop knockout. For this, *in vitro*-transcribed minigenome RNA was transfected all at once into 293T cells following transfection of helper plasmid DNA encoding for L, NP and VP35, but not VP30. Reporter protein expression was analyzed 48 hr post RNA transfection. Several approaches were utilized to analyze reporter protein expression, such as fluorescence signal quantification by FACS, epi-fluorescence microscopic image driven fluorescence quantification using ImageJ, and transcript quantification by RTQA. In absence of VP30, there was no significant difference in eGFP expression between the dual-reporter minigenome and the knockout version, indicating that the stem-loop may not be important, which is in contrast to previously published work (Weik et al., 2002) (Figure 39A) (Appendix 21A-D & 22A & B). Transcript quantification by RTQA supported the result (Figure 39B). Importantly, there was still a reduction in RNA editing, confirming a role of VP30 for this process (Figure 39).

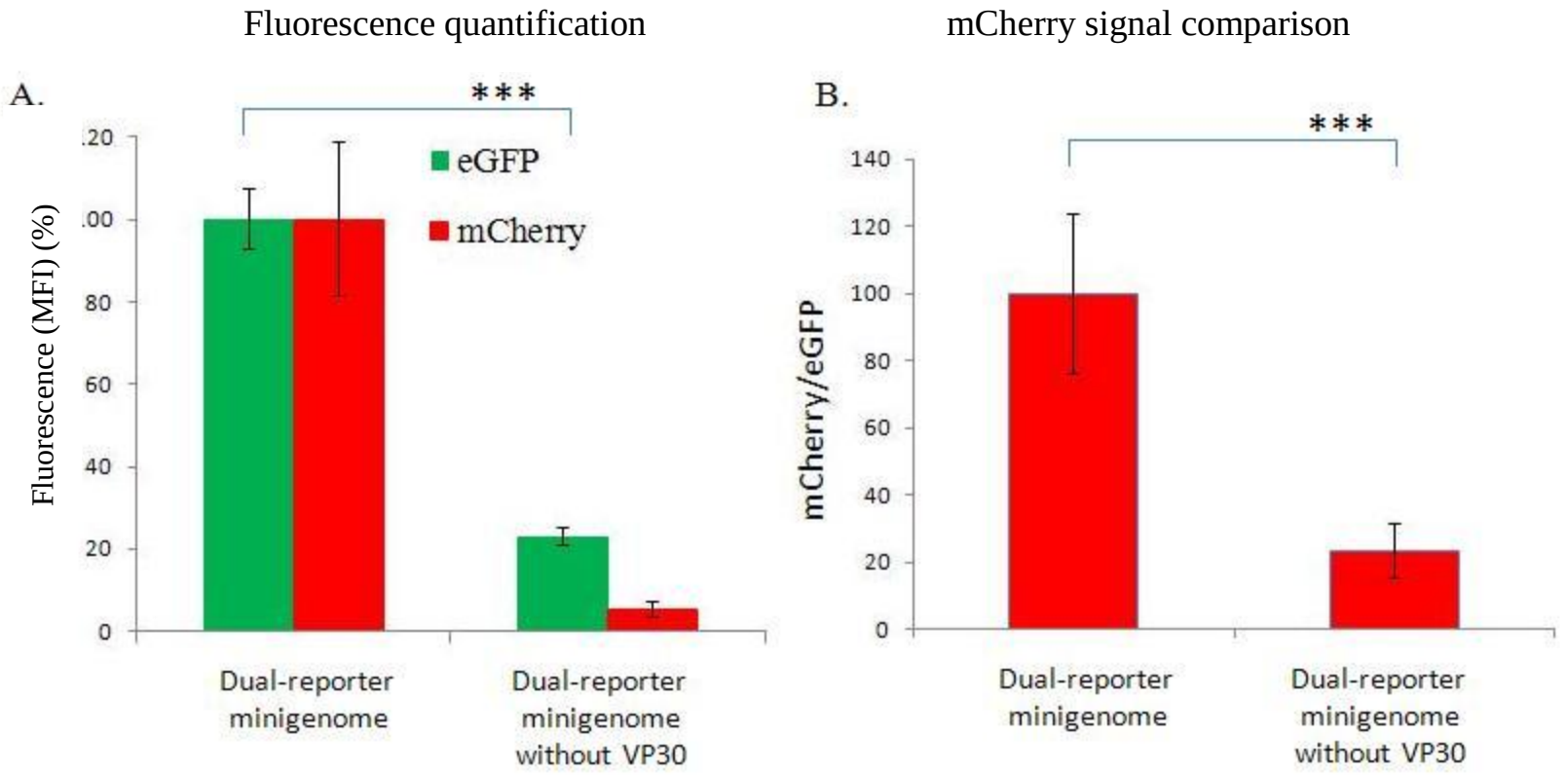

Figure 38. **VP30 mediates RNA editing.** *In vitro*-transcribed minigenome RNA was transfected into 293T cells following transfection of helper plasmid DNA with or without the plasmid expressing VP30. Reporter expression was analyzed by FACS 48 hr post-transfection. **A.** In the absence of the VP30 a reduction in eGFP expression and an even larger reduction in mCherry expression when comparing fluorescence signals, mean fluorescence intensity (MFI) (two tailed unpaired t-test, $P<0.001$). **B.** To determine mCherry reduction in the low eGFP expression (indicative of transcription) in absense of VP30 e, mCherry signal was normalized with eGFP signal. Reduction in RNA editing in absence ofVP30 is evident (two tailed unpaired t-test, $P<0.001$). Error bars: mean+/- standard deviation of 3 replicates.

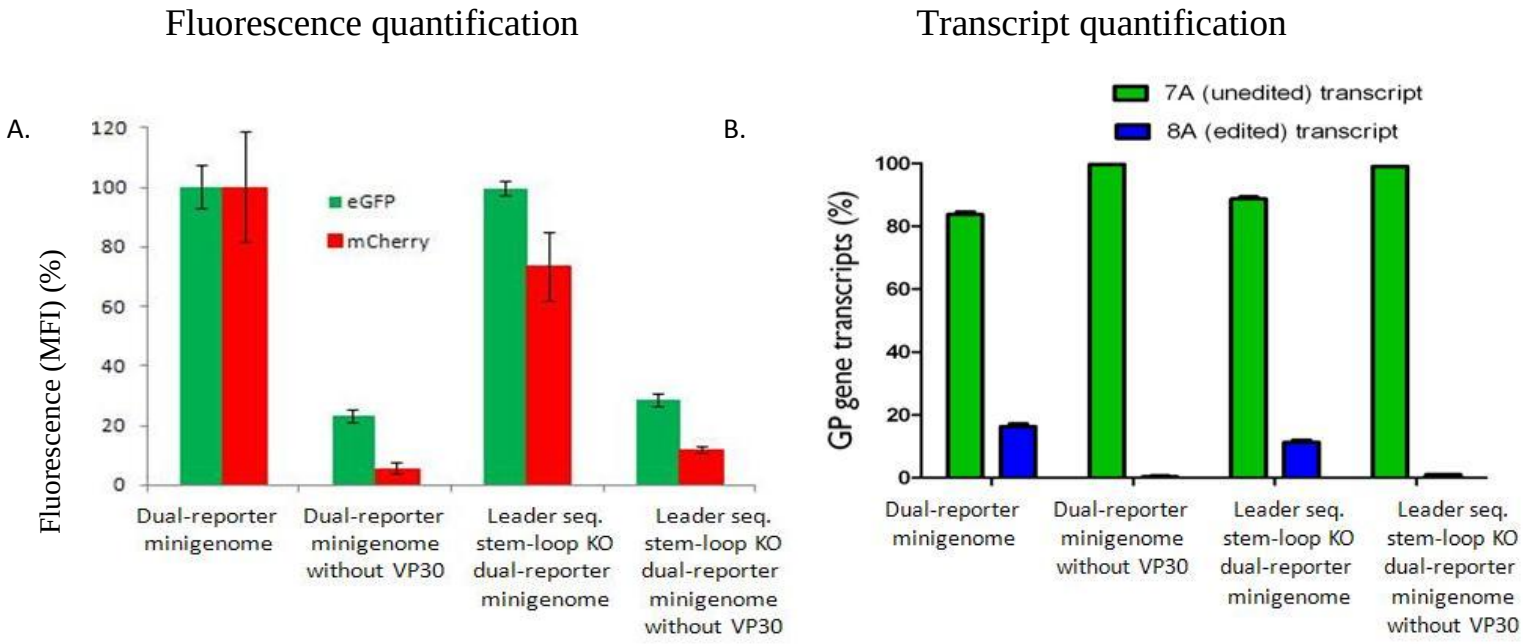

Figure 39. **VP30 mediates RNA editing independent of its function in transcript activation.** VP30 based transcript activation depends on a 3' leader sequence stem-loop (Weik et al., 2002). *In vitro*-transcribed RNA from the dual-reporter minigenome and a dual-reporter genome with a stem-loop knock-out (KO) was transfected separately in 293T cells for rescue (Figure 7 and see 2.9.2). **A.** Total fluorescence, mean fluorescence intensity (MFI), for eGFP and mCherry are shown from these minigenomes rescues with or without VP30. **B.** Transcripts were quantified from the same minigenome rescues showing that edited transcripts (mCherry expression) were almost undetectable by the rapid transcript quantification assay (RTQA) from both minigenomes in the absence of VP30. Quantification was done in triplicate from three independent minigenome rescues. Error bars: mean+/- standard deviation of 3 replicates.

3.3.3.4 Secondary Structure formation of the cis-acting sequences is important for RNA editing

Given the role of VP30 in overcoming a secondary structure (stem-loop) prior to the NP transcription start signal, the ES and its surrounding up- and downstream cis-acting sequences (110 nt) were analyzed for similar secondary structures using the prediction webserver mfold (Zuker, 2003).The system predicted two secondary structures for the upstream 45 nt of the ES (Figure 40A), which were formed by nucleotides 1-24 nt and 38-45 nt (plus sense). To determine the role of these stem-loops, the first putative stem-loop was destabilized by the introduction of several mutations (Figure 40B) into the dual-reporter minigenome based on a prediction by the mutational webserver XRNAmute (Alexander and Danny, 2008). In vitro-transcribed minigenome RNA was transfected into 293T cells and reporter protein expression and transcripts were analyzed and quantified by FACS and RTQA, respectively. Mutations had no impact on RNA editing, indicating that the predicted first stem-loop within the upstream sequence (45 nt) is not important for RNA editing (Figure 41A & B). Subsequently, mutations were introduced into the second predicted stem-loop of the upstream cis-acting sequences (either G39A and C44T or G38A and G39A) (Figure 40C & D). The minigenome DNA was transfected into 293T cells and reporter protein expression was analyzed 48 hr post-transfection. The signal for mCherry was reduced (Figure 41C) (Appendix 23), indicating the importance of the second stem-loop for RNA editing.

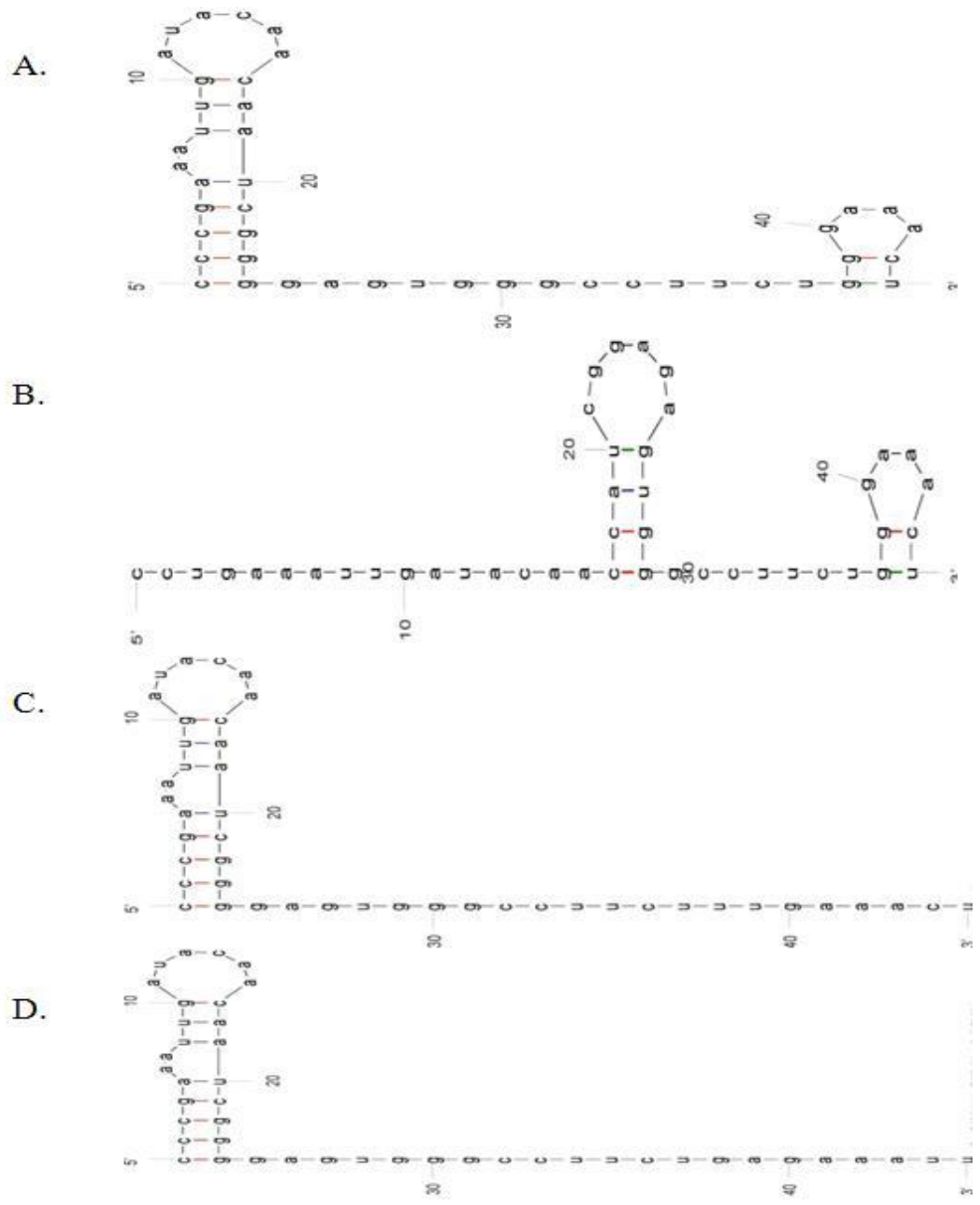

Figure 40. **Two predicted stem-loops in the upstream sequence of the editing site (ES). A.** The mFold RNA secondary structure prediction webserver predicted two stem-loops within the upstream cis-acting sequences (position 1-24 nt and 38- 45 nt) (plus sense). **B.** Three mutations (C3U, A18C, and G24A) were introduced to destabilize the first stem-loop structure (position 1-24). **C.** Two mutations (G38A and G39A) were introduced to destabilize the second stem-loop structure (position 38-45). **D.** Two different mutations (G39A and C44T) were introduced to destabilize the second stem-loop structure (position 38-45).

Fluorescence quantification

Transcript quantification

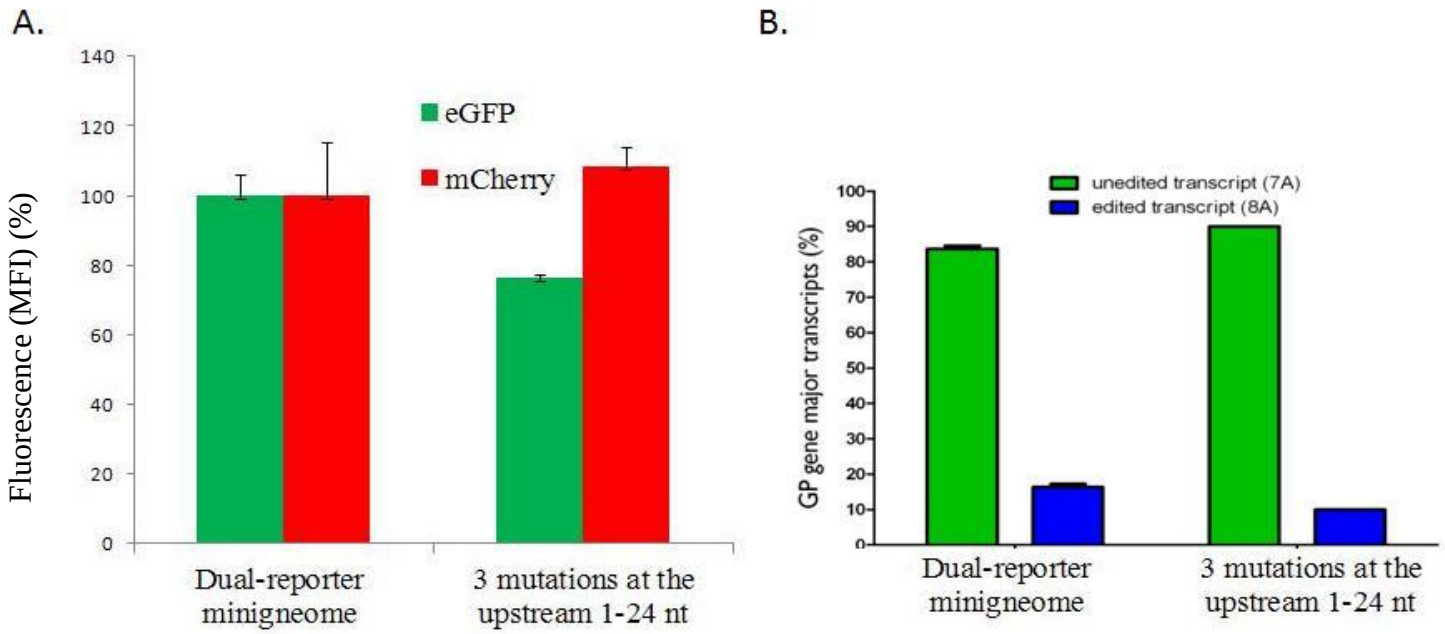

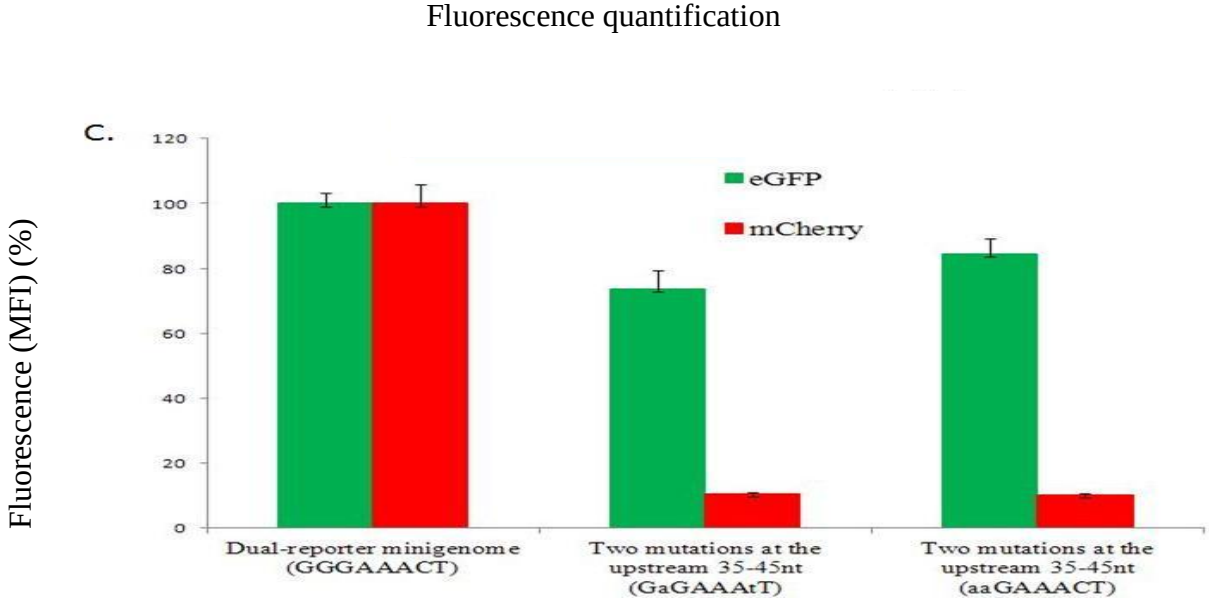

Figure 41. **Secondary structure of cis-acting editing site (ES) upstream sequence is important for RNA editing.** The cis-acting upstream sequence forms two predicted stem-loops (position 1-24 and 38-45) upstream of the ES (Figure 40A). **A & B. The first stem-loop has no effect on RNA editing.** Three mutations were introduced (C3U, A18C, and G24A) to destabilize the predicted first stem-loop (position 1-24) (Figure 40B). *In vitro*-transcribed minigenome RNA was transfected into 293T and protein expression and transcripts were analyzed 48 post-transfection by fluorescence activated cell sorting (FACS) and rapid transcript quantification assay (RTQA), respectively. In the dual-reporter minigenome, destabilization of the first predicted stem-loop did neither influence the transcript ratio nor reporter protein expression indicating that this stem-loop structure has no importance for RNA editing. **C. the second stem-loop is important for RNA editing.** Two different sets of mutations [G38A and G39A (Figure 40C) or G39A and C44T (Figure 40D)] were introduced to destabilize the predicted stem-loop. The minigenome DNA was transfected into 293T cells and reporter protein expression was analyzed by FACS 48 hr post-transfection. With both mutants, the mCherry signal was reduced, indicating the importance of this second stem-loop (position 38-45) for RNA editing. Error bars: mean+/- standard deviation of 3 replicates.

4. DISCUSSION

4.1 Identification of ssGP

4.1.1 ssGP-specific Transcripts

NNS RNA viruses use their genomes very efficiently. For example, the paramyxoviruses use 95% of their RNA genomes to encode their proteins. In addition, certain viruses increase their coding capacity by using RNA editing, which is a universal feature of almost all paramyxoviruses (Kolakofsky et al., 1991; Steward et al., 1993). Interestingly, EBOV utilizes a similar feature to increase its genome encoding capacity by producing multiple proteins from the GP gene. The sole surface protein $GP_{1,2}$ is encoded by an edited transcript, whereas sGP is encoded by an unedited transcript (Volchkov et al., 1995; Volchkov et al., 2005). Among the NNS RNA viruses, genes with RNA editing encode both structural and nonstructural proteins with editing involved in the expression of both (Anthony Sanchez, 2007; Hausmann et al., 1999a; Robert A. Lamb, 2007; Volchkov et al., 2005). As an example, the P protein of paramyxoviruses is one of the major components of the nucleocapsid, which is the viral active transcription/replication complex (Bourhis et al., 2006; Matsumura et al., 1999; Robert A. Lamb, 2007; Wiegand et al., 2007). RNA editing of the hepatitis delta antigen (HDAg) p24 gene by ADAR results in HDAg p27 during HDV genome transcription. Both of these proteins are essential for the HDV life cycle, as p24 is required for HDV replication, whereas p27 is required for viral RNA packaging (Casey et al., 1992; Casey and Gerin, 1995; Kuo et al., 1989; Ryu et al., 1992). For EBOV, $GP_{1,2}$ plays a major role in viral pathogenesis by dictating cellular tropism of EBOV (Anthony Sanchez, 2007;

Feldmann et al., 2003; Feldmann et al., 2001). Despite well-defined functions for the structural proteins generated through RNA editing, the roles of similarly produced nonstructural proteins are not well-characterized, except for certain paramyxoviruses for which these genes have been identified as IFN antagonists (Park et al., 2003; Rodriguez et al., 2002; Shaw et al., 2004). A well-defined function has not been assigned for sGP yet, despite its abundance during infection (Anthony Sanchez, 2007; Feldmann et al., 2001). However, there have been several proposed functions for sGP, such as blocking EBOV neutralizing antibodies (Kindzelskii et al., 2000; Yang et al., 1998), interfering with the innate immune response by binding to CD16b to inhibit early neutrophil activation (Yang et al., 1998), or counteracting the permeability increasing effect of pro-inflammatory mediators such as TNF-α, thereby interfering with leukocyte extravasation (Falzarano et al., 2006; Wahl-Jensen et al., 2005a). Previously, it has been hypothesized that EBOV produces a second small soluble nonstructural protein, ssGP, from the GP gene through RNA editing. Specifically, RNA editing would allow switching into the third ORF, either by deletion of one or insertion of two A residues at the GP gene ES (Volchkov et al., 2000; Volchkova et al., 1998) (Figure 11). However, neither transcription nor expression of ssGP had been achieved prior to this work.

Therefore, the first objective of my studies was to identify whether ssGP is actually produced during EBOV infection. Initial evidence that ssGP might be produced came from the detection of ssGP-specific transcripts. I could demonstrate that ZEBOV infection *in vivo* and *in vitro* resulted in the production of three distinct GP gene-specific transcripts. I did confirm that the major GP gene transcripts encode for sGP and $GP_{1,2}$ with a similar ratio as described previously by others (Sanchez et al., 1996; Volchkov et

al., 1995). In addition to these transcripts, I identified approximately 5% of all GP gene transcripts as ssGP-specific (Figure 12). This provided primary evidence that ssGP may be expressed during EBOV infection.

Transcript analysis revealed that 3% of the transcripts contained a higher number of insertions, suggesting that the EBOV editing process is not absolutely accurate. Interestingly, deletions were rarely found and were only present as a single A residue deletion (Figure 13). However, this rare occurrence of deletions during RNA editing is not surprising, because RNA editing mostly involves nucleotide insertion or substitution, as shown for paramyxoviruses and ADAR, respectively (Casey et al., 1992; Casey and Gerin, 1995; Hausmann et al., 1999a). Transcripts with a higher number of nucleotide insertions were reported for paramyxoviruses, where up to fourteen non-template G residues have been found in P gene derived transcripts and only rarely deletions of nucleotides were noted (Galinski et al., 1992; Kulkarni et al., 2009; Lo et al., 2009; Pelet et al., 1991). Similar or even higher numbers of non-template nucleotide insertions were noticed for EBOV RNA editing. In particular, insertion of 0, 3, 6, 9, 12, & 15 non-template nucleotides insertions were found for sGP-specific transcripts; 5, 8, 11, 14, & 17 non-template insertions for ssGP-specific transcripts; and 1, 4, 7 10, 13, & 16 non-template nucleotide insertions for $GP_{1,2}$-specific transcripts (Figure 13). Interestingly, all insertions were A residues, altering the ORFs by incorporation of 1-5 additional lysine residues. The functional consequence of these additional lysines has yet to be determined.

Potential errors during RNA-dependent DNA amplification as a source of nucleotide insertions at the ES were excluded by analyzing amplification of a synthetic RNA including the ZEBOV ES and surrounding sequences. No insertions were observed

during amplification of the synthetic RNA. In addition, distinct GP gene-specific transcripts could also be a result of a quasispecies in the original virus stock used for infection. Therefore, I applied the same approach to RNA isolated from the ZEBOV seed-stock used in these experiments. I detected a minor proportion (6% of transcripts) of the '8A' variant directly encoding for the transmembrane protein $GP_{1,2}$ but no transcripts that would directly encode for ssGP. This finding does not come unexpected, since an '8U' virus had been plaque-purified earlier, and was used for the initial molecular characterization of EBOV (Sanchez et al., 1993). In addition, an '8A' ZEBOV has been genetically engineered and characterized in vitro to demonstrate the importance of RNA editing for virus cytopathogenicity (Volchkov et al., 2001). A recent study has confirmed that ZEBOV passaging in Vero E6 cells resulted in rapid accumulation of '8U' at the ES in the viral genome. This '8U' virus excceeded the wild-type '7U' virus in 4-5 cell passages. In contrast, *in vivo* the '8U' ZEBOV variant immediately reverted back to '7U' wild-type ZEBOV, indicating the importance of a wild-type ES for efficient replication and spread in the infected host (Volchkova et al., 2011). Importantly, the lack of detection of genomic RNA directly encoding for ssGP (without RNA editing) suggests that such a virus variant is not viable, as one would predict given the important function of $GP_{1,2}$ for the viral life cycle.

4.1.2 ssGP Protein Detection

All expression products from the GP gene carry the same N-terminal amino acid sequence, including the SP, which directs them into the ER (Anthony Sanchez, 2007; Feldmann et al., 2001). Therefore, all products are potentially exposed to similar co- and post-translational modifications. Like sGP, ssGP is also expected to be secreted from

infected cells during EBOV infection due to the lack of a transmembrane anchor. A similar predicted MW for sGP and ssGP (32.6 and 29.5, kDa respectively), similar processing and co- and post-translational modifications (i.e. glycosylation), the expected low abundance of ssGP (<5% of transcripts) (Figure 12), and the lack of ssGP-specific antibodies provided a major challenge for the detection of ssGP during EBOV infection. Therefore, all protein preparations were subjected to PNGaseF treatment prior to protein analysis. PNGaseF removes all N-linked glycans, which is the most prominent form of glycosylation detected for sGP (Falzarano et al., 2006; Sanchez et al., 1998) and also predicted for ssGP. This strategy provided preliminary evidence for ssGP expression during in vitro infection as demonstrated by reducing SDS-PAGE analysis (Figure 16).

For further confirmation, nano-LC-ESI-MS/MS was utilized to identify a unique ssGP-specific peptide. Based on sequence analysis using a peptide cutter webserver (www.expasy.org), only treatment with formic acid (Hua et al., 2006) or digestion with the endoproteinase AspN resulted in a unique C-terminal peptide that could be used for ssGP identification (Appendix 6). In a control experiment, this C-terminal ssGP-specific peptide was detected by nano-LC-ESI-MS/MS and database searching (Mascot, Matrix Science) (Udeshi et al., 2008) from formic acid digested, purified, recombinant-expressed ssGP (Figure 17); but, the method failed when applied to the supernatant from ZEBOV infected Vero E6 cell (MOI of 1) treated with formic acid or AspN (data not shown). The low abundance of ssGP, also indicated by the low prevalence of ssGP transcripts (< 5%), during infection is likely the reason, as mass spectrometry has limitations for the detection of low abundant proteins (Lubec and Afjehi-Sadat, 2007; Ossipova et al., 2006; Shevchenko et al., 1996).

In another attempt, antiserum was raised against the C-terminal ssGP-specific peptide to overcome the limitations in detection. However, the antiserum cross-reacted with sGP and GP_1, the larger fragment of $GP_{1,2}$ (data not shown). This was not unexpected, since only the last two amino acid of the peptide were unique to ssGP.

2-D gel electrophoresis is a powerful tool to separate proteins with similar biochemical characteristics. As a result, proteins with small differences in their MW and p*I* can be visualized and identified on the same gel. Proteins separate on 2-D gel based on their p*I* in the first dimension, followed by SDS-PAGE separation based on their MW in the second dimension (Wu, 2006). Therefore, 2-D electrophoresis was utilized to separate sGP and ssGP, which differed in their predicted p*I* (8.17 and 6.26, respectively) and MW (32.6 and 29.5, kDa respectively). In combination with deglycosylation (PNGaseF treatment), these two different proteins were separated, thus providing final proof that ssGP is indeed expressed during EBOV infection (Figure 18). This finding was also supported by visualizing Cy-labeled proteins in the infected supernatants on 2-D DIGE (Appendix 9 & 10). 2-D DIGE based protein detection enhances reproducibility and separation compared with traditional 2-D gel electrophoresis (Zhou et al., 2002).

4.1.3 ssGP Biophysical Properties

All GP gene products possess an identical N-terminal (1-295 aa) primary sequence, including a SP (1-32 aa), suggesting that ssGP may undergo similar processing pathways and co- and post- translational modifications as has been described for sGP and $GP_{1,2}$. It was previously shown that there is a substantial difference between $GP_{1,2}$ and sGP, the latter of which is not O-glycosylated (Anthony Sanchez, 2007; Barrientos et al.,

2004; Barrientos et al., 2007; Falzarano et al., 2006; Feldmann et al., 1994). To characterize ssGP, recombinant-expressed ssGP with or without a tag, was utilized. It was apparent that ssGP migrated like a dimer on non-reducing SDS-PAGE similar to sGP (Figure 14C). In the case of sGP, the homodimer appears in a parallel orientation with intermolecular disulfide bonds between two Cys53 and Cys306 (Barrientos et al., 2004; Falzarano et al., 2006). However, ssGP lacks the Cys306 position; therefore, site-directed mutagenesis of HA-tagged recombinant-expressed ssGP determined that mature ssGP also appears as a homodimer consisting of two monomeric ssGP molecules, which are connected via an intermolecular disulfide bond that links the two Cys53 residues (Figure 19). As with sGP, it could be speculate that the remaining four cysteines (aa position 108, 121, 135, and 147) are involved in intramolecular disulfide bond formation and stabilization of the molecule (Barrientos et al., 2004; Falzarano et al., 2006). sGP has been shown to be C-mannosylated (Falzarano et al., 2007). ssGP possesses the C-mannosylation motif (WXXW); however, this post-translational modification has yet to be identified for ssGP. Together with the slight differences in migration pattern under non-reducing conditions (Figure 15B), these data suggests that ssGP seems to have a similar structure to sGP, showing minor differences due to a slightly lower MW and a more unstable structure of the homodimer (Figure 42). The determination of the glycosylation status of ssGP using endoglycosidases and exoglycosidases revealed the existence of complex hybrid type N-linked carbohydrates (Figure 20), while evidence of O-glycosylation could not be found (Figure 21). Therefore, ssGP glycosylation is very similar to that of sGP (Barrientos et al., 2007; Falzarano et al., 2006; Ritchie et al., 2010). This differs from $GP_{1,2}$, the other GP gene product generated through RNA editing,

which is also glycosylated (Feldmann et al., 1994; Ito et al., 1999; Ritchie et al., 2010; Sanchez et al., 1998) and the solely O-glycosylated Δ-peptide, the C-terminal proteolytic cleavage fragment of the sGP precursor (Volchkova et al., 1999). The ORF encoding for ssGP possesses six predicted N-liked glycosylation motifs, which all seem to be used based on the MW-shift after complete N-linked deglycosylation following PNGaseF treatment (Figure 20).

4.1.4 ssGP Function

To characterize ssGP function, an experimental approach was taken to establish a binding assay for sGP or ssGP on known target cells such as Vero E6 cells (generally used for virus growth) and primary human monocytes (primary *in vivo* target cell) (Stroher et al., 2001). However, interactions between nonstructural proteins and susceptible cells were inconclusive, despite multiple attempts (data not shown). Then, attempts to show binding of these proteins to human primary neutrophils were also carried out. It has previously been shown that sGP interacts with human neutrophils through an interaction with CD16b (Kindzelskii et al., 2000; Yang et al., 1998); however, this finding was contested by others (Maruyama et al., 1998; Sui and Marasco, 2002). In this study, a similar FACS based binding assay showed that neither ssGP nor sGP bound to the surface of purified human neutrophils. The interaction of a viral surface protein with its receptor is likely mediated through a specific structure at the RBD. Hence, nonstructural glycoproteins (sGP and ssGP) of EBOV do not seem to bind to susceptible cells, despite possessing the putative RBD (Kuhn et al., 2006).

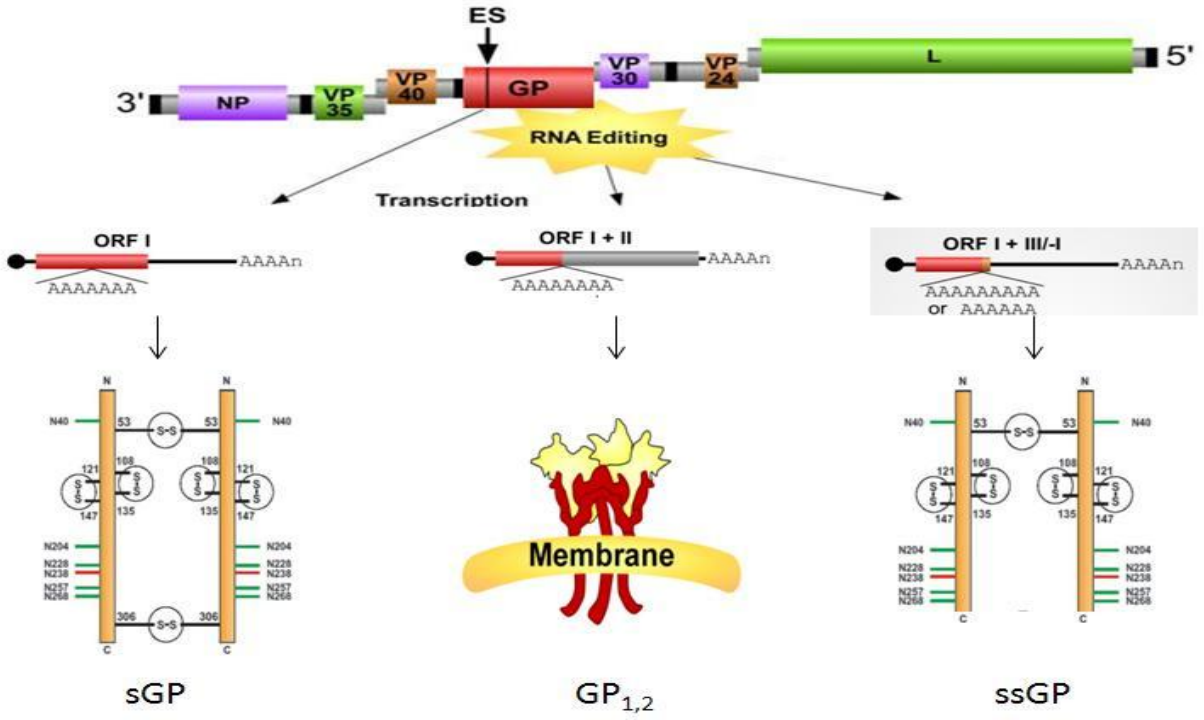

Figure 42. **EBOV GP gene produces multiple proteins through RNA editing.** RNA editing produces multiple GP gen-products. The soluble glycoprotein (sGP) is encoded by the unedited transcript and forms a disulfide linked homodimer. The transmembrane glycoprotein ($GP_{1,2}$) is encoded by an edited transcript and forms a homotrimer. The small soluble glycoprotein (ssGP) is encoded by another edited transcript and forms a less stringent homodimer. The schematic figure here was expanded using a scheme published previously (Falzarano, 2010; Falzarano et al., 2006) with permission.

Supporting this hypothesis is the finding that sGP and ssGP and $GP_{1,2}$ differ in their tertiary structure, which could destroy a functional RBD. sGP and ssGP are homodimers (Barrientos et al., 2004; Falzarano et al., 2006), whereas $GP_{1,2}$ is a heterotrimer that consists of the two disulfide-linked proteolytic cleavage fragments, GP_1 and GP_2 (Anthony Sanchez, 2007; Feldmann et al., 2001; Ito et al., 1999; Sanchez et al., 1998). Furthermore, both sGP and ssGP differ in their glycosylation pattern from $GP_{1,2}$ in that they lack O-linked and largely lack high-mannose type N-linked carbohydrates (Figure 20 & 21). In particular, high-mannose N-glycosylated carbohydrates on surface proteins are known to efficiently enhance interaction with potential host cell attachment molecules, such as LSECtin, DC-SIGN, and DC-SIGNR, found on dendritic and endothelial cells, as described for HIV, hepatitis C virus, MARV, and EBOV (Lin et al., 2003; Marzi et al., 2004; Powlesland et al., 2008; Simmons et al., 2003). Therefore, these differences in structure and co- and post-translational processing may be the reasons for the failure in detecting binding to susceptible cells.

Endothelial cells are considered secondary target cells for EBOV infection, whereas monocytes/macrophages and dendritic cells are primary target cells (Geisbert et al., 2003b; Stroher et al., 2001). It has been postulated that sGP secreted from primary target cells can activate endothelial cells involving the loss of barrier function, an important role in EBOV pathogenesis (Feldmann et al., 1996a; Hensley and Geisbert, 2005; Sullivan et al., 2003; Yang et al., 1998). Despite abundant release from infected cells, sGP did not activate endothelial cells, but instead sGP was shown to rescue the endothelial barrier function after treatment of TNF-α and thus may function as an anti-inflammatory molecule (Wahl-Jensen et al., 2005b). Despite similarities in primary

sequence, processing/modifications and structure, ssGP did not rescue the endothelial barrier function similar to sGP. This may be explained by the lack of Cys306 in ssGP, which has been previously shown to be involved in intermolecular disulfide bond formation (Barrientos et al., 2004; Falzarano et al., 2006) and was shown to be essential for the effect of sGP on endothelial barrier function (Falzarano et al., 2006).

Despite the failure to establish a function for ssGP, several potential functions can be proposed: (1) Antibody decoy, because all the GP gene products (ssGP, sGP, and $GP_{1,2}$) have the same N-terminal primary amino acid sequences; therefore, nonstructural proteins (sGP and ssGP) could shield virus from neutralization by acting as a decoy to $GP_{1,2}$ specific antibodies. A similar function has been identified for the secreted form of the envelope protein (sG) of respiratory syncytia virus (RSV), which acts as a decoy for RSV-specific antibodies (Collins and Graham, 2008). However, the very low (<5%) ssGP abundance speaks against its effectiveness as a decoy during infection. (2) Cellular binding, because ssGP is highly N-glycosylated and shows sequence similarities including the putative RBD with other GP gene products (sGP and $GP_{1,2}$). Therefore, it could potentially bind to susceptible cells by interacting with potential lectin-based EBOV receptors. A similar binding has been shown for West Nile virus (WNV) nonstructural protein 1 (NS1), which after release binds to the cell surface (Chung et al., 2006). Despite having similar N-terminal sequence similarities, the tertiary structure of ssGP is different from those of other EBOV glycoproteins (sGP and $GP_{1,2}$) which might speak against a binding of ssGP to EBOV receptors as supported by data presented here. (3) Host response modulation, because ssGP might initiate cellular signaling on the surface of target cells. A similar function has been recently associated with a newly

identified influenza A virus protein expressed via ribosomal frameshifting from gene segment 3 (Jagger et al., 2012). (4) Host immune response evasion, which has been shown for other viral nonstructural proteins (Chung et al., 2006; Park et al., 2003; Samuel and Diamond, 2006; Shaw et al., 2004). ssGP could potentially interact with immune regulatory molecules or their receptors to evade host immune responses. A potential anti-inflammatory role has been described for sGP (Wahl-Jensen et al., 2005b), which is absent with ssGP. (5) Cellular secretory pathway competition, because ssGP could compete with cellular components that use those pathways. For example, one of the virus strategies of immune evasion is restricting antigen presentation by cellular human leukocyte antigen (HLA) (Hurley and Bonifacino, 2012; Iannello et al., 2006; Ploegh, 1998).

4.2 RNA Editing- an Inherent Feature of EBOV

RNA editing was mostly considered as a rare event in a few organisms compared to alternative splicing. Recent advances in bioinformatic data mining, deep sequencing and proteomics changed the view of RNA editing and found that RNA editing occurs more frequently in fundamentally all kingdoms of life (Jantsch, 2010). RNA editing is an important mechanism to generate protein diversification in different organisms and consequently plays a role in evolution (Gerber and Keller, 2001; Hajduk and Ochsenreiter, 2010). RNA editing was first described in parasitic protozoa, and its mitochondrial genome was identified to be edited at the RNA level via a U insertion/deletion mechanism (Jantsch, 2010). The human cellular editing enzyme ADAR plays an important role in antiviral defense and proteome diversification (Jantsch, 2010). Interestingly, ADAR-driven RNA editing has also been described to enhance RNA virus

replication (Gélinas et al., 2011). In contrast to the widely-studied ADAR-driven editing (base substitution), viral polymerase-driven site-specific RNA editing (mainly insertion of non-template nucleotide) has mainly been characterized in the paramyxoviruses (P gene editing). In particular, edited products of the paramyxovirus P gene (V and W/D) have been identified as playing an important role in host immune evasion (Hausmann et al., 1999a). Similar to paramyxoviruses, all known species in the genus *Ebolavirus*, including the most recently identified BEBOV (Towner et al., 2008), possess a highly conserved ES (7U) in the GP gene (Figure 24) and are therefore thought to undergo site-specific RNA editing during transcription. This results in the production of multiple glycoproteins, including the nonstructural sGP and ssGP and the structural $GP_{1,2}$ (Figure 11 and 42) (Anthony Sanchez, 2007; Feldmann et al., 2001). However, RNA editing had only been experimentally addressed for ZEBOV species (Sanchez et al., 1996; Volchkov et al., 1995). A difference in the GP gene RNA editing frequency among all the species in the *Ebolavirus* genus might contribute to the variability in pathogenesis among them, because $GP_{1,2}$ dictates cellular tropism (Anthony Sanchez, 2007). Therefore, the second objective of this study was to identify and characterize RNA editing in all EBOV species during infection on transcript and protein levels.

4.2.1 Rapid Transcript Quantification Assay (RTQA) for RNA Editing

Viral RNA editing alters the RNA transcript (nucleotide sequence change) by insertion or deletion of nucleotides and thus edited transcripts differ from the unedited ones. Several methods have been developed to detect and quantify editing in eukaryotes (Nakae et al., 2008). RNA editing includes mainly site-specific single-nucleotide modifications (base deamination) (Gerber and Keller, 2001), which has been previously

quantified by primer extension reactions performed on total RNA (Navaratnam et al., 1991) or RT-PCR templates (Navaratnam et al., 1991), or by hybridization techniques, that are capable of discriminating single nucleotide differences in RT-PCR products (Navaratnam et al., 1991; Schiffer and Heinemann, 1999; Sommer et al., 1991). Further, restriction enzymes that cleave RT-PCR products (either edited or unedited) were used for detection and quantification of editing (Paschen and Djuricic, 1994). Several advanced high-throughput methods recently became available for the detection of edited RNA, such as denaturing high performance liquid chromatography (DHPLC), allele-specific real-time PCR with TaqMan probes, and PCR with allele-specific primers (ASP) (Nakae et al., 2008). More recently, a pyrosequencing approach (Sodhi et al., 2005) and TaqMan-based real-time quantitative assays to differentiate edited versus unedited PCR products using fluorescent probes (Wong et al., 2009) have been reported. Previously, NNS viral RNA editing was mainly quantified using a cloning-sequencing approach (Kulkarni et al., 2009; Lo et al., 2009), which has several limitations, including being time-consuming, labor-intensive and highly expensive for large numbers of samples. Therefore, a new method, RTQA, which is based on amplified fragment length polymorphism (AFLP), was developed to detect and quantify viral RNA editing. RTQA has several advantages over the commonly used AFLP (Vos et al., 1995) for the detection of single nucleotide polymorphism, such as not using of restriction enzymes. RTQA uses capillary electrophoresis that has proven to differentiate between PCR fragments generated from polymorphic transcripts (Poyau et al., 2007) mostly base substitution (Mátyás et al., 2002). In contrast to the base substitution, EBOV RNA editing (insertion of non-template nucleotide) derived transcripts largely differ by a single nucleotide.

Therefore, it was necessary to first evaluate the method for its suitability, reproducibility, sensitivity, and specificity. For this, PCR fragments differing by a single nucleotide were mixed in known proportion as reference standards for accurate quantification (Appendices 12 & 13). Next, quantification of transcripts was done on transcripts (unedited and edited) derived from the dual-reporter cassettes confirming the suitability for detection and quantification (data not shown). RTQA is a PCR based assay, therefore it can quantify transcripts of very low copy number; the specificity of this method is high based on primer specificity.

4.2.2 RTQA Quantified viral RNA editing

GP gene transcripts (differing by a single nucleotide) were quantified by RTQA from both in vitro and *in vivo* ZEBOV infection and the transcript ratio between sGP and $GP_{1,2}$-specific transcripts in infected Vero E6 cells was determined to be 80 and 20%, respectively, as reported previously (Volchkov et al., 1995). This was confirmed by the cloning-sequencing method (Figure 12). For this analysis, I omitted the quantification of ssGP transcript mainly due to the very low level of transcripts detected during infection (Figure 12). In addition, ssGP-trasncript detection through RTQA is complicated because ssGP could be encoded by two different transcripts (one has 6A and another has 9A at the editing site) therefore it adds additional trasncrpts to quantify simulateneously. As RTQA only optimized for two (sGP, 7A and $GP_{1,2}$) transcripts, four transcript quantifation requires further optimization by the titratation that would cumbersome. In addition, RTQA is based on PCR technology therefore any miss priming during ampllication process could create more background.

Subsequently, RTQA quantification was used to analyze RNA editing in Vero E6 cells infected with the different species of EBOV. 15- 40% of the transcripts were edited in all cases expect for REBOV infection, where only 10% of transcripts were edited (Figure 26). Similarly, RNA editing was confirmed for EBOV infection of primary target cells such, as primary human macrophages (Bray and Geisbert, 2005; Geisbert et al., 2003b; Stroher et al., 2001) (Figure 26). RNA editing seems to be rather stable among the different EBOV species. This is in contrast to most paramyxoviruses, for which the RNA editing frequency of the P gene can range from 31-82%, despite a similar ES in the P gene, as demonstrated for Sendai and Nipah virus, respectively (Kulkarni et al., 2009). Translation products appeared similar in size for all EBOV species (Figure 27). All sGPs were found N-glycosylated with six predicted N-glycosylation motifs conserved among all EBOV species. It is interesting to note that there was a difference in editing between the human pathogenic species (ZEBOV, SEBOV, CIEBOV, and BEBOV) and the human apathogenic REBOV. However, further studies need to show if a difference in editing would account for differences in pathogenicity (Hoenen et al., 2006a). Thus, I determined that RNA editing is an inherent feature of all members of the genus *Ebolavirus*. In contrast, MARV appears to not use RNA editing and produces only $GP_{1,2}$ from the GP gene (Anthony Sanchez, 2007).

Remarkably, the EBOV RNA editing frequency was stable over the course of infection (up to 144 hr post-infection). This was not the case for Nipah virus infection where at the very early time points (2.5 hr) editing was only 10%, but shifted to 94% and 91% at 9.5 and 24 hr post-infection, respectively. Later time points showed a decrease in the percentage of edited transcripts (Kulkarni et al., 2009). At this point the reason for

this difference is unknown and needs to be further analyzed. Although EBOV RNA editing seems stable during infection, its potential contribution to virus replication or immune evasion has yet to be determined. sGP has a potential anti-inflammatory role (Wahl-Jensen et al., 2005b), but EBOV VP35 and VP24 have been identified as antagonists of the host innate immune response (Cárdenas et al., 2006; Feng et al., 2007). In terms of paramyxoviruses, the P gene edited products play important roles in immune evasion (Park et al., 2003; Shaw et al., 2004). It also needs to be considered that RNA editing may play a more important role in the natural reservoir rather than the end host; future studies need to address this possibility.

4.3 Characterization of RNA Editing

The EBOV GP gene and paramyxoviruses P gene contain at least two ORFs that overlap at the ES, and as a result they can produce fusion proteins between the N-and C-terminal ORFs. Retroviruses and coronaviruses use ribosomal frameshifting to access alternative ORFs (Brierley et al., 1989; Jacks and Varmus, 1985; Weiss et al., 1990), whereas paramyxoviruses and EBOV utilize transcriptional frameshifting (RNA editing) through insertion of non-template G and A residues, respectively (Hausmann et al., 1999a; Volchkov et al., 1995). RNA editing in the *Paramyxoviridae* family occurs in the P gene at a short stretch of 5' A_nG_n residues (plus sense) (Hausmann et al., 1999a; Jacques et al., 1994). The P proteins from members of the genera *Morbillivirus*, *Respirovirus*, *Henipavirus*, and *Avulavirus* are expressed from unedited transcripts, whereas the V and W/D (W protein in Nipah virus and D protein in parainfluenza virus 3) proteins require the insertion of one or two G residues at the ES, respectively. For paramyxoviruses, it has been postulated that RNA editing occurs through a mechanism of

viral polymerase stuttering/elongation similar to polyadenylation of RNA transcripts, indicating that the ES may have evolved from polyadenylation sites (Hausmann et al., 1999a). Currently, there is no published information available on the mechanism for EBOV RNA editing. In this study, I developed an altered minigenome system to characterize EBOV RNA editing.

4.3.1 RNA editing is GP gene-specific

The minigenome system is an artificial system for studying virus transcription and replication. Minigenome systems for filoviruses have already been established (Groseth et al., 2005; Mühlberger, 2007; Mühlberger et al., 1998; Muhlberger et al., 1999); however, the minigenome system has not been utilized to characterize RNA editing. Despite the availability of a minigenome based on either viral or cellular polymerase, in this study the bacteriophage T7-polymerase-based ZEBOV minigenome system was utilized. In this system, RNA editing was first demonstrated using the entire GP gene ORF, allowing studies on RNA editing without the infectious virus, which needs BSL4 containment. Minigenome studies were initially done in several cell types such as 293T and Vero E6 cells (data not shown). Most subsequent studies, however, used the highly transfectable 293T cells, because of higher expression and thus more easy quantification. For transcript quantification experiments, I solely used in vitro-transcribed minigenome RNA to avoid any DNA contamination in the quantification process.

Paramyxoviruses RNA editing is highly regulated by cis-acting sequences (Hausmann et al., 1999a). In order to study the structural requirements for EBOV RNA editing, I established a minigenome carrying a truncated GP gene covering the ES and 45

and 58 nt up- and downstream of it (total 110 nt) (truncated GP minigenome). The ratios obtained for unedited and edited transcripts were similar when transcripts derived from the truncated GP gene minigenome, the GP minigenome or ZEBOV infection were analyzed, demonstrating the usefulness of the truncated GP gene minigenome to characterize the mechanism of RNA editing (Figure 30). Interestingly, the ZEBOV L gene also has a series of seven uridine residues similar to the GP gene ES, which is, however, not conserved in all EBOV species. A similarly constructed truncated L minigenome did not show any evidence for RNA editing (Figure 30), which is in line with no reports for multiple L gene-derived transcripts during EBOV infection. Therefore, EBOV RNA editing appears to be GP gene-specific, which further suggests additional structural requirements for RNA editing, since the primary ES sequence is present in some EBOV L genes. A high degree of specificity in the selection of site-specific nucleotide insertion in the paramyxoviruses P gene editing has been described (Hausmann et al., 1999a; Steward et al., 1993). Similarly, the template sequence of dsRNA was identified as being important for ADAR-driven RNA editing (Nishikura et al., 1991).

4.3.2 Primary and Secondary Requirements for RNA Editing

In order to confirm and quantify RNA editing at protein level, a dual-reporter minigenome was developed. Two fluorescent reporters, eGFP and mCherry, were chosen because their excitation and emission spectra are far apart; therefore, no fluorescence resonance energy transmission (FRET) based interference and no background noise were observed when tested by FACS and confocal microscopy (Appendices 14 & 15). The downstream reporter (mCherry) was engineered with a C-terminal NLS to allow for

better separation of edited (nuclear localization) and unedited (cytoplasmic localization) products (Figure 32). Fluorescence reporters have advantages over commonly used luciferase-based reporters, such as no substrate requirement, the ability for continuous observation, and the ability to observe single cells (Wang et al., 2002).

One complicating factor studying EBOV RNA editing in a minigenome system is the potential occurrence of RNA editing by other viral polymerases in addition to the EBOV L polymerase, because DNA-dependent RNA polymerases, such as those from vaccinia virus and bacteriophage T7 (used in this study), appear to be able to recognize the ZEBOV GP gene ES (Volchkov et al., 1995). This might be explained by the high similarity of the EBOV ES sequence to polyadenylation sites in those organisms. Whether paramyxovirus polymerase complexes can recognize the EBOV GP gene ES is currently unknown. The possibility of non-template A residue insertion during the T7 driven DNA-based transcription was ruled out by detecting only eGFP (expressed from unedited transcripts) but not mCherry (expressed from edited transcripts) (Appendix 16).

In order to define the structural requirements for RNA editing, I first investigated the role of the primary ES sequence by introducing point-mutations at AAGAAAA or AAAAAGA. A to G mutations at positions 3 or 6 of the ES sequence completely abolished RNA editing, indicating the importance of the primary ES sequence. Previously, a recombinant ZEBOV with identical mutations in an 8A-ES (AAGAAGAA) was generated and rescued, and was shown to have impaired sGP production (edited transcript for this recombinant virus) and increased cell cytotoxicity (Volchkov et al., 2001). It should be mentioned that the mutations in the ES were silent (no amino acid change) and, thus did not affect the structure of $GP_{1,2}$ in the recombinant virus.

Having established the importance of the primary structure of the ES for RNA editing, I next analyzed RNA editing using a minigenome containing only the EBOV GP gene ES without any surrounding up- and downstream sequences. RNA editing was dramatically reduced to almost undetectable levels, indicating a requirement of surrounding cis-acting sequences for RNA editing. This was not surprising because cis-acting sequences are known to be required for paramyxovirus P gene editing (Hausmann et al., 1999a). This probably also explains why RNA editing does not occur with the ZEBOV L gene (Figure 30).

To further define the cis-acting sequences for RNA editing, dual-reporter minigenome with deletions of either the upstream 45 nt or downstream 58 nt were generated and analyzed. In both cases, reduction in RNA editing was observed, suggesting that cis-acting sequences reside on both sides of the ES (Figure 35). This is in contrast to paramyxovirus P gene RNA editing, which only seems to require upstream cis-acting sequences (Hausmann et al., 1999a). Despite differences in mechanism and sequence specificity, ADAR-based RNA editing seems to require interaction with a base-paired region that extended up to 20 nt downstream of the edited nucleotide (Lehmann and Bass, 1999; Polson et al., 1996). Similar to ADAR, the apolipoprotein B (apoB) mRNA editing enzyme (APOBEC) (specifically APOBEC1) deaminates (C to U) in ssDNA or RNA. This enzyme has a preference to edit AU rich sequence, and this sequence specificity reside downstream from the ES in the apoB mRNA (Anant et al., 1995; Jantsch and Vesely, 2000).

Having established that cis-acting up- and downstream sequences surrounding the ES are important for RNA editing, it was of interest to further define the exact regions. A

deletion approach was taken to narrow down the up- and downstream sequences required for editing. As small as 18 nt up- and 9 nt downstream sequences were identified as sufficient for editing (Figure 37). Therefore, cis-acting sequences for editing apparently reside between 18 nt up- and 9 nt downstream of the ES. The paramyxovirus cis-acting sequence is strictly conserved within virus genera and resides just upstream of the P gene ES (Hausmann et al., 1999a). Cis-acting sequences not only regulate the editing frequency but also determine the number of G residues insertion during editing. For an example, Sendai virus contains specific alterations within the conserved motif sequence changed editing from a precisely controlled G residue insertion to an uncontrolled A residue insertion (similar to polyadenylation) (Hausmann et al., 1999a; Hausmann et al., 1999b).

4.3.3 Viral Factor for RNA Editing

ZEBOV and REBOV minigenome-driven reporter expression requires all four proteins of the RNP complex (NP, VP35, VP30, and L) (Groseth et al., 2005; Muhlberger et al., 1999). In contrast, MARV minigenome rescue only requires three RNP proteins (NP, VP35, and L) (Muhlberger et al., 1998; Muhlberger et al., 1999). EBOV VP30 has been described to act as a transcription activator (Modrof et al., 2003; Modrof et al., 2002). Oligomerization and phosphorylation of VP30 are important for this function (Hartlieb et al., 2003; Martinez et al., 2008; Modrof et al., 2002). More recently, VP30 has also been assigned a function in the viral replication cycle (Martinez et al., 2011). The only other members of the order *Mononegavirales* that requires a fourth protein for transcription are the pneumoviruses (Fearns and Collins, 1999). The reconstitution of the RNP complex by transient expression using helper-plasmids for optimal reporter

expression was carefully worked out for the ZEBOV minigenome system previously (Muhlberger et al., 1999). In this study, the optimal conditions were used for both plasmid-driven and *in vitro*-transcribed RNA based minigenome rescues. In my studies, dual-reporter minigenome systems did not transcribe or express in absence of NP, L, or VP35. This is not surprising as these proteins are known essential parts of the EBOV RNP complex. Interestingly, and in contrast to previous publications (Muhlberger et al., 1999; Weik et al., 2002), in absence of VP30 both plasmid DNA-driven and *in vitro*-transcribed RNA based minigenomes resulted in reduced but certainly positive transcription and expression. More importantly, in the absence of VP30 RNA editing was impaired using the minigenome system (Figure 38). Therefore, this data indicates a potential novel role of VP30 for EBOV RNA editing.

VP30 based EBOV transcription regulation has not been fully understood; however, it has been shown that VP30 acts as an early anti-terminator for the transcription of the first gene (NP) (Weik et al., 2002). Mutations resulting in the destabilization of the RNA stem-loop of the EBOV leader sequence suggested that VP30 may function in helping the polymerase complex to overcome the stem-loop-driven inhibition at the very early stage of transcription (Weik et al., 2002). A recent study has shown that VP30 preferentially to the sequences near the predicted stem-loop of the leader sequence (John et al., 2007). Therefore, it was important to investigate whether the reduction in RNA editing in the absence of VP30 was not actually caused by a general reduction in transcription. To do this, a leader sequence stem-loop knock out (KO) dual-reporter minigenome was generated by changing six nucleotides (Figure 8B), which had previously been identified as being important for the formation of the leader sequence

stem-loop (Weik et al., 2002). Unexpectedly, this mutant did show a reduction in transcription and expression (Appendix 21 and 22) in the absence of VP30, which is in contrast to the earlier work published by others (Weik et al., 2002). However, taking the reduced transcription and reporter gene expression into account, there was still an obvious reduction in RNA editing in the absence of VP30 (Figure 39), confirming a role of VP30 in RNA editing. Given the role of VP30 in overcoming transcription termination at the stem-loop structure in the EBOV genome leader sequence, one might speculate that a similar stem-loop structure might be present in the cis-acting sequences surrounding the EBOV GP gene ES. Like EBOV VP30, M2-1 of RSV functions in transcript anti-termination (Weik et al., 2002), but the mechanism is unknown (Blondot et al., 2012).

4.3.4 Structural Importance of cis-acting Sequences in RNA Editing

To understand the structural importance of the cis-acting sequences for RNA editing by the EBOV polymerase, a mutational study was undertaken. RdRPs, a class of template dependent polymerases, are key enzymes for viral transcription and replication (Buck, 1996; O'Reilly and Kao, 1998). A unique feature of NNS RNA virus RdRPs is the need of an encapsidated genome as the template for transcription (Ishihama and Barbier, 1994). Filovirus transcription start-signals are predicted to form RNA secondary structures, a unique feature among NNS RNA viruses (Muhlberger et al., 1996; Sanchez et al., 1993). Despite no information on structural requirements for RNA editing (insertion of non-template nucleotide) with NNS viruses, the importance of RNA secondary structures for RNA editing has been well established for ADAR-driven RNA editing [conversion of adenosine (A) residue to inosine (I)] (Brennicke et al., 1999; Casey et al., 1992; Gerber and Keller, 2001; Linnstaedt et al., 2009; Smith et al., 1997; Tian et

al., 2011). In addition, structural features, particularly secondary structures in the immediate vicinity, enable ADARs to recognize specific adenosine for base substitution (Casey et al., 1992; Lehmann and Bass, 1999). ADARs have been studied well for cellular double-stranded RNA (dsRNA) deamination as well as deamination of the HDV genome and anti-genome (Casey, 2006). ADAR-based editing has not been described for EBOV; in contrast, EBOV RNA editing has only been shown to depend on the viral polymerase (Volchkov et al., 1995). Interestingly, the 5' end of the mRNA species of most of the filovirus genes can form stable secondary structures (Muhlberger et al., 1996). Despite the evidence for RNA secondary structures at the leader sequences and its importance for EBOV transcription (Weik et al., 2002), secondary structures at the vicinity of an ES have yet to be determined. A first evidence for the existence of secondary structures located within the cis-acting upstream ES sequences was obtained from computer-assisted prediction analysis (www.mFold.rna.albany.edu). The program predicted two RNA secondary structures at position 1-24 and 38-45 within the 45 nt-long upstream cis-acting sequences (Figure 40A). While destabilization of the first stem-loop (position 1-24) had no effect on RNA editing, destabilization of the second stem-loop (position 38-45) resulted in impaired RNA editing (Figure 41). The second predicted stem-loop is located within the 9 nt upstream region determined earlier to be sufficient for RNA editing. This region is conserved in all EBOV species further supporting (Figure 24) the importance of the secondary structure of the cis-acting sequence in editing; however, the exact mechanism remains unclear. ADAR-based RNA editing is highly regulated by the secondary structure formation of the editing region in the dsRNA substrate (Lehmann and Bass, 1999; Polson et al., 1996). Despite these being deffernce

between mechanism and substrate ADAR and APOBEC1 based editing, it could be speculated that a stem-loop formed by the upstream 9 nt of the EBOV ES will stall the RNP complex at the vicinity of the ES during GP gene transcription. VP30 could play a similar role in overcoming transcript termination as has been described for the leader sequence (Weik et al., 2002). Alternatively, VP30 could bind to the cis-acting sequence at the vicinity of the ES, allowing the RNP complex driven transcription to proceed through re-alignment of the RNP complex to the RNA template. This may lead to a back-sliding of the RNP complex at the uridine stretch of the ES. For this, VP30 would need to bind to the RNA template, which has been shown to occur through its N-terminal Cys_3His_1 motif (John et al., 2007). However, VP30 binding to the cis-acting sequences of the ES remains to be determined. A proposed model for EBOV RNA editing is depicted in Figure 43.

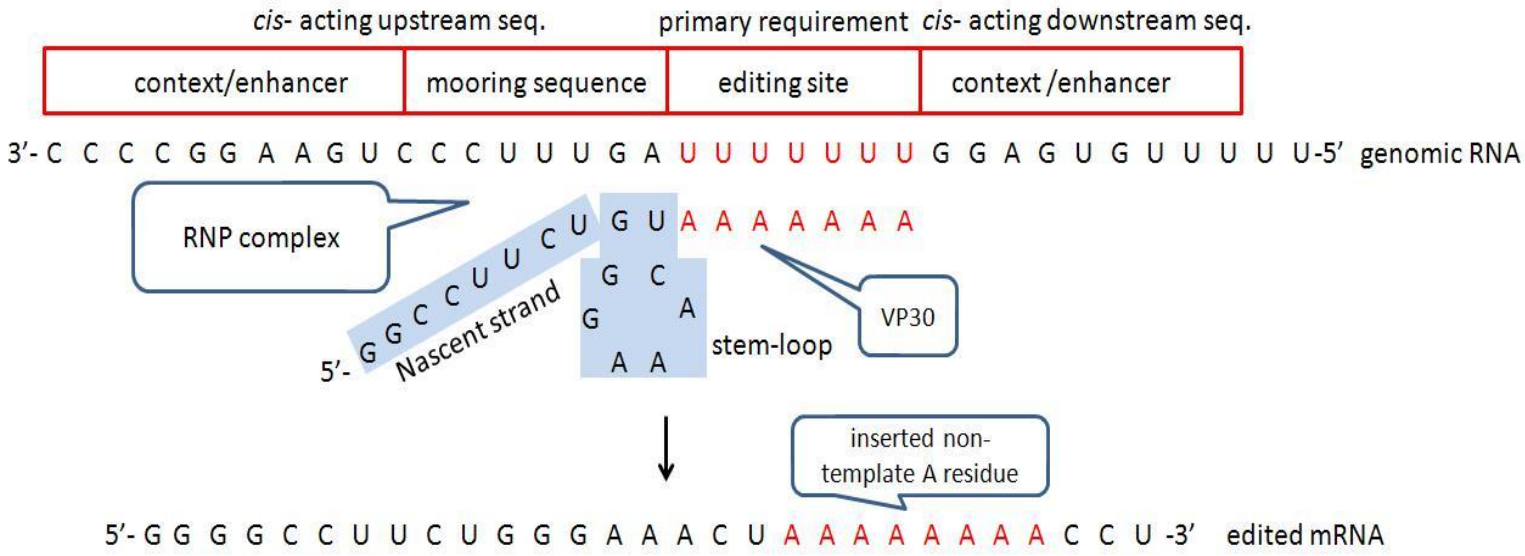

Figure 43. **Proposed mechanism of EBOV RNA editing**. The ES (a hepta uridine stretch, shown here in red) is a primary, but not sole, requirement for RNA editing. The stem-loop formed by the immediate upstream 9 nt of the ES has been identified compulsory for RNA editing and is termed here 'mooring sequence'. The context in which the two identified sequence elements are placed (ES and mooring sequence) has a significant effect on editing and is termed 'enhancer'. The ribonucleoprotein (RNP) complex uses genomic RNA transcription, thus allowing production of mRNA. The stem-loop formed at the mooring sequence potentially stalls the RNP complex. Subsequently, VP30 overcomes the transcription stop allowing transcription to proceed. During this process RNP slippage can occur when it encounters the primary ES resulting in insertion of non-template adenosine residue and thus RNA editing occurs.

4.4 Summary

RNA editing is one of many mechanisms that organisms use for protein diversification as part of the evolutionary process. By RNA editing, viruses uniquely increase their genome encoding capacity by producing multiple proteins from the same gene— EBOV RNA editing is one of the prime examples; however, the mechanism of RNA editing remains an enigma. Therefore, this study was undertaken to identify RNA editing as a common feature of all EBOVs, to study the mechanism of RNA editing, and to characterize previously unknown protein product generated by RNA editing. A better understanding of RNA editing and its role in virus replication might identify targets for novel and urgently needed intervention strategies. Similar to the paramyxoviruses' P gene editing, EBOV RNA editing produces multiple proteins from the GP gene. The primary GP gene-product is sGP, which is abundant in infection; however, a function for sGP has yet not been identified. One out of five GP gene transcripts is edited and produces the transmembrane glycoprotein $GP_{1,2}$, which dictates entry and tropism of EBOV. Here, I could identify a novel third EBOV GP gene-product small soluble glycoprotein (ssGP), which is generated through RNA editing.

Briefly, ssGP is expressed to low abundance during EBOV replication *in vitro* and *in vivo*. This could be demonstrated at the transcript and protein levels. ssGP is apparently N-glycosylated and secreted from the infected cells. The mature form of ssGP is a homodimer formed by two cysteine-mediated a disulfide bond between two monomeric molecules. No obvious function could yet be assigned to ssGP; but, despite biochemical and structural similarities with sGP, it does not have the same anti-inflammatory function as sGP.

Discussion

RNA editing plays an important role in the EBOV life cycle, however, it had only been described for *Zaire ebolavirus*, the type-species of EBOV. In this study, quantification of GP gene transcripts and detection of the corresponding proteins demonstrated that RNA editing is an inherent feature of the genus, *Ebolavirus*. Transcript quantification was achieved by a rapid transcript quantification assay (RTQA), a new method specifically developed for these studies.

In order to study the requirements for EBOV RNA editing a new dual-reporter minigenome was developed allowing studies on RNA editing without using infectious virus (requires BSL4). I could identify the primary sequence of the ES as an important but not sufficient requirement for RNA editing. Important cis-acting sequences reside between 18 nt up- and 9 nt downstream of the ES. The secondary structure of the upstream located cis-acting sequence as well as VP30, a putative viral factor, are the additional important elements for EBOV RNA editing. Overall, this thesis provided a unique scientific contribution to the field of filoviruses in particular and NNS viruses in general. The inherent feature of RNA editing for all EBOV has identified a potential novel target for antiviral therapy.

4.5 Future Directions

Viruses have strategies (e.g. RNA editing) to increase their coding capacity to produce multiple proteins (either structural or nonstructural or both). This study has broadened the understanding of Ebola virus RNA editing, which uniquely produces multiple proteins from the GP gene. Therefore, identification of the second nonstructural protein, ssGP clearly emphasizes the nead to continue further research to understand the role of sGP and ssGP in EBOV infection. The functions of viral nonstructural proteins are diverse and it has been shown that these proteins play important roles in pathogenesis (Geiss et al., 2002; Reyes, 2002; Shaw et al., 2004). Therefore, a functional characterization of ssGP along with sGP would potentially resolve the enigma of EBOV these proteins function. For that, a series of cells could be screened to determine an interaction between ssGP or sGP and host cellular receptor(s) using FACS analysis.

The role of VP30 in editing needs to be addressed in future studies. As a start, a binding experiment between VP30 and the surrounding nucleotide sequence of the GP gene ES might further define its role in editing, which could be done *in vitro*; a similar approach has been described previously (John et al., 2007). Similarly, a deletion approach in the VP30 gene would allow identifying the domains involved in RNA editing. The sequence and structural requirements for RNA editing need to be further analyzed in order to better understand the mechanism and to identify target for intervention. The newly developed RTQA has the potential to be applied here and in other strategies to analyze transcripts of in vitro and *in vivo* infection.

5. REFERENCES

Abràmoff, M.D., Magalhães, P.J., Ram, S.J., 2004. Image processing with ImageJ. *Biophotonics International* 11, 36-42.

Alazard-Dany, N., Volchkova, V., Reynard, O., Carbonnelle, C., Dolnik, O., Ottmann, M., Khromykh, A., Volchkov, V.E., 2006. Ebola virus glycoprotein GP is not cytotoxic when expressed constitutively at a moderate level. *J Gen Virol* 87, 1247-1257.

Aleksandrowicz, P., Marzi, A., Biedenkopf, N., Beimforde, N., Becker, S., Hoenen, T., Feldmann, H., Schnittler, H.J., 2011. Ebola Virus Enters Host Cells by Macropinocytosis and Clathrin-Mediated Endocytosis. Journal of Infectious Diseases 204, S957-S967.

Alexander, C., Danny, B., 2008. An efficient method for the prediction of deleterious multiple-point mutations in the secondary structure of RNAs using suboptimal folding solutions. BMC Bioinformatics 9, 222.

Alvarez, C.P., Lasala, F., Carrillo, J., Muñiz, O., Corbí, A.L., Delgado, R., 2002. C-type lectins DC-SIGN and L-SIGN mediate cellular entry by Ebola virus in cis and in trans. Journal of Virology 76, 6841.

Anant, S., MacGinnitie, A., Davidson, N., 1995. The binding of apobec-1 to mammalian apo B RNA is stabilized by the presence of complementation factors which are required for post-transcriptional editing, p. 99.

Anthony Sanchez, T.W.Giesbert., Heinz Felddmann, 2007. Filoviridae:Marburg and Ebola Viruses, in: David M. Knipe, P.P.M.H., MD; Diane E. Griffin, MD, PhD; Robert A. Lamb, PhD, ScD; Malcolm A. Martin, MD; Bernard Roizman, ScD; Stephen E. Straus, MD (Ed.), Fields Virology, 5th ed. Lippincott Williams and Wilkins, Philadelphia, pp. 1409-1448.

Arnaout, M., Mahalingam, B., Xiong, J.P., 2005. Integrin structure, allostery, and bidirectional signaling. *Annu. Rev. Cell Dev. Biol*. 21, 381-410.

Ascenzi, P., Bocedi, A., Heptonstall, J., Capobianchi, M.R., Di Caro, A., Mastrangelo, E., Bolognesi, M., Ippolito, G., 2008. Ebolavirus and Marburgvirus: insight the Filoviridae family. *Mol Aspects Med* 29, 151-185.

Baize, S., Leroy, E., Georges, A., Georges-Courbot, M.C., Capron, M., Bedjabaga, I., Lansoud-Soukate, J., Mavoungou, E., 2002. Inflammatory responses in Ebola virus-infected patients. *Clinical & Experimental Immunology* 128, 163-168.

Baize, S., Leroy, E.M., Georges-Courbot, M.C., Capron, M., Lansoud-Soukate, J., Debre, P., Fisher-Hoch, S.P., McCormick, J.B., Georges, A.J., 1999. Defective humoral responses and extensive intravascular apoptosis are associated with fatal outcome in Ebola virus-infected patients. *Nat Med* 5, 423-426.

Bale, S., Liu, T., Li, S., Wang, Y., Abelson, D., Fusco, M., Woods, V.L., Jr., Ollmann Saphire, E., 2011. Ebola Virus Glycoprotein Needs an Additional Trigger, beyond Proteolytic Priming for Membrane Fusion. *PLoS Negl Trop Dis* 5, e1395.

Barnes, B., Lubyova, B., Pitha, P.M., 2002. Review: on the role of IRF in host defense. *Journal of Interferon & Cytokine Research* 22, 59-71.

Baron, R.C., McCormick, J.B., Zubeir, O.A., 1983. Ebola virus disease in southern Sudan: hospital dissemination and intrafamilial spread. *Bull World Health Organ* 61, 997-1003.

Barrientos, L.G., Martin, A.M., Rollin, P.E., Sanchez, A., 2004. Disulfide bond assignment of the Ebola virus secreted glycoprotein SGP. *Biochem Biophys Res Commun* 323, 696-702.

Barrientos, L.G., Martin, A.M., Wohlhueter, R.M., Rollin, P.E., 2007. Secreted glycoprotein from Live Zaire ebolavirus-infected cultures: preparation, structural and biophysical characterization, and thermodynamic stability. *J Infect Dis* 196 Suppl 2, S220-231.

Bashirova, A.A., Geijtenbeek, T.B.H., van Duijnhoven, G.C.F., van Vliet, S.J., Eilering, J.B.G., Martin, M.P., Wu, L., Martin, T.D., Viebig, N., Knolle, P.A., 2001. A dendritic cell–specific intercellular adhesion molecule 3–grabbing nonintegrin (DC-SIGN)–related

protein is highly expressed on human liver sinusoidal endothelial cells and promotes HIV-1 infection. *The Journal of Experimental Medicine* 193, 671.

Baskerville, A., Bowen, E.T., Platt, G.S., McArdell, L.B., Simpson, D.I., 1978. The pathology of experimental Ebola virus infection in monkeys. *J Pathol* 125, 131-138.

Basler, C.F., Mikulasova, A., Martinez-Sobrido, L., Paragas, J., Muhlberger, E., Bray, M., Klenk, H.D., Palese, P., Garcia-Sastre, A., 2003. The Ebola virus VP35 protein inhibits activation of interferon regulatory factor 3. J*ournal of Virology* 77, 7945.

Basler, C.F., Wang, X., Mühlberger, E., Volchkov, V., Paragas, J., Klenk, H.D., García-Sastre, A., Palese, P., 2000. The Ebola virus VP35 protein functions as a type I IFN antagonist. *Proceedings of the National Academy of Sciences* 97, 12289.

Bausch, D.G., Nichol, S.T., Muyembe-Tamfum, J.J., Borchert, M., Rollin, P.E., Sleurs, H., Campbell, P., Tshioko, F.K., Roth, C., Colebunders, R., Pirard, P., Mardel, S., Olinda, L.A., Zeller, H., Tshomba, A., Kulidri, A., Libande, M.L., Mulangu, S., Formenty, P., Grein, T., Leirs, H., Braack, L., Ksiazek, T., Zaki, S., Bowen, M.D., Smit, S.B., Leman, P.A., Burt, F.J., Kemp, A., Swanepoel, R., 2006. Marburg hemorrhagic fever associated with multiple genetic lineages of virus. *N Engl J Med* 355, 909-919.

Bausch, D.G., Sprecher, A.G., Jeffs, B., Boumandouki, P., 2008. Treatment of Marburg and Ebola hemorrhagic fevers: a strategy for testing new drugs and vaccines under outbreak conditions. *Antiviral Res* 78, 150-161.

Bavari, S., Bosio, C.M., Wiegand, E., Ruthel, G., Will, A.B., Geisbert, T.W., Hevey, M., Schmaljohn, C., Schmaljohn, A., Aman, M.J., 2002. Lipid raft microdomains. *The Journal of Experimental Medicine* 195, 593-602.

Becker, S., 2007. Fighting filoviruses. *Expert Rev Vaccines* 6, 1.

Beniac, D.R., Melito, P.L., Hiebert, S.L., Rabb, M.J., Lamboo, L.L., Jones, S.M., Booth, T.F., 2012. The Organisation of Ebola Virus Reveals a Capacity for Extensive, Modular Polyploidy. *PLoS One* 7, e29608.

Bharat, T.A., Noda, T., Riches, J.D., Kraehling, V., Kolesnikova, L., Becker, S., Kawaoka, Y., Briggs, J.A., 2012. Structural dissection of Ebola virus and its assembly determinants using cryo-electron tomography. *Proc Natl Acad Sci* U S A. pnas.1120453109.

Blondot, M.L., Dubosclard, V., Fix, J., Lassoued, S., Aumont-Nicaise, M., Bontems, F., Eléouët, J.F., Sizun, C., 2012. Structure and Functional Analysis of the RNA-and Viral Phosphoprotein-Binding Domain of Respiratory Syncytial Virus M2-1 Protein. *PLoS Pathogens* 8, e1002734.

Bosio, C.M., Aman, M.J., Grogan, C., Hogan, R., Ruthel, G., Negley, D., Mohamadzadeh, M., Bavari, S., Schmaljohn, A., 2003. Ebola and Marburg viruses replicate in monocyte-derived dendritic cells without inducing the production of cytokines and full maturation. *Journal of Infectious Diseases* 188, 1630.

Bourhis, J.M., Canard, B., Longhi, S., 2006. Structural disorder within the replicative complex of measles virus: functional implications. *Virology* 344, 94-110.

Bray, M., 2003. Defense against filoviruses used as biological weapons. *Antiviral Res* 57, 53-60.

Bray, M., 2009. Filoviruses, in: Douglas D. Richman, R.J.W., Frederick G. Heyden (Ed.), Clinical Virology, 3rd ed. American Society of Microbiology, Washington, DC, pp. 923-941.

Bray, M., Davis, K., Geisbert, T., Schmaljohn, C., Huggins, J., 1998. A mouse model for evaluation of prophylaxis and therapy of Ebola hemorrhagic fever. *J Infect Dis* 178, 651-661.

Bray, M., Geisbert, T.W., 2005. Ebola virus: the role of macrophages and dendritic cells in the pathogenesis of Ebola hemorrhagic fever. *Int J Biochem Cell Biol* 37, 1560-1566.

Brecher, M., Schornberg, K.L., Delos, S.E., Fusco, M.L., Saphire, E.O., White, J.M., 2012. Cathepsin cleavage potentiates the Ebola virus glycoprotein to undergo a subsequent fusion-relevant conformational change. *Journal of Virology* 86, 364-372.

References

Breman, J.G., Johnson, K.M., van der Groen, G., Robbins, C.B., Szczeniowski, M.V., Ruti, K., Webb, P.A., Meier, F., Heymann, D.L., 1999. A search for Ebola virus in animals in the Democratic Republic of the Congo and Cameroon: ecologic, virologic, and serologic surveys, 1979-1980. Ebola Virus Study Teams. *J Infect Dis 179 Suppl 1*, S139-147.

Brennicke, A., Marchfelder, A., Binder, S., 1999. RNA editing. *FEMS Microbiology Reviews* 23, 297-316.

Brierley, I., Digard, P., Inglis, S.C., 1989. Characterization of an efficient coronavirus ribosomal frameshifting signal: requirement for an RNA pseudoknot. *Cell* 57, 537-547.

Brindley, M.A., Hughes, L., Ruiz, A., McCray, P.B., Jr., Sanchez, A., Sanders, D.A., Maury, W., 2007. Ebola virus glycoprotein 1: identification of residues important for binding and postbinding events. *Journal of Virology* 81, 7702-7709.

Buck, K.W., 1996. Comparison of the replication of positive-stranded RNA viruses of plants and animals. *Advances in Virus Research* 47, 159-251.

Bukreyev, A., Rollin, P.E., Tate, M.K., Yang, L., Zaki, S.R., Shieh, W.J., Murphy, B.R., Collins, P.L., Sanchez, A., 2007. Successful topical respiratory tract immunization of primates against Ebola virus. *Journal of Virology* 81, 6379.

Bukreyev, A., Volchkov, V., Blinov, V., Netesov, S., 1993. The VP35 and VP40 proteins of filoviruses:: Homology between Marburg and Ebola viruses. *FEBS Lett* 322, 41-46.

Bukreyev, A., Yang, L., Zaki, S.R., Shieh, W.J., Rollin, P.E., Murphy, B.R., Collins, P.L., Sanchez, A., 2006. A single intranasal inoculation with a paramyxovirus-vectored vaccine protects guinea pigs against a lethal-dose Ebola virus challenge. *Journal of Virology* 80, 2267-2279.

Calain, P., Monroe, M.C., Nichol, S.T., 1999. Ebola virus defective interfering particles and persistent infection. *Virology* 262, 114-128.

Cárdenas, W.B., 2010. Evasion of the Interferon-Mediated Antiviral Response by Filoviruses. *Viruses* 2, 262-282.

Cárdenas, W.B., Loo, Y.M., Gale Jr, M., Hartman, A.L., Kimberlin, C.R., Martinez-Sobrido, L., Saphire, E.O., Basler, C.F., 2006. Ebola virus VP35 protein binds double-stranded RNA and inhibits alpha/beta interferon production induced by RIG-I signaling. *Journal of Virology* 80, 5168.

Carette, J.E., Raaben, M., Wong, A.C., Herbert, A.S., Obernosterer, G., Mulherkar, N., Kuehne, A.I., Kranzusch, P.J., Griffin, A.M., Ruthel, G., 2011. Ebola virus entry requires the cholesterol transporter Niemann-Pick C1. *Nature* 477, 340-343.

Carstea, E.D., Morris, J.A., Coleman, K.G., Loftus, S.K., Zhang, D., Cummings, C., Gu, J., Rosenfeld, M.A., Pavan, W.J., Krizman, D.B., 1997. Niemann-Pick C1 disease gene: homology to mediators of cholesterol homeostasis. *Science* 277, 228-231.

Casey, J., 2006. RNA editing in hepatitis delta virus. Hepatitis Delta Virus, 67-89.

Casey, J.L., Bergmann, K.F., Brown, T.L., Gerin, J.L., 1992. Structural requirements for RNA editing in hepatitis delta virus: evidence for a uridine-to-cytidine editing mechanism. *Proc Natl Acad Sci* U S A 89, 7149-7153.

Casey, J.L., Gerin, J.L., 1995. Hepatitis D virus RNA editing: specific modification of adenosine in the antigenomic RNA. *Journal of Virology* 69, 7593-7600.

Casillas, A.M., Nyamathi, A.M., Sosa, A., Wilder, C.L., Sands, H., 2003. A current review of Ebola virus: pathogenesis, clinical presentation, and diagnostic assessment. *Biol Res Nurs* 4, 268-275.

Chandran, K., Sullivan, N.J., Felbor, U., Whelan, S.P., Cunningham, J.M., 2005. Endosomal proteolysis of the Ebola virus glycoprotein is necessary for infection. *Science* 308, 1643-1645.

Chung, K.M., Liszewski, M.K., Nybakken, G., Davis, A.E., Townsend, R.R., Fremont, D.H., Atkinson, J.P., Diamond, M.S., 2006. West Nile virus nonstructural protein NS1 inhibits

complement activation by binding the regulatory protein factor H. *Proceedings of the National Academy of Sciences* 103, 19111-19116.

Churkin, A., Gabdank, I., Barash, D., 2011. The RNAmute web server for the mutational analysis of RNA secondary structures. *Nucleic acids research* 39, W92-W99.

Claude, P., 1978. Morphological factors influencing transepithelial permeability: a model for the resistance of the zonula occludens. *J Membr Biol* 39, 219-232.

Collins, P.L., Graham, B.S., 2008. Viral and host factors in human respiratory syncytial virus pathogenesis. *Journal of Virology* 82, 2040-2055.

Conner, S.D., Schmid, S.L., 2003. Regulated portals of entry into the cell. Nature 422, 37-44.

Conrad, J.L., Isaacson, M., Smith, E.B., Wulff, H., Crees, M., Geldenhuys, P., Johnston, J., 1978. Epidemiologic investigation of Marburg virus disease, Southern Africa, 1975. A*m J Trop Med Hyg* 27, 1210-1215.

Côté, M., Misasi, J., Ren, T., Bruchez, A., Lee, K., Filone, C.M., Hensley, L., Li, Q., Ory, D., Chandran, K., 2011. Small molecule inhibitors reveal Niemann-Pick C1 is essential for Ebola virus infection. *Nature* 477, 344-348.

Cozelmann, k.K., 2004. Reverse Genetics of Mononegavirales, in: Kawaoka, Y. (Ed.), Biology of negative strand RNA viruses: the power of reverse genetics. Springer, pp. 1-32.

Davis, K.J., Anderson, A.O., Geisbert, T.W., Steele, K.E., Geisbert, J.B., Vogel, P., Connolly, B.M., Huggins, J.W., Jahrling, P.B., Jaax, N.K., 1997. Pathology of experimental Ebola virus infection in African green monkeys. Involvement of fibroblastic reticular cells. *Arch Pathol Lab Med* 121, 805-819.

DePaola, N., Phelps, J.E., Florez, L., Keese, C.R., Minnear, F.L., Giaever, I., Vincent, P., 2001. Electrical impedance of cultured endothelium under fluid flow. *Annals of biomedical engineering* 29, 648-656.

Dessen, A., Volchkov, V., Dolnik, O., Klenk, H.D., Weissenhorn, W., 2000. Crystal structure of the matrix protein VP40 from Ebola virus. *Embo J* 19, 4228-4236.

Dieterich, P., Odenthal-Schnittler, M., Mrowietz, C., Krämer, M., Sasse, L., Oberleithner, H., Schnittler, H.J., 2000. Quantitative morphodynamics of endothelial cells within confluent cultures in response to fluid shear stress. *Biophysical Journal* 79, 1285-1297.

Dolnik, O., Kolesnikova, L., Becker, S., 2008. Filoviruses: interactions with the host cell. *Cellular andMmolecular Life Sciences* 65, 756-776.

Dolnik, O., Volchkova, V., Garten, W., Carbonnelle, C., Becker, S., Kahnt, J., Stroher, U., Klenk, H.D., Volchkov, V., 2004. Ectodomain shedding of the glycoprotein GP of Ebola virus. *EMBO J* 23, 2175-2184.

Dominguez-Soto, A., Aragoneses-Fenoll, L., Martin-Gayo, E., Martinez-Prats, L., Colmenares, M., Naranjo-Gomez, M., Borras, F.E., Munoz, P., Zubiaur, M., Toribio, M.L., 2007. The DC-SIGN–related lectin LSECtin mediates antigen capture and pathogen binding by human myeloid cells. *Blood* 109, 5337-5345.

Dowell, S.F., Mukunu, R., Ksiazek, T.G., Khan, A.S., Rollin, P.E., Peters, C.J., 1999. Transmission of Ebola hemorrhagic fever: a study of risk factors in family members, Kikwit, Democratic Republic of the Congo, 1995. Commission de Lutte contre les Epidemies a Kikwit. *J Infect Dis 179 Suppl* 1, S87-91.

Dube, D., Brecher, M.B., Delos, S.E., Rose, S.C., Park, E.W., Schornberg, K.L., Kuhn, J.H., White, J.M., 2009. The primed ebolavirus glycoprotein (19-kilodalton GP1,2): sequence and residues critical for host cell binding. *Journal of Virology* 83, 2883-2891.

Dye, J.M., Herbert, A.S., Kuehne, A.I., Barth, J.F., Muhammad, M.A., Zak, S.E., Ortiz, R.A., Prugar, L.I., Pratt, W.D., 2012. Postexposure antibody prophylaxis protects nonhuman primates from filovirus disease. *Proceedings of the National Academy of Sciences* 109, 5034-5039.

References

Ebihara, H., Takada, A., Kobasa, D., Jones, S., Neumann, G., Theriault, S., Bray, M., Feldmann, H., Kawaoka, Y., 2006. Molecular determinants of Ebola virus virulence in mice. *PLoS Pathog* 2, e73.

Egelman, E., Wu, S., Amrein, M., Portner, A., Murti, G., 1989. The Sendai virus nucleocapsid exists in at least four different helical states. *Journal of Virology* 63, 2233.

Elliott, L.H., Kiley, M.P., McCormick, J.B., 1985. Descriptive analysis of Ebola virus proteins. *Virology* 147, 169-176.

Emond, R., Evans, B., Bowen, E., Lloyd, G., 1977. A case of Ebola virus infection. *British Medical Journal* 2, 541-544.

Empig, C.J., Goldsmith, M.A., 2002. Association of the caveola vesicular system with cellular entry by filoviruses. *Journal of Virology* 76, 5266.

Falzarano, D., 2010. Structure-Function analysis of Ebola virus glycoproteins, Department of Medical Microbiology. University of Manitoba, Winnipeg.

Falzarano, D., Krokhin, O., Van Domselaar, G., Wolf, K., Seebach, J., Schnittler, H.J., Feldmann, H., 2007. Ebola sGP--the first viral glycoprotein shown to be C-mannosylated. *Virology* 368, 83-90.

Falzarano, D., Krokhin, O., Wahl-Jensen, V., Seebach, J., Wolf, K., Schnittler, H.J., Feldmann, H., 2006. Structure-function analysis of the soluble glycoprotein, sGP, of Ebola virus. *Chembiochem* 7, 1605-1611.

Fearns, R., Collins, P.L., 1999. Role of the M2-1 transcription antitermination protein of respiratory syncytial virus in sequential transcription. *Journal of Virology* 73, 5852-5864.

Feldmann, H., Bugany, H., Mahner, F., Klenk, H.D., Drenckhahn, D., Schnittler, H.J., 1996a. Filovirus-induced endothelial leakage triggered by infected monocytes/macrophages. *Journal of Virology* 70, 2208-2214.

Feldmann, H., Geisbert, T.W., 2011. Ebola haemorrhagic fever. *The Lancet* 377, 849-862.

Feldmann, H., Jones, S., Klenk, H.D., Schnittler, H.J., 2003. Ebola virus: from discovery to vaccine. *Nat Rev Immunol* 3, 677-685.

Feldmann, H., Jones, S.M., Daddario-DiCaprio, K.M., Geisbert, J.B., Ströher, U., Grolla, A., Bray, M., Fritz, E.A., Fernando, L., Feldmann, F., 2007. Effective post-exposure treatment of Ebola infection. *PLoS Pathogens* 3, e2.

Feldmann, H., Klenk, H.D., 1996. Marburg and Ebola viruses. *Adv Virus Res* 47, 1-52.

Feldmann, H., Nichol, S.T., Klenk, H.D., Peters, C.J., Sanchez, A., 1994. Characterization of filoviruses based on differences in structure and antigenicity of the virion glycoprotein. *Virology* 199, 469-473.

Feldmann, H., Slenczka, W., Klenk, H.D., 1996b. Emerging and reemerging of filoviruses. *Arch Virol Suppl* 11, 77-100.

Feldmann, H., Volchkov, V.E., Volchkova, V.A., Stroher, U., Klenk, H.D., 2001. Biosynthesis and role of filoviral glycoproteins. *J Gen Virol* 82, 2839-2848.

Feng, Z., Cerveny, M., Yan, Z., He, B., 2007. The VP35 protein of Ebola virus inhibits the antiviral effect mediated by double-stranded RNA-dependent protein kinase PKR. *Journal of Virology* 81, 182.

Ferron, F., Longhi, S., Henrissat, B., Canard, B., 2002. Viral RNA-polymerases-a predicted 2'-O-ribose methyltransferase domain shared by all Mononegavirales. *Trends in biochemical sciences* 27, 222-224.

Fisher-Hoch, S., McCormick, J., 1999. Experimental filovirus infections. *Current Topics in Microbiology and Immunology* 235, 117.

Formenty, P., Hatz, C., Le Guenno, B., Stoll, A., Rogenmoser, P., Widmer, A., 1999. Human infection due to Ebola virus, subtype Cote d'Ivoire: clinical and biologic presentation. *Journal of Infectious Diseases* 179, S48.

Formenty, P., Libama, F., Epelboin, A., Allarangar, Y., Leroy, E., Moudzeo, H., Tarangonia, P., Molamou, A., Lenzi, M., Ait-Ikhlef, K., Hewlett, B., Roth, C., Grein, T., 2003. [Outbreak

of Ebola hemorrhagic fever in the Republic of the Congo, 2003: a new strategy?]. *Med Trop* (Mars) 63, 291-295.

Freeman, G.J., Casasnovas, J.M., Umetsu, D.T., DeKruyff, R.H., 2010. TIM genes: a family of cell surface phosphatidylserine receptors that regulate innate and adaptive immunity. *Immunological Reviews* 235, 172-189.

Galinski, M.S., Troy, R.M., Banerjee, A.K., 1992. RNA editing in the phosphoprotein gene of the human parainfluenza virus type 3. *Virology* 186, 543-550.

Garbutt, M., Liebscher, R., Wahl-Jensen, V., Jones, S., Moller, P., Wagner, R., Volchkov, V., Klenk, H.D., Feldmann, H., Stroher, U., 2004. Properties of replication-competent vesicular stomatitis virus vectors expressing glycoproteins of filoviruses and arenaviruses. *Journal of Virology* 78, 5458.

Garoff, H., Hewson, R., Opstelten, D.J.E., 1998. Virus maturation by budding. *Microbiology and molecular biology reviews* 62, 1171.

Gear, J.S., Cassel, G.A., Gear, A.J., Trappler, B., Clausen, L., Meyers, A.M., Kew, M.C., Bothwell, T.H., Sher, R., Miller, G.B., Schneider, J., Koornhof, H.J., Gomperts, E.D., Isaacson, M., Gear, J.H., 1975. Outbreake of Marburg virus disease in Johannesburg. *Br Med J* 4, 489-493.

Geisbert, T.W., Daddario-DiCaprio, K.M., Williams, K.J., Geisbert, J.B., Leung, A., Feldmann, F., Hensley, L.E., Feldmann, H., Jones, S.M., 2008. Recombinant vesicular stomatitis virus vector mediates postexposure protection against Sudan Ebola hemorrhagic fever in nonhuman primates. *Journal of Virology* 82, 5664-5668.

Geisbert, T.W., Hensley, L.E., Jahrling, P.B., Larsen, T., Geisbert, J.B., Paragas, J., Young, H.A., Fredeking, T.M., Rote, W.E., Vlasuk, G.P., 2003a. Treatment of Ebola virus infection with a recombinant inhibitor of factor VIIa/tissue factor: a study in rhesus monkeys. *The Lancet* 362, 1953-1958.

Geisbert, T.W., Hensley, L.E., Kagan, E., Yu, E.Z., Geisbert, J.B., Daddario-DiCaprio, K., Fritz, E.A., Jahrling, P.B., McClintock, K., Phelps, J.R., 2006. Postexposure protection of guinea pigs against a lethal ebola virus challenge is conferred by RNA interference. *Journal of Infectious Diseases* 193, 1650-1657.

Geisbert, T.W., Hensley, L.E., Larsen, T., Young, H.A., Reed, D.S., Geisbert, J.B., Scott, D.P., Kagan, E., Jahrling, P.B., Davis, K.J., 2003b. Pathogenesis of Ebola hemorrhagic fever in cynomolgus macaques: evidence that dendritic cells are early and sustained targets of infection. *Am J Pathol* 163, 2347-2370.

Geisbert, T.W., Lee, A.C., Robbins, M., Geisbert, J.B., Honko, A.N., Sood, V., Johnson, J.C., de Jong, S., Tavakoli, I., Judge, A., Hensley, L.E., Maclachlan, I., 2010. Postexposure protection of non-human primates against a lethal Ebola virus challenge with RNA interference: a proof-of-concept study. *Lancet* 375, 1896-1905.

Geisbert, T.W., Young, H.A., Jahrling, P.B., Davis, K.J., Larsen, T., Kagan, E., Hensley, L.E., 2003c. Pathogenesis of Ebola hemorrhagic fever in primate models: evidence that hemorrhage is not a direct effect of virus-induced cytolysis of endothelial cells. *Am J Pathol* 163, 2371-2382.

Geiss, G.K., Salvatore, M., Tumpey, T.M., Carter, V.S., Wang, X., Basler, C.F., Taubenberger, J.K., Bumgarner, R.E., Palese, P., Katze, M.G., 2002. Cellular transcriptional profiling in influenza A virus-infected lung epithelial cells: the role of the nonstructural NS1 protein in the evasion of the host innate defense and its potential contribution to pandemic influenza. *Proceedings of the National Academy of Sciences* 99, 10736.

Gélinas, J.F., Clerzius, G., Shaw, E., Gatignol, A., 2011. Enhancement of replication of RNA viruses by ADAR1 via RNA editing and inhibition of RNA-activated protein kinase. *Journal of Virology* 85, 8460-8466.

Georges-Courbot, M.C., Sanchez, A., Lu, C.Y., Baize, S., Leroy, E., Lansout-Soukate, J., Tevi-Benissan, C., Georges, A.J., Trappier, S.G., Zaki, S.R., Swanepoel, R., Leman, P.A.,

Rollin, P.E., Peters, C.J., Nichol, S.T., Ksiazek, T.G., 1997. Isolation and phylogenetic characterization of Ebola viruses causing different outbreaks in Gabon. *Emerg Infect Dis* 3, 59-62.

Gerber, A.P., Keller, W., 2001. RNA editing by base deamination: more enzymes, more targets, new mysteries. *Trends in Biochemical Sciences* 26, 376-384.

Gomis-Rüth, F.X., Dessen, A., Timmins, J., Bracher, A., Kolesnikowa, L., Becker, S., Klenk, H.D., Weissenhorn, W., 2003. The matrix protein VP40 from Ebola virus octamerizes into pore-like structures with specific RNA binding properties. *Structure* 11, 423-433.

Gramberg, T., Hofmann, H., Möller, P., Lalor, P.F., Marzi, A., Geier, M., Krumbiegel, M., Winkler, T., Kirchhoff, F., Adams, D.H., 2005. LSECtin interacts with filovirus glycoproteins and the spike protein of SARS coronavirus. *Virology* 340, 224-236.

Grolla, A., Lucht, A., Dick, D., Strong, J.E., Feldmann, H., 2005. Laboratory diagnosis of Ebola and Marburg hemorrhagic fever. *Bull Soc Pathol Exot* 98, 205-209.

Groseth, A., Charton, J.E., Sauerborn, M., Feldmann, F., Jones, S.M., Hoenen, T., Feldmann, H., 2009. The Ebola virus ribonucleoprotein complex: a novel VP30-L interaction identified. *Virus Res* 140, 8-14.

Groseth, A., Feldmann, H., Theriault, S., Mehmetoglu, G., Flick, R., 2005. RNA polymerase I-driven minigenome system for Ebola viruses. *Journal of Virology* 79, 4425-4433.

Groseth, A., Hoenen, T., Eickmann, M., Becker, S., Filoviruses: Ebola, Marburg and Disease. eLS.

Günther, S., Feldmann, H., Geisbert, T.W., Hensley, L.E., Rollin, P.E., Nichol, S.T., Ströher, U., Artsob, H., Peters, C.J., Ksiazek, T.G., 2011. Management of Accidental Exposure to Ebola Virus in the Biosafety Level 4 Laboratory, Hamburg, Germany. *Journal of Infectious Diseases* 204, S785-S790.

Haasnoot, J., De Vries, W., Geutjes, E.J., Prins, M., De Haan, P., Berkhout, B., 2007. The Ebola virus VP35 protein is a suppressor of RNA silencing. *PLoS Pathogens* 3, e86.

Hajduk, S., Ochsenreiter, T., 2010. RNA editing in kinetoplastids. *RNA Biology* 7, 229.

Han, Z., Boshra, H., Sunyer, J.O., Zwiers, S.H., Paragas, J., Harty, R.N., 2003. Biochemical and functional characterization of the Ebola virus VP24 protein: implications for a role in virus assembly and budding. *Journal of Virology* 77, 1793.

Harrison, S.C., 2008. Viral membrane fusion. Nature structural & molecular biology 15, 690-698.

Hartlieb, B., Modrof, J., Muhlberger, E., Klenk, H.D., Becker, S., 2003. Oligomerization of Ebola virus VP30 is essential for viral transcription and can be inhibited by a synthetic peptide. *J Biol Chem* 278, 41830-41836.

Hartlieb, B., Muziol, T., Weissenhorn, W., Becker, S., 2007. Crystal structure of the C-terminal domain of Ebola virus VP30 reveals a role in transcription and nucleocapsid association. *Proceedings of the National Academy of Sciences* 104, 624.

Hartman, A.L., Towner, J.S., Nichol, S.T., 2010. Ebola and marburg hemorrhagic fever. *Clin Lab Med* 30, 161-177.

Harty, R.N., Brown, M.E., Wang, G., Huibregtse, J., Hayes, F.P., 2000. A PPxY motif within the VP40 protein of Ebola virus interacts physically and functionally with a ubiquitin ligase: implications for filovirus budding. *Proceedings of the National Academy of Sciences* 97, 13871.

Hausmann, S., Garcin, D., Delenda, C., Kolakofsky, D., 1999a. The versatility of paramyxovirus RNA polymerase stuttering. *Journal of Virology* 73, 5568-5576.

Hausmann, S., Garcin, D., Morel, A.S., Kolakofsky, D., 1999b. Two nucleotides immediately upstream of the essential A6G3 slippery sequence modulate the pattern of G insertions during Sendai virus mRNA editing. *Journal of Virology* 73, 343-351.

Hensley, L.E., Geisbert, T.W., 2005. The contribution of the endothelium to the development of coagulation disorders that characterize Ebola hemorrhagic fever in primates.Thrombosis and Haemostasis-Stuttgart- 94, 254.

References

Hensley, L.E., Mulangu, S., Asiedu, C., Johnson, J., Honko, A.N., Stanley, D., Fabozzi, G., Nichol, S.T., Ksiazek, T.G., Rollin, P.E., 2010. Demonstration of cross-protective vaccine immunity against an emerging pathogenic Ebolavirus species. *PLoS Pathogens* 6, e1000904.

Hensley, L.E., Young, H.A., Jahrling, P.B., Geisbert, T.W., 2002. Proinflammatory response during Ebola virus infection of primate models: possible involvement of the tumor necrosis factor receptor superfamily. *Immunol Lett* 80, 169-179.

Hoenen, T., Groseth, A., Falzarano, D., Feldmann, H., 2006a. Ebola virus: unravelling pathogenesis to combat a deadly disease. *Trends Mol Med* 12, 206-215.

Hoenen, T., Groseth, A., Kolesnikova, L., Theriault, S., Ebihara, H., Hartlieb, B., Bamberg, S., Feldmann, H., Stroher, U., Becker, S., 2006b. Infection of naive target cells with virus-like particles: implications for the function of Ebola virus VP24. *Journal of Virology* 80, 7260.

Hoenen, T., Volchkov, V., Kolesnikova, L., Mittler, E., Timmins, J., Ottmann, M., Reynard, O., Becker, S., Weissenhorn, W., 2005. VP40 octamers are essential for Ebola virus replication. *Journal of Virology* 79, 1898.

Hua, L., Low, T.Y., Sze, S.K., 2006. Microwave-assisted specific chemical digestion for rapid protein identification. *Proteomics* 6, 586-591.

Huang, Y., Xu, L., Sun, Y., Nabel, G.J., 2002. The assembly of Ebola virus nucleocapsid requires virion-associated proteins 35 and 24 and posttranslational modification of nucleoprotein. *Mol Cell* 10, 307-316.

Huggins, J., Zhang, Z.X., Bray, M., 1999. Antiviral drug therapy of filovirus infections: S-adenosylhomocysteine hydrolase inhibitors inhibit Ebola virus in vitro and in a lethal mouse model. *Journal of Infectious Diseases* 179, S240.

Huggins, J.W., 1989. Prospects for treatment of viral hemorrhagic fevers with ribavirin, a broad-spectrum antiviral drug. *Review of Infectious Diseases* 11, S750.

Hunt, C.L., Lennemann, N.J., Maury, W., 2012. Filovirus Entry: A Novelty in the Viral Fusion World. *Viruses* 4, 258-275.

Hurley, J.H., Bonifacino, J.S., 2012. Nef-arious goings-on at the Golgi. *Nat Struct Mol Biol* 19, 661-662.

Iannello, A., Debbeche, O., Martin, E., Attalah, L.H., Samarani, S., Ahmad, A., 2006. Viral strategies for evading antiviral cellular immune responses of the host. *Journal of leukocyte Biology* 79, 16-35.

Ignatyev, G., Steinkasserer, A., Streltsova, M., Atrasheuskaya, A., Agafonov, A., Lubitz, W., 2000. Experimental study on the possibility of treatment of some hemorrhagic fevers. *J Biotechnol* 83, 67-76.

Ikegami, T., Niikura, M., Saijo, M., Miranda, M.E., Calaor, A.B., Hernandez, M., Acosta, L.P., Manalo, D.L., Kurane, I., Yoshikawa, Y., 2003. Antigen capture enzyme-linked immunosorbent assay for specific detection of Reston Ebola virus nucleoprotein. *Clinical and Vaccine Immunology* 10, 552.

Iseni, F., Baudin, F., Garcin, D., Marq, J.B., Ruigrok, R.W.H., Kolakofsky, D., 2002. Chemical modification of nucleotide bases and mRNA editing depend on hexamer or nucleoprotein phase in Sendai virus nucleocapsids. *RNA* 8, 1056-1067.

Ishihama, A., Barbier, P., 1994. Molecular anatomy of viral RNA-directed RNA polymerases. *Archives of Virology* 134, 235-258.

Ito, H., Watanabe, S., Sanchez, A., Whitt, M.A., Kawaoka, Y., 1999. Mutational analysis of the putative fusion domain of Ebola virus glycoprotein. *J Virol* 73, 8907-8912.

Iwasa, A., Shimojima, M., Kawaoka, Y., 2011. sGP Serves as a Structural Protein in Ebola Virus Infection. *Journal of Infectious Diseases* 204, S897-S903.

Iwase, H., Hotta, K., 1993. Release of O-linked glycoprotein glycans by endo-alpha-N-acetylgalactosaminidase. *Methods Mol Biol* 14, 151-159.

References

Jaax, N.K., Davis, K.J., Geisbert, T.J., Vogel, P., Jaax, G.P., Topper, M., Jahrling, P.B., 1996. Lethal experimental infection of rhesus monkeys with Ebola-Zaire (Mayinga) virus by the oral and conjunctival route of exposure. *Arch Pathol Lab Med* 120, 140-155.

Jacks, T., Varmus, H.E., 1985. Expression of the Rous sarcoma virus pol gene by ribosomal frameshifting. *Science* 230, 1237.

Jacques, J.P., Hausmann, S., Kolakofsky, D., 1994. Paramyxovirus mRNA editing leads to G deletions as well as insertions. *EMBO J* 13, 5496-5503.

Jagger, B.W., Wise, H.M., Kash, J.C., Walters, K.A., Wills, N.M., Xiao, Y.L., Dunfee, R.L., Schwartzman, L.M., Ozinsky, A., Bell, G.L., Dalton, R.M., Lo, A., Efstathiou, S., Atkins, J.F., Firth, A.E., Taubenberger, J.K., Digard, P., 2012. An Overlapping Protein-Coding Region in Influenza A Virus Segment 3 Modulates the Host Response. *Science* 337, 199-204.

Jahrling, P.B., Geisbert, J., Swearengen, J.R., Jaax, G.P., Lewis, T., Huggins, J.W., Schmidt, J.J., LeDuc, J.W., Peters, C.J., 1996. Passive immunization of Ebola virus-infected cynomolgus monkeys with immunoglobulin from hyperimmune horses. *Arch Virol Suppl* 11, 135-140.

Jahrling, P.B., Marty, A.M., Geisbert, T.W., 2007. Viral hemorrhagic fevers. Medical Aspects of Biological Warfare, Office of the Surgeon General, United States Army, and Borden Institute, Walter Reed Army Medical Center, Washington, DC, 271-310.

James, P., Quadroni, M., Carafoli, E., Gonnet, G., 1994. Protein identification in DNA databases by peptide mass fingerprinting. *Protein Science* 3, 1347-1350.

Janshoff, A., Wegener, J., Sieber, M., Galla, H.J., 1996. Double-mode impedance analysis of epithelial cell monolayers cultured on shear wave resonators. *European Biophysics Journal* 25, 93-103.

Jantsch, M.F., 2010. Reaching complexity through RNA editing. RNA Biol 7, 191.

Jantsch, M.F., Vesely, C., 2000. RNA binding domains and RNA recognition by RNA-editing machineries. In: Madame Curie Bioscience Database [Internet]. Austin (TX): Landes Bioscience; 2000-. .

Jasenosky, L.D., Neumann, G., Lukashevich, I., Kawaoka, Y., 2001. Ebola virus VP40-induced particle formation and association with the lipid bilayer. *Journal of Virology* 75, 5205.

John, S.P., Wang, T., Steffen, S., Longhi, S., Schmaljohn, C.S., Jonsson, C.B., 2007. Ebola virus VP30 is an RNA binding protein. *Journal of Virology* 81, 8967.

Johnson, E., Jaax, N., White, J., Jahrling, P., 1995. Lethal experimental infections of rhesus monkeys by aerosolized Ebola virus. *Int J Exp Pathol* 76, 227-236.

Johnson, E.D., Johnson, B.K., Silverstein, D., Tukei, P., Geisbert, T.W., Sanchez, A.N., Jahrling, P.B., 1996. Characterization of a new Marburg virus isolated from a 1987 fatal case in Kenya. *Arch Virol Suppl* 11, 101-114.

Jones, S.M., Feldmann, H., Ströher, U., Geisbert, J.B., Fernando, L., Grolla, A., Klenk, H.D., Sullivan, N.J., Volchkov, V.E., Fritz, E.A., 2005. Live attenuated recombinant vaccine protects nonhuman primates against Ebola and Marburg viruses. *Nature Medicine* 11, 786-790.

Kindzelskii, A.L., Yang, Z., Nabel, G.J., Todd, R.F., 3rd, Petty, H.R., 2000. Ebola virus secretory glycoprotein (sGP) diminishes Fc gamma RIIIB-to-CR3 proximity on neutrophils. *J Immunol* 164, 953-958.

King, A., Lefkowitz, E., Adams, M.J., 2011. Virus Taxonomy: Ninth Report of the International Committee on Taxonomy of Viruses. An Elsevier Title.

Kissling, R.E., Robinson, R.Q., Murphy, F.A., Whitfield, S.G., 1968. Agent of disease contracted from green monkeys. *Science* 160, 888.

Kobinger, G.P., Feldmann, H., Zhi, Y., Schumer, G., Gao, G., Feldmann, F., Jones, S., Wilson, J.M., 2006. Chimpanzee adenovirus vaccine protects against Zaire Ebola virus. *Virology* 346, 394-401.

References

Kolakofsky, D., Curran, J., Pelet, T., Jacques, J., 1993. Paramyxovirus P gene mRNA editing. RNA editing. Ellis Horwood, Chichester, England, 105-123.

Kolakofsky, D., Hausmann, S., 1998. Cotranscriptional paramyxovirus mRNA editing: a contradiction in terms. Modification and editing of RNA. ASM Press, Washington, DC, 413-420.

Kolakofsky, D., Pelet, T., Garcin, D., Hausmann, S., Curran, J., Roux, L., 1998. Paramyxovirus RNA synthesis and the requirement for hexamer genome length: the rule of six revisited. *Journal of Virology* 72, 891-899.

Kolakofsky, D., Vidal, S., Curran, J., 1991. Paramyxovirus RNA synthesis and P gene expression. The Paramyxoviruses D. Kingsbury (Ed.) Plenum Press, New York.

Kolesnikova, L., Bugany, H., Klenk, H.D., Becker, S., 2002. VP40, the matrix protein of Marburg virus, is associated with membranes of the late endosomal compartment. *Journal of Virology* 76, 1825.

Kondratowicz, A.S., Lennemann, N.J., Sinn, P.L., Davey, R.A., Hunt, C.L., Moller-Tank, S., Meyerholz, D.K., Rennert, P., Mullins, R.F., Brindley, M., 2011. T-cell immunoglobulin and mucin domain 1 (TIM-1) is a receptor for Zaire Ebolavirus and Lake Victoria Marburgvirus. *Proceedings of the National Academy of Sciences* 108, 8426.

Kortepeter, M.G., Martin, J.W., Rusnak, J.M., Cieslak, T.J., Warfield, K.L., Anderson, E.L., Ranadive, M.V., 2008. Managing potential laboratory exposure to Ebola virus by using a patient biocontainment care unit. *Emerging Infectious Diseases* 14, 881.

Kuhn, J.H., 2008. Filoviruses. A compendium of 40 years of epidemiological, clinical, and laboratory studies. Arch Virol Suppl 20, 13-360.

Kuhn, J.H., Becker, S., Ebihara, H., Geisbert, T.W., Johnson, K.M., Kawaoka, Y., Lipkin, W.I., Negredo, A.I., Netesov, S.V., Nichol, S.T., Palacios, G., Peters, C.J., Tenorio, A., Volchkov, V.E., Jahrling, P.B., 2010. Proposal for a revised taxonomy of the family Filoviridae: classification, names of taxa and viruses, and virus abbreviations. *Archives of Virology* 155, 2083-2103.

Kuhn, J.H., Radoshitzky, S.R., Guth, A.C., Warfield, K.L., Li, W., Vincent, M.J., Towner, J.S., Nichol, S.T., Bavari, S., Choe, H., Aman, M.J., Farzan, M., 2006. Conserved receptor-binding domains of Lake Victoria marburgvirus and Zaire ebolavirus bind a common receptor. *J Biol Chem* 281, 15951-15958.

Kulkarni, S., Volchkova, V., Basler, C.F., Palese, P., Volchkov, V.E., Shaw, M.L., 2009. Nipah virus edits its P gene at high frequency to express the V and W proteins. *Journal of Virology* 83, 3982-3987.

Kuo, M.Y., Chao, M., Taylor, J., 1989. Initiation of replication of the human hepatitis delta virus genome from cloned DNA: role of delta antigen. *J Virol* 63, 1945-1950.

Le Guenno, B., Formenty, P., Boesch, C., 1999. Ebola virus outbreaks in the Ivory Coast and Liberia, 1994-1995. *Curr Top Microbiol Immunol* 235, 77-84.

Le Guenno, B., Formenty, P., Wyers, M., Gounon, P., Walker, F., Boesch, C., 1995. Isolation and partial characterisation of a new strain of Ebola virus. Lancet 345, 1271-1274.

Ledgerwood, J., Costner, P., Desai, N., Holman, L., Enama, M., Yamshchikov, G., Mulangu, S., Hu, Z., Andrews, C., Sheets, R., 2010. A replication defective recombinant Ad5 vaccine expressing Ebola virus GP is safe and immunogenic in healthy adults. Vaccine 29, 304-313.

Lee, J.E., Fusco, M.L., Hessell, A.J., Oswald, W.B., Burton, D.R., Saphire, E.O., 2008. Structure of the Ebola virus glycoprotein bound to an antibody from a human survivor. *Nature* 454, 177-182.

Lee, J.E., Saphire, E.O., 2009. Ebolavirus glycoprotein structure and mechanism of entry. *Future Virology* 4, 621-635.

References

Lee, R.J., Wang, S., Low, P.S., 1996. Measurement of endosome pH following folate receptor-mediated endocytosis. Biochimica et Biophysica Acta (BBA)-Molecular Cell Research 1312, 237-242.

Lehmann, K.A., Bass, B.L., 1999. The importance of internal loops within RNA substrates of ADAR11. *Journal of Molecular Biology* 291, 1-13.

Lenard, J., 1996. Negative-strand virus M and retrovirus MA proteins: all in a family? *Virology* 216, 289-298.

Leroy, E., Baize, S., Volchkov, V., Fisher-Hoch, S., Georges-Courbot, M., Lansoud-Soukate, J., Capron, M., Debre, P., McCormick, J., Georges, A., 2000. Human asymptomatic Ebola infection and strong inflammatory response. *The Lancet* 355, 2210-2215.

Leroy, E., Gonzalez, J., Baize, S., 2011. Ebola and Marburg haemorrhagic fever viruses: major scientific advances, but a relatively minor public health threat for Africa. *Clinical Microbiology and Infection* 17, 964-976.

Leroy, E.M., Baize, S., Mavoungou, E., Apetrei, C., 2002. Sequence analysis of the GP, NP, VP40 and VP24 genes of Ebola virus isolated from deceased, surviving and asymptomatically infected individuals during the 1996 outbreak in Gabon: comparative studies and phylogenetic characterization. *Journal of General Virology* 83, 67.

Leroy, E.M., Epelboin, A., Mondonge, V., Pourrut, X., Gonzalez, J.P., Muyembe-Tamfum, J.J., Formenty, P., 2009. Human Ebola outbreak resulting from direct exposure to fruit bats in Luebo, Democratic Republic of Congo, 2007. *Vector-borne and Zoonotic Diseases* 9, 723-728.

Leung, L.W., Hartman, A.L., Martinez, O., Shaw, M.L., Carbonnelle, C., Volchkov, V.E., Nichol, S.T., Basler, C.F., 2006. Ebola virus VP24 binds karyopherin α1 and blocks STAT1 nuclear accumulation. *Journal of Virology* 80, 5156-5167.

Levy, D.E., Marié, I., Smith, E., Prakash, A., 2002. Review: Enhancement and Diversification of IFN Induction by IRF-7-Mediated Positive Feedback. *Journal of Interferon & Cytokine Research* 22, 87-93.

Licata, J.M., Simpson-Holley, M., Wright, N.T., Han, Z., Paragas, J., Harty, R.N., 2003. Overlapping motifs (PTAP and PPEY) within the Ebola virus VP40 protein function independently as late budding domains: involvement of host proteins TSG101 and VPS-4. *Journal of Virology* 77, 1812.

Lin, G., Simmons, G., Pohlmann, S., Baribaud, F., Ni, H., Leslie, G.J., Haggarty, B.S., Bates, P., Weissman, D., Hoxie, J.A., Doms, R.W., 2003. Differential N-linked glycosylation of human immunodeficiency virus and Ebola virus envelope glycoproteins modulates interactions with DC-SIGN and DC-SIGNR. *J Virol* 77, 1337-1346.

Linnstaedt, S.D., Kasprzak, W.K., Shapiro, B.A., Casey, J.L., 2009. The fraction of RNA that folds into the correct branched secondary structure determines hepatitis delta virus type 3 RNA editing levels. *RNA* 15, 1177-1187.

Lo, M.K., Harcourt, B.H., Mungall, B.A., Tamin, A., Peeples, M.E., Bellini, W.J., Rota, P.A., 2009. Determination of the henipavirus phosphoprotein gene mRNA editing frequencies and detection of the C, V and W proteins of Nipah virus in virus-infected cells. *J Gen Virol* 90, 398-404.

Lubec, G., Afjehi-Sadat, L., 2007. Limitations and pitfalls in protein identification by mass spectrometry. *Chemical Reviews-Columbus* 107, 3568-3584.

Lupton, H.W., Lambert, R.D., Bumgardner, D.L., Moe, J.B., Eddy, G.A., 1980. Inactivated vaccine for Ebola virus efficacious in guineapig model. *Lancet* 2, 1294-1295.

MacNeil, A., Farnon, E.C., Wamala, J., Okware, S., Cannon, D.L., Reed, Z., Towner, J.S., Tappero, J.W., Lutwama, J., Downing, R., 2010. Proportion of deaths and clinical features in bundibugyo ebola virus infection, Uganda. *Emerg Infect Dis* 16, 1969.

References

Mahanty, S., Hutchinson, K., Agarwal, S., McRae, M., Rollin, P.E., Pulendran, B., 2003. Cutting edge: impairment of dendritic cells and adaptive immunity by Ebola and Lassa viruses. *J Immunol* 170, 2797-2801.

Malashkevich, V.N., Schneider, B.J., McNally, M.L., Milhollen, M.A., Pang, J.X., Kim, P.S., 1999. Core structure of the envelope glycoprotein GP2 from Ebola virus at 1.9-A resolution. *Proc Natl Acad Sci* U S A 96, 2662-2667.

Manicassamy, B., Wang, J., Jiang, H., Rong, L., 2005. Comprehensive analysis of Ebola virus GP1 in viral entry. *Journal of Virology* 79, 4793.

Martin, J.E., Sullivan, N.J., Enama, M.E., Gordon, I.J., Roederer, M., Koup, R.A., Bailer, R.T., Chakrabarti, B.K., Bailey, M.A., Gomez, P.L., 2006. A DNA vaccine for Ebola virus is safe and immunogenic in a phase I clinical trial. Clinical and Vaccine Immunology 13, 1267.

Martinez, M.J., Biedenkopf, N., Volchkova, V., Hartlieb, B., Alazard-Dany, N., Reynard, O., Becker, S., Volchkov, V., 2008. Role of Ebola virus VP30 in transcription reinitiation. *J Virol* 82, 12569-12573.

Martinez, M.J., Volchkova, V.A., Raoul, H., Alazard-Dany, N., Reynard, O., Volchkov, V.E., 2011. Role of VP30 Phosphorylation in the Ebola Virus Replication Cycle. *Journal of Infectious Diseases* 204, S934-S940.

Martinez, O., Johnson, J., Manicassamy, B., Rong, L., Olinger, G.G., Hensley, L.E., Basler, C.F., 2010. Zaire Ebola virus entry into human dendritic cells is insensitive to cathepsin L inhibition. *Cellular Microbiology* 12, 148-157.

Martinez, O., Valmas, C., Basler, C.F., 2007. Ebola virus-like particle-induced activation of NF-[kappa] B and Erk signaling in human dendritic cells requires the glycoprotein mucin domain. *Virology* 364, 342-354.

Martini, G., Knauff, H., Schmidt, H., Mayer, G., Baltzer, G., 1968a. Über eine bisher unbekannte, von affen eingeschleppte infektionskrankheit: Marburg-virus-krankheit. *Dtsch. Med. Wochenschr* 93, 559-571.

Martini, G.A., Knauff, H.G., Schmidt, H.A., Mayer, G., Baltzer, G., 1968b. A hitherto unknown infectious disease contracted from monkeys. "Marburg-virus" disease. *Ger Med Mon* 13, 457-470.

Maruyama, T., Buchmeier, M.J., Parren, P.W.H.I., Burton, D.R., 1998. Ebola virus, neutrophils, and antibody specificity. *Science* 282, 843-843.

Marzi, A., Gramberg, T., Simmons, G., Moller, P., Rennekamp, A.J., Krumbiegel, M., Geier, M., Eisemann, J., Turza, N., Saunier, B., Steinkasserer, A., Becker, S., Bates, P., Hofmann, H., Pohlmann, S., 2004. DC-SIGN and DC-SIGNR interact with the glycoprotein of Marburg virus and the S protein of severe acute respiratory syndrome coronavirus. *Journal of Virology* 78, 12090-12095.

Mateo, M., Reid, S.P., Leung, L.W., Basler, C.F., Volchkov, V.E., 2010. Ebolavirus VP24 binding to karyopherins is required for inhibition of interferon signaling. *Journal of Virology* 84, 1169.

Matsumura, H., Ikemura, N., Ito, Y., Kuribayashi, K., 1999. RNA editing-like phenomenon in paramyxovirus V gene mRNA observed in insect cells infected with a recombinant baculovirus. *J Gen Virol* 80 (Pt 1), 117-123.

Mátyás, G., Giunta, C., Steinmann, B., Hossle, J.P., Hellwig, R., 2002. Quantification of single nucleotide polymorphisms: a novel method that combines primer extension assay and capillary electrophoresis. *Human Mutation* 19, 58-68.

Mehedi, M., Groseth, A., Feldmann, H., Ebihara, H., 2011. Clinical aspects of Marburg hemorrhagic fever. *Future Virology* 6, 1091-1106.

Mercer, J., Helenius, A., 2009. Virus entry by macropinocytosis. Nature cell biology 11, 510-520.

Miller, E.H., Chandran, K., 2012. Filovirus entry into cells–new insights. *Current Opinion in Virology* 2, 206-214.

References

MMWR, 2009. Imported Case of Marburg Hemorrhagic Fever—Colorado, 2008, Morbidity and mortality weekly report

Modrof, J., Becker, S., Muhlberger, E., 2003. Ebola virus transcription activator VP30 is a zinc-binding protein. *Journal of Virology* 77, 3334-3338.

Modrof, J., Muhlberger, E., Klenk, H.D., Becker, S., 2002. Phosphorylation of VP30 impairs ebola virus transcription. *J Biol Chem* 277, 33099-33104.

Mpanju, O.M., Towner, J.S., Dover, J.E., Nichol, S.T., Wilson, C.A., 2006. Identification of two amino acid residues on Ebola virus glycoprotein 1 critical for cell entry. Virus Res 121, 205-214.

Mueller, U.G., Wolfenbarger, L.L.R., 1999. AFLP genotyping and fingerprinting. *Trends in Ecology & Evolution* 14, 389-394.

Mühlberger, E., 2007. Filovirus replication and transcription. *Future Virology* 2, 205-215.

Muhlberger, E., Lotfering, B., Klenk, H.D., Becker, S., 1998. Three of the four nucleocapsid proteins of Marburg virus, NP, VP35, and L, are sufficient to mediate replication and transcription of Marburg virus-specific monocistronic minigenomes. *Journal of Virology* 72, 8756-8764.

Mühlberger, E., Lötfering, B., Klenk, H.D., Becker, S., 1998. Three of the four nucleocapsid proteins of Marburg virus, NP, VP35, and L, are sufficient to mediate replication and transcription of Marburg virus-specific monocistronic minigenomes. *Journal of Virology* 72, 8756-8764.

Muhlberger, E., Trommer, S., Funke, C., Volchkov, V., Klenk, H.D., Becker, S., 1996. Termini of all mRNA species of Marburg virus: sequence and secondary structure. *Virology* 223, 376-380.

Muhlberger, E., Weik, M., Volchkov, V., Klenk, H., Becker, S., 1999. Comparison of the transcription and replication strategies of Marburg virus and Ebola virus by using artificial replication systems. *Journal of Virology* 73, 2333.

Muhlberger, E.a.B., S, 2002. Marburg Virus Replication and Nucleocapsid Formation: Different Jobs, Same Players, in: Holzenburg, A., Bogner, E. (Eds.), Structure-function Relationships of Human Pathogenic Viruses. Springer, pp. 89-107.

Mupapa, K., Massamba, M., Kibadi, K., Kuvula, K., Bwaka, A., Kipasa, M., Colebunders, R., Muyembe-Tamfum, J., 1999. Treatment of Ebola hemorrhagic fever with blood transfusions from convalescent patients. *Journal of Infectious Diseases* 179, S18-S23.

Murphy, F.A., 1978. Pathology of Ebola virus infection. Ebola virus haemorrhagic fever (SR Pattyn, ed.). Elsevier, Amsterdam, The Netherlands, 43-49.

Nakae, A., Tanaka, T., Miyake, K., Hase, M., Mashimo, T., 2008. Comparing methods of detection and quantitation of RNA editing of rat glycine receptor alpha3P185L. *International Journal of Biological Sciences* 4, 397.

Nanbo, A., Imai, M., Watanabe, S., Noda, T., Takahashi, K., Neumann, G., Halfmann, P., Kawaoka, Y., 2010. Ebolavirus is internalized into host cells via macropinocytosis in a viral glycoprotein-dependent manner. *PLoS Pathogens* 6, e1001121.

Navaratnam, N., Patel, D., Shah, R., Greeve, J.C., Powell, L.M., Knott, T.J., Scott, J., 1991. An additional editing site is present in apolipoprotein B mRNA. *Nucleic Acids Research* 19, 1741-1744.

Negredo, A., Palacios, G., Vázquez-Morón, S., González, F., Dopazo, H., Molero, F., Juste, J., Quetglas, J., Savji, N., de la Cruz Martínez, M., 2011. Discovery of an Ebolavirus-Like Filovirus in Europe. *PLoS Pathogens* 7, e1002304.

Neumann, G., Noda, T., Takada, A., Jasenosky, L.D., Kawaoka, Y., 2004. Roles of filoviral matrix-and glycoproteins in the viral life cycle. Ebola and Marburg Viruses: *Molecular and Cellular Biology*, 137–170.

Nishikura, K., Yoo, C., Kim, U., Murray, J., Estes, P., Cash, F., Liebhaber, S., 1991. Substrate specificity of the dsRNA unwinding/modifying activity. *Embo J* 10, 3523.

Niwa, H., Yamamura, K., Miyazaki, J., 1991. Efficient selection for high-expression transfectants with a novel eukaryotic vector. *Gene* 108, 193-199.

Noda, T., Sagara, H., Suzuki, E., Takada, A., Kida, H., Kawaoka, Y., 2002. Ebola virus VP40 drives the formation of virus-like filamentous particles along with GP. *Journal of Virology* 76, 4855-4865.

O'Reilly, E.K., Kao, C.C., 1998. Analysis of RNA-dependent RNA polymerase structure and function as guided by known polymerase structures and computer predictions of secondary structure. *Virology* 252, 287-303.

Ogino, T., Banerjee, A.K., 2007. Unconventional mechanism of mRNA capping by the RNA-dependent RNA polymerase of vesicular stomatitis virus. *Molecular Cell* 25, 85-97.

Okumura, A., Pitha, P.M., Yoshimura, A., Harty, R.N., 2010. Interaction between Ebola virus glycoprotein and host toll-like receptor 4 leads to induction of proinflammatory cytokines and SOCS1. *Journal of Virology* 84, 27-33.

Olinger, G.G., Bailey, M.A., Dye, J.M., Bakken, R., Kuehne, A., Kondig, J., Wilson, J., Hogan, R.J., Hart, M.K., 2005. Protective cytotoxic T-cell responses induced by venezuelan equine encephalitis virus replicons expressing Ebola virus proteins. *Journal of Virology* 79, 14189.

Ossipova, E., Fenyö, D., Eriksson, J., 2006. Optimizing search conditions for the mass fingerprint-based identification of proteins. *Proteomics* 6, 2079-2085.

Ou, W., Delisle, J., Konduru, K., Bradfute, S., Radoshitzky, S.R., Retterer, C., Kota, K., Bavari, S., Kuhn, J.H., Jahrling, P.B., 2011. Development and characterization of rabbit and mouse antibodies against ebolavirus envelope glycoproteins. *Journal of Virological Methods* 174, 99-109.

Palacios, G., Quan, P.L., Jabado, O.J., Conlan, S., Hirschberg, D.L., Liu, Y., Zhai, J., Renwick, N., Hui, J., Hegyi, H., Grolla, A., Strong, J.E., Towner, J.S., Geisbert, T.W., Jahrling, P.B., Buchen-Osmond, C., Ellerbrok, H., Sanchez-Seco, M.P., Lussier, Y., Formenty, P., Nichol, M.S., Feldmann, H., Briese, T., Lipkin, W.I., 2007. Panmicrobial oligonucleotide array for diagnosis of infectious diseases. *Emerg Infect Dis* 13, 73-81.

Panchal, R.G., Ruthel, G., Kenny, T.A., Kallstrom, G.H., Lane, D., Badie, S.S., Li, L., Bavari, S., Aman, M.J., 2003. In vivo oligomerization and raft localization of Ebola virus protein VP40 during vesicular budding. *Proc Natl Acad Sci* U S A 100, 15936.

Park, M.S., Shaw, M.L., Munoz-Jordan, J., Cros, J.F., Nakaya, T., Bouvier, N., Palese, P., Garcia-Sastre, A., Basler, C.F., 2003. Newcastle disease virus (NDV)-based assay demonstrates interferon-antagonist activity for the NDV V protein and the Nipah virus V, W, and C proteins. *Journal of Virology* 77, 1501-1511.

Paschen, W., Djuricic, B., 1994. Extent of RNA editing of glutamate receptor subunit GluR5 in different brain regions of the rat. *Cellular and Molecular Neurobiology* 14, 259-270.

Pelet, T., Curran, J., Kolakofsky, D., 1991. The P gene of bovine parainfluenza virus 3 expresses all three reading frames from a single mRNA editing site. *Embo J* 10, 443-448.

Peters, C., 1997. Ebola and hantaviruses. *FEMS Immunology & Medical Microbiology* 18, 281-289.

Peterson, A.T., Bauer, J.T., Mills, J.N., 2004. Ecologic and geographic distribution of filovirus disease. *Emerg Infect Dis* 10, 40-47.

Peterson, A.T., Lash, R., Carroll, D.S., Johnson, K.M., 2006. Geographic potential for outbreaks of Marburg hemorrhagic fever. The American journal of tropical medicine and hygiene 75, 9.

Pinzon, J.E., Wilson, J., Tucker, C., 2005. Climate-based health monitoring systems for eco-climatic conditions associated with infectious diseases. *Bulletin de la Société de pathologie exotique* 98, 239-243.

Pinzon, J.E., Wilson, J.M., Tucker, C.J., Arthur, R., Jahrling, P.B., Formenty, P., 2004. Trigger events: enviroclimatic coupling of Ebola hemorrhagic fever outbreaks. *The American Journal of Tropical Medicine and Hygiene* 71, 664.

References

Ploegh, H.L., 1998. Viral strategies of immune evasion. *Science* 280, 248-253.

Polson, A.G., Bass, B.L., Casey, J.L., 1996. RNA editing of hepatitis delta virus antigenome by dsRNA-adenosine deaminase. *Nature* 380, 454-456.

Powell, D.W., 1981. Barrier function of epithelia. *Am J Physiol* 241, G275-288.

Powlesland, A.S., Fisch, T., Taylor, M.E., Smith, D.F., Tissot, B., Dell, A., Pohlmann, S., Drickamer, K., 2008. A novel mechanism for LSECtin binding to Ebola virus surface glycoprotein through truncated glycans. *J Biol Chem* 283, 593-602.

Poyau, A., Vincent, L., Berthommé, H., Paul, C., Nicolas, B., Pujol, J.F., Madjar, J.J., 2007. Identification and relative quantification of adenosine to inosine editing in serotonin 2c receptor mRNA by CE. *Electrophoresis* 28, 2843-2852.

Prêle, C.M., Woodward, E.A., Bisley, J., Keith-Magee, A., Nicholson, S.E., Hart, P.H., 2008. SOCS1 regulates the IFN but not NFκB pathway in TLR-stimulated human monocytes and macrophages. *The Journal of Immunology* 181, 8018.

Radoshitzky, S.R., Warfield, K.L., Chi, X., Dong, L., Kota, K., Bradfute, S.B., Gearhart, J.D., Retterer, C., Kranzusch, P.J., Misasi, J.N., Hogenbirk, M.A., Wahl-Jensen, V., Volchkov, V.E., Cunningham, J.M., Jahrling, P.B., Aman, M.J., Bavari, S., Farzan, M., Kuhn, J.H., 2011. Ebolavirus {delta}-Peptide immunoadhesins inhibit marburgvirus and ebolavirus cell entry. *Journal of Virology* 85, 8502-8513.

Rec, W.E., 2005. Outbreak of Ebola haemorrhagic fever in Yambio, south Sudan, April - June 2004. *Wkly Epidemiol Rec* 80, 370-375.

Rec, W.E., 2007. Outbreak news. Ebola virus haemorrhagic fever, Democratic Republic of the Congo--update. *Wkly Epidemiol Rec* 82, 345-346.

Reed, D.S., Mohamadzadeh, M., 2007. Status and challenges of filovirus vaccines. *Vaccine* 25, 1923-1934.

Reid, S.P., Leung, L.W., Hartman, A.L., Martinez, O., Shaw, M.L., Carbonnelle, C., Volchkov, V.E., Nichol, S.T., Basler, C.F., 2006. Ebola virus VP24 binds karyopherin {alpha} 1 and blocks STAT1 nuclear accumulation. *Journal of Virology* 80, 5156.

Reyes, G.R., 2002. The nonstructural NS5A protein of hepatitis C virus: an expanding, multifunctional role in enhancing hepatitis C virus pathogenesis. *Journal of Biomedical Science* 9, 187-197.

Risi, G.F., Bloom, M.E., Hoe, N.P., Arminio, T., Carlson, P., Powers, T., Feldmann, H., Wilson, D., 2010. Preparing a Community Hospital to Manage Work-related Exposures to Infectious Agents in BioSafety Level 3 and 4 Laboratories. *Emerging Infectious Diseases* 16, 373.

Ritchie, G., Harvey, D.J., Stroeher, U., Feldmann, F., Feldmann, H., Wahl-Jensen, V., Royle, L., Dwek, R.A., Rudd, P.M., 2010. Identification of N-glycans from Ebola virus glycoproteins by matrix-assisted laser desorption/ionisation time-of-flight and negative ion electrospray tandem mass spectrometry. *Rapid Commun Mass Spectrom* 24, 571-585.

Robert A. Lamb, G.D.P., 2007. Paramyxoviridae: The viruses and Their Replication, in: David M. Knipe, P.P.M.H., MD; Diane E. Griffin, MD, PhD; Robert A. Lamb, PhD, ScD; Malcolm A. Martin, MD; Bernard Roizman, ScD; Stephen E. Straus, MD (Ed.), *Fields Virology*, 5th ed. Lippincott Williams and Wilkins, Philadelphia, pp. 1449-1496.

Rodriguez, J.J., Parisien, J.P., Horvath, C.M., 2002. Nipah virus V protein evades alpha and gamma interferons by preventing STAT1 and STAT2 activation and nuclear accumulation. *Journal of Virology* 76, 11476-11483.

Ruigrok, R.W.H., Crépin, T., Kolakofsky, D., 2011. Nucleoproteins and nucleocapsids of negative-strand RNA viruses. *Current Opinion in Microbiology* 14, 504-510.

Ruigrok, R.W.H., Schoehn, G., Dessen, A., Forest, E., Volchkov, V., Dolnik, O., Klenk, H.D., Weissenhorn, W., 2000. Structural characterization and membrane binding properties of the matrix protein VP40 of ebola virus1. *Journal of Molecular Biology* 300, 103-112.

References

Ryabchikova, E., Kolesnikova, L., Netesov, S., 1999. Animal pathology of filoviral infections. *Curr Top Microbiol Immunol* 235, 145.

Ryabchikova, E., Price, B.B.S., 2004. Ebola and Marburg viruses: a view of infection using electron microscopy. Battelle Press.

Ryu, W.S., Bayer, M., Taylor, J., 1992. Assembly of hepatitis delta virus particles. *Journal of Virology* 66, 2310-2315.

Sadek, R.F., Khan, A., Kilmarx, P., Ksiazek, T., Peters, C., 1996. Outbreak of Ebola hemorrhagic fever, Zaire, 1995: a closer numerical look. Proceedings of the Epidemiology section of the American Statistical Association (Anaheim, CA). Alexandria, VA: ASA, 62-65.

Sadek, R.F., Khan, A.S., Stevens, G., Peters, C., Ksiazek, T.G., 1999. Ebola hemorrhagic fever, Democratic Republic of the Congo, 1995: determinants of survival. *Journal of Virology* 179, S24-S27.

Saeed, M.F., Kolokoltsov, A.A., Albrecht, T., Davey, R.A., 2010. Cellular entry of ebola virus involves uptake by a macropinocytosis-like mechanism and subsequent trafficking through early and late endosomes. *PLoS pathogens* 6, e1001110.

Samuel, M.A., Diamond, M.S., 2006. Pathogenesis of West Nile virus infection: a balance between virulence, innate and adaptive immunity, and viral evasion. *Journal of Virology* 80, 9349-9360.

Sanchez, A., Kiley, M.P., Holloway, B.P., Auperin, D.D., 1993. Sequence analysis of the Ebola virus genome: organization, genetic elements, and comparison with the genome of Marburg virus. *Virus Research* 29, 215-240.

Sanchez, A., Ksiazek, T.G., Rollin, P.E., Miranda, M.E.G., Trappier, S.G., Khan, A.S., Peters, C.J., Nichol, S.T., 1999. Detection and molecular characterization of Ebola viruses causing disease in human and nonhuman primates. *Journal of Infectious Diseases* 179, S164-S169.

Sanchez, A., T. W. Geisbert, H. Feldmann, 2007. Filoviridae: Marburg and Ebola Viruses 5th ed. Lippincott Williams and Wilkins, Philadelphia.

Sanchez, A., Trappier, S.G., Mahy, B.W., Peters, C.J., Nichol, S.T., 1996. The virion glycoproteins of Ebola viruses are encoded in two reading frames and are expressed through transcriptional editing. *Proc Natl Acad Sci* U S A 93, 3602-3607.

Sanchez, A., Yang, Z.Y., Xu, L., Nabel, G.J., Crews, T., Peters, C.J., 1998. Biochemical analysis of the secreted and virion glycoproteins of Ebola virus. *Journal of Virology* 72, 6442-6447.

Sanger, F., Coulson, A.R., 1975. A rapid method for determining sequences in DNA by primed synthesis with DNA polymerase. *Journal of Molecular Biology* 94, 441-448.

Sarwar, U.N., Sitar, S., Ledgerwood, J.E., 2011. Filovirus emergence and vaccine development: a perspective for health care practitioners in travel medicine. Travel Med Infect Dis 9, 126-134.

Schiffer, H.H., Heinemann, S.F., 1999. A quantitative method to detect RNA editing events. *Analytical Biochemistry* 276, 257.

Schnittler, H., Wilke, A., Gress, T., Suttorp, N., Drenckhahn, D., 1990. Role of actin and myosin in the control of paracellular permeability in pig, rat and human vascular endothelium. *J Physiol* 431, 379-401.

Schnittler, H.J., Feldmann, H., 1998. Marburg and Ebola hemorrhagic fevers: does the primary course of infection depend on the accessibility of organ-specific macrophages? *Clin Infect Dis* 27, 404-406.

Schnittler, H.J., Franke, R.P., Akbay, U., Mrowietz, C., Drenckhahn, D., 1993. Improved in vitro rheological system for studying the effect of fluid shear stress on cultured cells. *American Journal of Physiology-Cell Physiology* 265, C289-C298.

Schornberg, K., Matsuyama, S., Kabsch, K., Delos, S., Bouton, A., White, J., 2006. Role of endosomal cathepsins in entry mediated by the Ebola virus glycoprotein. *Journal of Virology* 80, 4174.

References

Schumann, M., Gantke, T., Muhlberger, E., 2009. Ebola virus VP35 antagonizes PKR activity through its C-terminal interferon inhibitory domain. *Journal of Virology*, JVI. 00523-00509v00521.

Seebach, J., Dieterich, P., Luo, F., Schillers, H., Vestweber, D., Oberleithner, H., Galla, H.J., Schnittler, H.J., 2000. Endothelial barrier function under laminar fluid shear stress. *Laborator Investigation* 80, 1819-1831.

Seebach, J., Madler, H., Wojciak-Stothard, B., Schnittler, H., 2005. Tyrosine phosphorylation and the small GTPase rac cross-talk in regulation of endothelial barrier function. Thrombosis and haemostasis-Stuttgart- 94, 620.

Seibel, N.M., Eljouni, J., Nalaskowski, M.M., Hampe, W., 2007. Nuclear localization of enhanced green fluorescent protein homomultimers. *Analytical Biochemistry* 368, 95-99.

Shaw, M.L., Garcia-Sastre, A., Palese, P., Basler, C.F., 2004. Nipah virus V and W proteins have a common STAT1-binding domain yet inhibit STAT1 activation from the cytoplasmic and nuclear compartments, respectively. *Journal of Virology* 78, 5633-5641.

Shevchenko, A., Wilm, M., Vorm, O., Mann, M., 1996. Mass spectrometric sequencing of proteins from silver-stained polyacrylamide gels. *Analytical Chemistry* 68, 850-858.

Shimojima, M., Takada, A., Ebihara, H., Neumann, G., Fujioka, K., Irimura, T., Jones, S., Feldmann, H., Kawaoka, Y., 2006. Tyro3 family-mediated cell entry of Ebola and Marburg viruses. *Journal of Virology* 80, 10109-10116.

Siegert, R., Shu, H.L., Slenczka, H.L., Peters, D., Muller, G., 1968. The aetiology of an unknown human infection transmitted by monkeys (preliminary communication). *Ger Med Mon* 13, 1-2.

Simmons, G., Reeves, J.D., Grogan, C.C., Vandenberghe, L.H., Baribaud, F., Whitbeck, J.C., Burke, E., Buchmeier, M.J., Soilleux, E.J., Riley, J.L., Doms, R.W., Bates, P., Pohlmann, S., 2003. DC-SIGN and DC-SIGNR bind ebola glycoproteins and enhance infection of macrophages and endothelial cells. *Virology* 305, 115-123.

Smith, D.H., Johnson, B.K., Isaacson, M., Swanapoel, R., Johnson, K.M., Killey, M., Bagshawe, A., Siongok, T., Keruga, W.K., 1982. Marburg-virus disease in Kenya. *Lancet* 1, 816-820.

Smith, H., Gott, J.M., Hanson, M.R., 1997. A guide to RNA editing. *RNA* 3, 1105.

Smith, P.W., Anderson, A.O., Christopher, G.W., Cieslak, T.J., Devreede, G., Fosdick, G.A., Greiner, C.B., Hauser, J.M., Hinrichs, S.H., Huebner, K.D., 2006. Designing a biocontainment unit to care for patients with serious communicable diseases: a consensus statement. *Biosecurity and bioterrorism: biodefense strategy, practice, and science* 4, 351-365.

Sodhi, M.S.K., Airey, D.C., Lambert, W., Burnet, P.W.J., Harrison, P.J., Sanders-Bush, E., 2005. A rapid new assay to detect RNA editing reveals antipsychotic-induced changes in serotonin-2C transcripts. *Molecular Pharmacology* 68, 711-719.

Sommer, B., Köhler, M., Sprengel, R., Seeburg, P.H., 1991. RNA editing in brain controls a determinant of ion flow in glutamate-gated channels. *Cell* 67, 11.

Steward, M., Vipond, I.B., Millar, N.S., Emmerson, P.T., 1993. RNA editing in Newcastle disease virus. *Journal of General Virology* 74, 2539-2548.

Stroher, U., West, E., Bugany, H., Klenk, H.D., Schnittler, H.J., Feldmann, H., 2001. Infection and activation of monocytes by Marburg and Ebola viruses. *Journal of Virology* 75, 11025-11033.

Stuart, K., Allen, T.E., Heidmann, S., Seiwert, S.D., 1997. RNA editing in kinetoplastid protozoa. *Microbiol Mol Biol Rev* 61, 105-120.

Sui, J., Marasco, W.A., 2002. Evidence against Ebola virus sGP binding to human neutrophils by a specific receptor. *Virology* 303, 9-14.

Sullivan, N., Yang, Z.Y., Nabel, G.J., 2003. Ebola virus pathogenesis: implications for vaccines and therapies. *Journal of Virology* 77, 9733-9737.

Sullivan, N.J., Sanchez, A., Rollin, P.E., Yang, Z., Nabel, G.J., 2000. Development of a preventive vaccine for Ebola virus infection in primates. *Nature* 408, 605-609.

Swanepoel, R., Leman, P., Burt, F., Zachariades, N., Braack, L., Ksiazek, T., Rollin, P., Zaki, S., Peters, C., 1996. Experimental inoculation of plants and animals with Ebola virus. *Emerg Infect Dis* 2, 321.

Swenson, D.L., Warfield, K.L., Warren, T.K., Lovejoy, C., Hassinger, J.N., Ruthel, G., Blouch, R.E., Moulton, H.M., Weller, D.D., Iversen, P.L., Bavari, S., 2009. Chemical modifications of antisense morpholino oligomers enhance their efficacy against Ebola virus infection. *Antimicrob Agents Chemother* 53, 2089-2099.

Takada, A., Ebihara, H., Feldmann, H., Geisbert, T.W., Kawaoka, Y., 2007a. Epitopes required for antibody-dependent enhancement of Ebola virus infection. *J Infect Dis 196 Suppl* 2, S347-356.

Takada, A., Ebihara, H., Jones, S., Feldmann, H., Kawaoka, Y., 2007b. Protective efficacy of neutralizing antibodies against Ebola virus infection. *Vaccine* 25, 993-999.

Takada, A., Fujioka, K., Tsuiji, M., Morikawa, A., Higashi, N., Ebihara, H., Kobasa, D., Feldmann, H., Irimura, T., Kawaoka, Y., 2004. Human macrophage C-type lectin specific for galactose and N-acetylgalactosamine promotes filovirus entry. *Journal of Virology* 78, 2943.

Takada, A., Robison, C., Goto, H., Sanchez, A., Murti, K.G., Whitt, M.A., Kawaoka, Y., 1997. A system for functional analysis of Ebola virus glycoprotein. *Proc Natl Acad Sci* U S A 94, 14764-14769.

Takada, A., Watanabe, S., Ito, H., Okazaki, K., Kida, H., Kawaoka, Y., 2000. Downregulation of [beta] 1 integrins by Ebola virus glycoprotein: implication for virus entry. *Virology* 278, 20-26.

Thomas, S.M., Lamb, R.A., Paterson, R.G., 1988. Two mRNAs that differ by two nontemplated nucleotides encode the amino coterminal proteins P and V of the paramyxovirus SV5. *Cell* 54, 891.

Tian, N., Yang, Y., Sachsenmaier, N., Muggenhumer, D., Bi, J., Waldsich, C., Jantsch, M.F., Jin, Y., 2011. A structural determinant required for RNA editing. *Nucleic Acids Research* 39, 5669-5681.

Timen, A., Koopmans, M.P.G., Vossen, A.C.T.M., van Doornum, G.J.J., Günther, S., van den Berkmortel, F., Verduin, K.M., Dittrich, S., Emmerich, P., Osterhaus, A.D.M.E., 2009. Response to imported case of Marburg hemorrhagic fever, the Netherlands. *Emerging Infectious Diseases* 15, 1171.

Timmins, J., Ruigrok, R.W.H., Weissenhorn, W., 2004. Structural studies on the Ebola virus matrix protein VP40 indicate that matrix proteins of enveloped RNA viruses are analogues but not homologues. *FEMS Microbiology Letters* 233, 179-186.

Timmins, J., Scianimanico, S., Schoehn, G., Weissenhorn, W., 2001. Vesicular release of ebola virus matrix protein VP40. *Virology* 283, 1-6.

Towner, J.S., Amman, B.R., Sealy, T.K., Carroll, S.A.R., Comer, J.A., Kemp, A., Swanepoel, R., Paddock, C.D., Balinandi, S., Khristova, M.L., 2009. Isolation of genetically diverse Marburg viruses from Egyptian fruit bats. *PLoS Pathogens* 5, e1000536.

Towner, J.S., Khristova, M.L., Sealy, T.K., Vincent, M.J., Erickson, B.R., Bawiec, D.A., Hartman, A.L., Comer, J.A., Zaki, S.R., Stroher, U., Gomes da Silva, F., del Castillo, F., Rollin, P.E., Ksiazek, T.G., Nichol, S.T., 2006. Marburgvirus genomics and association with a large hemorrhagic fever outbreak in Angola. *Journal of Virology* 80, 6497-6516.

Towner, J.S., Pourrut, X., Albarino, C.G., Nkogue, C.N., Bird, B.H., Grard, G., Ksiazek, T.G., Gonzalez, J.P., Nichol, S.T., Leroy, E.M., 2007. Marburg virus infection detected in a common African bat. *PLoS One* 2, e764.

Towner, J.S., Sealy, T.K., Khristova, M.L., Albarino, C.G., Conlan, S., Reeder, S.A., Quan, P.L., Lipkin, W.I., Downing, R., Tappero, J.W., Okware, S., Lutwama, J., Bakamutumaho, B.,

Kayiwa, J., Comer, J.A., Rollin, P.E., Ksiazek, T.G., Nichol, S.T., 2008. Newly discovered ebola virus associated with hemorrhagic fever outbreak in Uganda. *PLoS Pathog* 4, e1000212.

Tsuda, Y., Safronetz, D., Brown, K., LaCasse, R., Marzi, A., Ebihara, H., Feldmann, H., 2011. Protective efficacy of a bivalent recombinant Vesicular Stomatitis Virus vaccine in the Syrian hamster model of lethal Ebola virus infection. *Journal of Infectious Diseases* 204, S1090-S1097.

Tucker, C.J., Wilson, J.M., Mahoney, R., Anyamba, A., Linthicum, K., Myers, M.F., 2002. Climatic and ecological context of the 1994-1996 Ebola outbreaks. *Photogrammetric Engineering and Remote Sensing* 68, 147-152.

Udeshi, N.D., Compton, P.D., Shabanowitz, J., Hunt, D.F., Rose, K.L., 2008. Methods for analyzing peptides and proteins on a chromatographic timescale by electron-transfer dissociation mass spectrometry. *Nature Protocols* 3, 1709-1717.

Villinger, F., Rollin, P.E., Brar, S.S., Chikkala, N.F., Winter, J., Sundstrom, J.B., Zaki, S.R., Swanepoel, R., Ansari, A.A., Peters, C.J., 1999. Markedly elevated levels of interferon (IFN)-γ, IFN-α, interleukin (IL)-2, IL-10, and tumor necrosis factor-α associated with fatal Ebola virus infection. *Journal of Infectious Diseases* 179, S188.

Visomirski-Robic, L.M., Gott, J.M., 1997a. Insertional editing in isolated Physarum mitochondria is linked to RNA synthesis. *RNA* 3, 821-837.

Visomirski-Robic, L.M., Gott, J.M., 1997b. Insertional editing of nascent mitochondrial RNAs in Physarum. *Proc Natl Acad Sci* U S A 94, 4324-4329.

Volchkov, V.E., Becker, S., Volchkova, V.A., Ternovoj, V.A., Kotov, A.N., Netesov, S.V., Klenk, H.D., 1995. GP mRNA of Ebola virus is edited by the Ebola virus polymerase and by T7 and vaccinia virus polymerases. *Virology* 214, 421-430.

Volchkov, V.E., Blinov, V.M., Netesov, S.V., 1992. The envelope glycoprotein of Ebola virus contains an immunosuppressive-like domain similar to oncogenic retroviruses. *FEBS Lett* 305, 181-184.

Volchkov, V.E., Chepurnov, A.A., Volchkova, V.A., Ternovoj, V.A., Klenk, H.D., 2000. Molecular Characterization of Guinea Pig-Adapted Variants of Ebola Virus* 1. *Virology* 277, 147-155.

Volchkov, V.E., Feldmann, H., Volchkova, V.A., Klenk, H.D., 1998. Processing of the Ebola virus glycoprotein by the proprotein convertase furin. *Proc Natl Acad Sci* U S A 95, 5762-5767.

Volchkov, V.E., Volchkova, V.A., Chepurnov, A.A., Blinov, V.M., Dolnik, O., Netesov, S.V., Feldmann, H., 1999. Characterization of the L gene and 5' trailer region of Ebola virus. *J Gen Virol* 80 (Pt 2), 355-362.

Volchkov, V.E., Volchkova, V.A., Dolnik, O., Feldmann, H., Klenk, H.D., 2005. Polymorphism of filovirus glycoproteins. *Advances in Virus Research* 64, 359-381.

Volchkov, V.E., Volchkova, V.A., Muhlberger, E., Kolesnikova, L.V., Weik, M., Dolnik, O., Klenk, H.D., 2001. Recovery of infectious Ebola virus from complementary DNA: RNA editing of the GP gene and viral cytotoxicity. *Science* 291, 1965-1969.

Volchkova, V.A., Dolnik, O., Martinez, M.J., Reynard, O., Volchkov, V.E., 2011. Genomic RNA editing and its impact on Ebola virus adaptation during serial passages in cell culture and infection of guinea pigs. *Journal of Infectious Diseases* 204, S941-S946.

Volchkova, V.A., Feldmann, H., Klenk, H.D., Volchkov, V.E., 1998. The nonstructural small glycoprotein sGP of Ebola virus is secreted as an antiparallel-orientated homodimer. *Virology* 250, 408-414.

Volchkova, V.A., Klenk, H.D., Volchkov, V.E., 1999. Delta-peptide is the carboxy-terminal cleavage fragment of the nonstructural small glycoprotein sGP of Ebola virus. *Virology* 265, 164-171.

References

Vos, P., Hogers, R., Bleeker, M., Reijans, M., van De Lee, T., Hornes, M., Friters, A., Pot, J., Paleman, J., Kuiper, M., 1995. AFLP: a new technique for DNA fingerprinting. *Nucleic Acids Research* 23, 4407-4414.

Wahl-Jensen, V., Kurz, S.K., Hazelton, P.R., Schnittler, H.J., Stroher, U., Burton, D.R., Feldmann, H., 2005a. Role of Ebola virus secreted glycoproteins and virus-like particles in activation of human macrophages. *Journal of Virology* 79, 2413-2419.

Wahl-Jensen, V.M., Afanasieva, T.A., Seebach, J., Stroher, U., Feldmann, H., Schnittler, H.J., 2005b. Effects of Ebola virus glycoproteins on endothelial cell activation and barrier function. *Journal of Virology* 79, 10442-10450.

Wang, D., Raja, N.U., Trubey, C.M., Juompan, L.Y., Luo, M., Woraratanadharm, J., Deitz, S.B., Yu, H., Swain, B.M., Moore, K.M., Pratt, W.D., Hart, M.K., Dong, J.Y., 2006. Development of a cAdVax-based bivalent ebola virus vaccine that induces immune responses against both the Sudan and Zaire species of Ebola virus. *Journal of Virology* 80, 2738-2746.

Wang, J., Manicassamy, B., Caffrey, M., Rong, L., 2011. Characterization of the receptor-binding domain of Ebola glycoprotein in viral entry. *Virol Sin* 26, 156-170.

Wang, Y., Yu, Y., Shabahang, S., Wang, G., Szalay, A., 2002. Renilla luciferase-Aequorea GFP (Ruc-GFP) fusion protein, a novel dual reporter for real-time imaging of gene expression in cell cultures and in live animals. *Molecular Genetics and Genomics* 268, 160-168.

Warfield, K.L., Bosio, C.M., Welcher, B.C., Deal, E.M., Mohamadzadeh, M., Schmaljohn, A., Aman, M.J., Bavari, S., 2003. Ebola virus-like particles protect from lethal Ebola virus infection. *Proceedings of the National Academy of Scien*ces 100, 15889.

Warfield, K.L., Swenson, D.L., Olinger, G.G., Nichols, D.K., Pratt, W.D., Blouch, R., Stein, D.A., Aman, M.J., Iversen, P.L., Bavari, S., 2006. Gene-specific countermeasures against Ebola virus based on antisense phosphorodiamidate morpholino oligomers. *PLoS Pathog* 2, e1.

Warren, T., Warfield, K., Wells, J., Swenson, D., Donner, K., Van Tongeren, S., Garza, N., Dong, L., Mourich, D., Crumley, S., 2010. Advanced antisense therapies for postexposure protection against lethal filovirus infections. *Nature Medicine* 16, 991-994.

Wegener, J., Zink, S., Rösen, P., Galla, H.J., 1999. Use of electrochemical impedance measurements to monitor β-adrenergic stimulation of bovine aortic endothelial cells. *Pflügers Archiv European Journal of Physiology* 437, 925-934.

Weik, M., Modrof, J., Klenk, H.D., Becker, S., Muhlberger, E., 2002. Ebola virus VP30-mediated transcription is regulated by RNA secondary structure formation. *Journal of Virology* 76, 8532-8539.

Weiss, R.B., Dunn, D.M., Atkins, J.F., Gesteland, R.F., 1990. Ribosomal frameshifting from-2 to+ 50 nucleotides. *Prog Nucleic Acid Res Mol Biol* 39, 159-183.

Weissenhorn, W., Calder, L.J., Wharton, S.A., Skehel, J.J., Wiley, D.C., 1998a. The central structural feature of the membrane fusion protein subunit from the Ebola virus glycoprotein is a long triple-stranded coiled coil. *Proceedings of the National Academy of Sciences* 95, 6032.

Weissenhorn, W., Carfi, A., Lee, K.H., Skehel, J.J., Wiley, D.C., 1998b. Crystal structure of the Ebola virus membrane fusion subunit, GP2, from the envelope glycoprotein ectodomain. *Mol Cell* 2, 605-616.

Welsch, S., Kolesnikova, L., Krähling, V., Riches, J.D., Becker, S., Briggs, J.A.G., 2010. Electron tomography reveals the steps in filovirus budding. *PLoS pathogens* 6, e1000875.

Whelan, S., Barr, J., Wertz, G., 2004. Transcription and replication of nonsegmented negative-strand RNA viruses. *Current Topics in Microbiology and Immunology* 283, 61.

WHO, 2002. Ebola hemorrhagic fever in Gabon-Update 23 WHO.

WHO, 2003a. Ebola haemorrhagic fever in the Republic of the Congo- Update 11. WHO.

WHO, 2003b. Ebola hemorrhagic fever in the Republic of the Congo- Update 12. WHO.

References

Wiegand, M.A., Bossow, S., Schlecht, S., Neubert, W.J., 2007. De novo synthesis of N and P proteins as a key step in Sendai virus gene expression. *Journal of Virology* 81, 13835-13844.

Wilson, J.A., Bray, M., Bakken, R., Hart, M.K., 2001. Vaccine potential of Ebola virus VP24, VP30, VP35, and VP40 proteins. *Virology* 286, 384-390.

Wilson, J.A., Hart, M.K., 2001. Protection from Ebola virus mediated by cytotoxic T lymphocytes specific for the viral nucleoprotein. *Journal of Virology* 75, 2660.

Wong, K., Lyddon, R., Dracheva, S., 2009. TaqMan-based, real-time quantitative polymerase chain reaction method for RNA editing analysis. *Analytical Biochemistry* 390, 173-180.

Workgroup, P., 2000. Biological and chemical terrorism: strategic plan for preparedness and response. MMWR 49, 1-14.

Wu, T.L., 2006. Two-dimensional difference gel electrophoresis.*Methods in Molecular Biology-Clifton Then Totowa-* 328, 71.

Yamayoshi, S., Noda, T., Ebihara, H., Goto, H., Morikawa, Y., Lukashevich, I.S., Neumann, G., Feldmann, H., Kawaoka, Y., 2008. Ebola virus matrix protein VP40 uses the COPII transport system for its intracellular transport. *Cell Host & Microbe* 3, 168-177.

Yang, L., Sanchez, A., Ward, J.M., Murphy, B.R., Collins, P.L., Bukreyev, A., 2008. A paramyxovirus-vectored intranasal vaccine against Ebola virus is immunogenic in vector-immune animals. *Virology* 377, 255-264.

Yang, Z., Delgado, R., Xu, L., Todd, R.F., Nabel, E.G., Sanchez, A., Nabel, G.J., 1998. Distinct cellular interactions of secreted and transmembrane Ebola virus glycoproteins. *Science* 279, 1034-1037.

Yasuda, J., Nakao, M., Kawaoka, Y., Shida, H., 2003. Nedd4 regulates egress of Ebola virus-like particles from host cells. *Journal of Virology* 77, 9987.

Yonezawa, A., Cavrois, M., Greene, W.C., 2005. Studies of Ebola virus glycoprotein-mediated entry and fusion by using pseudotyped human immunodeficiency virus type 1 virions: involvement of cytoskeletal proteins and enhancement by tumor necrosis factor alpha. *Journal of Virology* 79, 918.

Zaki, S.R., Goldsmith, C.S., 1999. Pathologic features of filovirus infections in humans. *Curr Top Microbiol Immunol* 235, 97-116.

Zeitlin, L., Pettitt, J., Scully, C., Bohorova, N., Kim, D., Pauly, M., Hiatt, A., Ngo, L., Steinkellner, H., Whaley, K.J., 2011. Enhanced potency of a fucose-free monoclonal antibody being developed as an Ebola virus immunoprotectant. *Proceedings of the National Academy of Sciences* 108, 20690-20694.

Zheng, H., Fu, T.B., Lazinski, D., Taylor, J., 1992. Editing on the genomic RNA of human hepatitis delta virus. *Journal of Virology* 66, 4693-4697.

Zhou, G., Li, H., DeCamp, D., Chen, S., Shu, H., Gong, Y., Flaig, M., Gillespie, J.W., Hu, N., Taylor, P.R., 2002. 2-D differential in-gel electrophoresis for the identification of esophageal scans cell cancer-specific protein markers. Molecular & Cellular Proteomics 1, 117-123.

Zuker, M., 2003. Mfold web server for nucleic acid folding and hybridization prediction. *Nucleic Acids Research* 31, 3406-3415.

Appendix 1. Primer Sequences

A. r.ssGP and r.sGP Plasmids

No.	Primer	Sequence (5'- 3')	Plasmid
1	F ssGP6A	agccggccagatctatcccacttgg	pDISPLAY
2	R ssGP6A	gacctgcagttactagtgaggttttttagttttcccagaagg	
3	F ssGP9A	agccggccagatctatcccacttgg	
4	R ssGP9A	gcctgcagttactagtgaggttttttttagtttcccagaagg	
5	F sGP/ssG9A	atcggaattcatgggcgttacagg	pCAGGS
6	R sGP	ttctcgagttagcgccggactctgac	
7	RssGP9A	atctcgagttactagtgaggttttttttagtttcccag	

B. Minigenome

No.	Primer	Sequence (5'- 3')
8	F GP BsmB1 mini	acttcgtctctgagtatgggcgttacagg
9	R GP BsmB1 mini	ttggcgtctcgcaaactaaaagacaaatttgc
10	F GP ES110 BsmB1 mini	attccgtctctgagtcccgaaattgatacaac
11	R GP ES110 BsmB1 mini	ttggcgtctcacaaaggctccgtttgatac
12	F L 110 BsmB1 mini	aacccgtctcggagtctttttaaaacctgatg
13	R L 110 BsmB1 mini	atatcgtctcgcaaaattcttgtagccgttttaagg
14	F BsmB1 pATX	atcgtctcaaaggcggtaatacggttatcc
15	R BsmB1 pATX	ttcgtctctcaggtggcacttttcggg
16	F GP ES110 BsmB1 pATX	atcgtctcacctgcccgaaattgatacaac
17	R GP ES110 BsmB1 pATX	ttcgtctcgccttggctccgtttgatacaac
18	F eGFP pATX-ES	atacgtctcacctgatggtgagcaagggcgag
19	R eGFP pATX-ES	tatcgtctcacgggcttgtacagctcgtccatg
20	F pATX-ES eGFP	acgcgtctcgcccgaaattgatacaacaatcggg
21	R pATX-ES eGFP	actcgtctcacaggtggcacttttcggggaaatg
22	F mCherry pATX-eGFP-ES	acgcgtctcgcctttacttgtacagctcg
23	R mCherry pATX-eGFP-ES	acgcgtctcgccttcttgtacagctcgtcc
24	F pATX-eGFP-ES mCherry	atacgtctcgaaggcggtaatacggttatcc
25	R pATX-eGFP-ES mCherry	attcgtctcgggctccgtttgatacttc
26	F NLS pATX-eGFP-ES-mCherry	acgcgtctcgcaaggatccaaaaaagaagagaaagg
27	R NLS pATX-eGFP-ES-mCherry	atacgtctcgccttttatctagatccggtggatcc
28	F pATX-eGFP-ES-mCherry NLS	attcgtctcgaaggcggtaatacggttatccacag
29	R pATX-eGFP-ES-mCherry NLS	attcgtctcacttgtacagctcgtccatgccg
30	F eGFP7AmCherryNLS pTM1	aatgaattcatggtgagcaagggcgag
31	R eGFP7AmCherryNLS pTM1	attctcgagttatctagatccggtggatc
32	F eGFP7AmCherryNLS pCAGGS	atagagctcatggtgagcaagggcg
33	R eGFP7AmCherryNLS pCAGGS	attgctagcggctccgtttgatacaactgtg

C. Mutagenesis & Deletion

No.	Primer	Sequence (5'- 3')
34	F ssGPCys53Gly	gtcgacaaactagttggtcgtgacaaactgtcatcc
35	R ssGPCys53Gly	ggatgacagtttgtcacgaccaactagtttgtcgac
36	F GP ES8A	acaggggagtgggaaactaaaaaaaacctcactagaaaaattcgc
37	R GP ES8A	gcgaatttttctagtgaggtttttttagtttcccactcccctgt
38	F nt C3337Amini	acgaggccctttagtctcgcgcgtttcggtg
39	R nt C3337Amini	tcaccgaaacgcgcgagactaaagggcctcg
40	F nt 3383Amini	atgcagctcccggaaacggtcacagcttgtc
41	R nt 3383Amini	agacaagctgtgaccgtttccgggagctgc
42	F ES 3rd AtoG	tgggccttctgggaaactaagaaaacctcactagaaaaattcg
43	R ES 3rd AtoG	cgaatttttctagtgaggttttcttagtttcccagaaggccca
44	F ES 6th AtoG	tgggccttctgggaaactaaaaagacctcactagaaaaattcg
45	R ES 6th AtoG	cgaatttttctagtgaggtcttttagtttcccagaaggccca
46	F leader-ssKO (1st 3)	actatgaggaagattaataaagctcctctcattgaaatttatatcg
47	R leader-ssKO (1st 3)	cgatataaatttcaatgagaggagctttattaatcttcctcatagt
48	F leader-ssKO (2nd 3)	tgaggaagattaataaagctagcctcattgaaatttatatcgaattt
49	R leader-ssKO (2nd 3)	aaattcgatataaatttcaatgaggctagctttattaatcttcctca
50	F ES SS KO (1-24) C3T	gcatggacgagctgtacaagcctgaaattgatacaacaatcgg
51	R ES SS KO (1-24) C3T	ccgattgttgtatcaatttcaggcttgtacagctcgtccatgc
52	F ES SS KO (1-24) A18C	acaagcccgaaattgatacaaccatcggggagtgggccttctgg
53	R ES SS KO (1-24) A18C	ccagaaggcccactccccgatggttgtatcaatttcgggcttgt
54	F ES SS KO (1-24) G24A	acaagcctgaaattgatacaaccatcggagagtgggccttctgg
55	R ES SS KO (1-24) G24A	ccagaaggcccactctccgatggttgtatcaatttcaggcttgt
56	F ES upstream 45 nt deletion	atggacgagctgtacaagaaaaaaacctcactagaaaaattcg
57	R ES upstream 45 nt deletion	cgaatttttctagtgaggtttttttcttgtacagctcgtccatgc
58	F ES dwnstream 58 nt deletion	tctgggaaactaaaaaaacgtgagcaagggcgaggag
59	R ES dwnstream 58 nt deletion	ctcctcgcccttgctcacgtttttttagtttcccaga
60	F ES only (upstream deleted)	atggacgagctgtacaagaaaaaaacctcactagaaaaattcg
61	R ES only (upstream deleted)	cgaatttttctagtgaggtttttttcttgtacagctcgtccat
62	F ES upstream 9 nt deletion	atggacgagctgtacaaggatacaacaatcggggag
63	R ES upstream 9 nt deletion	cttgtacagctcgtccatcttgtacagctcgtccat
64	F ES upstream 18 nt deletion	atggacgagctgtacaagatcggggagtgggccttc
65	R ES upstream 18 nt deletion	gaaggcccactccccgatcttgtacagctcgtccat
66	F ES upstream 27 nt deletion	atggacgagctgtacaagtgggccttctgggaaac
67	R ES upstream 27 nt deletion	gtttcccagaaggcccacttgtacagctcgtccat
68	F ES dwnstream 13 nt deletion	attcgtctcacgtgagcaagggcgaggagg
69	R ES dwnstream13 nt deletion	acgcgtctcgcacgacaactgtgaaagacaactc
70	F ES dwnstream 22 nt deletion	attcgtctcacgtgagcaagggcgaggagg
71	R ES downstream 22 nt deletion	attcgtctcgcacgaaagacaactcttcactgcg
72	F ES dwnstream 31 nt deletion	attcgtctcacgtgagcaagggcgaggagg
73	R ES downstream 31 nt deletion	attcgtctcgcacgtcttcactgcgaatttttctag
74	F ES dwnstream 49 nt deletion	attcgtctcacgtgagcaagggcgaggagg
75	R ES dwnstream 49 nt deletion	acgcgtctcgcacgctagtgaggtttttttagtttcc

76	F ES SS KO (38-45) G39A&C44T	aacaatcggggagtgggccttctgagaaattaaaaaaacc
77	R ES SS KO (38-45) G39A&C44T	ggtttttttaatttctcagaaggcccactccccgattgtt
78	F ES SS KO (38-45) C44T	tgggccttctgggaaattaaaaaaacctcactag
79	R ES SS KO (38-45) C44T	ctagtgaggttttttaatttcccagaaggccca
80	F ES SS KO (38-45) G38A & G39A	gagtgggccttctaagaaactaaaaaaacctcactag
81	R ES SS KO (38-45) G38A & G39A	ctagtgaggttttttagtttcttagaaggcccactc

D. Sequencing

No.	Primer	Sequence (5'- 3')
82	F ES clone check	acaccacagtttctgctccagc
83	R ES clone check	tgactgtgcacttgaaccattgc
84	F ES110 check	actcccgaaattgatacaacaatcg
85	R ES110 check	attggctccgtttgatacaactgtg
86	F mini check	aaagtgccacctgacgtctaagaaacc
87	R mini check	actctcagtacaatctgctctgatgcc
88	F ZEBOV leader check	aggatcttttgtgtgcgaataactatgagg
89	R ZEBOV leader check	actcggaattttgtgattccgagcaatttg
90	F eGFP seq check	aacggcatcaaggtgaacttcaagatcc
91	R eGFP seq check	atgttgccgtcctccttgaagtcgatgc
92	F pATX seq check	ttaaagggaataagggcgacacgg
93	R pATX seq check	tcaaaacgccagcaacgc
94	F nt5958 ZEBOV	agagtaggggtcgtcaggtcc
95	oligo-dT primer	ttttttttttttttt
96	F ZEBOV L 110seq	aaacctgatgaaacatttgtacattcagg
97	R ZEBOV L 110seq	attcttgtagccgttttaagggactgagg
98	F CEBOV 110seq	ctgttgataccagcatgggtgagtgg
99	R CEBOV 110seq	ggtttctggtacaggtacgaaagacaac
100	F SEBOV 110seq	atatcaatgctgatattggtgaatgg
101	R SEBOV 110seq	gttgagcgataaagcttcgaaagac
102	F REBOV 110seq	aaattgaaccagatgttggtgagtgg
103	R REBOV 110seq	gtgggttgatagaatttggaaatgc
104	F BEBOV 110seq	ctgttgacaccggcgtaggtgaatgg
105	R BEBOV 110seq	ggctcttggtacaaatatgacagac

E. Rapid Assay

No.	Primer	Sequence (5'- 3')
106	F ZEBOVGP ES 110seq	6FAM-aaattgatacaacaatcggggagtgg
107	R ZEBOVGP ES 110seq	tccgtttgatacaactgtgaaagac
108	F ZEBOV L 110seq	6FAM-aaacctgatgaaacatttgtacattcagg
109	R ZEBOV L 110seq	attcttgtagccgttttaagggactgagg
110	F CEBOV 110seq	6FAM-ctgttgataccagcatgggtgagtgg
111	R CEBOV 110seq	ggtttctggtacaggtacgaaagacaac
112	F SEBOV 110seq	6FAM-atatcaatgctgatattggtgaatgg
113	R SEBOV 110seq	gttgagcgataaagcttcgaaagac
114	F REBOV 110seq	6FAM-aaattgaaccagatgttggtgagtgg
115	R REBOV 110seq	gtgggttgatagaatttggaaatgc
116	F BEBOV 110seq	6FAM-ctgttgacaccggcgtaggtgaatgg
117	R BEBOV 110seq	ggctcttggtacaaatatgacagac
118	F d50upESG7m	6FAM-ccgccgccgggatcactctcggcatgg
119	R d50upESG7m	tccgtttgatacaactgtgaaagac

Appendix 2. Reagents

A. Buffers for Protein Purification:

Equilibrium buffer:

8 ml of 20 mM Tris (pH 7.5); 8 ml of 0.1 NaCl; and 0.08 ml of 0.1 mM EDTA (TNE) in 375.92 ml distilled water. Filter sterilized.

Wash buffer:

Equilibrium buffer + 0.05% Tween-20 (100% stock).

Column storage buffer:

Equilibrium buffer + 0.09% sodium azide (2% stock solution)

Regeneration buffer:

0.1 M glycine, pH 2.0

B. Buffers for peptide identification:

100 mM NH_4HCO_3 solution:

1.5812 g in 200 ml distilled water.

10 mM DTT solution:

0.00154 gm DTT in 1 ml 100 mM NH_4HCO_3 solution

65 mM IAA solution:

0.01 gm IAA in 1 ml 100 mM NH_4HCO_3 solution

C. Coommassie brilliant blue R-250 stain

Coommassie brilliant blue R-250	1.25 g
Glacial acetic acid	50 ml
Methanol	225 ml
Distilled water	225 ml

Coommassie destain

Glacial acetic acid	50 ml
Methanol	225 ml
Distilled water	225 ml

D. 4x SDS-PAGE gel loading buffer:

1 M Tris-HCL (pH 6.8)	2 ml
SDS	0.8 g
10% glycerol	4 ml
B marcaptoethanol	0.4 ml
0.5 M EDTA	1 ml
Bromophenol blue	8 mg

E. 6x gel loading buffer:

Bromophenol blue	0.025 mg
Sucrose	4 g
Sterile distilled water	10 ml

F. Western blotting gel:

Resolving gel buffer (for 10% mini gel 3.2 ml/gel):

Distilled water	4.8 ml
40% acrylamide	2.5 ml
1.5 M Tris (pH 8.8)	2.5 ml
10% SDS	100 ul
10% ammonium persulfate	100 ul
TEMED	4 ul

Stacking gel buffer (for 4% mini gel 1 ml/gel):

Distilled water	3.15 ml
40% acrylamide	500 ul
0.5 M Tris (pH 6.8)	1.25 ml
10% SDS	50 ul
10% ammonium persulfate	50 ul
TEMED	8 ul

A. .

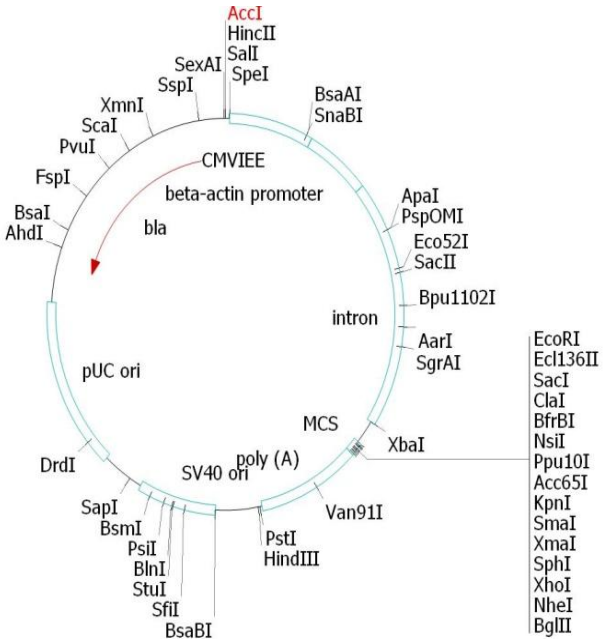

B.

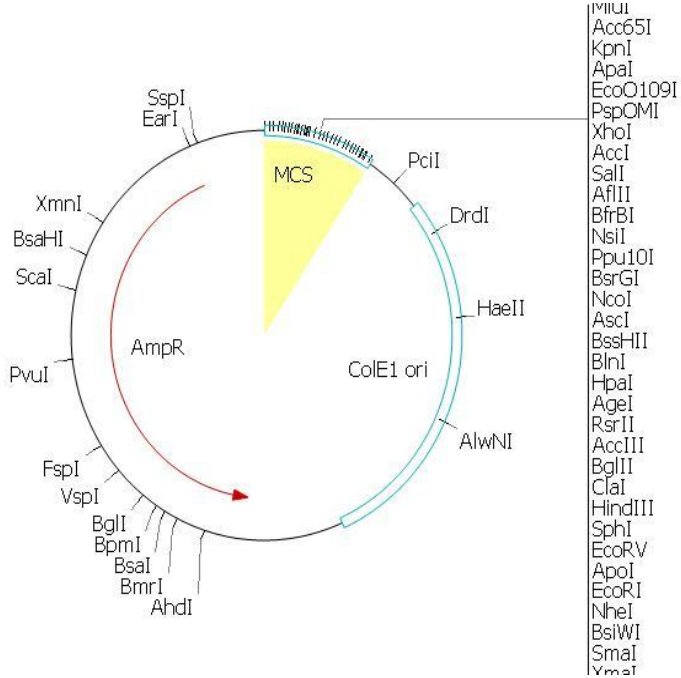

Appendix 3. **Vector maps of pCAGGS-MCS and pATX-MCS. A.** pCAGGS. beta-actin promoter: chicken β- actin/rabbit β-globin hybrid promoter, CMVIEE: human cytomegalovirus immediate early promoter enhancer, pUC ori: pUC origin of replication, SV40: SV40 origin of replication (SV40 ori), poly (A) signal, and MCS: multiple cloning sites. **B.** pATX. AmpR: ampicillin resistance gene, ColE1 ori: origin of replication and, and MCS: multiple cloning sites.

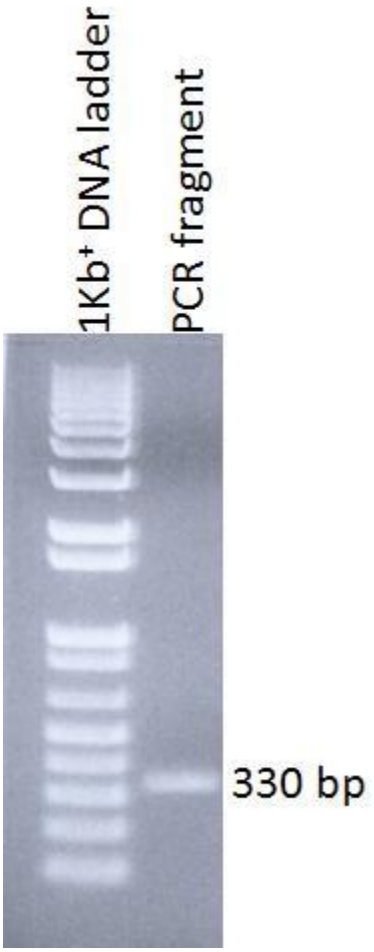

Appendix 4. **PCR fragment for cloning and sequencing**. A GP gene editing region 330 bp PCR fragment was amplified from transcript RNA derived from ZEBOV infection (in vitro and *in vivo*) for cloning into the TOPO TA 2.1 vector for sequencing.

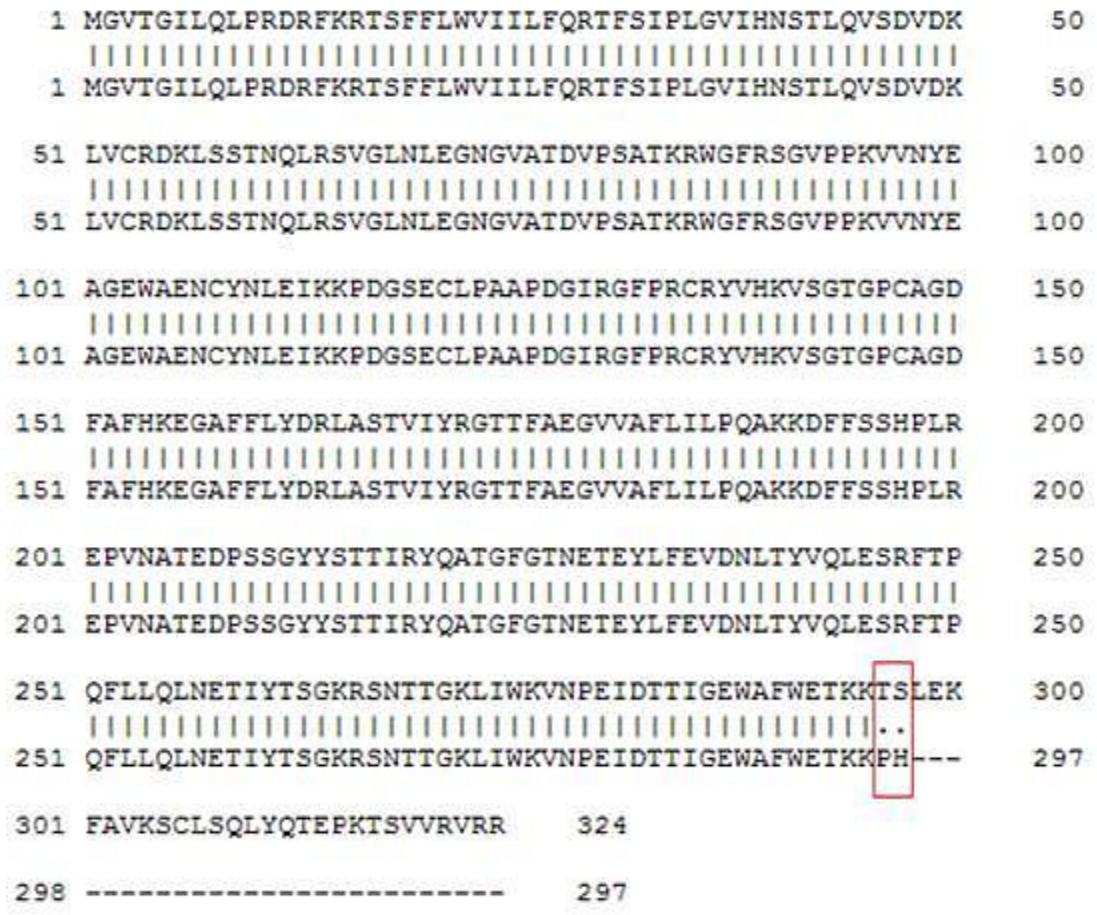

Appendix 5. **ssGP C-terminal amino acids (aa) are unique.** Amino acid sequence alignment between sGP (upper sequence) and ssGP (lower sequence) reveals that the C-terminus of ssGP is unique (box).

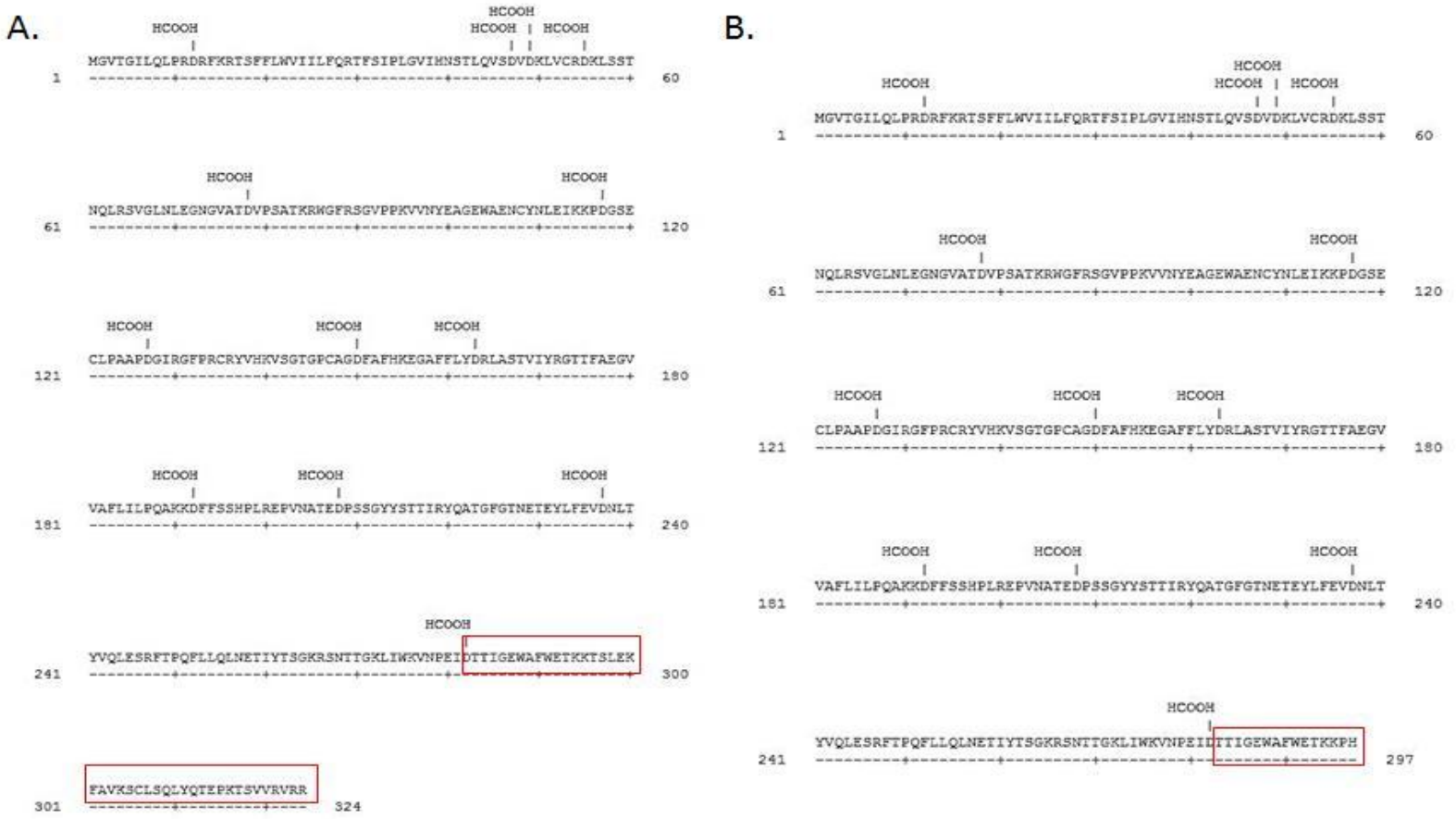

Appendix 6. **Formic acid cleavage sites on ssGP and sGP.** Predicted peptide fragments for formic acid digestion according to the peptide cutter webserver (www.expasy.org) for sGP (A) and ssGP (B) reveals that the C-terminal peptide (boxed) differs between sGP and ssGP. The ssGP C-terminal peptide (282-TTIGEWAFWETKKPH-297) has a MW of 1830.9173 Da, which is smaller than that of the sGP C-terminal peptide (282-TTIGEWAFWETKKTSLEKFAVKSCLSQLYQTEPKTSVVRVRR-324; MW 4775.5228 Da).

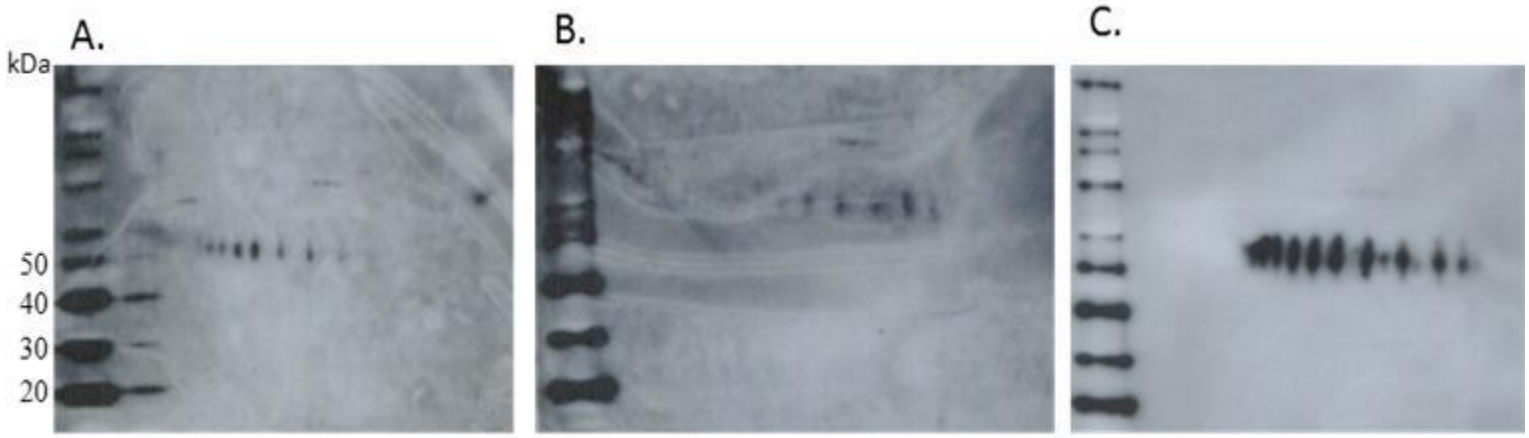

Appendix 7. **2 dimensional (2-D) gel electrophoresis separating r.ssGP and r.sGP**. Vero E6 cells were transfected with plasmids expressing r.ssGP or r.sGP. Supernatants [r.ssGP (A), r.sGP (B) or both (C)] were run on 2-D gel electrophoresis with a pH gradient (pH 3-10) in the first dimension and 4% SDS-PAGE in the second dimension. Proteins were detected by immunoblotting using MAb 42/3.7 (1:10,000 dilution). There was no clear separation between r.sGP and r.ssGP.

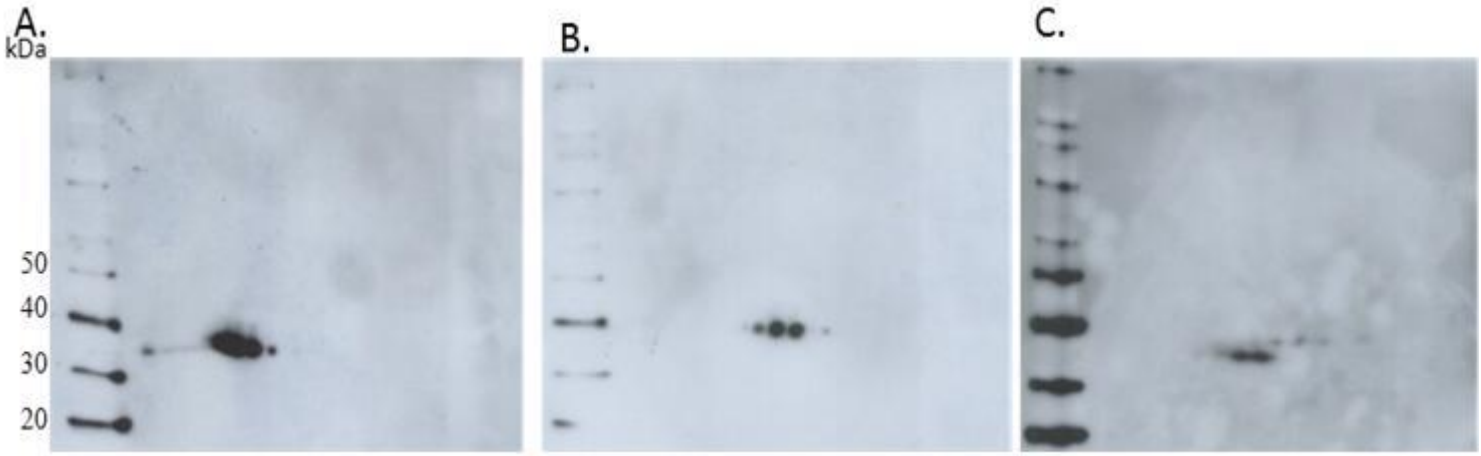

Appendix 8. **2 dimensional (2-D) gel electrophoresis for separating deglycosylated r.ssGP and r.sGP.** Vero E6 cells were transfected with plasmids expressing r.ssGP or r.sGP. Supernatants [r.ssGP (A), r.sGP (B) or both (C)] treated with PNGaseF prior to separation on 2-D gel electrophoresis using a pH gradient (4-7) for the first dimension and 4% SDS-PAGE for the second dimension. Proteins were detected by immunoblotting using MAb 42/3.7 (1:10,000 dilution). The analysis allowed separation between deglycosylated r.ssGP and r.sGP (see C).

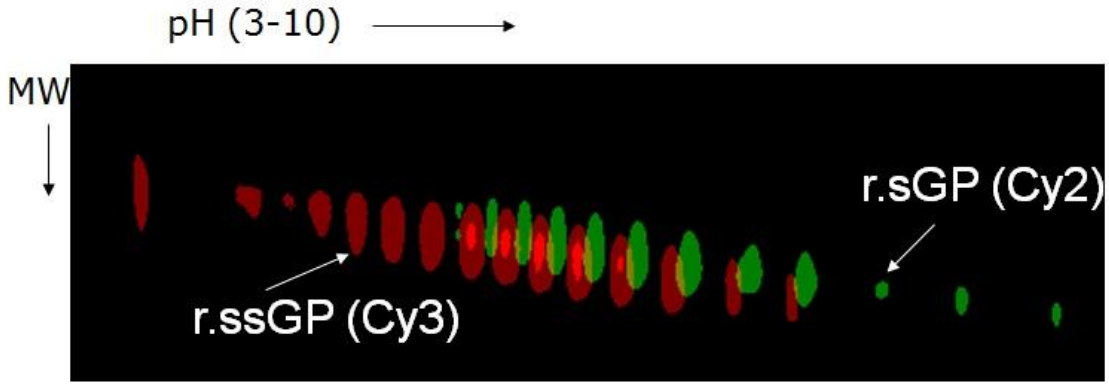

Appendix 9. **2 dimensional difference gel electrophoresis (2-D DIGE) for separating r.sGP and r.ssGP.** Purified r.ssGP and r.sGP were dyed with Cy3 and Cy2, respectively, and mixed. The mixture was subjected to 2-D DIGE with a pH gradient (3-10) in the first dimension and 4% SDS-PAGE in the second dimension. Cy dyes were visualized at respective fluorescence spectrum using the Typhoon 9400 scanner (GE Healthcare). r.ssGP and r.sGP could be separated based on their isoelectric point (p*I*) and molecular weight (MW).

A.

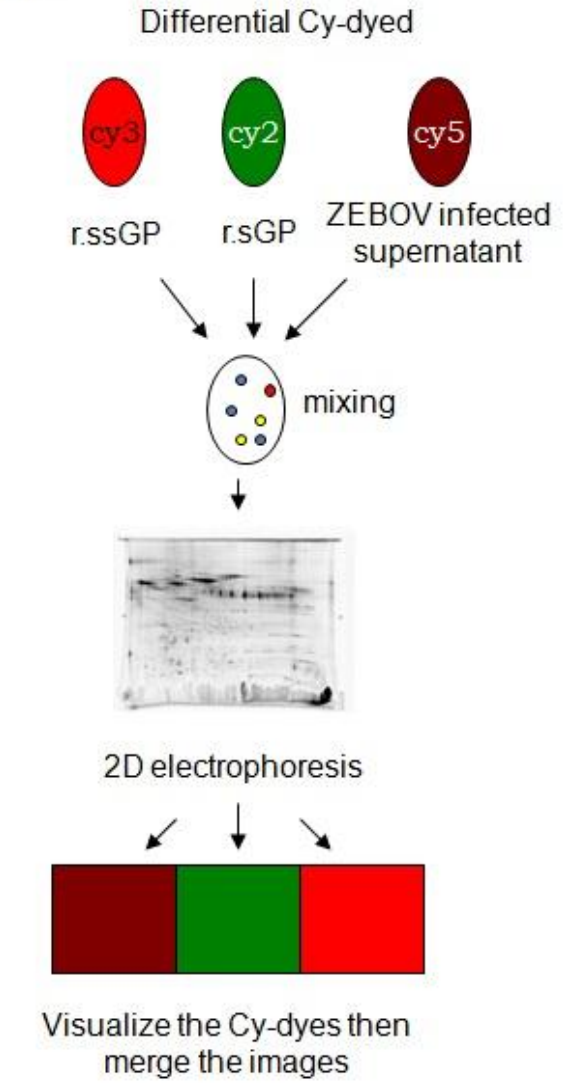
Differential Cy-dyed
cy3
cy2
cy5
r.ssGP
r.sGP
ZEBOV infected supernatant
mixing
2D electrophoresis
Visualize the Cy-dyes then merge the images

B.

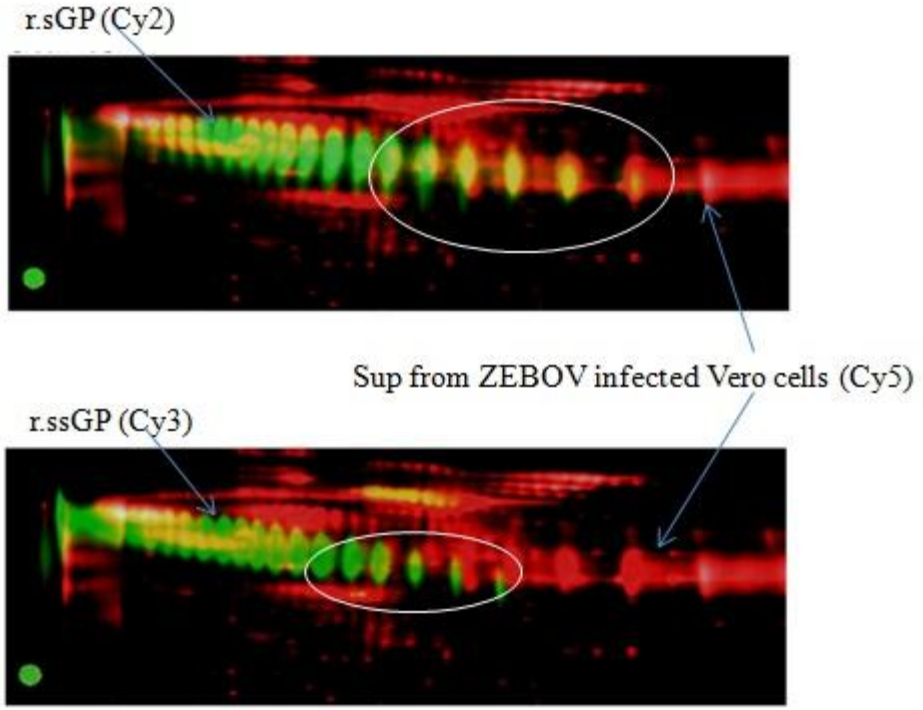
r.sGP (Cy2)
Sup from ZEBOV infected Vero cells (Cy5)
r.ssGP (Cy3)

Appendix 10. **2 dimensional difference gel electrophoresis (2-D DIGE) detected ssGP**. **A. Scheme of 2-D DIGE**. Purified r.ssGP, r.sGP, and concentrated supernatant from ZEBOV infected Vero E6 cells (MOI of 1) were labeled with Cy3, Cy2, and Cy5, respectively, and mixed prior to application to 2-D DIGE with a pH gradient (pH 3-10) in the first dimension and 4% SDS-PAGE in the second dimension. Cy dyes were visualized at respective fluorescence spectrum using the Typhoon 9400 scanner. **B. Top image, gel scanned for Cy2 and Cy5**. The migration pattern of r.sGP (green) overlapped with a certain proportions of labeled proteins (yellow) derived from supernatants of ZEBOV infected Vero E6 cells (red). **Bottom image**, **gel scanned for Cy3 and Cy5**. The migration pattern of r.ssGP (green) overlapped with a certain proportion of labeled proteins (yellow) derived from supernatants of ZEBOV infected Vero E6 cells (red). This indicates that sGP and ssGP are expressed and secreted during EBOV infection.

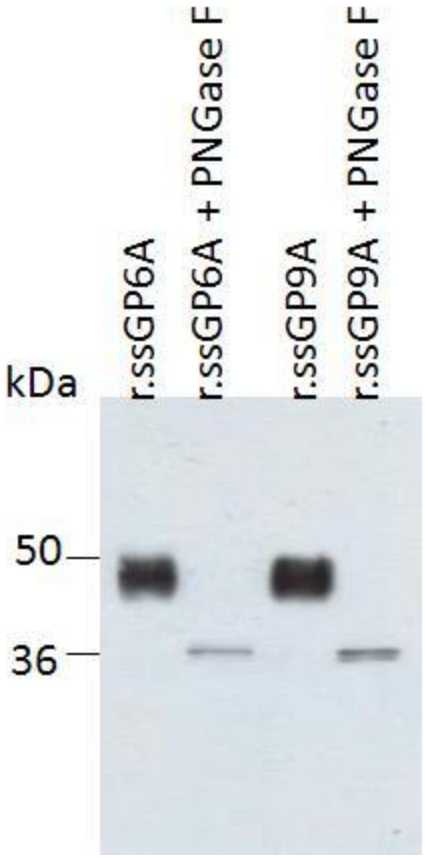

Appendix 11. **ssGP is N-glycosylated.** 293T cells were transfected with expression plasmids encoding two distinct forms of HA-tagged ssGP (ssGP6A and ssGP9A; difference by one amino acid) and supernatants were collected from the transfected cells at 72 hr post-transfection. Proteins were purified using HA-affinity chromatography, treated with PNGaseF, separated under reducing 10% SDS-PAGE, and detected by immunoblotting using anti-HA peroxidase (1:10,000 dilution). PNGaseF treatment resulted in a molecular weight (MW) shift suggesting all six potential N-linked glycosylation motifs are glycosylated.

A.

Sample Name	Sample in put in % (7A_8A)	% 7A-Obtained (Raw)	% 8A-Obtained (Raw)
Unedited (7A)_edited (8A)	0_100	15.8%	84.2%
Unedited (7A)_edited (8A)	0_100	15.3%	84.7%
Unedited (7A)_edited (8A)	0_100	16.3%	83.7%
Unedited (7A)_edited (8A)	100_0	100.0%	0.0%
Unedited (7A)_edited (8A)	100_0	100.0%	0.0%
Unedited (7A)_edited (8A)	100_0	100.0%	0.0%
Unedited (7A)_edited (8A)	10_90	21.1%	78.9%
Unedited (7A)_edited (8A)	10_90	20.9%	79.1%
Unedited (7A)_edited (8A)	10_90	20.7%	79.3%
Unedited (7A)_edited (8A)	20_80	27.1%	72.9%
Unedited (7A)_edited (8A)	20_80	26.9%	73.1%
Unedited (7A)_edited (8A)	20_80	26.7%	73.3%
Unedited (7A)_edited (8A)	30_70	32.6%	67.4%
Unedited (7A)_edited (8A)	30_70	32.6%	67.4%
Unedited (7A)_edited (8A)	30_70	33.4%	66.6%
Unedited (7A)_edited (8A)	40_60	40.7%	59.3%
Unedited (7A)_edited (8A)	40_60	40.6%	59.4%
Unedited (7A)_edited (8A)	40_60	40.0%	60.0%
Unedited (7A)_edited (8A)	50_50	48.2%	51.8%
Unedited (7A)_edited (8A)	50_50	47.8%	52.2%
Unedited (7A)_edited (8A)	50_50	47.8%	52.2%
Unedited (7A)_edited (8A)	60_40	55.5%	44.5%
Unedited (7A)_edited (8A)	60_40	55.8%	44.2%
Unedited (7A)_edited (8A)	60_40	57.1%	42.9%
Unedited (7A)_edited (8A)	70_30	65.3%	34.7%
Unedited (7A)_edited (8A)	70_30	65.6%	34.4%
Unedited (7A)_edited (8A)	70_30	66.2%	33.8%
Unedited (7A)_edited (8A)	80_20	75.5%	24.5%
Unedited (7A)_edited (8A)	80_20	74.7%	25.3%
Unedited (7A)_edited (8A)	80_20	75.4%	24.6%
Unedited (7A)_edited (8A)	90_10	83.8%	16.2%
Unedited (7A)_edited (8A)	90_10	84.3%	15.7%
Unedited (7A)_edited (8A)	90_10	83.6%	16.4%

B.

7A-Standard Deviation	
0	0.51%
10	0.23%
20	0.20%
30	0.44%
40	0.38%
50	0.25%
60	0.86%
70	0.47%
80	0.46%
90	0.39%
100	0.00%

8A-Standard Deviation	
0	0.00%
10	0.39%
20	0.46%
30	0.47%
40	0.86%
50	0.25%
60	0.38%
70	0.44%
80	0.20%
90	0.23%
100	0.51%

C.

Genotype % Conversion								
7A= y = -2162.3923x⁶ + 6665.5481x⁵ - 8128.0786x⁴ + 5079.0668x³ - 1816.0436x² + 513.2139x - 51.3087								
8A= y = 2162.3923x⁶ - 6308.8057x⁵ + 7236.2225x⁴ - 4025.6124x³ + 1127.7183x² - 40.6008x + 0.0055								
Sample Name 7A_8A	%7A Avg.	%8A Avg.	%7A Conversion	%7A St. Dev	%8A Conversion	%8A St. Dev	%7A	%8A
0_100	16%	84%	0.1%	0.51%	99.9%	0.00%	0.1%± 0.51%	99.9%± 0.00%
100_0	100%	0%	100.0%	0.00%	0.0%	0.51%	100.0%± 0.00%	0.0%± 0.51%
10_90	21%	79%	9.9%	0.23%	90.1%	0.39%	9.9%± 0.23%	90.1%± 0.39%
20_80	27%	73%	20.2%	0.20%	79.8%	0.46%	20.2%± 0.20%	79.8%± 0.46%
30_70	33%	67%	29.5%	0.44%	70.5%	0.47%	29.5%± 0.44%	70.5%± 0.47%
40_60	40%	60%	40.3%	0.38%	59.7%	0.86%	40.3%± 0.38%	59.7%± 0.86%
50_50	48%	52%	50.2%	0.25%	49.8%	0.25%	50.2%± 0.25%	49.8%± 0.25%
60_40	56%	44%	59.7%	0.86%	40.3%	0.38%	59.7%± 0.86%	40.3%± 0.38%
70_30	66%	34%	70.0%	0.47%	30.1%	0.44%	70.0%± 0.47%	30.1%± 0.44%
80_20	75%	25%	80.2%	0.46%	19.8%	0.20%	80.2%± 0.46%	19.8%± 0.20%
90_10	84%	16%	89.9%	0.39%	10.1%	0.23%	89.9%± 0.39%	10.1%± 0.23%

Appendix 12. **Rapid transcript quantification assay (RTQA). A.** Raw data from quantifying different ratios of PCR fragments 7A unedited and 8A edited using the 3730xl genetic analyzer (Applied Biosystems). **B.** Standard deviation for the quantified PCR fragments. **C.** A curve fit equation for the % genotype conversion (top) and converted raw data using the curve fit equation for the % genotype conversion (bottom). This standard series was developed for transcript quantification using the rapid transcript quantification assay (RTQA).

Sample Name	In put (7A)	In put (8A)	Allele (7A)	Allele (8A)	Size (7A)	Size (8A)	Height (7A)	Height (8A)	Percent (7A)	Mapover to titration 7A	Percent (8A)	Mapover to titration 8A	Peak Area (7A)	Peak Area (8A)
unedited (7A)-edited (8A)	0%	100%	7A	**8A**	105.38	106.36	2019	10318	16.4%	0% ± 0.5%	83.6%	100% ± 0.7%	11712	56703
unedited (7A)-edited (8A)	0%	100%	7A	**8A**	105.45	106.35	1858	9190	16.8%	1% ± 0.5%	83.2%	99% ± 0.7%	10825	52010
unedited (7A)-edited (8A)	0%	100%	7A	**8A**	105.41	106.41	585	3096	15.9%	0% ± 0.5%	84.1%	100% ± 0.5%	3364	17779
unedited (7A)-edited (8A)	10%	90%	7A	8A	105.52	106.42	2180	7094	23.5%	10% ± 0.5%	76.5%	90% ± 0.7%	12750	38869
unedited (7A)-edited (8A)	10%	90%	7A	8A	105.41	106.41	2114	6591	24.3%	11% ± 0.7%	75.7%	89% ± 0.1%	12011	37438
unedited (7A)-edited (8A)	10%	90%	7A	8A	105.46	106.37	1964	6592	23.0%	9% ± 0.5%	77.0%	91% ± 0.7%	11113	35874
unedited (7A)-edited (8A)	20%	80%	7A	8A	105.51	106.39	2993	6624	31.1%	20% ± 0.1%	68.9%	80% ± 0.2%	16899	36512
unedited (7A)-edited (8A)	20%	80%	7A	8A	105.45	106.29	3494	7775	31.0%	20% ± 0.1%	69.0%	80% ± 0.2%	19323	42678
unedited (7A)-edited (8A)	20%	80%	7A	8A	105.38	106.38	3224	7145	31.1%	20% ± 0.1%	68.9%	80% ± 0.2%	18210	39645
unedited (7A)-edited (8A)	30%	70%	7A	8A	105.48	106.39	3818	6149	38.3%	30% ± 0.2%	61.7%	70% ± 0.2%	21619	34015
unedited (7A)-edited (8A)	30%	70%	7A	8A	105.49	106.41	3687	5989	38.1%	30% ± 0.1%	61.9%	70% ± 0.2%	19708	32401
unedited (7A)-edited (8A)	30%	70%	7A	8A	105.43	106.33	2717	4440	38.0%	30% ± 0.1%	62.0%	70% ± 0.2%	15370	24227
unedited (7A)-edited (8A)	40%	60%	7A	8A	105.5	106.41	5511	6657	45.3%	39% ± 0.2%	54.7%	61% ± 0.2%	30604	36195
unedited (7A)-edited (8A)	40%	60%	7A	8A	105.47	106.45	5421	6510	45.4%	40% ± 0.2%	54.6%	60% ± 0.2%	30436	35828
unedited (7A)-edited (8A)	40%	60%	7A	8A	105.5	106.4	5840	7151	45.0%	39% ± 0.2%	55.0%	61% ± 0.2%	31194	38876
unedited (7A)-edited (8A)	50%	50%	7A	8A	105.44	106.34	5395	4574	54.1%	51% ± 0.5%	45.9%	49% ± 0.7%	29443	25454
unedited (7A)-edited (8A)	50%	50%	7A	8A	105.46	106.34	4773	4205	53.2%	50% ± 0.2%	46.8%	50% ± 0.5%	27646	23323
unedited (7A)-edited (8A)	50%	50%	7A	8A	105.45	106.35	5828	5128	53.2%	50% ± 0.2%	46.8%	50% ± 0.5%	33203	29095
unedited (7A)-edited (8A)	60%	40%	7A	8A	105.48	106.38	6206	3809	62.0%	61% ± 0.7%	38.0%	39% ± 0.2%	33505	20649
unedited (7A)-edited (8A)	60%	40%	7A	8A	105.48	106.38	5562	3410	62.0%	61% ± 0.7%	38.0%	39% ± 0.2%	31233	18343
unedited (7A)-edited (8A)	60%	40%	7A	8A	105.48	106.37	4271	2486	63.2%	63% ± 0.7%	36.8%	37% ± 0.2%	24551	13748
unedited (7A)-edited (8A)	70%	30%	7A	8A	105.48	106.38	7084	3231	68.7%	69% ± 0.7%	31.3%	31% ± 0.2%	37802	18214
unedited (7A)-edited (8A)	70%	30%	7A	8A	105.54	106.34	5988	2783	68.3%	69% ± 0.7%	31.7%	31% ± 0.2%	34025	15429
unedited (7A)-edited (8A)	70%	30%	7A	8A	105.42	106.32	6244	2881	68.4%	69% ± 0.7%	31.6%	31% ± 0.2%	35160	15812
unedited (7A)-edited (8A)	80%	20%	7A	8A	105.49	106.39	7675	2119	78.4%	80% ± 0.2%	21.6%	20% ± 0.3%	41635	11209
unedited (7A)-edited (8A)	80%	20%	7A	8A	105.51	106.32	6892	1873	78.6%	80% ± 0.2%	21.4%	20% ± 0.3%	39125	10024
unedited (7A)-edited (8A)	80%	20%	7A	8A	105.53	106.43	8131	2254	78.3%	80% ± 0.2%	21.7%	20% ± 0.3%	44855	12238
unedited (7A)-edited (8A)	90%	10%	7A	8A	105.49	106.38	6737	927	87.9%	90% ± 0.2%	12.1%	10% ± 0.3%	36970	4923
unedited (7A)-edited (8A)	90%	10%	7A	8A	105.54	106.44	7670	1107	87.4%	89% ± 0.2%	12.6%	11% ± 0.3%	41754	5827
unedited (7A)-edited (8A)	90%	10%	7A	8A	105.45	106.35	8426	1186	87.7%	90% ± 0.2%	12.3%	10% ± 0.3%	46153	6083
unedited (7A)-edited (8A)	100%	0%	7A		105.5		8195	0	100.0%	100% ± 0.0%	0.0%	0% ± 0.0%	45856	
unedited (7A)-edited (8A)	100%	0%	7A		105.48		11247	0	100.0%	100% ± 0.0%	0.0%	0% ± 0.0%	59190	
unedited (7A)-edited (8A)	100%	0%	7A		105.46		9340	0	100.0%	100% ± 0.0%	0.0%	0% ± 0.0%	50064	

Appendix 13. **Data-sheet of quantified PCR fragments using the rapid transcript quantification assay (RTQA).** A series of PCR fragments (7A unedited and 8A edited) mixed to known proportions were applied to the 3730xl genetic analyzer and analyzed by the GeneMapper software (Applied Biosystems). The data sheet shows the actual input and calculated output data for each combination in the grey and red columns, respectively.

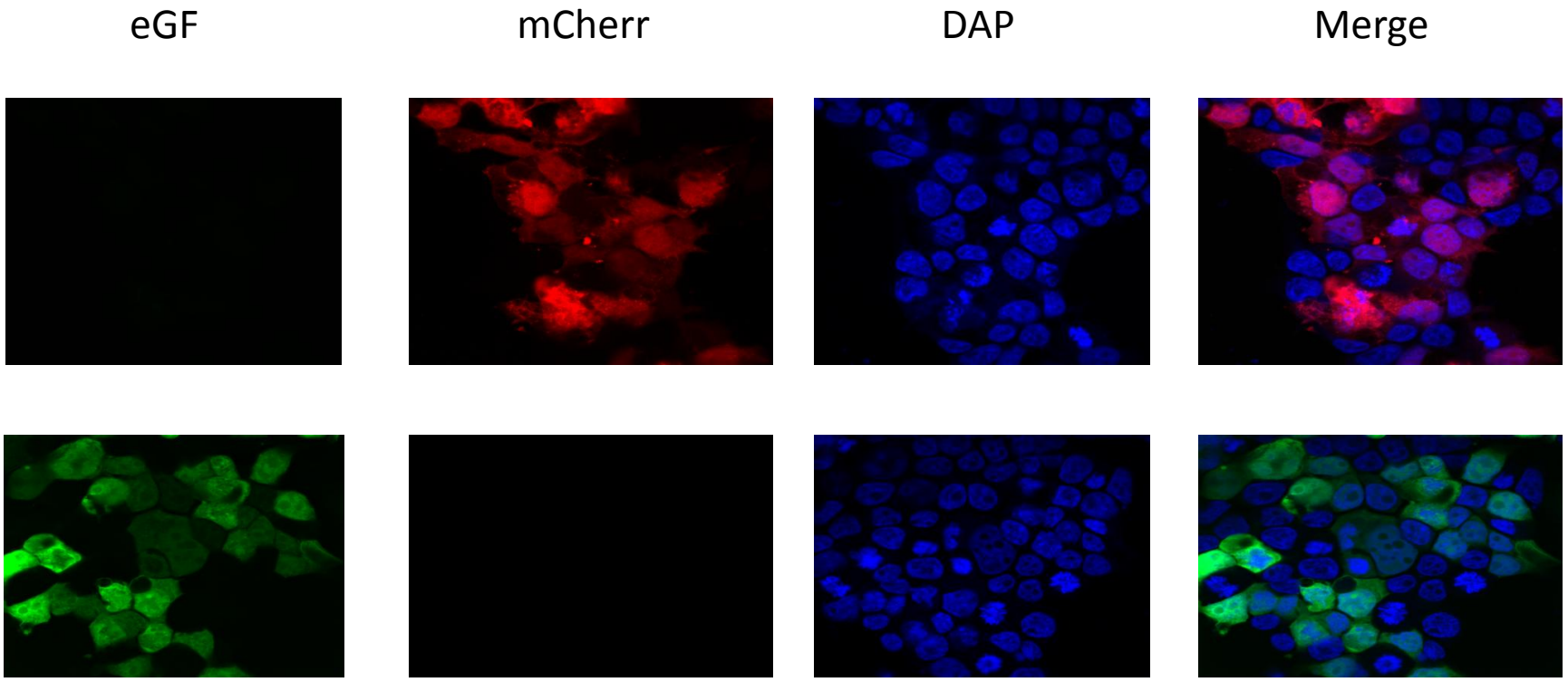

Appendix 14. **eGFP and mCherry are far apart in their respective fluorescence spectra.** Transient expression of eGFP (top panel) and mCherry (bottom panel) following transfection of corresponding pCAGGS plasmid DNA into 293T cells was analyzed at 48 hr post-transfection using the confocal microscope Zeiss LSM 710 at their respective fluorescence spectra. There is no obvious overlap of fluorescence in the respective channels.

Fluorescence Quantification

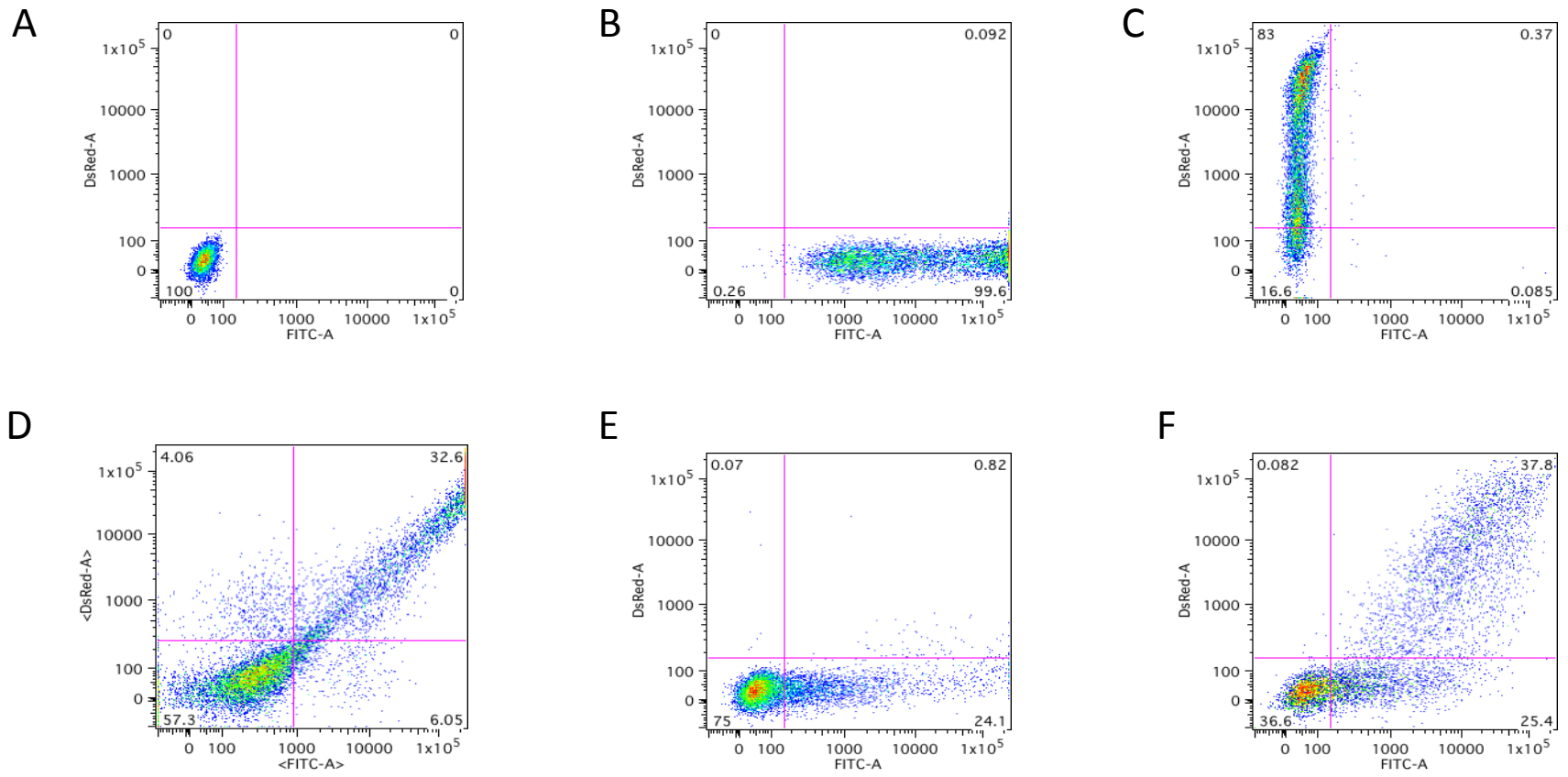

Appendix15. **Reporter expression from the dual-reporter cassette quantified by Flow Cytometer.** Plasmid DNA was transfected into 293T cells. Cells were fixed 48 hr post-transfection with 2% PFA and expression of reporter proteins was analyzed by FACS. **A.** 293T cells, non-transfected **B.** eGFP expression (no mCherry background), **C.** mCherry expression (low to no eGFP background), **D.** eGFP and mCherry expression, **E.** unedited dual-reporter cassette, eGFP-110nt-mCherry-NLS (only eGFP signal), F. edited dual-reporter cassette, eGFP-111nt-mCherry-NLS (mCherry signal in eGFP expressing cells detected). FITC and DsRed are the channels for eGFP and mCherry signal acquisition, respectively. Numerical number in each quadrant shows % positive cells for respective fluorescence signal(s).

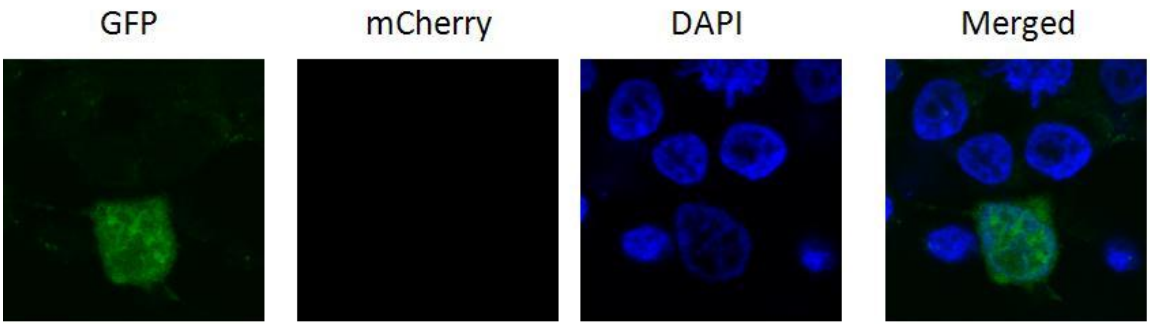

Appendix 16. **T7 bacteriophage polymerase does not mediate RNA editing.** The dual-reporter cassette (eGFP-110nt-mCherry-NLS) was inserted into the pTM1 expression plasmid for T7 driven transcription. 293T cells were transfected with pTM1-(eGFP-110nt-mCherry-NLS) and pCAGGS-T7 for T7 expression and 72 hr post-transfection cells were fixed with 2% paraformaldehyde (PFA) and analyzed for reporter protein expression using confocal microscope. Only cytoplasmic eGFP expression was observed indicating the absence of RNA editing under T7 driven transcription.

Fluorescence quantification

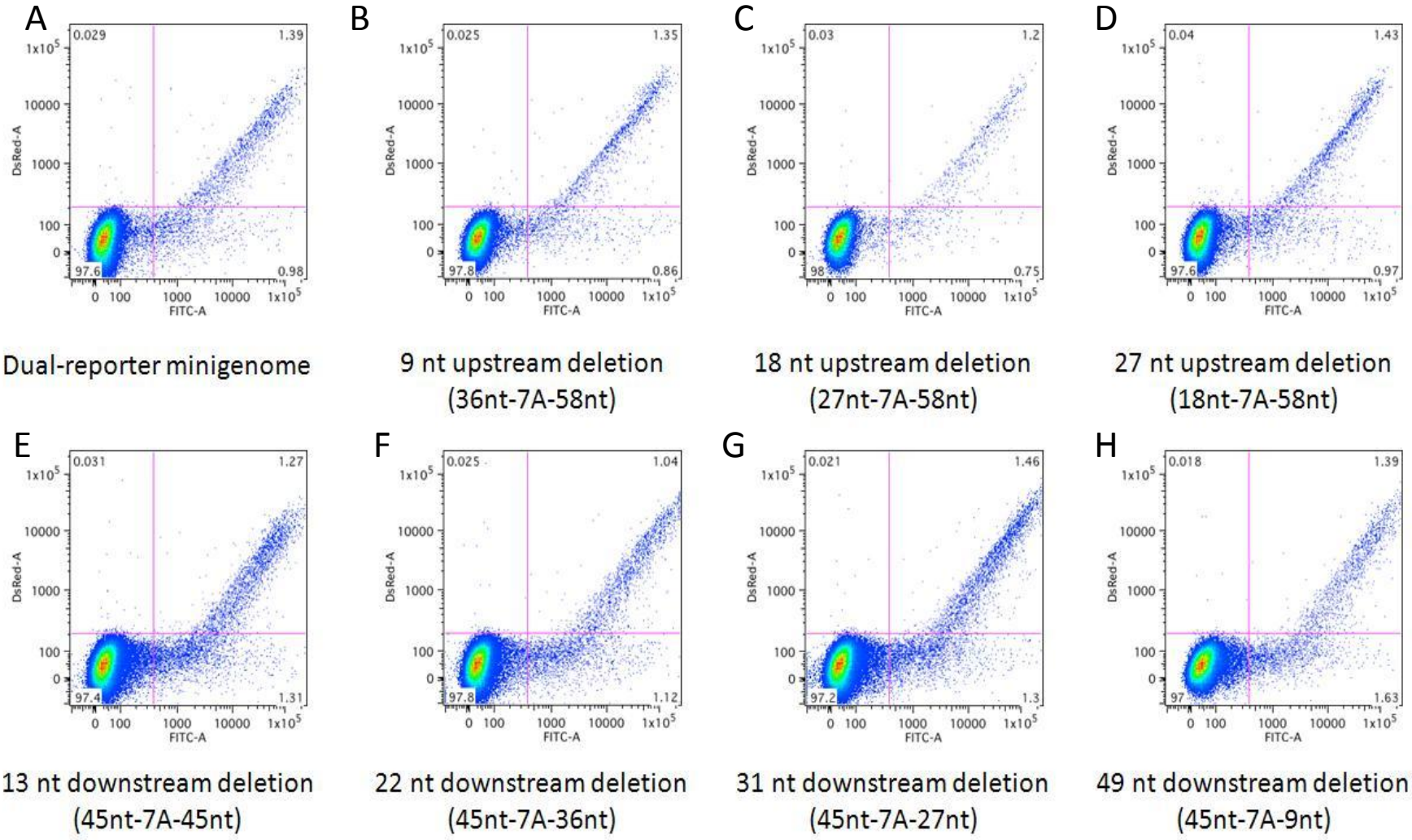

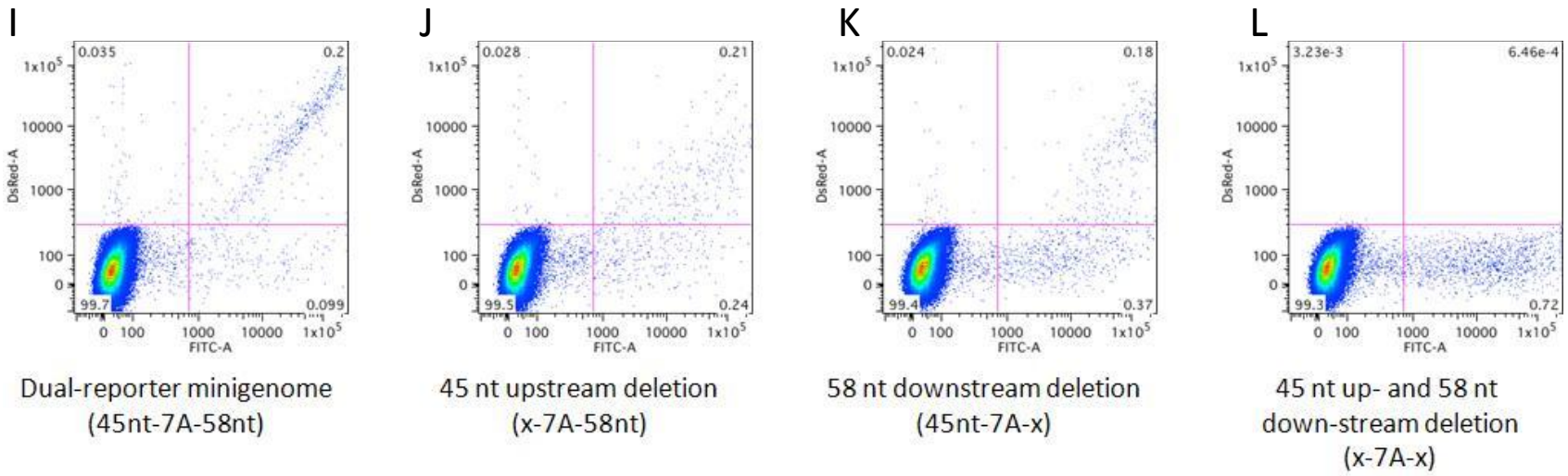

Appendix 17. **Fluorescence signal quantification.** Minigenome DNA of several mutated dual-reporter minigenomes was transfected into 293T cells and reporter protein expression was analyzed at 48 hr post-transfection. Total eGFP and mCherry signals were quantified using fluorescence activated cell sorting (FACS). The images represent one of three independent rescues: **A.** dual-reporter minigenome (no mutation), **B.** Deletion of 9 nt from the upstream cis-acting sequence, **C.** Deletion of 18 nt from the upstream cis-acting sequence, **D.** Deletion of 27 nt from the upstream cis-acting sequence, **E.** Deletion of 13 nt from the downstream, **F.** Deletion of 22 nt from the downstream cis-acting sequence, **G.** Deletion of 31 nt from the downstream cis-acting sequence, **H.** deletion of 49 nt from the downstream cis-acting sequence. FITC and DsRed are the channels for eGFP and mCherry signal acquisition, respectively. Similarly, additional deleted dual-reporter minigenomes were rescued using in vitro-transcribed RNA in 293T cells at 48 hr post-transfection. **I.** dual-reporter minigenome (no mutation), **J.** deletion of 45 nt upstream cis-acting sequence, **K.** Deletion of 58 nt downstream cis-acting sequence, and **L.** Deletion of 45 nt up- and 58 nt downstream cis-acting sequences.

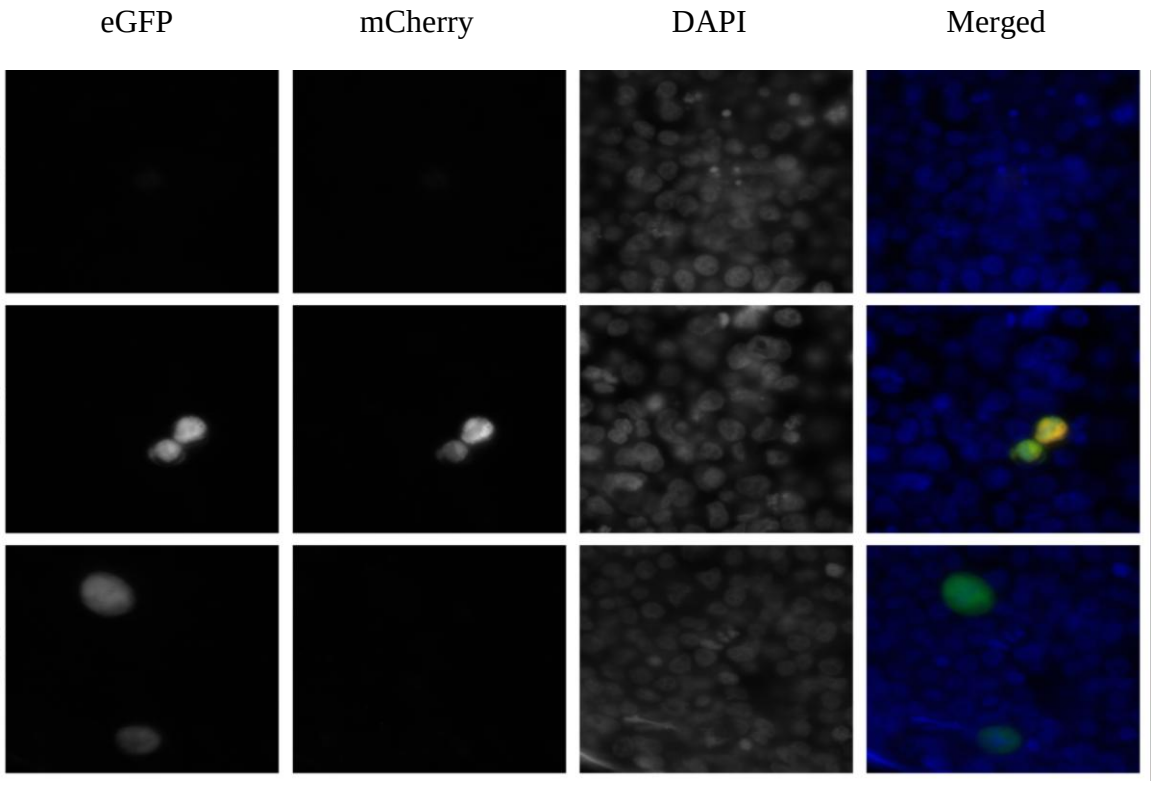

Appendix 18. **VP30, a putative transacting factor for RNA editing.** In vitro-transcribed dual-reporter minigenome RNA was transfected into 293T cells in absence of VP30 and reporter protein expression was analyzed 48 hr post-transfection. Under epi-fluorescence microscope from dual-reporter minigenome rescue without L plasmid (negative control) (top panel), with VP30 plasmid (middle panel), and without VP30 plasmid (bottom panel). In absence of VP30 eGFP expression confirmed transcription, but failed to provide editing supported by undetectable mCherry signal.

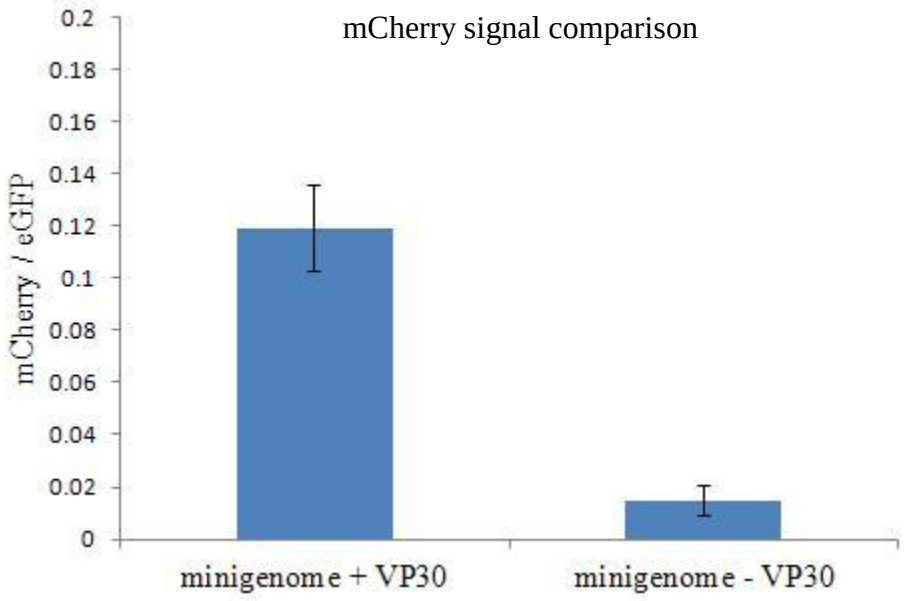

Appendix 19. **Editing reduced in absence of VP30.** In vitro-transcribed dual-reporter minigenome RNA was transfected into 293T cells in the presence or absence of VP30 and reporter protein expression was analyzed using an epi-fluorescence microscope 48 hr post-transfection. Fluorescence signals (mean fluorescence intensity) were quantified using ImageJ software. mCherry signals were found to be very low in the absence of VP30 (mean of three independent minigenome rescues).

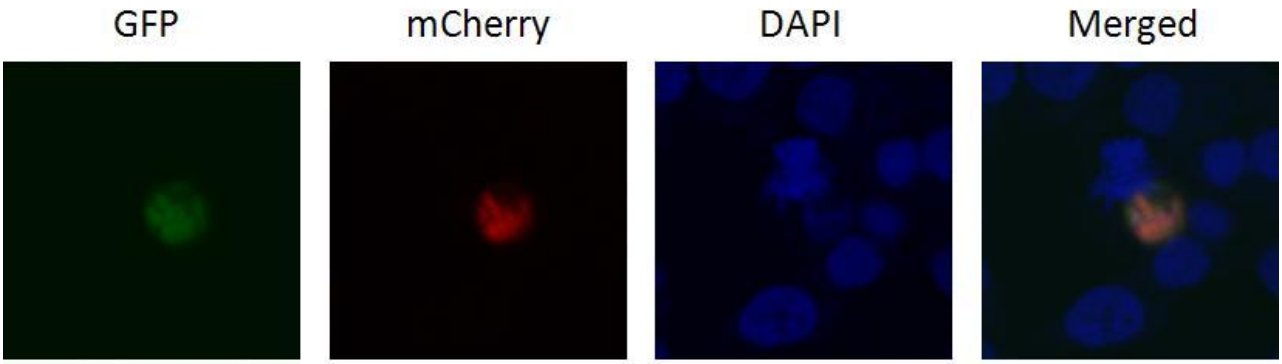

Appendix 20. **Leader sequence stem-loop knockout (KO) allows RNA editing.** The leader sequence stem-loop was destabilized in the dual-reporter minigenome by introducing three mutations (see Figure 8B). In vitro-transcribed mutated minigenome RNA was transfected into 293T cells and reporter protein expression was analyzed 48 hr post-transfection. RNA editing was observed as indicated by eGFP-mCherry fusion protein expression in the nucleus.

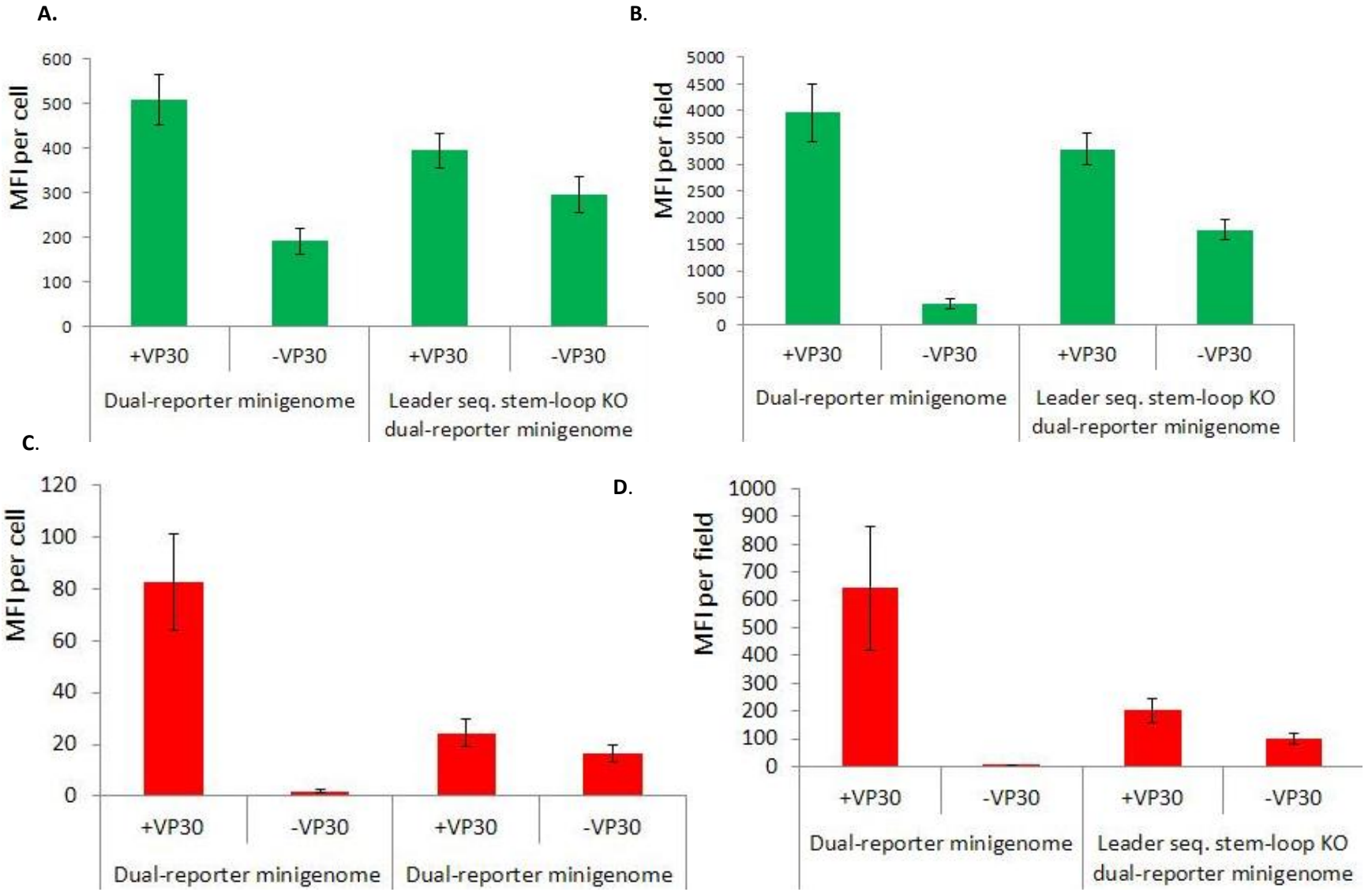
A.
MFI per cell
600
500
400
300
200
100
0
+VP30
-VP30
+VP30
-VP30
Dual-reporter minigenome
Leader seq. stem-loop KO dual-reporter minigenome
B.
MFI per field
5000
4500
4000
3500
3000
2500
2000
1500
1000
500
0
+VP30
-VP30
+VP30
-VP30
Dual-reporter minigenome
Leader seq. stem-loop KO dual-reporter minigenome
C.
MFI per cell
120
100
80
60
40
20
0
+VP30
-VP30
+VP30
-VP30
Dual-reporter minigenome
Dual-reporter minigenome
D.
MFI per field
1000
900
800
700
600
500
400
300
200
100
0
+VP30
-VP30
+VP30
-VP30
Dual-reporter minigenome
Leader seq. stem-loop KO dual-reporter minigenome

Appendix 21. **ImageJ based fluorescence quantification in absence of VP30.** In vitro-transcribed dual-reporter minigenome RNA (wild-type and leader stem-loop knockout) (see Figure 8B) was transfected into 293T cells with or without VP30 plasmid and reporter protein expression was analyzed 48 hr post-transfection. Mean fluorescence intensity (MFI) was calculated using ImageJ software from images taken under an epi-fluorescence microscope. Quantification for eGFP signal only per cell (A) and per field (B). Quantification for mCherry signal only per cell (C) and per field (D).

A.

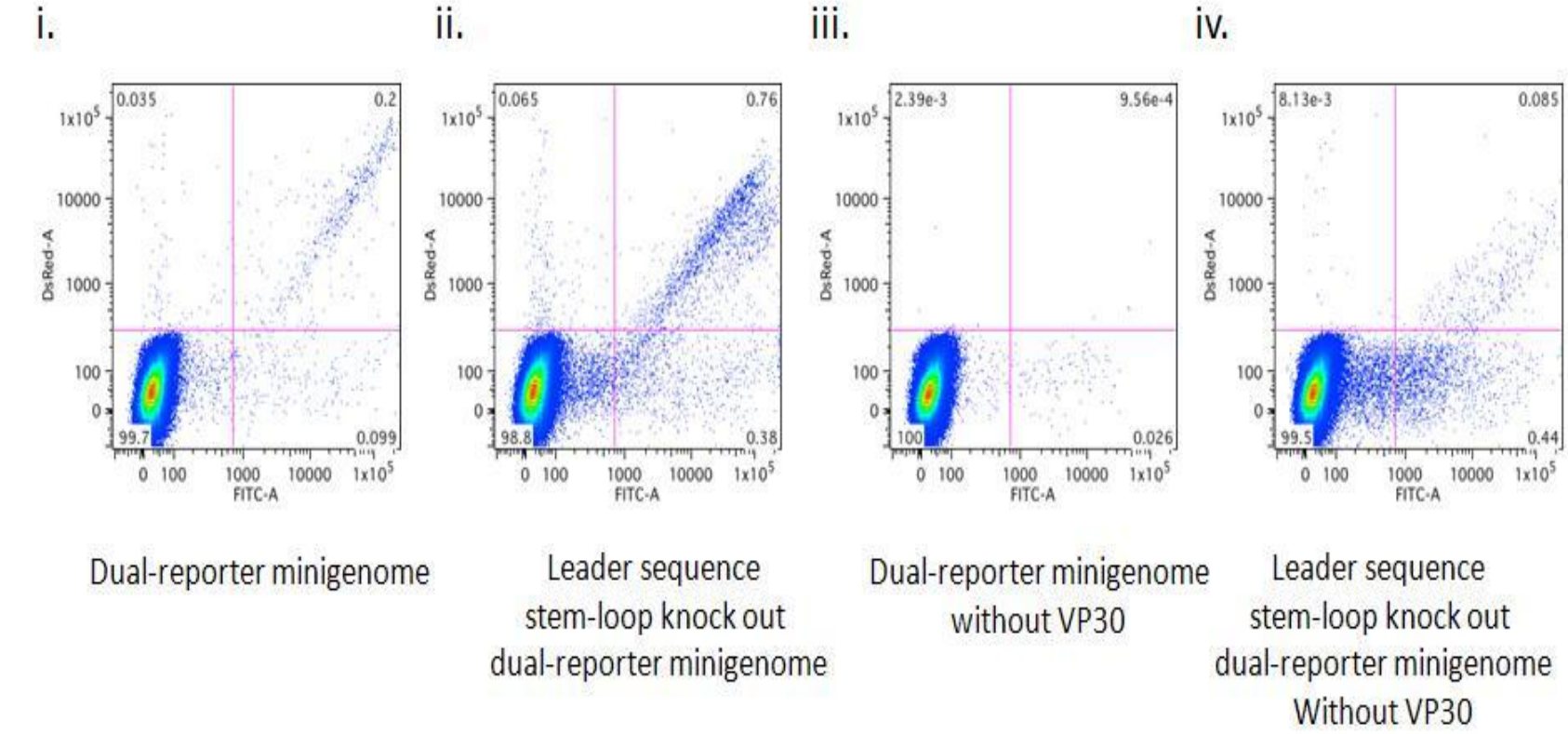
i.
ii.
iii.
iv.
0.035
0.2
99.7
0.099
0.065
0.76
98.8
0.38
2.39e-3
9.56e-4
100
0.026
8.13e-3
0.085
99.5
0.44
DsRed-A
FITC-A
1x10^5
10000
1000
100
0
0 100 1000 10000 1x10^5
Dual-reporter minigenome
Leader sequence stem-loop knock out dual-reporter minigenome
Dual-reporter minigenome without VP30
Leader sequence stem-loop knock out dual-reporter minigenome Without VP30

B.

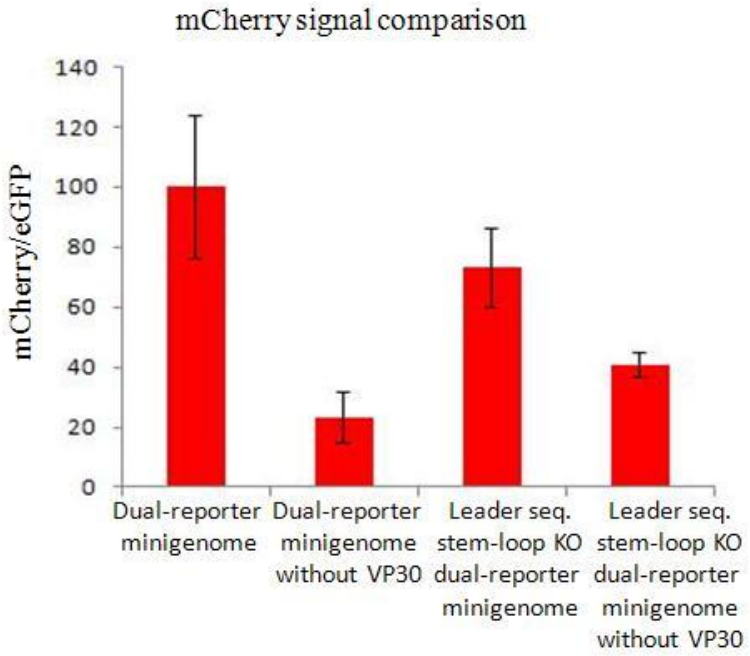
mCherry signal comparison
mCherry/eGFP
140
120
100
80
60
40
20
0
Dual-reporter minigenome
Dual-reporter minigenome without VP30
Leader seq. stem-loop KO dual-reporter minigenome
Leader seq. stem-loop KO dual-reporter minigenome without VP30

Appendix 22. **Editing reduced in the SSKO minigenome in absence of VP30.** In vitro-transcribed dual-reporter minigenome RNA (wild-type and leader stem-loop knockout) (see Figure 8B) was transfected into 293T cells with or without VP30 plasmid and reporter protein expression was analyzed 48 hr post-transfection. eGFP and mCherry signals were quantified by fluorescence activated cell sorting (FACS). **A.** FACS images representing one of three independent rescues: (i) dual-reporter minigenome, (ii) leader sequence stem-loop KO dual-reporter minigenome, (iii) dual-reporter minigenome without VP30, and (iv) leader sequence stem-loop KO dual-reporter minigenome without VP30. FITC and DsRed are the channels for eGFP and mCherry signal acquisition, respectively. **B.** mCherry signals in eGFP expressing cells were compared minigenome rescues with or without VP30.

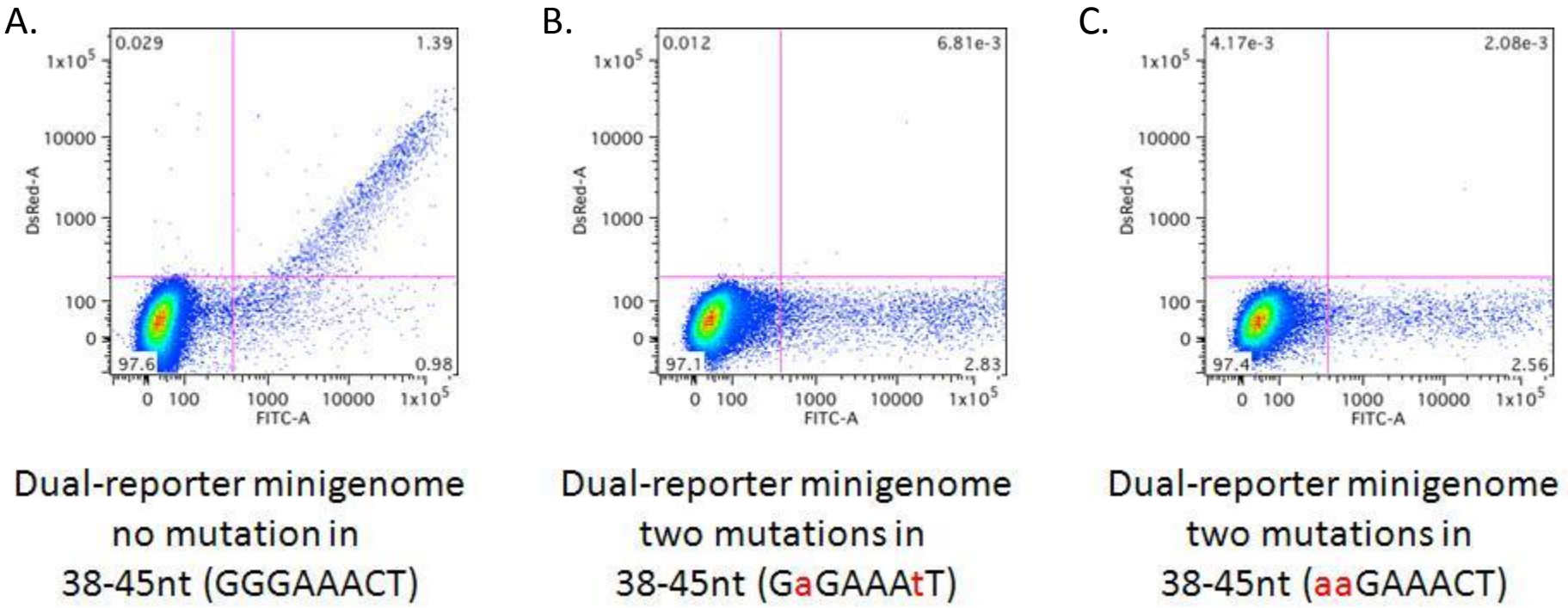

Appendix 23. **Secondary structure (second stem-loop) of the upstream cis-acting sequence is important for RNA editing.** The predicted second stem-loop of the upstream cis-acting sequence was destabilized through mutations [5'G38A and C44T and 5'G38A and G39A]. Dual-reporter minigenome was transfected into 293T cells and reporter protein expression was analyzed by fluorescence activated cell sorting (FACS) at 48 hr post-transfection. FITC and DsRed are the channels for eGFP and mCherry signal acquisition, respectively. RNA editing was abolished in both mutated minigenomes (B and C) in comparison to the non-mutated minigenome (A) indicating that the second predicted stem-loop is important for RNA editing.

Appendices